



Structural pathobiology of cervical wear by robot-simulated three-year toothbrushing

Inaugural – Dissertation

zur

Erlangung des Grades Doctor medicinae dentariae
der Universität Witten/Herdecke

Fakultät für Gesundheit

vorgelegt von Katharina Wilke

aus Albstadt

2023

Dekanin: Prof. Dr. rer. medic Margareta Halek

Dekan: Prof. Dr. med. dent. Stefan Zimmer

Mentor: Prof. Dr. med. Dr. h.c. Peter Gängler

Zweitgutachter: apl. - Prof. Dr. med. dent. A. Rainer Jordan

Tag der Disputation: 29.11.2023

Table of Contents

1	INTRODUCTION.....	1
2	AIM OF STUDY	3
3	SCIENTIFIC BACKGROUND	4
3.1	Mechanisms of tooth wear	4
3.1.1	Abrasion	4
3.1.2	Attrition.....	5
3.1.3	Erosion	5
3.1.4	“Abfraction” – disputed	6
3.1.5	Cervical wear.....	6
3.2	Age-related changes in microstructure.....	7
3.2.1	Structure of human enamel	7
3.2.2	Phases of amelogenesis	8
3.2.3	Age changes of enamel	9
3.2.4	Properties and ageing of dentin.....	9
3.2.5	Properties and ageing of root cementum	10
3.3	Clinical tooth wear indices	11
4	MATERIAL AND METHODS	12
4.1	Experimental design.....	12
4.2	Human tooth model.....	13
4.3	Video observation.....	15
4.4	Robot simulation	16
4.4.1	Six-axis robot arm	16
4.4.2	Toothbrush adjustment	18
4.4.3	Artificial oral cavity.....	18
4.4.4	Toothbrushing programme	19
4.4.5	Executed brushing strokes	19
4.4.6	Overview of manual toothbrushes Rapid Relief and Jubilee	21
4.5	Replication technique	22
4.5.1	Positioning of replicas in the sample chamber	23
4.5.2	Planimetry fields	23
4.6	Scanning electron microscope (SEM).....	24
4.7	3D-SEM.....	25
4.7.1	Calibration protocol	25
4.7.2	Alignment and measurements.....	27
4.7.3	Visualisation of abrasion volume	28
4.8	Accuracy verification.....	28

5	RESULTS	29
5.1	Morphological feature coding	29
5.1.1	Functional abrasion marks (FAM)	30
5.1.2	Appearance perikymata (AP)	30
5.1.3	Exposed prismatic enamel (EPE)	31
5.1.4	Enamel infractions (EI)	31
5.1.5	Open dentin tubules (ODT)	32
5.1.6	Dental calculus (DC)	32
5.1.7	Peninsula formation (PF)	33
5.1.8	Cemento-enamel junction types	33
5.2	Combined wear feature images	34
5.2.1	Incisor A41 – <i>Rapid Relief</i> (flexible neck)	34
5.2.2	Incisor A42 – <i>Rapid Relief</i> (flexible neck)	35
5.2.3	Canine A43 – <i>Rapid Relief</i> (flexible neck)	36
5.2.4	Premolar A44 – <i>Rapid Relief</i> (flexible neck)	37
5.2.5	Premolar A45 – <i>Rapid Relief</i> (flexible neck)	38
5.2.6	Molar A46 – <i>Rapid Relief</i> (flexible neck)	39
5.2.7	Molar A47 – <i>Rapid Relief</i> (flexible neck)	40
5.2.8	Incisor B41 – <i>Jubilee</i> (rigid neck)	41
5.2.9	Incisor B42 – <i>Jubilee</i> (rigid neck)	42
5.2.10	Canine B43 – <i>Jubilee</i> (rigid neck)	43
5.2.11	Premolar B44 – <i>Jubilee</i> (rigid neck)	44
5.2.12	Premolar B45 – <i>Jubilee</i> (rigid neck)	45
5.2.13	Molar B46 – <i>Jubilee</i> (rigid neck)	46
5.2.14	Molar B47 – <i>Jubilee</i> (rigid neck)	47
5.3	Cervical wear lesions	48
5.3.1	Incisor A41 – Cervical wear lesion – <i>Rapid Relief</i>	48
5.3.2	Incisor A42 – Cervical wear lesion – <i>Rapid Relief</i>	48
5.3.3	Canine A43 – Cervical wear lesion – <i>Rapid Relief</i>	49
5.3.4	Premolar A44 – Cervical wear lesion – <i>Rapid Relief</i>	49
5.3.5	Premolar A45 – Cervical wear lesion – <i>Rapid Relief</i>	50
5.3.6	Molar A46 – Cervical wear lesion – <i>Rapid Relief</i>	50
5.3.7	Molar A47 – Cervical wear lesion – <i>Rapid Relief</i>	51
5.3.8	Incisor B41 – Cervical wear lesion – <i>Jubilee</i>	51
5.3.9	Incisor B42 – cervical wear lesion – <i>Jubilee</i>	52
5.3.10	Canine B43 – Cervical wear lesion – <i>Jubilee</i>	52
5.3.11	Premolar B44 – Cervical wear lesion – <i>Jubilee</i>	53
5.3.12	Premolar B45 – Cervical wear lesion – <i>Jubilee</i>	53
5.3.13	Molar B46 – Cervical wear lesion – <i>Jubilee</i>	54
5.3.14	Molar B47 – Cervical wear lesion – <i>Jubilee</i>	54
5.4	Volume loss	55
5.4.1	Incisor A42 – Reshaper 3D	55

5.4.2	Premolar A44 – Reshaper 3D	55
5.4.3	Molar A46 – Reshaper 3D	56
5.4.4	Incisor B41 – Reshaper 3D	57
5.4.5	Incisor B42 – Reshaper 3D	57
5.4.6	Canine B43 – Reshaper 3D	58
5.4.7	Premolar B45 – Reshaper 3D	58
5.5	Tooth comparison	59
5.5.1	Coding of abrasion patterns per tooth: Toothbrush <i>Rapid Relief</i>	59
5.5.2	Coding of abrasion patterns per tooth: Toothbrush <i>Jubilee</i>	60
5.6	Descriptive analysis of abrasion patterns	61
5.6.1	Functional abrasion marks (FAM)	61
5.6.2	Appearance perikymata (AP)	62
5.6.3	Exposed prismatic enamel (EPE)	63
5.6.4	Enamel infractions (EI)	64
5.6.5	Open dentin tubules (ODT)	65
5.6.6	Dental calculus (DC)	66
5.6.7	Peninsula formation (PF).....	67
5.6.8	Cemento-enamel junction types (CEJ)	68
5.6.9	Morphology of cervical abrasion lesions.....	69
5.7	Statistical evaluation.....	70
5.7.1	Absolute and relative frequency	71
5.7.2	Bar chart coding sum comparison.....	72
5.7.3	Box plot abrasion patterns comparison	72
5.7.4	Mean value, variance, standard deviation and standard error	73
5.7.5	Hypothesis testing of abrasion patterns	74
5.7.6	Statistical evaluation of 3D measurements	76
5.7.7	Shapiro–Wilk test.....	78
5.7.8	Quantile–quantile plot	78
5.7.9	ANOVA: Young vs old teeth.....	79
6	DISCUSSION	81
6.1	Replication technique	81
6.1.1	Storage and pre-cleaning of human teeth	81
6.1.2	Adaptation of the replication technique.....	82
6.2	Advantages of the robot simulation	84
6.2.1	Brushing machines	85
6.2.2	Alternative: In vivo models	85
6.2.3	Average brushing duration.....	86
6.2.4	Brushed tooth surfaces	86
6.2.5	Toothbrush motion frequency	87
6.2.6	Calculation of brushing strokes.....	87
6.2.7	Frequency of toothbrushing techniques.....	88

6.2.8	Brushing force	89
6.2.9	Artificial oral cavity.....	90
6.2.10	Manual toothbrushes.....	91
6.3	Toothbrushing-induced morphological changes	92
6.3.1	Functional abrasion marks (FAM)	93
6.3.2	Appearance perikymata (AP)	95
6.3.3	Exposed prismatic enamel (EPE)	95
6.3.4	Enamel infractions (EI)	96
6.3.5	Open dentin tubules (ODT)	97
6.3.6	Dental calculus (DC)	97
6.3.7	Peninsula formation (PF).....	98
6.3.8	Cemento-enamel junction (CEJ).....	98
6.3.9	Morphology of cervical abrasion lesions.....	101
6.4	Advantages 3D-SEM	102
6.4.1	Comparative analysis of volume loss in publications	102
6.4.2	Imaging errors of 3D SEM	104
6.4.3	Sputter coat.....	104
6.4.4	Software alignment.....	104
6.4.5	Measurement inaccuracies	105
6.5	Statistical limitations	106
6.6	Alternative methods	107
6.6.1	Profilometry	107
6.6.2	Non-contacting profilometry and confocal laser scanning microscopy	107
6.6.3	Digital laser microscope (Keyence)	107
6.6.4	Optical coherence tomography (OCT).....	108
6.6.5	Atomic force microscopy (AFM).....	109
6.6.6	Reflectometer (SRI)	109
6.6.7	Intra-oral scanners (IOS)	109
6.6.8	Other approaches to quantify tooth wear	110
6.6.9	Alternative software	110
7	CONCLUSIONS.....	111
8	SUMMARY	113
9	REFERENCES.....	115
10	DANKSAGUNG	129
11	CURRICULUM VITAE.....	130
12	EIDESSTATTLICHE ERKLÄRUNG	131

APPENDIX	I
A.1 Vote of the Ethics Committee	i
A.2 Information for study participants (tooth donation)	ii
A.3 Declaration of consent (tooth donation)	iii
A.4 Method for video observations	iv
A.5 Information for study participants (video observation)	v
A.6 Video observation consent form	vi
A.7 Questionnaire on tooth brushing habits	vii
A.8 Video evaluation table	viii
A.9 Evaluation of robot tooth brushing programmes	ix
A.10 3D SEM calibration protocol	x
A.11 Key parameters for in vitro tooth brushing studies	x

1 Introduction

Tooth wear is a natural phenomenon and a physiological component of the ageing process. Current systematic reviews support the assumption that tooth wear is widespread in all age groups. In permanent teeth, the average prevalence of tooth wear is between 20% and 45%, affecting approximately one in three adults worldwide (Bartlett et al. 2013, Schlueter and Luka 2018). A distinction is made between cervical, occlusal and approximal tooth wear. Occlusal tooth wear occurs mainly due to abrasion and attrition and is well defined. Incisors become thinner and shorter, cusps are flattened, fissures widen and surface details are lost. The ultrastructure of enamel determines the fracture resistance that maintains the shape and function of teeth and also influences how the form of a tooth changes as it wears down. Overall, mammal teeth are adapted to withstand significant stress and wear to remain functional throughout life (Ungar 2015). But the stomatognathic system is highly adaptable and capable of compensating occlusal tooth wear by continuous eruption throughout life (Ainamo and Ainamo 1984, Gängler 1986). Approximal wear is caused solely by tribological wear due to the physiological mobility and friction of the teeth and is compensated by mesial migration of the dentition, whereby rounded contact points are transformed into flat contact surfaces. In the case of tooth loss, migration can lead to mesial inclination if the tooth is not occlusally supported by an antagonist. Occlusal and proximal wear are physiological ageing processes. Cervical root wear results mainly by abrasion and erosion and is less well defined, removing enamel, cementum and dentin, resulting in typical cervical lesions. Cervical wear is primarily found in humans and very rarely in other animals, and is therefore considered a pathological phenomenon that is due to oral hygiene and erosive diets (Gängler et al. 2005). Anthropologists studying archaeological human crania consider the formation of cervical wear lesions to be a *modern* clinical phenomenon (Kaidonis 2008).

Brushing too vigorously with abrasive dentifrice is a significant cause of the gingival recession and subsequent cervical abrasion lesions in combination with dentin hypersensitivity (Bergström and Lavstedt 1979, Heasman et al. 2015, Demarco et al. 2021). Abrasive cervical lesions (Fig.1) can occur on all teeth but are most common on the buccal sides of incisors, canines and premolars (Addy et al. 1987). According to recent studies, the overall prevalence of cervical root wear is 29.0–46.7%, more prevalent in older populations and men (Bartlett et al. 2013, Teixeira et al. 2020). An extensive cervical lesion can harm the structural integrity and cosmetic appearance of the tooth as well as the vitality of the dental pulp.

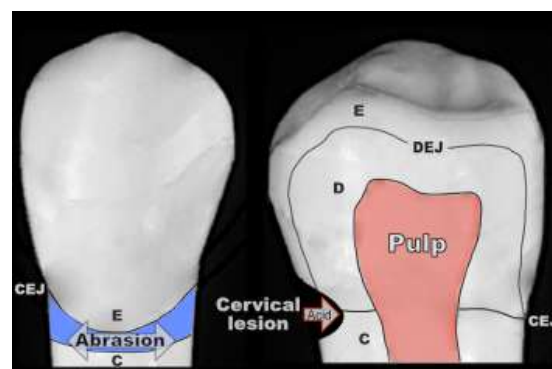


Figure 1: Cervical abrasion lesion. Buccal side (left) and lateral cross section (right). Dental structures: enamel (E), dentin (D), cementum (C), dentino-enamel junction (DEJ), cemento-enamel junction (CEJ). **Blue:** The cervical region, which is vulnerable to toothbrush abrasion.

If these lesions progress uncontrolled, this can lead to tooth fractures, inflammation and devitalisation of the pulp, periapical bone infections and, ultimately, tooth loss (Ceruti et al. 2006). Besides caries and periodontal disease, tooth wear is considered one of the most common factors leading to clinical problems in the human dentition (Mehta et al. 2020). Improvements in oral hygiene and treatment options for caries and periodontitis have made it possible to preserve teeth in advanced age. This makes it increasingly important to focus on the issue of tooth wear (Ganss et al. 2011, Lussi and Carvalho 2014). In the absence of profound structural damage, treatment of tooth wear is primarily based on correcting cosmetic impairment (Bartlett and O’Toole 2021). Nevertheless, in recent decades, as many as 2–10% of adolescents have shown severe tooth wear, some of which require early restorative treatment (Bartlett et al. 2013, Lussi and Carvalho 2014). The consequences of tooth wear are, besides caries, the main reason for restorations on permanent tooth surfaces (Nascimento et al. 2011). In addition, tooth wear rarely affects a single tooth. Often several sextants or quadrants are affected simultaneously, which, depending on the severity, may require complex rehabilitations when indirect restorations are considered, resulting in costly tooth wear treatment (Bartlett and O’Toole 2019). Therefore, it is recommended to focus on preventing and controlling the progression of cervical lesions and delaying extensive treatment. There is good evidence that early diagnosis and appropriate preventive measures can reduce tooth wear and thus obviate the need for complicated restorative treatment in the future (O’Toole et al. 2018a). Standard preventive measures include dietary adjustments, careful hygiene practices and adhesive techniques to alleviate the dentin hypersensitivity (O’Toole et al. 2018b). Nevertheless, various methods, such as profilometry or 3D confocal laser microscopy, have been proposed to search for objective systems to investigate tooth wear. However, no standard method for early detection of tooth wear has yet been established. Due to different study designs, variable sample sizes, different clinical indices and different diagnostic tools used to quantify tooth wear of different aetiology, there are notable differences in the prevalence data collected (Schlueter and Luka 2018). Among many different clinical evaluation indices, the *Smith and Knight tooth wear index* from Smith and Knight (1984) and the *Basic Erosive Wear Examination* (BEWE) index has been most widely established in recent years, with the latter being easier for dentists to implement due to its simplicity and comparability (Bardsley 2008, Bartlett et al. 2008, 2011). However, the BEWE index does not record dentin exposure in detail and does not allow an objective classification of the tooth wear (Olley et al. 2014). Moreover, the terms and definitions applied also considerably influence the prevalence data. With terms such as “*root defect*”, “*abrasion*” or “*abfraction*”, the prevalence tends to be underestimated by investigators compared to when the more general term “*non-carious cervical lesion*” is applied (Teixeira et al. 2020). Cervical tooth wear is progressive, so a lifelong approach to monitoring and prevention should be taken.

2 Aim of Study

This study aims to gain insight into the alterations in the morphological characteristics of cervical wear lesions of human teeth after a clinically validated, robot-assisted, three-year simulated toothbrushing programme in an artificial oral cavity. To investigate the influence of tooth age on wear, 14 teeth from three different age groups (juvenile, young adults and middle-aged adults) will be positioned within an anatomical dental arch. The study aims to distinguish between harmful and beneficial effects of toothbrushing on oral health.

The present study had three objectives:

1. Characterising abrasion patterns of early toothbrushing lesions by scanning electron microscopy summarised in a catalogue of criteria for evaluating tooth wear.
2. Quantitative analysis of volume loss due to toothbrushing using scanning electron microscopy equipped with a *4Q-BSE detector* and a 3D point clouds processing software.
3. Analysis of changing abrasion patterns on natural teeth due to three-year robot simulated toothbrushing.

It is hypothesised that both the morphological abrasion patterns and the extent of volume loss could vary depending on the age of the teeth.

Finally, a catalogue of pathobiological abrasion patterns and the coding of changes over time due to tooth brushing can contribute to a deeper understanding of cervical wear as a basis for further research. The importance of early detection and diagnosis of wear characteristics for initiating appropriate preventive measures cannot be overestimated.

This research aims to achieve a clinically significant objective by formulating a methodology that can assess dental care products for their ability to both preserve tooth structure and deliver effective plaque control, thereby ensuring optimal dental health for consumers. Within this framework, the primary working hypothesis to be explored in the advancement of the new methodology posits that utilizing a dentifrice and a manual toothbrush equipped with a flexible ball joint brush neck is less abrasive compared to using a manual toothbrush with a rigid brush neck.

3 Scientific Background

3.1 Mechanisms of tooth wear

In general, tooth wear is the cumulative surface loss of mineralised tooth substance due to physical or chemical-physical attrition, abrasion and erosion (Eccles 1982). The main mechanisms of tooth wear are illustrated in *Figure 2*. A historical review shows that researchers in North America focused on attrition, while in Europe the priority was the investigation of erosion (Bartlett et al. 1999).

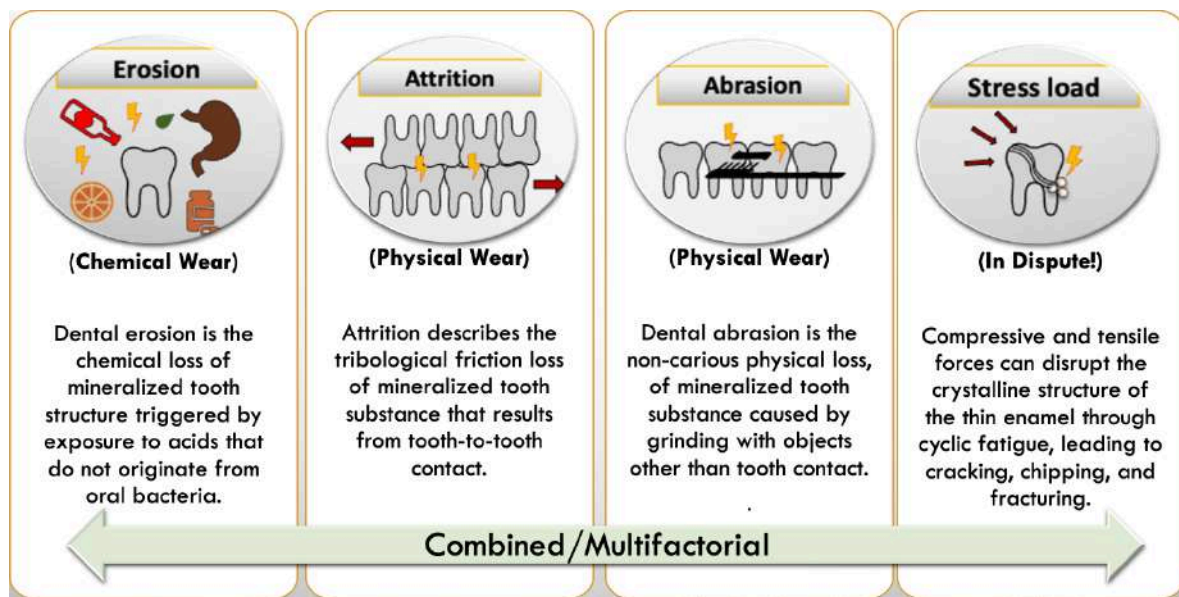


Figure 2: Three main mechanisms cause tooth wear: erosion, attrition and abrasion. The influence of occlusal loading on cervical wear is controversial.

3.1.1 Abrasion

The term abrasion is derived from the Latin verb "*abradere*". It describes the loss of mineralised tooth substance caused by mechanical processes such as grinding or rubbing with objects other than teeth. Occlusally, the enamel can be abraded by a granular diet, and the extent of occlusal degradation is influenced by the abrasiveness of the food (Imfeld 1996). Nowadays, foods are predominantly of tender consistency, so occlusal abrasion due to food intake occurs only to a marginal extent (Gängler et al. 2005). Other forms of dental abrasion can be related to habits such as nail biting, pipe smoking or piercings (Lee et al. 2012). Abrasion from toothbrushing is considered a predominant wear mechanism in the cervical tooth region (Davis and Winter 1976, Radentz et al. 1976, Litonjua et al. 2004, Dzakovich and Oslak 2008, Heasman et al. 2015). The horizontal brushing technique is considered harmful to the gum tissue and tooth structure when used forcefully (Mierau et al. 1989, Mierau 1992, Wiegand and Schlueter 2014). Other factors that influence the abrasion process include the type of toothbrush, stiffness of the bristles, the abrasiveness of dentifrice, and frequency and duration of brushing (Wiegand et al. 2009, Bizhang et al. 2016, Lippert et al. 2017, Turssi et al. 2019b, 2019a).

3.1.2 Attrition

Attrition is the tribological loss of mineralised tooth substance due to tooth-to-tooth contact. The defects appear flat and polished, with the ground facets matching the teeth. Bruxism, in particular, can lead to excessive occlusal wear and, in the worst case, to tooth fractures and temporomandibular joint disorders due to the permanent static overload (Roberts and Stocum, 2018). Tooth malocclusions such as head bite, overbite, crossbite and parafunctions can also contribute to a pathological progression of attrition (Carlsson et al. 2003, Yadav et al. 2020, Kapagiannidou et al. 2021). Also, an unsupported partial dentition can increase the amount of occlusal wear on the remaining teeth. During life, an average mesial migration of 1 cm was observed due to approximal tooth attrition. Point-like approximal tooth contacts are transformed into contact surfaces.

3.1.3 Erosion

Erosion is the chemical loss of mineralised tooth structure caused by exposure to acids that do not originate from oral bacteria. According to studies, 46% of teenagers (McGuire et al. 2009) and 80% of adults (Okunseri et al. 2015) are affected by erosive tooth wear. A distinction is made between extrinsic and intrinsic acid load (Eccles 1979, Ganss and Lussi 2014). Extrinsic factors include acidic foods, especially low pH drinks such as carbonated sodas and wine, citrus fruits or vinegar (Saads Carvalho and Lussi 2020, Hartz et al. 2021). Tooth enamel consists of more than 90% hydroxyapatite. It is therefore very susceptible to demineralisation as soon as the pH value in the oral cavity falls below 5.5 (Moazzez et al. 2000). In several studies, the main focus of research into erosive tooth wear has been the excessive consumption of acidic drinks, particularly by children and adolescents (Kreulen et al. 2010, Saads Carvalho and Lussi 2020). Nevertheless, the erosive potential of an acidic beverage depends not only on its pH but also on its mineral content, buffering capacity and calcium-chelating properties. Evidence shows that additional milk and yoghurt consumption is associated with a lower prevalence of erosive tooth wear (Salas et al. 2015). In addition, the combination of wine and cheese has proven to be a smart social strategy, as the cheese buffers the acidity of the wine while providing calcium and phosphate ions to the enamel for remineralisation (Larsen and Nyvad 1999). Intrinsic factors include the influence of acids due to reflux diseases, bulimia or xerostomia (Bartlett 2006). In particular, gastro-oesophageal reflux disease and hyposalivation, disease-related or caused by medication, are considered clear risk indicators for severe erosive tooth wear (Bartlett et al. 1996, Carvalho et al. 2016b). Acids demineralise the outer enamel, and an irregular structure is created, comparable to the honeycomb etching pattern in adhesive dentistry (Ganss and Lussi 2014, Bartlett and O'Toole 2021). The demineralised zone can extend up to 100 µm into the tooth structure and can deteriorate the mechanical properties of enamel and dentin, increasing the tooth's susceptibility to abrasion by the toothbrush (Zentner and Duschner 1996). It has been shown that even delaying toothbrushing two hours after a meal does not protect against enamel erosion (Ganss et al. 2007a). Consequently, it is more critical to change harmful toothbrushing habits to

prevent tooth erosion than to encourage patients to wait to brush their teeth. In contrast, fluoride application during toothbrushing positively affects remineralisation and caries prevention (Bartlett et al. 2013). In an optimal mineralised environment, either through fluoride or calcium replacement, especially with viscous fluoride gels, the integrity of the enamel surface can be recovered (Parker et al. 2014, O'Toole et al. 2015, Amaechi et al. 2020). Without prevention, the loss of the surface gradually leads to visible tooth wear (Fig. 3).



Figure 3: Tooth with typical features of occlusal erosion: Occlusal structures have been flattened, cusps rounded and cusp slopes hollowed out.

3.1.4 “Abfraction” – disputed

“Abfraction” is a theoretical concept that assumes that occlusal load causes stress and tensions in the tooth structure, resulting in micro-infractions in the cervical area, predisposing this area to erosion and abrasion (Lee and Eakle 1984). Coy (1982) suggested bruxism as the main cause of the characteristic wedge-shaped lesions at the cervical tooth region. The term “*abfraction*” was finally defined by Grippo (1991), referring to “*breaking away*”. As early as the 1970s, studies using finite element analysis (FEA) showed that, under model assumptions, stresses are concentrated in the cervical region of the teeth, especially under non-axial loading (Yettram et al. 1976). But one criticism is that most FEA studies use two-dimensional models, although three-dimensional models would be more suitable for measuring torsional strains. FEA studies also show equal loading on the tooth’s buccal and lingual side, contrary to clinical findings, as cervical lesions occur far more frequently on the buccal side (Bhundia et al. 2019). Present studies have frequently observed the occurrence of cervical lesions in association with occlusal wear, but the correlation could neither be confirmed nor rejected (Takehara et al. 2008, Silva et al. 2013). However, patients affected by bruxism and cervical lesions were also found to report excessive toothbrushing behaviour (Bader et al. 1996, Jiang et al. 2011). Anthropological researchers also questioned the role of occlusal forces, as no cervical lesions were found in cranial findings despite severe occlusal wear (Aubry et al. 2003, Kaidonis 2008, Urzúa et al. 2015). Therefore, the ORCA Consensus Report 2020 did not include the term “*abfraction*” as a separate tooth wear mechanism (Schlueter et al. 2020).

3.1.5 Cervical wear

Due to growing life expectancy and success in caries prevention, non-carious cervical lesions are increasingly becoming a major dental problem affecting up to two thirds of the population (Teixeira et al. 2020). Cervical wear is characterised by the loss of tooth structure due to wear near the cemento-enamel junction, where all three hard tooth substances – dentin, cementum and enamel – intersect. The thin cervical enamel layer is formed by ameloblasts, which no longer have a *Tomes process* in this final phase of enamel formation (Thompson 2020). In consequence, this thin enamel layer is less

structured, has a lower mineral and higher protein content, and has a low density of *Hunter-Schreger bands* (Lynch et al. 2010). Furthermore, the cementum represents a relatively weak junction with the enamel, while it forms a relatively strong and hygroscopic bond with the root dentin. The average cervical cementum thickness is only about 20–40 μm . Therefore, exposed cementum is particularly susceptible to wear processes due to toothbrush abrasion and erosion (Jaeggi and Lussi 1999). Meta-analyses have shown the association between cervical wear and frequency, toothbrushing technique and toothbrush stiffness (Heasman et al. 2015). Only 2% of these lesions are found on lingual or palatal surface (Sangnes and Gjermo 1976). This is consistent with the fact that the inner surfaces are neglected by the majority of participants from video observation studies during toothbrushing (Schlueter et al. 2018). When severe, cervical wear lesions affect the cosmetic and function of the stomatognathic system and can be associated with dentin hypersensitivity (Bartlett et al. 2013). Cervical wear lesions are often wedge-shaped with an inward peak or saucer-shaped (*Fig. 4*) (Hur et al. 2011, Worawongvasu 2021). Finally, there is evidence that cervical tooth wear is mainly caused by a combination of physical (abrasive) and chemical (erosive) factors (Bhundia et al. 2019, Schlueter et al. 2020). Therefore, possible preventive measures include a change in diet, a change in toothbrushing technique, and especially control of the pressure and frequency of toothbrushing (Bader et al. 1993).



Figure 4: Saucer-shaped cervical wear lesions on two maxillary premolars. The individual suffers from reflux and formerly exhibited a vigorous horizontal brushing technique. The patient also complains of dentin hypersensitivity.

3.2 Age-related changes in microstructure

In order to assess the structural changes of the tooth surface, a deeper understanding of the dental microstructure is required. The general percentage of inorganic components in hard tooth tissue ranges from cementum (50%), bone (60%), dentin (70%) and enamel (95%) (Steiniger et al. 2010).

3.2.1 Structure of human enamel

Microstructurally, tooth enamel consists of bundles of hundreds of parallel hydroxyapatite crystals arranged in long cylinders called prisms or rods, which account for 95% of the weight and 87% of the volume and are arranged in identical manner in all primates (Lee et al. 2010). The inorganic components of enamel are mainly composed of calcium (Ca^{2+}), phosphate (PO_4^{3-}), hydroxide (OH), fluoride (F^-), carbonate (CO_3^{2-}) and sodium (Na^+) ions (Shellis et al. 2014). Enamel is designed to withstand mechanical stresses, temperature differences, intermittent corrosive chemical environments and chewing (Lacruz et al. 2017). The layer of enamel is on average 1.6–1.7 mm thick, with a maximum thickness of 2.3–3.5 mm in the occlusal cusp area, while the enamel layer in the cervical area is only 0.1–0.01 mm thin (Kunin et al. 2015). The organic components and the water content of 4–5 wt. % act as a bonding agent between hydroxyapatite crystals and enable prisms to slide under the

load (He and Swain 2007). The hardness at the matured enamel surface of $H > 6$ GPa and $E > 115$ GPa and the bio-nanocomposite structure provide high resistance to material fatigue and wear (Cuy et al. 2002, Thompson 2020). The denser packing and parallel alignment of the crystals in the outer enamel further increases the wear resistance at the tooth surface (He and Swain 2009). Conferring to Elhennawy et al. (2017), a reduction in the volume concentration of hydroxyapatite by 1% causes a decrease in the elastic modulus by 3 GPa. Therefore, the hardness of the enamel decreases with reduced mineralisation towards the dentin-enamel junction to about $H < 3$ GPa and $E < 70$ GPa (An et al. 2012). The overall enamel mineral content, which varies greatly from person to person, can thus be used as a predictor of the wear and caries resistance (Akkus et al. 2017).

3.2.2 Phases of amelogenesis

The formation of tooth enamel rods can be divided into five different phases:

1. Secretion of an organic matrix: Ameloblasts are arranged in a tight, overlapping row in the inner enamel epithelium. During differentiation, the Tomes process is formed at the proximal end of ameloblasts, which produces specific proteins, mainly amelogenin (80%), ameloblastin (10%) and enamelin (10%) (Habelitz and Bai 2021). Without proteins secreting calcium phosphate compounds, the mineralisation process fails and no enamel layer can be formed (Hu et al. 2008). **2. Crystal formation:** Enamel apatite bands are oriented perpendicular to the mineralisation front and formed by the migration of ameloblasts from the dentin-enamel junction to the surface (Ronnholm 1962, Daculsi et al. 1984). Enamel formation progresses at a rate of about $4 \mu\text{m}$ per day (Dean 1998). With enamel maturation, the nano crystallites reach a cross-section of $26 \times 68 \text{ nm}$ (Meckel et al. 1965) and a length of up to $1 \mu\text{m}$ (Wang et al. 2008). Enamel rods resulting from prismatic bundles consist of about 40,000 crystallites and are surrounded by a protein-rich shell (Kerebel et al. 1979).

3. Regulation of crystal growth: Enamel rods typically form a keyhole-like structure in which prisms can be divided into a head and a tail region by their different orientation. Four ameloblasts are involved in the formation of a keyhole-interlocked enamel prism (*Fig. 5*). The head is secreted by the Tomes process of an ameloblast and separated by the interprismatic substance that guides the mineralisation of each prism and forms the tail of the keyhole (Meckel et al. 1965). By etching the enamel, a prismatic head can be removed from the surface creating a characteristic honeycombed appearance (Meurman and Frank 1991). The periodic growth phases of enamel can be



Figure 5: Concept of the keyhole-like microstructure of human enamel rods by Meckel et al. (1965). In the section a “keyhole” configuration of prisms with an arcade-shaped head (prism rod) and cervical tail (interprismatic enamel) can be seen. Original plaster and resin models courtesy of Alfred Meckel.

recognised structurally as prismatic transverse *Retzius stripes*, which occur at intervals of about 7–8 days during human amelogenesis and mark the periodic resting phase between the secretory phases of the ameloblasts. The Retzius stripes reach the lateral tooth surfaces at an acute angle and bulge out there as perikymata (*kyma* (κύμα), Greek – wave). Perikymata form circular bands around the tooth crown and are a characteristic feature of juvenile teeth that are worn down with age (Osborn 1973). Enamel tufts originate in the inner enamel at the junction of the dentin. These are areas high in an organic matrix and therefore hypomineralised. Some enamel tufts run through the enamel to the surface and are then called enamel lamellae (Weatherell et al. 1968). Hunter-Schreger striations are an optical phenomenon caused by the alternating alignment of prism rods and can be seen as light and dark stripes in longitudinal and transverse sections. **4. Degradation of the organic matrix:** To complete the mineralisation process, mature ameloblasts transform into reduced ameloblasts in order to remove both degraded matrix proteins and water (Simmer et al. 2010). The crystals expand into the new space, become larger and interlock with each other (Smith 1998). At the beginning of amelogenesis and before final apoptosis, the ameloblasts produce a few layers of reduced enamel epithelium without a Tomes process. Once the enamel has reached its predetermined thickness, finally a prism-free enamel layer (20–80 µm) is formed (Ripa et al. 1966). After tooth eruption, the last ameloblasts in the cervical area of the tooth are replaced by the junctional epithelium (Smith 1998). **5. Crystal maturation:** During post-eruptive maturation, the mineral content and thickness of the aprismatic structure gradually increase due to progressive surface mineralisation. The initial maturation phase of permanent teeth in humans lasts about 3 to 6 years (Park et al. 2008). Therefore, exposed prismatic areas more frequently occur in juvenile teeth (Kunin et al. 2015). The OH⁻ ions of the hexagonal hydroxyapatite crystals are replaceable by other ions during maturation. Typical substitutions of hydroxyapatite which differ in the following solubility are: fluor hydroxyapatite < carbonate hydroxyapatite < magnesium hydroxyapatite (Young 1974). In particular, the incorporation of fluoride ions reduces the acid solubility of the crystal lattice (Griffin et al. 2007).

3.2.3 Age changes of enamel

Recently erupted teeth are more susceptible to wear, decalcification and caries because crystal maturation is still immature (Thompson 2020). The enamel structure is subject to a constant change in the demineralisation and remineralisation (Gängler et al. 2005). Prolonged exposure to minerals and fluoride compacts the crystal structure on the surface to a depth of 1–2 mm (He et al. 2011). At a physiological rate of wear, the enamel thickness of a 65-year-old has decreased by about a third on average (Kidd et al. 1984). Mechanical properties of enamel are ultimately determined by its unique chemical composition and on age and individual characteristics (Cuy et al. 2002).

3.2.4 Properties and ageing of dentin

Dentin is formed by odontoblasts and consists of 70% inorganic and 20% organic material. Mineralisation by odontoblasts initially occurs at a rate of ~2.8 µm/day and finally slows down to 0.5 µm/day

(Bleicher 2014). The anisotropic orientation of the crystals determines the physical properties of the dentin (Marten et al. 2010). The reaction possibilities of dentin are complex and represent a combination of different biological response patterns of odontoblasts (Arnold 2006). During life, odontoblasts maintain the ability to respond to external stimuli, such as caries or excessive wear, with secondary or tertiary dentin accumulation, increasing the hardness of dentin and narrowing the pulp chamber volume (Carvalho and Lussi 2017). The collagen network is less solid and more susceptible to mechanical wear. Therefore, the rate of wear accelerates once dentin is exposed (Bartlett and O'Toole 2021). When dentin is exposed to an erosive attack, the more mineralised peri-tubular dentin dissolves first. The resulting widening of the dentinal tubules can increase dentinal hypersensitivity in sensitive individuals (West et al. 2013, Seong et al. 2018). The accumulation of calcium phosphate crystals in dentin tubules gradually induces their sclerosis and increases the dentin's resistance to occlusal stress and tooth wear (Maeda 2020). This process usually begins in the third decade of life and progresses gradually until the lumens are (almost) entirely closed. A disadvantage of a fully sclerotised dentin is that it cannot be adequately supplied with interstitial fluid, which reduces fatigue and fracture resistance (Nazari et al. 2009). Consequently, dentin of older individuals has a higher elastic modulus (Xu et al. 2014). The gradual remodelling allows the dentin to partially adopt the function of the worn-down enamel over time (Arola et al. 2017).

3.2.5 Properties and ageing of root cementum

Cementum is formed by cementoblasts that differentiate from ectomesenchyme cells and is quite close in properties to bone. The main function of the primary cementum is the biomechanical anchorage of the collagen fibres of the periodontium to the alveolar bone (Lehnen et al. 2012). Secondary cementum is formed when the tooth goes into occlusion. A basic differentiation is made between cellular and acellular cementum. Acellular *Sharpey fibres*, formed by fibroblasts, cover the coronal two-thirds of the root and are oriented perpendicular to the surface *and* are mainly responsible for anchoring the tooth in the alveolar bone. To accomplish this task they are significantly thicker than the cellular fibres (Nanci and Ten Cate 2017). Cellular cementum is very similar to bone and consists of 60% inorganic minerals, but does not contain blood vessels and nerves. It is aligned parallel to the root surface and is predominantly located at the root apex. The middle third usually consists of mixed-fibre cementum. A third form described is the acellular-afibrillar cementum, which is present in 50% of permanent teeth in the cervical area where the marginal epithelium has been lost (Steiniger et al. 2010). It is considered responsible for the formation of cementum tongues and cementum isles on the enamel (Lüllmann-Rauch 2009). Between the ages of 20 and 60, the thickness of the cementum ultimately triples due to a continuous accumulation (Gupta et al. 2014). The layer thickness varies between 50 μm and 150 μm and increases in the course of ageing, especially in the apical third. In forensics, the relationship between the coronal shift of the cemento-enamel junction and the thickness of the cementum in the apical third is used to estimate the age (Raju et al. 2016).

3.3 Clinical tooth wear indices

Over the years, numerous clinical tooth wear indices have been developed, adapted and modified, as shown in *Table 1* (Bardsley 2008, O’Toole et al. 2018a). The wide range of indices complicates comparisons between different studies and investigations (Ganss and Lussi 2014). In recent years, the BEWE index has been established as a simple, validated instrument for basic dental care and has been used in several studies for wear control (Dixon et al. 2012, Marro et al. 2018). However, there are some disadvantages associated with clinical indices. For example, visual diagnosis of exposed dentin is very difficult. According to a study by Ganss et al. (2006), the accuracy of correlating visual decisions with histological findings was very low. Furthermore, as the conventional approach has been limited to the detection of wear lesions visible to the naked eye, the visible damage to the tooth structure may already result in pain and irreversible changes in tooth shape, function and cosmetics. Therefore, for a long time, clinical evaluation and monitoring of tooth wear was performed only by visual examination based on subjective indices. However, it has been proven that it is not possible to visually detect tooth wear at an early stage, particularly in enamel. There is a need for objective methods for early detection and differentiation of occlusal, proximal and cervical tooth wear in order to assess the progression and severity of tooth wear based on the different aetiologies and thus make the right prevention and treatment recommendations (Bartlett 2005, Loomans et al. 2017).

▪ **Table 1. Overview of the most popular clinical tooth wear indices**

<i>Index name</i>	<i>Description</i>	<i>Reference</i>
<i>Eccles index</i>	<i>Tooth structure loss is differentiated into three classes of lesions and assigned to the vestibular, oral and occlusal surfaces.</i>	<i>(Eccles 1979)</i>
<i>Tooth wear index (TWI)</i>	<i>Degree of wear damage to the teeth depending on age. In addition, the aetiology is taken into account (abrasion, erosion, attrition). The index differentiates between enamel and dentin loss.</i>	<i>(Smith and Knight 1984) Modified: (Millward et al. 1994)</i>
<i>Occlusal abrasion index</i>	<i>Grade 1</i> – Grounded facets; <i>Grade 2</i> – Levelling of cusps; <i>Grade 3</i> – Exposure of dentin; <i>Grade 4</i> – Exposure of secondary dentin; <i>Grade 5</i> – Pulp exposure.	<i>(Gängler 1995)</i>
<i>Lussi index</i> & <i>Visual Erosion Dental Examination (VEDE)</i>	<i>Examines erosion defects on the facial, occlusal and oral surfaces of tooth. VEDE has been used at the University of Oslo since 2005. It is a modification of Lussi’s tooth erosion index.</i>	<i>(Lussi 1996) (Mulic et al. 2010) (Margaritis et al. 2011)</i>
<i>Basic erosive wear examination (BEWE)</i>	<i>Considered a simple and standardised index for the clinical evaluation of erosions. For the evaluation, the dentition is divided into sextants and the vestibular, occlusal and palatal tooth surfaces are scored.</i>	<i>(Bartlett et al. 2008)</i>
<i>Exact tooth wear index</i>	<i>There are five severity levels for the classification of enamel wear lesions and six severity levels for the classification of dentin wear lesions.</i>	<i>(Fares et al. 2009)</i>

4 Material and Methods

4.1 Experimental design

The robot-simulated three-year toothbrushing cycle was performed for both manual toothbrushes in the ORMED Laboratory at the University of Witten-Herdecke. Replication of teeth and SEM evaluation were performed at the Centre for Electron Microscopy of University Hospital Jena. The flow chart (Fig. 6) visualises the work stages and their sequence in the methodology.

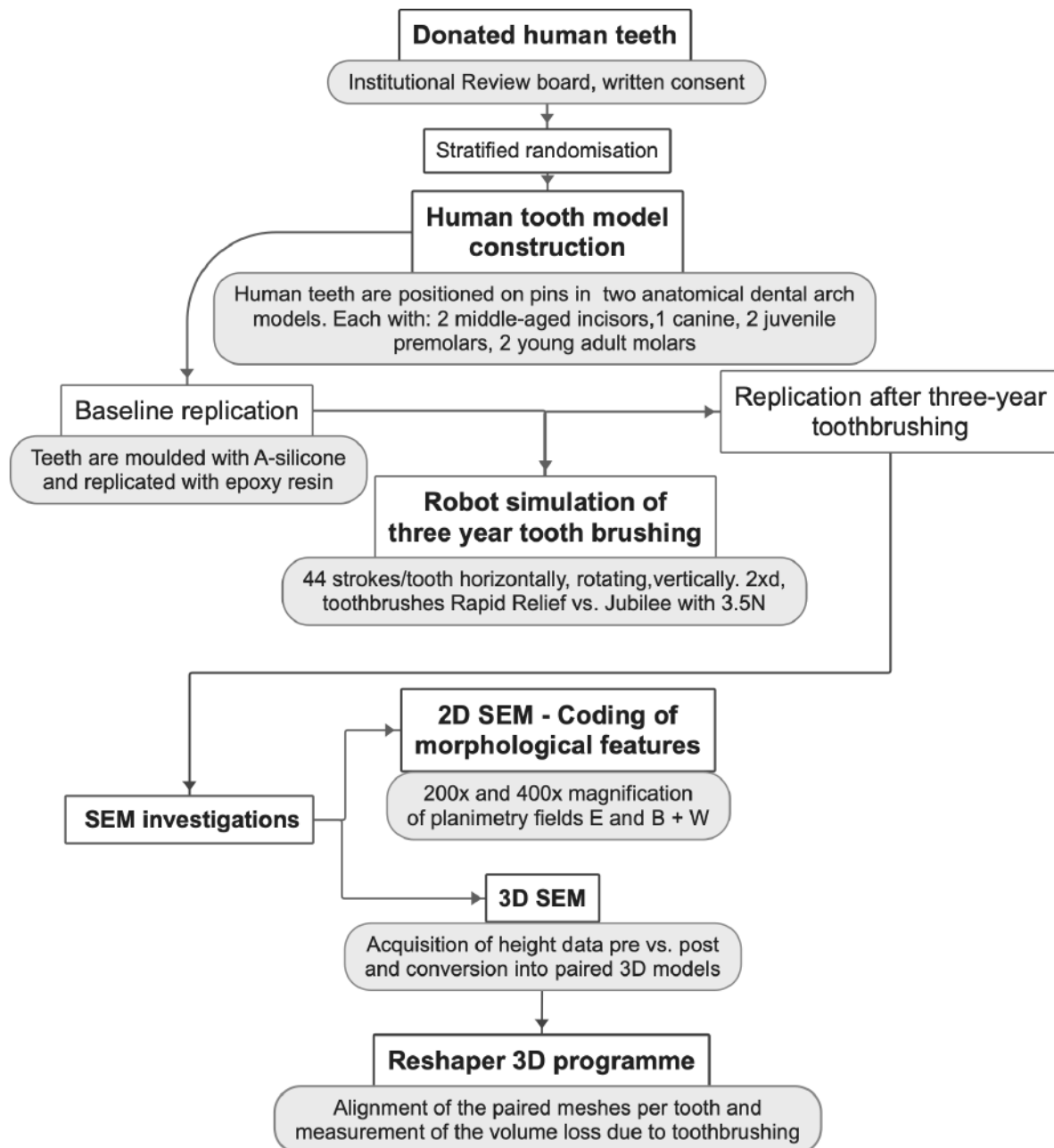


Figure 6: Experiment flow chart: The robot simulated three-year toothbrushing on 14 extracted human teeth in anatomical position, SEM-coding and 3D-SEM measurement of cervical volume loss after toothbrushing with two types of manual toothbrushes (flexible ball joint neck versus conventional rigid neck).

The project followed the principles of good clinical practice and, regarding the collection of dental donations, the Declaration of Helsinki. The study was submitted to the Ethics Committee of the University of Witten-Herdecke, and a positive vote was given on 3 May 2021. An amendment concerning extra-clinical video-based survey of toothbrushing strokes per time and toothbrushing habits was approved on 8 January 2022 (*application number: SR-67/2021*). The normative framework for the collection and use of extracted teeth in research and teaching followed Gross et al. (2015).

In addition to verbal information, patients were given written information. The tooth had to be extracted due to strict medical indications, and the donation was anonymous and voluntary. Small collection jars with 0.1% thymol solution were deposited in the dental collection offices (*Fig. 7*). After a successful collection phase, teeth were subjected to a professional dental cleaning with an ultrasonic device and prophylaxis cups. Finally, 1% NaOCl was applied to the cervical tooth area for 5 minutes. Teeth were then carefully brushed with a tapered manual toothbrush to remove remaining tissue remnants of the periodontium, which were in particular attached firmly at the juvenile premolars. The teeth were then rinsed under running water. Large carious defects were prepared and filled with bulk-fill composite to stabilise the teeth.



Figure 7: Two tooth collection jars with juvenile premolars in 0.1% thymol solution, which were extracted for orthodontic reasons. The jars were labelled as follows:

Patient age:

Extraction reason:

- PA Caries Endo Ortho

4.2 Human tooth model

For the validated robot arm to brush the teeth, it is necessary to position them in an anatomical position in the calibrated dental arch. For this purpose, the roots were cut off. The lower part of the tooth was hollowed out to approximately 0.5 mm. The teeth were attached to pins with *UNIFAST III* (*GC Corporation, Tokyo, Japan*). A silicone wall was used to check the correct position of the teeth in the dental arch (*Fig. 8*). The teeth were stored and moulded outside the model and reinserted for the subsequent toothbrushing cycles. *KaVo* artificial teeth were used for the 3rd molar and the canine in terminal position.



Figure 8: The tooth holder by *KaVo* is designed to simulate the physiological situation of a dentition (*eugnathia*) including the bony contour of the jaw. It has specially manufactured notches into which plastic teeth can be clicked. The silicone wall was used to ensure the position of the real teeth in the dental arch. Human teeth were polymerised on plastic pins and could thus be easily removed and repositioned from the model.

Each model included two incisors and one canine of middle-aged patients from 40 to 65 years of age that had to be extracted for periodontal reasons. These teeth have matured enamel and hypermineralised root dentin with 60–70% occluded tubules. Two juvenile premolars of 10–15-year-old

patients with presumably immature enamel were extracted for orthodontic reasons. The root cementum is thinly formed, and the dentin may show open tubules without peri- and intratubular mineralisation. In addition, two molars of young adults aged 18 to 35 years that had to be extracted for carious or surgical reasons were included. It can be assumed that these teeth have both aprismatic and prismatic enamel and hypermineralised root dentin with cementum residues. To enhance comparability, tooth pairs from a single patient (*same age*) were placed in separate models.

▪ **Final composition of human tooth model A (Fig. 9):**

Incisors and canines of patients aged 40-65 years.

Extracted for periodontitis reasons.

Age of patients:

Incisor 41: 55 yrs *Two anterior teeth*

Incisor 42: 40 yrs *served as reserve.*

Canine 43: 58 yrs

Two premolars of patients aged 10-15 years. **Two molars of patients aged 18-35 years.**

Extracted for orthodontic reasons. *Extracted for caries / endodontic reasons.*

Age of patients:

Premolar 44: 14 yrs **Molar 46: 36 yrs**

Premolar 45: 13 yrs **Molar 47: 19 yrs**



Figure 9: Human tooth model A – nine human teeth of different ages were aligned in anatomical position to be brushed with the **Rapid Relief** toothbrush.

▪ **Final composition of human tooth model B (Fig. 10):**

Incisors and canines of patients aged 40-65 years.

Extracted for periodontitis reasons.

Age of patients:

Incisor 41: 40 yrs *Two anterior teeth*

Incisor 42: 61 yrs *served as reserve.*

Canine 43: 58 yrs

Two premolars of patients aged 10-15 years. **Two molars of patients aged 18-35 years.**

Extracted for orthodontic reasons. *Extracted for caries / endodontic reasons.*

Age of patients:

Premolar 44: 14 yrs **Molar 46: 31 yrs**

Premolar 45: 13 yrs **Molar 47: 19 yrs**



Figure 10: Human tooth model B – nine human teeth of different ages were aligned in anatomical position to be brushed with the **Jubilee** toothbrush.

The trial set-up with intact human teeth was rarely chosen because most classical evaluation techniques require flattening and polishing of tooth specimens. A major advantage of this approach is the ability to investigate the impact of toothbrushing on unprocessed enamel, dentin and cementum simultaneously in a clinically relevant scenario.

4.3 Video observation

An additional video observation study was organised to determine the average number of tooth-brushing strokes per time and toothbrushing techniques of 50 volunteers. Subjects were recruited through social media. Interested participants received verbal and written information about the procedure and the purpose of the study. During the initial contact, a consent form was sent, and the inclusion and exclusion criteria were requested (Table 2). Participation was voluntary and could be withdrawn without giving reasons. The brushing speed and technique observed in the video were pseudonymised (by Art. 4 No. 5 DS-GVO) and included in the study by an encryption code (Table 3).

▪ **Table 2: Inclusion and exclusion criteria**

Inclusion criteria were:	Exclusion criteria were:
- Signed declaration of consent	- Fixed orthodontic appliances
- Age > 18 years old, European	- Mental or physical disabilities that could affect the performance of oral hygiene
- More than 20 teeth	- Removable dentures
- A video recording device	
- A manual toothbrush	

▪ **Table 3: Inclusion of subjects by an encryption code**

Subjects	Coding	Brushing speed (Double strokes/second)	Brushing technique (horizontal/rotating/vertical)	Questionnaire: (yes/no)	♂ ♀
01.	EEd5gd4t	3.6 Hz	rotating	yes	♀

The videos were edited so that only the mouth area could be seen, and after the study was completed, the videos were deleted. All subjects were instructed to brush their teeth with a manual toothbrush with dentifrice and videotape the procedure. Brushing should last for at least 30 seconds and should be done in front of a mirror for self-monitoring. Subjects were instructed to start with the buccal surfaces of the mandibular teeth on the right side, as the robot was programmed and validated for this region. Recorded videos were edited with iMovie, and brush strokes were counted at 25% slow mode speed. A video segment was selected in which brushing was continuous for at least 10 seconds, and strokes performed during that period were counted. The unit of measurement (hertz) is the SI unit for frequency and indicates the number of oscillations per second or also applies to the number of arbitrarily repeating processes per second. “Double stroke” means that a back-and-forth or circular movement is counted as one stroke (1 Hz). A total of 50 subjects (32 female and 18 male) aged 19–68 participated in the video observation study. The results are summarised in Table 4.

▪ **Table 4: Results of the video evaluation**

Brushing techniques:	20x rotating (40%) > 14x horizontal (29%) > 5x vertical (10%) & 11x mixed (22%) <i>Without mixed: 20x rotating (51%) > 14x horizontal (36%) > 5x vertical (13%)</i>
Brushing stroke frequency:	Rotating: 4.2 Hz Horizontal: 4.5Hz Vertical: 3.5 Hz Average brushing stroke frequency: 4.2 Hz

Schlueter et al. (2010) cited a sample size of 30 subjects as sufficient to capture typical oral hygiene habits. The data collected on the number of brush strokes mainly reflects the brushing behaviour of buccal surfaces. The registration of the average number of brush strokes per second was necessary for the extrapolation of the in vitro brush strokes performed by the robot to the clinical situation. This resulted in the following calculation:

$$\frac{\text{Total number of robot strokes}}{\text{Ø Human strokes per day and buccal tooth surface}} = \frac{44 \text{ strokes} \times (2 \times 30 \text{ days}) \times 36 \text{ months}}{2 \times 42 \text{ strokes}} = \frac{95,040}{84} = 1,131 \text{ days} = 3.09 \text{ years}$$

The robot performed 44 brushing strokes per tooth in one single brushing cycle, resulting in 31,680 brushing strokes per year and a total of 95,040 brushing strokes in the simulated three-year trial. (44 strokes per buccal tooth side per cycle result to 88 strokes/daily and results to following rounded strokes: ~600 strokes/week; ~2.600 strokes/month; ~7.800 strokes/12weeks; ~31.600 strokes/year; 95.000 strokes/three-years.)

4.4 Robot simulation

In vitro methods on human teeth have the advantage that they can shorten the investigation period. Furthermore, they offer the possibility to control all relevant aspects of toothbrushing.

4.4.1 Six-axis robot arm

The validated six-axis robot (FS02N, Kawasaki, Akashi, Hyogo, Japan) has a maximum movement speed of 3.8 mm/s. Its accuracy was specified as +/- 0.03 mm (Fig. 11). The robot was designed to simulate the toothbrushing movements of humans. For this purpose, parameters such as brushing force, brushing technique and brushing time were taken from clinical studies. Various holders of toothbrushes were available for the robot arm, depending on whether an examination was carried out with a manual toothbrush or an electric toothbrush. A touch panel was used to control the six-axis robot arm. A combined programme was selected in which three brushing techniques (horizontal, rotating, vertical) were alternately applied to the buccal surfaces of teeth. The parameters were documented in detail to ensure reproducibility, and a standard operating procedure was established for each step. The robot-assisted method enabled the relevant parameters of toothbrushing to be standardised. A list of critical parameters was based on recommendations of Parry et al. (2008) for good in vitro assessment in dental



Figure 11: The validated six-axis robot (FS02N, Kawasaki, Akashi, Hyogo, Japan) is holding the manual toothbrush "Jubilee Soft" with rigid neck and a flat trim.

abrasion studies (*Table 5*). These include the composition and abrasiveness of dentifrice, configuration and filament stiffness of the toothbrush (soft, medium, firm) and behavioural aspects, i.e., brushing technique, brushing force applied, brushing strokes per time and frequency of brushing. Individual differences in oral hygiene habits, as well as differences in the arrangement of teeth or composition of the saliva, could thus be excluded. Furthermore, by using an artificial oral cavity for wet brushing with dentifrice in combination with the standardised robot movements and brush force application, an optimised clinical simulation was ensured. A further advantage is the simultaneous examination of enamel, dentin and cementum on teeth in anatomical position. In addition to morphological characterisation, abrasion at the cervical area of the tooth was investigated by three years of robot-simulated toothbrushing with two different manual toothbrushes. This approach provided accurate reproducibility under clinical conditions.

▪ **Table 5: Robot parameters and combined artificial oral cavity**

1. Controlled brushing force	3.5 N
2. Defined brushing time	65 h per real human tooth model
3. Toothbrushing technique	2 x horizontal brushing (hb), 1 x rotating brushing (rb), 1 x vertical brushing (vb)
4. Controlled speed of brushing movement	2.6 Hz (hb); 1.7 Hz (rb), 1.5 Hz (vb)
5. Type of toothbrush	12x Rapid Relief Model A (<i>soft bristles</i>) 12x Jubilee Model B (<i>soft bristles</i>)
6. Defined dentifrice slurry	1:3 Sensodyne Extra Fresh / water pH 7.4; ~ 6500 ppm slurry particles
7. Maintaining homogeneity of slurry	Artificial oral cavity (AOC): Slurry pump and regular stirring. 14 ml/min - 7.5 rev/min
8. Renewing the slurry during brushing cycle	Change of slurry every 3 months (AOC 5h 15min)
9. AOC constant irrigation	Constant irrigation of real human teeth drop by drop
10. Expected measurable loss of tooth structures (<i>unknown</i>)	Three-year toothbrushing cycle performing a total of 95,040 buccal strokes per tooth
11. Control of room temperature	Room air conditioner 22°C
12. Straightforward, reproducible methodology	Updated SOP version (11/10/2022) (Standard operation procedure)

4.4.2 Toothbrush adjustment

The toothbrush was positioned and fixed in the horizontal and vertical plane with a holder adapted to the grip design and the corresponding locking screws. Correct positioning of the manual toothbrush was achieved by aligning the bristle field centrally and evenly on a crosshair alignment aid (Fig.12). Two tensiometer plates enabled force distribution over the whole brush head. For this purpose, a force of 1.75 Newton (N) was set on each of the tensiometer plates. A deviation of up to ± 0.025 N was tolerated as long as the total contact force was finally 3.5 N. The exact force setting had to be controlled and documented for each brushing cycle and assigned to the respective manual toothbrush. After setting the contact force, the robot arm was ready to execute the toothbrushing programme. A model carrier, which served as a fixed position for the six-axis robot, was used to ensure the reproducibility of the toothbrushing movements in each cycle.

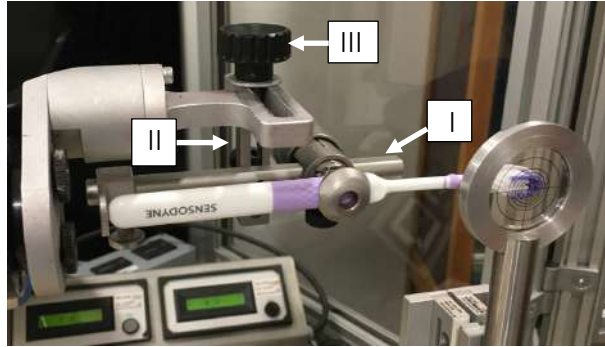


Figure 12: The holder is screwed onto the horizontal slide rail (I) and the manual toothbrush is fixed in the clamping jaws. The vertical rail (II) can be used to adjust the height, and the black knob and associated rail (III) can be used to adjust the manual toothbrush forwards or backwards towards the crosshair alignment field.

4.4.3 Artificial oral cavity

The artificial oral cavity (AOC) is used for permanently rinsing all human teeth to simulate a continuous toothbrushing process (Fig. 13). The commercial dentifrice *Sensodyne Extra Fresh* with medium abrasiveness was selected for suspension (ratio 1:3). For constant slurry irrigation, a peristaltic pump (*Concept 420smd*, SAIER, Gundelfingen, Germany) was installed and the pump speed was set to 7.50 rpm = 14 ml/min. The experimental set-up was designed to apply 1.0 g of toothpaste to teeth simulating a period of 2 minutes toothbrushing. Slurry was renewed every simulated three months together with the replacement of the manual toothbrush. A rubber dam was stretched under the human tooth model on the carrier to prevent slurry from accidentally dripping into the metal fixture with robot electronics underneath. Room temperature was kept at 22°C during the test to maintain a constant viscosity of the particle suspension. Table 6 presents an overview of the AOC data.

▪ Table 6: Overview of the artificial oral cavity

Slurry components:	4 x 75 ml Sensodyne Extra Fresh + 900 ml water	<i>In total: 1200 ml slurry ratio</i> 1:3 <i>PH: 7.4 with ~ 6500 ppm</i>
Peristaltic pump:	Type: <i>Concept 420smd</i> <i>SAIER, Gundelfingen, Germany</i> Speed: $V = 7.50$ U/min	For constant slurry irrigation and to simulate 1.0 g of dentifrice for brushing time of 2 minutes

4.4.4 Toothbrushing programme

The chosen programme was designed to simulate the toothbrushing routine of an average person during one session limited to the buccal surface of teeth. The programme combined three clinically most commonly observed toothbrushing techniques: 2 x horizontal brushing (17 s), 1 x rotating brushing (19 s) and 1 x vertical brushing (22 s). Since horizontal brushing was most commonly observed in vivo, it was performed twice.

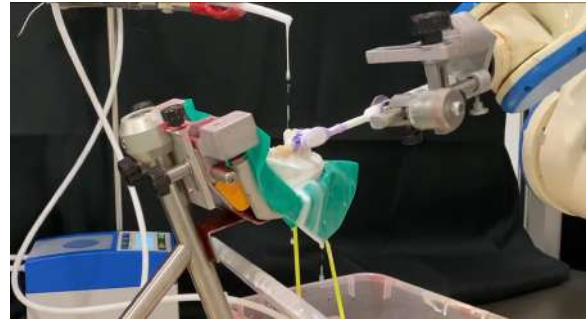



Figure 13: Robot arm in action including the AOC with a peristaltic pump for constant irrigation of the human teeth with slurry during the toothbrushing cycles.

4.4.5 Executed brushing strokes

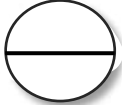
Since the robot arm brushed slower than an average human, the pure brushing time could not be transferred to the clinical situation. Therefore, the number of brush strokes performed by the robot per tooth was counted. A video was recorded to evaluate each toothbrushing programme. Since the brushing techniques (horizontal, rotating, vertical) were very different in their execution, the respective amplitude of motion was measured.

▪ Weighting of the different brushing strokes


Horizontal: For the horizontal brushing movement, as common in many studies, the reciprocating movement was counted as a “double” stroke.

<u>Stroke distance:</u>	<u>Motion frequency:</u>	<u>Number of strokes per cycle:</u>
$s = 3 \text{ cm}$ 	2.6 Hz – horizontal stroke (back-and-forth)	90 horizontal strokes

Rotation: During the rotating motion, the brush moved with one counted stroke over a complete circle of 360°.

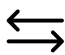


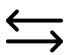


<u>Stroke distance:</u>	<u>Motion frequency:</u>	<u>Number of strokes per cycle:</u>
 $d = 1.8 \text{ cm}; U = \pi d = 5.6 \text{ cm}$	1.7 Hz – rotating stroke (360° circular movement)	33 rotating strokes

Vertical: The vertical brushing motion of the robot was much slower and only performed in one direction from the bottom to the top.

<u>Stroke distance:</u>	<u>Motion frequency:</u>	<u>Number of strokes per cycle:</u>
 $s = 1.8 \text{ cm}$ (60% of the horizontal 3 cm)	1.5 Hz – vertical stroke (from below to above)	11 vertical strokes (Due to the shorter distance covered, the counted number of vertical strokes is divided by three. $\frac{33}{3}$)

When weighing different strokes, only one-third of the vertical strokes were scored, because a vertical stroke is only in contact with the teeth in one direction. Therefore, based on the average movement speed (4.5 Hz), we calculated an average of 44–45 brushing strokes per buccal tooth surface. Based on our video observation, 42 strokes per tooth could be counted. Overall, the 44 strokes per tooth buccally performed by the robot corresponds with the clinical observations (*Table 7*). Accordingly, each tooth received 44 buccal brushing strokes per cycle. Consequently, the robot performed 31,680 strokes in one year and a total of 95,040 strokes per buccal tooth surface during the simulated three-year toothbrushing period. The data refers to persons aged 19-35 years without physical limitations, as the brushing speed can vary significantly in children and the elderly due to still missing or decreasing manual skills. This is generally a fact rarely considered when recommending a general toothbrushing time. Accordingly, the robot simulates the toothbrushing behaviour of a young adult to middle-aged person without physical limitations.

▪ **Table 7: Comparison robot vs human**


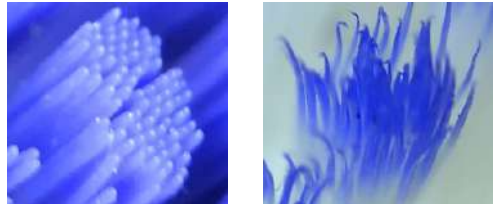
	Robot			Human		
Brushing technique:	 Horizontal	 360° rotation	 Vertical	 Horizontal	 360° rotation	 Vertical
Frequency:	2.6 Hz	1.7 Hz	1.5 Hz	4.5 Hz	4.2 Hz	3.5 Hz
Time (s):	34 Sec	19 sec	22 sec	17 sec*	24 sec*	6 sec*
Technique in %:	45%	25%	29%	36%*	51%*	13%*
				*Percentage of observed brushing techniques in the collective		
Stroke count:	90	33	11 ($\frac{1}{3}$)	76	100	21
Buccal mixed strokes per tooth: 10 sec in vivo*	<u>Counted per tooth:</u> 44 buccal strokes per robot brushing cycle			Mixed strokes in vivo for 10 sec: <i>Strokes proportionate to %*: 16 horizontal + 21 rotations + 5 verticals</i> 42 buccal strokes per tooth per brushing cycle in vivo		

***Total time:** Assuming 47 seconds for 11 teeth, based on the recommendation of Van der Weijden et al. (1993) that the optimal brushing time is 30 seconds for a quadrant (seven teeth).

A brushing cycle for 11 teeth lasted a total of 75 seconds and 30 seconds for repositioning. The robot only stopped after a complete simulated month had passed. Then the settings of the toothbrush could be checked before the next monthly programme was started. An average toothbrushing frequency of twice a day was assumed. Therefore, the cycle was repeated 60 times per month. A month of 30 days lasted 1 hour and 45 minutes. A three-year toothbrushing cycle lasted a total of 65 hours and consisted of 2,160 repetitions of one single toothbrushing cycle.

4.4.6 Overview of manual toothbrushes *Rapid Relief* and *Jubilee*

Table 8: Overview: Test toothbrush *Rapid Relief*

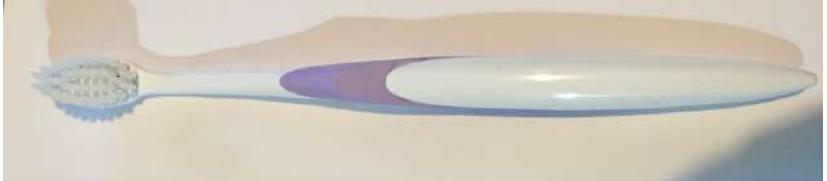

Toothbrush features			Test toothbrush: <i>Rapid Relief</i>		
Toothbrush in total	Length:	190 mm			
	Width:	14 mm			
Brush head	Length:	26 mm			
	Width:	12 mm			
Bristle board	Length:	24 mm	 <p style="display: flex; justify-content: space-around;"> Rounded filaments Tapered filaments </p>		
	Width:	11 mm			
Bristle tufts	Amount:	32 bristle tufts			
	Types:	Rounded & tapered			
Filaments	Amount:	Rounded:			80 filaments per tuft
		Tapered:	70 filaments per tuft		
	Length:	Rounded:	8.5–10 mm		
		Tapered:	12 mm		



Rapid Relief filaments

The last millimetre of filaments appears roughened under a stereomicroscope. The *Rapid Relief* toothbrush has an interdental trim and five tufts of tapered filaments on each side. The unique characteristic of the test toothbrush was a flexible brush neck due to a ball joint to reduce stiffness.

Table 9: Overview: Reference toothbrush *Jubilee*

Toothbrush Features			Reference toothbrush: <i>Jubilee</i>		
Toothbrush in total	Length:	191 mm			
	Width:	14 mm			
Brush head	Length:	25 mm			
	Width:	13 mm			
Bristle board	Length:	23 mm	 <p style="display: flex; justify-content: space-around;"> Rigid flat-trim brush head Rounded filaments </p>		
	Width:	12 mm			
Bristle tufts	Amount:	32 bristle tufts			
	Types:	Rounded			
Filaments	Amount:	80 filaments per tuft			
	Length:	10 mm			

The *Jubilee* toothbrush with soft, flat-trimmed bristles and a small brush head was developed for pain-sensitive teeth. Since the toothbrush had to be replaced every three months (simulated), a total of 12 of each manual toothbrush were needed for a three-year brushing cycle per human tooth model. A three-month toothbrushing cycle took a total of 5 hours and 15 minutes for the respective manual toothbrush.

4.5 Replication technique

The replication technique has been proven over decades for SEM examinations and enables even fragile areas of human teeth to be subjected to high-quality evaluation. At baseline and after the robot-simulated toothbrushing cycle, all buccal surfaces of teeth were moulded in two steps with an A-silicon (*Affinis Putty Soft and Affinis light body, Coltene Holding AG, Altstätten, Switzerland*). First the teeth were moulded with putty, then rinsed under lukewarm water and brushed with a rotating soft prophyl brush under double-distilled water. Before the precision impression, teeth were coated with *tubulicid blue* for 5 minutes and then dried with air. The low-viscosity silicone was applied to the buccal surface of teeth with an automatic mixing tip (*Fig. 14*).



Figure 14: The green *Affinis light body* impressions were cut into flat squares and labelled with the respective tooth identification number. After 30 minutes of set-up time, the impressions could be cast with epoxy resin. In advance, the impressions were checked with stereo microscope for oil and cleanliness.

The epoxy resin (*Easy-Mix N 5000 Epoxyd, Weicon, Münster, Germany*) is a two-component cartridge that is cured overnight in a heating cabinet at 37°C and can be easily applied to impressions.

Rising bubbles had to be carefully removed with a small ball tamper. This epoxy resin has a linear shrinkage of approximately 2% and therefore reproduces dimensions in a slightly reduced scale. Cured epoxy resin remains dimensionally stable. Replicas were carefully removed from the impressions the next day, glued onto small pen sample holders, and labelled on the bottom with the respective tooth identification number. Subsequently, epoxy resin replicas were sputtered with a 20 nm thin gold layer (Au); see *Fig. 15* (*Sputter CCU-010 HV, Zizers, Switzerland*).



Figure 15: A sputtered tooth replica glued on a pen holder for SEM investigation.

Sputtering was necessary to avoid electrical charging effects on the surface of the samples during the SEM investigations. The 28 sputtered replicas were stored in custom-designed, sealable plastic sample boxes. Immediately before SEM investigation, replicas had to be purified with air. For 3D volume measurements, replicas were later sputtered with an additional 80 nm gold layer to exclude incorrect measurements due to material delineations.

4.5.1 Positioning of replicas in the sample chamber

The characteristic morphological features were examined using the secondary electron mode. The scan resolution was set to 1024 x 768 pixels. Digitisation made it possible to save the rasterised images in a file. By optimising the specimen sizes, all seven replicas of one tooth model fit on the sample table (Fig. 16). This enabled the examination of a complete set of teeth in a single setting.

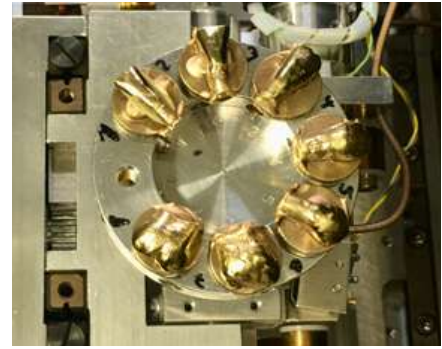


Figure 16: All seven replicas of a tooth model fit on the sample table, so that the morphological investigation could be performed in one setting.

4.5.2 Planimetry fields

The clinical validation of tooth surfaces is based on nine planimetric fields, buccally and lingually and more than three approximal fields x,y,z, mesially and distally (Gängler et al. 2013). The areas selected for SEM investigations were the middle of the smooth surfaces between the planimetry fields E and G + H and a cervical region of the teeth between fields B + W (Fig. 17).

Investigation areas (Fig. 17):

- I Abrasion patterns on the enamel at the equator line in the middle crossing point of the fields E and G + H.
- II Change of morphological features at the planimetry field B and the mirrored area at the root surface W.

Standard magnifications **100x and 400x**.

Respective regions were compared pre and post the three-year robot-simulated brushing cycle.

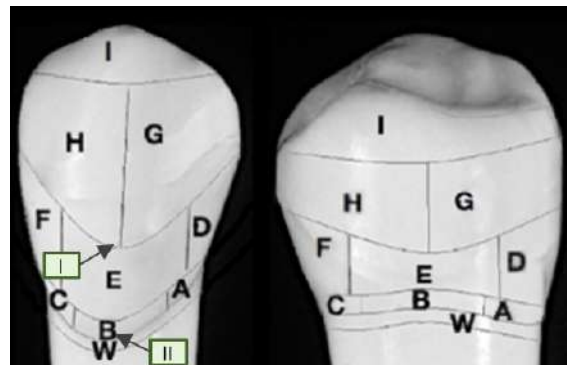


Figure 17: Crown and root fields for planimetry assessment. Arrows I and II point to the regions investigated under SEM.

The SEM has already been used for quantitative and qualitative analysis of teeth, with magnifications of 200 – 1000x proving useful for micromorphological surface studies (Dietz 2012, Montag et al. 2018).

Selected teeth for 3D SEM: **A42, A44, A46, B41, B42, B43, B45**

4.6 Scanning electron microscope (SEM)

The scanning electron microscopes (SEM) ability to produce high-resolution images makes it ideal for studying the surface structures and morphology of enamel and other dental hard tissues (Risnes et al. 2019). The outstanding feature of SEM is that this technique can provide a high depth of field while maintaining high magnification. At 1000x magnification and a resolution of 100 nm, the depth of field of the SEM is 100 μm , while the resolution of an optical microscope is only 0.2 μm . Imaging uneven, rough surfaces, such as the surface of teeth, requires a high depth of field. SEM was invented by Manfred von Ardenne in 1937 and has become increasingly popular since 1965.

The operating principle of the SEM device is shown in *Figure 18*.

The primary electron beam is focused on the sample surface utilising magnetic lenses and scans the sample in a linear pattern and is accelerated with voltages between 1 and 30 kV, leading to multiple interactions with the sample surfaces. For this study, secondary and backscattered electrons were the most important.

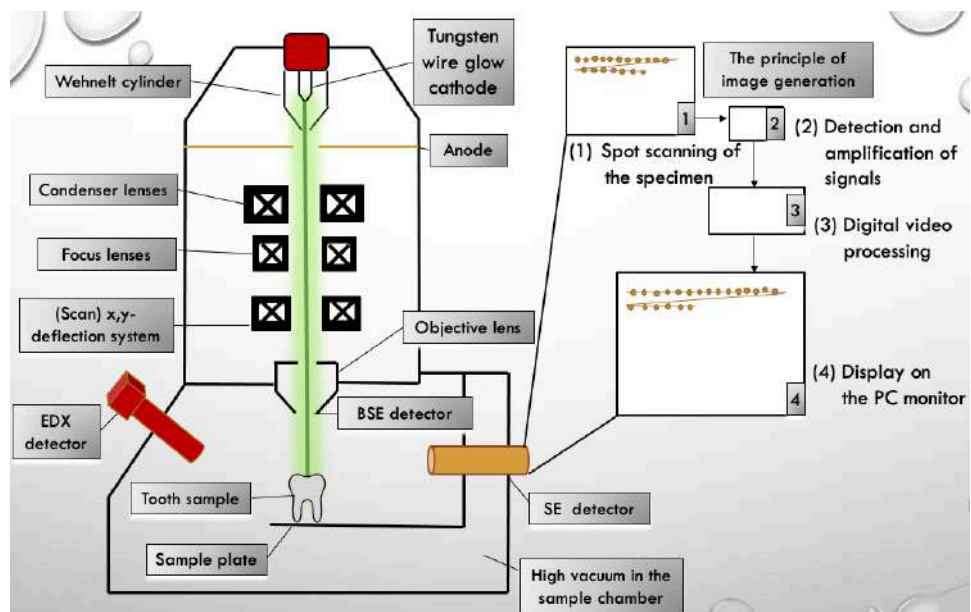


Figure 18: Device components of SEM (LEO-1450, Zeiss, Oberkochen, Germany). The high vacuum is generated by a turbomolecular pump directly connected to the sample chamber, which is equipped with a four-axis sample table (x-y-z tilting). The door can be opened by ventilating the chamber to place the samples on the table. The electron beam is generated by a glowing cathode consisting of a hairpin-shaped tungsten filament (\varnothing 100 μm). The number of electrons leaving the cathode is controlled by the Wehnelt cylinder (emission current). The different detectors are connected to a computer to convert the scanned electrical signals into digitised data.

Secondary electrons are very low in energy, while backscattered electrons have almost the same energy as primary electrons. Secondary electrons emerge directly at the sample surface (1–10 nm) and are very slow with an emergence energy of ≤ 50 eV, but map the sample's topography quite well and offer the best lateral point resolution. The detector is located on the side wall and is usually an *Everhart–Thornley detector*. With the secondary electron mode, images with magnifications of up to 2000x can be achieved. For the 3D measurements, it was necessary to switch to the high-energy backscattered electrons, which originate from the samples' deeper layers (1–2 μm).

4.7 3D-SEM

Backscattered electrons for the 3D evaluations were collected by an Si-conductor four-quadrant detector (*4Q-BSE detector*) directly arranged around the primary beam exit (*Fig. 19*). In contrast to the stereo method, which requires two consecutive images, each with different tilt angles, 3D reconstruction with the *4Q-BSE detector* can be performed in one single scan. 4Q-BSE mode enables reproducible measurements of height differences with an accuracy of up to 0.1 μm . A large working distance was chosen to achieve a good depth of field despite the low magnification. In addition, a small aperture diaphragm and a suitable beam current were set for a larger probe diameter to keep chromatic and spherical errors low. However, due to the size of cervical lesions, low magnification had to be used, so lower resolution was sufficient for this application.

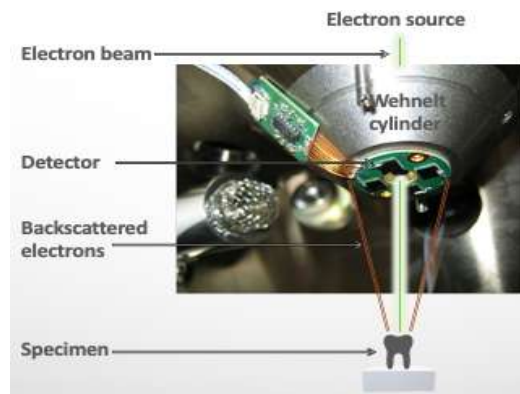


Figure 19: The 4-Quadrant-BSE detector (SEM 515, Philips, Eindhoven, Netherlands; software: Point electronic GmbH, Halle, Germany) enables the creation of a height profile of the sample surface by positioning four backscattered electron detectors directly around the exit aperture of the primary beam.

4.7.1 Calibration protocol

The distance between each of the *4Q-BSE detectors* is about 30 mm, which should be many times larger than the dimension of the scanning field on the sample. At this low magnification, however, the scan field becomes so large that the strongly varying angles of incidence depending on the detector simulate a curvature of the object. This imaging error was a disturbing factor for 3D profilometry, as it could lead to distortions in the volume measurement. But together with the paired tooth replicas (pre and post), a calibration block was used correct this imaging error.



Figure 20: Two replicas (pre and post) and the calibration block together on the sample table.

Tooth replicas (*Fig. 20*)

Placed together on the sample table adjusted to the same height (*Fig. 21*).

Calibration block

With a flat plane for spherical correction, points spaced one millimetre apart for length scaling, and a spherical notch for height determination.



Figure 21: The two replicas and the calibration body were adjusted to the same height.

Calibration of the geometric alignment required a thorough knowledge of the operation of SEM, including the correct positioning of the sample and set of the electron beam. Therefore, a uniform adjustment protocol for the correction of aberrations was implemented (*Appendix 9*).

Sample position and angle as well as electron beam setting could be read from the SEM display and are based on the standard calibration for magnification, scan rotation and working distance.

Magnification was set to allow the entire cervical lesion to be monitored. In the case of molars, two scans (mesial and distal) were required. The *DIPS 2.9 software* (Point electronic GmbH, Halle, Germany) was used to analyse and measure the topography. The notches on the specimen allowed the displayed magnification to be checked and corrected to the actual value (Fig. 22). A spherical correction was performed based on the plane of the calibration body. The topography image was used to display the curvature to adjust the value for the spherical correction until the surface was displayed flat.

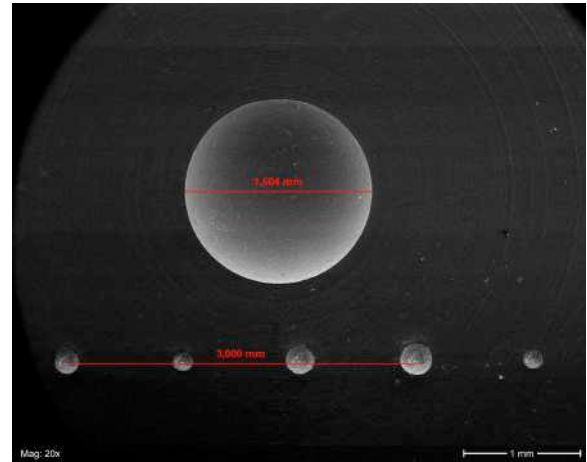


Figure 22: After calibration, the program DIPS shows the real distance between the small notches of 1 mm and the diameter of the large hemisphere of 1.6 mm.

Spherical aberration was corrected with DISS 5 (Point electronic GmbH, Halle, Germany). DISS (Digital Image Scanning System) is an active image acquisition and processing system for SEM (Fig. 23). The next step was to remeasure the depth of the groove with *MicroShape* (Point electronic GmbH).

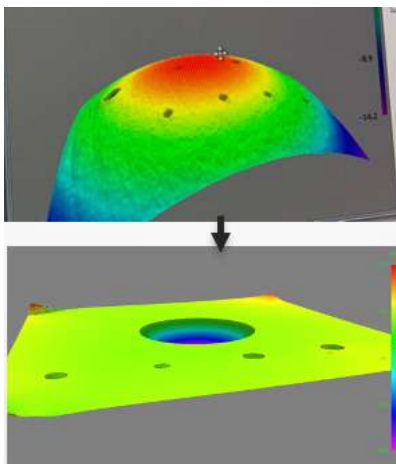


Figure 23: After the spherical correction with DISS 5 the surface that was previously considered falsely curved is displayed flat according to reality.

The actual depth of the spherical cavity of the reference body was previously calculated using the known geometry parameters to be $t = 328.7 \mu\text{m}$. After correcting the calibration, the software measured a groove depth of $t = 328.1 \mu\text{m}$. The number of pixels was set to 1024 x 1024, as the resulting resolution was sufficient for this purpose. This reduced the scanning speed to 1:01 min. At 2048 x 2048 pixels, a scan would take about 4 minutes. Images were digitally processed by DISS 5. Using the four images from different angles, an elevation data set was created in *.al3d format*. The height profile data sets created were saved under the name of the tooth examined pre and post and respective date of recording. The *MicroShape* software was then used to generate a 3D data set in *.ply format* through a mathematical transformation.

Alignment and measurement of the 3D models, pre and post, was subsequently performed using the *Leica Reshaper 3D* surface mapping software (Leica Geosystems, Heerbrugg, Switzerland).

4.7.2 Alignment and measurements

The abrasion volume was measured using the software *Leica's Reshaper 3D* (*Leica Geosystems, Heerbrugg, Switzerland*). This is a versatile software solution for processing all types of point clouds and meshes for a variety of applications. With integrated software tools, volumes, distances and angles could be calculated and 3D comparisons could be made between the paired (pre and post) tooth models. A coloured surface model can also be created to visually illustrate the measurement result. A different data set had to be created to calculate the resulting volume of cervical lesions. For this purpose, the pre-data network was aligned with the post-data network. Either the software calculated the least squares correlation related to the whole model, or the user sets several reference points beforehand for the alignment. Due to substantial surface changes caused by the brushing cycle, alignment via reference points performed better. For this purpose, the user set a number of alignment points on both paired models, and based on these points the models were calculated in superposition (*Fig. 24*). Measuring the entire tooth, however, resulted in inaccuracies due to the optical distortions of the scans in the marginal areas. Therefore, the cervical areas were outlined with a manual polyline to reduce possible distortion of the margins (*Fig. 25*).

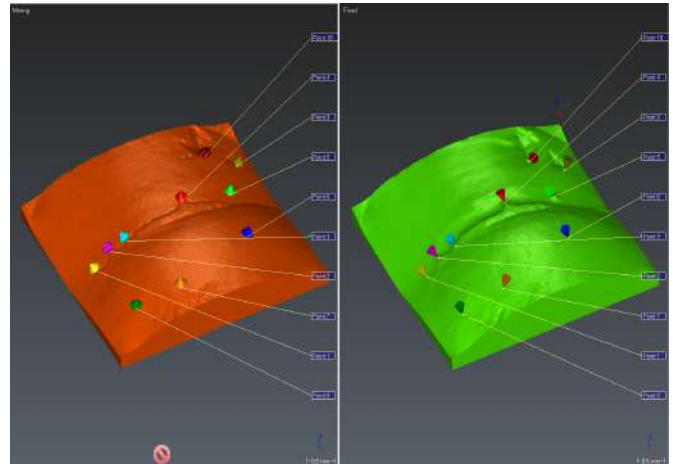


Figure 24: With the point alignment tool, distinctive points on both pairs of teeth (pre and post) can be selected and then aligned by the software to calculate the volume difference.

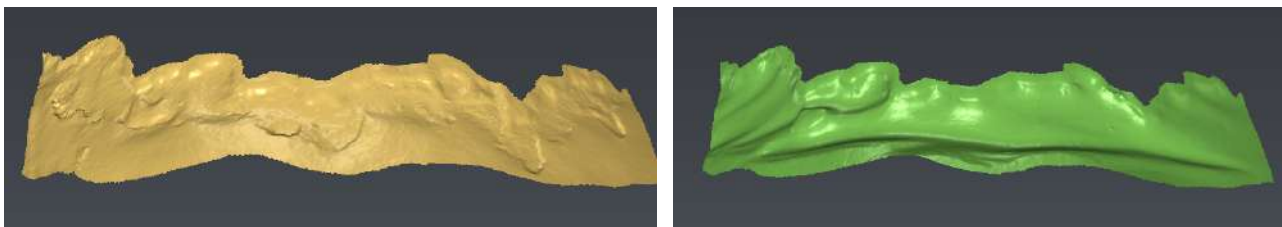


Figure 25: The cervical lesions of tooth A42 were cut out with a polyline. The pre-data mesh was shown in yellow and the post-data mesh in green. The models are superimposed to calculate the volume loss.

To adjust the inclination angles of the models, a freehand readjustment was necessary since a deviating inclination could lead to considerable differences in the volume calculation. The height profile and surface levelness were highlighted in colour after alignment. A partially calculated “*theoretical application volume*” represented the method’s measurement inaccuracy and should thus be as low as possible. Finally, *Reshaper 3D* was used to calculate the area of the abrasive cervical lesion in mm^2 and the volume difference between the data meshes of teeth in mm^3 . The abrasion volume is given in cubic millimetres as well as nanolitres (nl), the latter for better size comparison with dental tools or materials.

4.7.3 Visualisation of abrasion volume

Since the human mind has difficulties imagining the extent of volumes in pure terms of cubic metres, a dental comparison from daily practice will be used to visualise the size of the abrasion volume. This procedure is standard in physics and the field of life sciences.

Visualisation with a G30 endo irrigation canula:



G30

Canula diameter: 0.3 mm

Estimated inner diameter: 0.15 mm

Radius: ~ 0.08 mm

Cylinder volume: $\pi \cdot r^2 \cdot h = \pi \cdot 0.08 \text{ mm}^2 \cdot 1 \text{ mm} = 0.02 \text{ mm}^3 = 20 \text{ nl}$

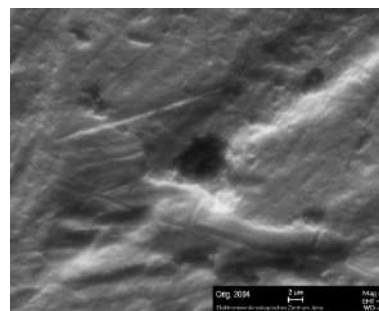
Consequently, **1 mm** of the endo irrigation canula has a **capacity of 20 nl**.

Transcendent

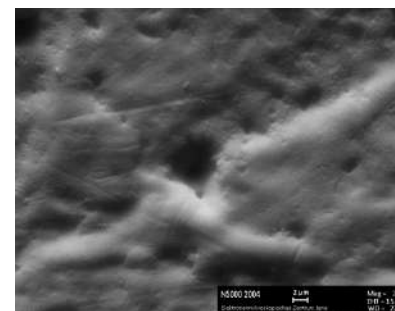
For an abrasion lesion of 60 nanolitres, 3 mm of the cannula would have to be filled with irrigation solution, equivalent to about one drop of irrigation solution on a glass plate.

4.8 Accuracy verification

To check the accuracy of the materials used, a 1-cent piece was moulded with the A-silicon (*Affinis light body*, Coltene Holding AG, Altstätten, Switzerland) and was also replicated with the epoxy resin (*Easy-Mix N 5000 Epoxyd*, Weicon, Münster, Germany). Figure 26 shows comparison of the original cent and the replicated cent.



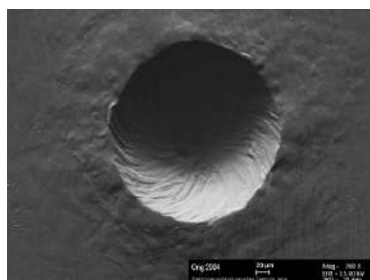
Original cent



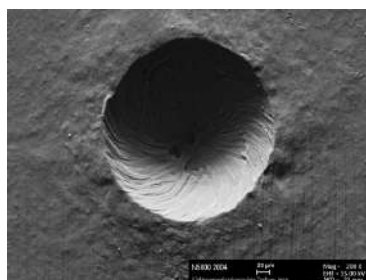
Replication of 1 cent

Figure 26: At 2000x magnification of the globe region (British Isles) on the front of a 1-cent piece, detail reproduction was satisfactory and far better than with all the other materials tested.

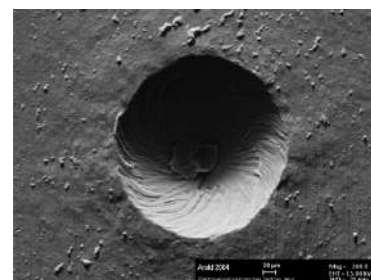
Also, the spherical cavity in the reference body was imprinted and replicated to evaluate the replication technique and measurement accuracy (Fig. 27). Incorporating an epoxy resin cartridge system considerably simplified the replication process compared to the classic *EPON 812* method.



Original reference body



Affinis and N5000



Affinis and EPON 812 equivalent

Figure 27: Replication of the reference body. While silicone particles stuck to the surface of EPON 812 equivalent replica, replication with two-component cartridge system epoxy resin (*Easy-Mix N 5000* by Weicon) turned out successful. Therefore, EPON 812 was excluded from standard operating procedures for this study.

5 Results

5.1 Morphological feature coding

In order to quantify cervical wear, a new system was developed to code morphological features that can be significantly altered by tooth brushing.

▪ **Table 10: Coding of abrasion patterns**

Abbr.	Feature	Code	Description
FAM	Functional abrasion marks	FAM 0	Few, shallow marks
		FAM 1	Some oriented marks
		FAM 2	Deeper criss-cross marks
		FAM 3	Many deep criss-cross marks
AP	Appearance perikymata	AP 0	Anatomical perikymata
		AP 1	Rounded perikymata
		AP 2	Shallow perikymata
		AP 3	No perikymata
EPE	Exposed prismatic enamel	EPE 0	No exposed prismatic enamel
		EPE 1	Some separated areas (< 20% of tooth area)
		EPE 2	Fluctuating areas (20–40% of tooth area)
		EPE 3	Extended areas (> 40% of tooth area)
EI	Enamel infractions	EI 0	No infractions
		EI 1	Vertical closed infractions
		EI 2	Gaping vertical infractions
		EI 3	Horizontal and inclined gaping infractions
ODT	Open dentin tubules	ODT 0	No open dentin tubules
		ODT 1	Few open dentin tubules
		ODT 2	Clustered open dentin tubules
		ODT 3	Uniformly distributed open dentin tubules
DC	Dental calculus	DC 0	No calculus
		DC 1	Few calculus remnants (< 30% of tooth area)
		DC 2	Some calculus islands (30–60% of tooth area)
		DC 3	Heavy calculus formation (> 60% of tooth area)
PF	Peninsula formation	PF 0	Straight CEJ
		PF 1	Slightly undulating CEJ
		PF 2	Undulating CEJ with peninsulas
		PF 3	Undulating CEJ with peninsulas and enamel islands
CEJ types	Cemento-enamel junction	Type 1	Cementum overlaps enamel
		Type 2	Edge-to-edge contact of cementum and enamel
		Type 3	Gap between cementum and enamel

Abrasion patterns represent the complex changes that occur over a lifetime and are individually more pronounced in older teeth. The following scanning electron microscope images illustrate the different abrasion patterns with image coding panels of the defined wear stages from 0 to 3.

5.1.1 Functional abrasion marks (FAM)

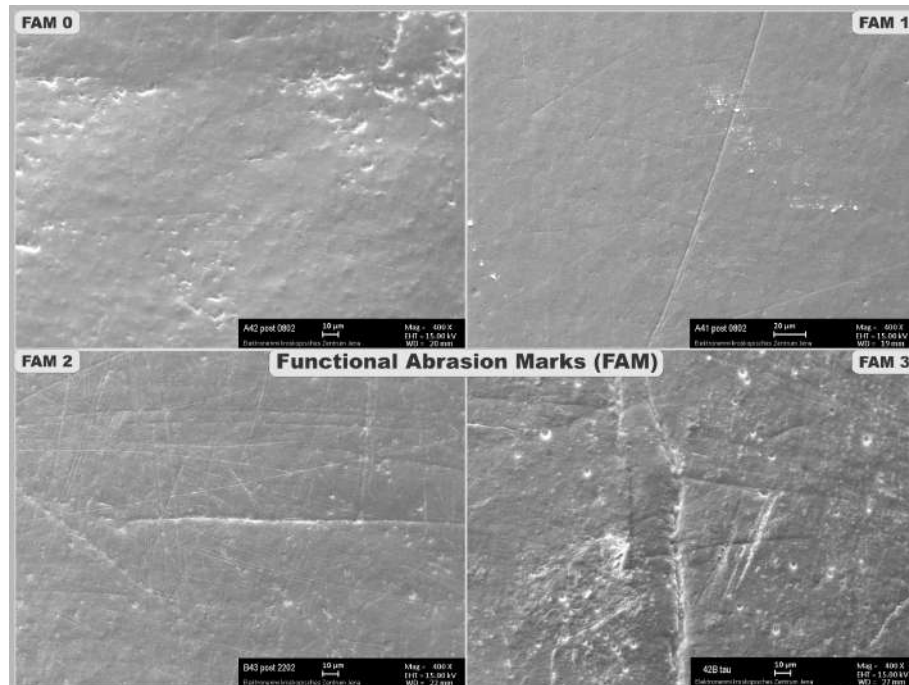


Figure 28: Functional abrasion marks (FAM) coding 0–3, SEM magnification 400x. FAM 0: Few, shallow marks; **FAM 1:** Some oriented marks; **FAM2:** Deeper criss-cross marks; **FAM 3:** Many deep criss-cross marks.

5.1.2 Appearance perikymata (AP)

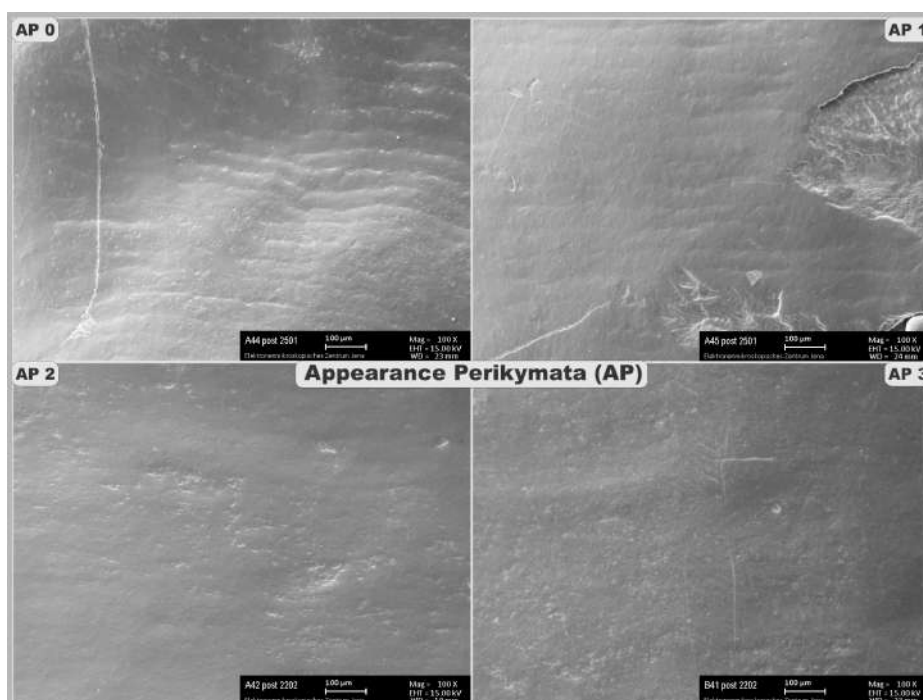


Figure 29: Appearance perikymata (AP) coding 0–3, SEM magnification 100x. AP 0: Anatomical perikymata; **AP 1:** Rounded perikymata; **AP 2:** Shallow perikymata; **AP 3:** No perikymata.

5.1.3 Exposed prismatic enamel (EPE)

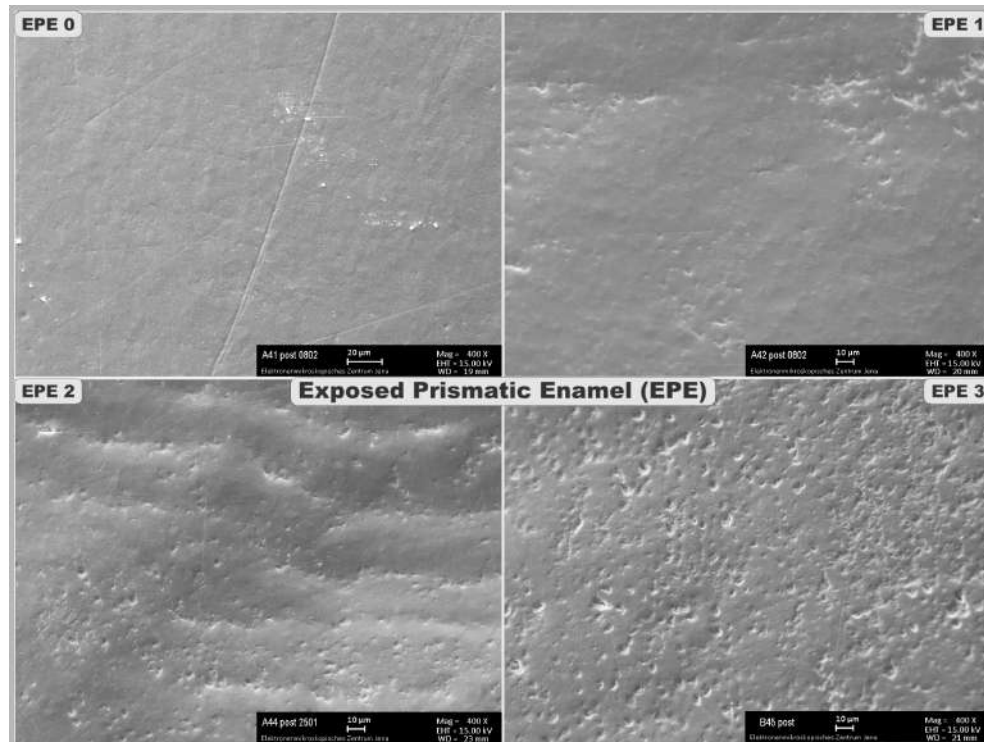


Figure 30: Exposed prismatic enamel (EPE) coding 0–3, SEM magnification 400x. **EPE 0**: No exposed prismatic enamel; **EPE 1**: Some separated areas (< 20% of tooth area); **EPE 2**: Fluctuating areas (20–40% of tooth area); **EPE 3**: Extended areas (> 40% of tooth area).

5.1.4 Enamel infractions (EI)

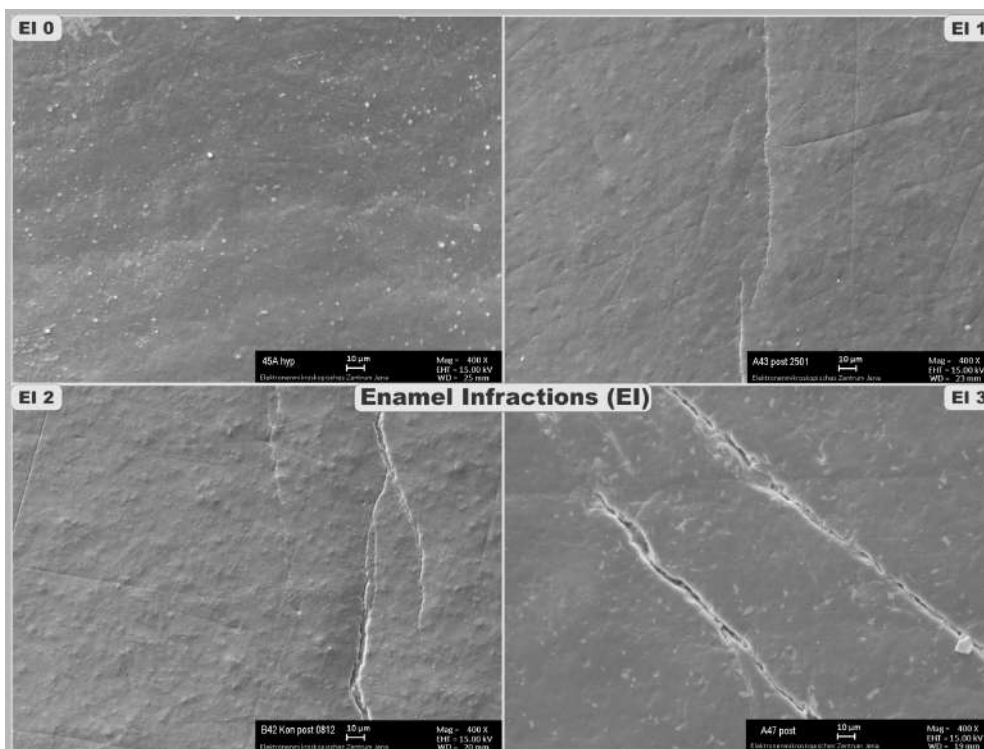


Figure 31: Enamel infractions (EI) coding 0–3, SEM magnification 400x. **EI 0**: No infractions; **EI 1**: Vertical closed infractions; **EI 2**: Gaping vertical infractions; **EI 3**: Horizontal and inclined gaping infractions.

5.1.5 Open dentin tubules (ODT)

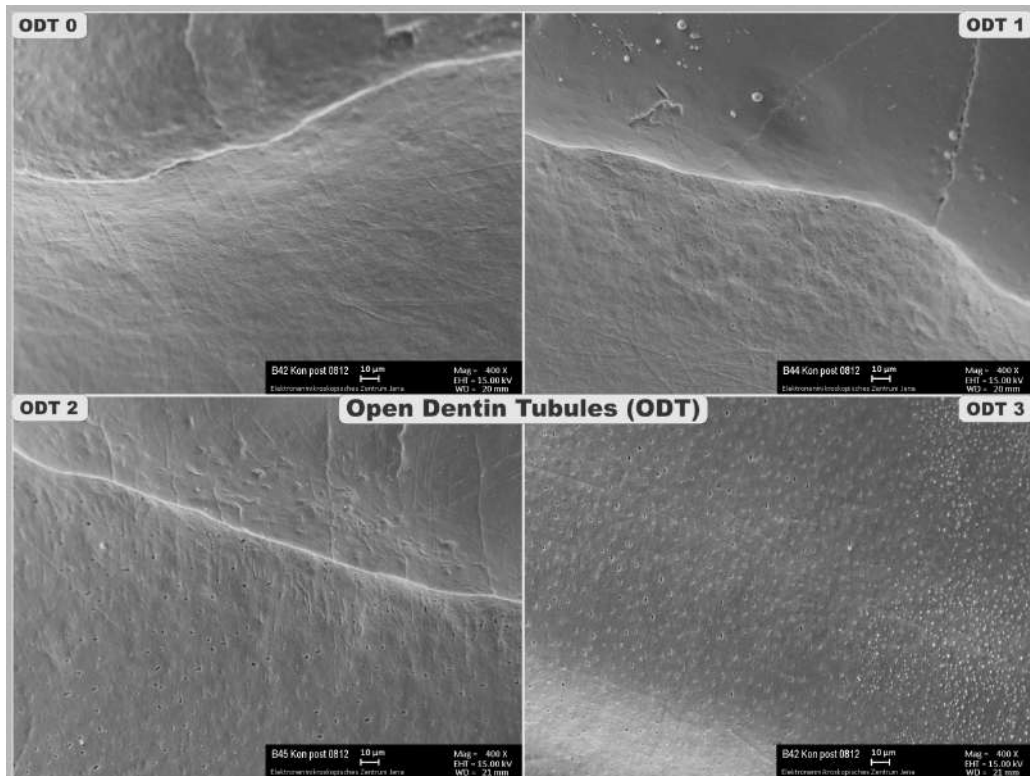


Figure 32: Open dentin tubules (ODT) coding 0–3, SEM magnification 400x. ODT 0: No open dentin tubules; ODT 1: Few open dentin tubules; ODT 2: Clustered open dentin tubules; ODT 3: Uniformly distributed open dentin tubules.

5.1.6 Dental calculus (DC)

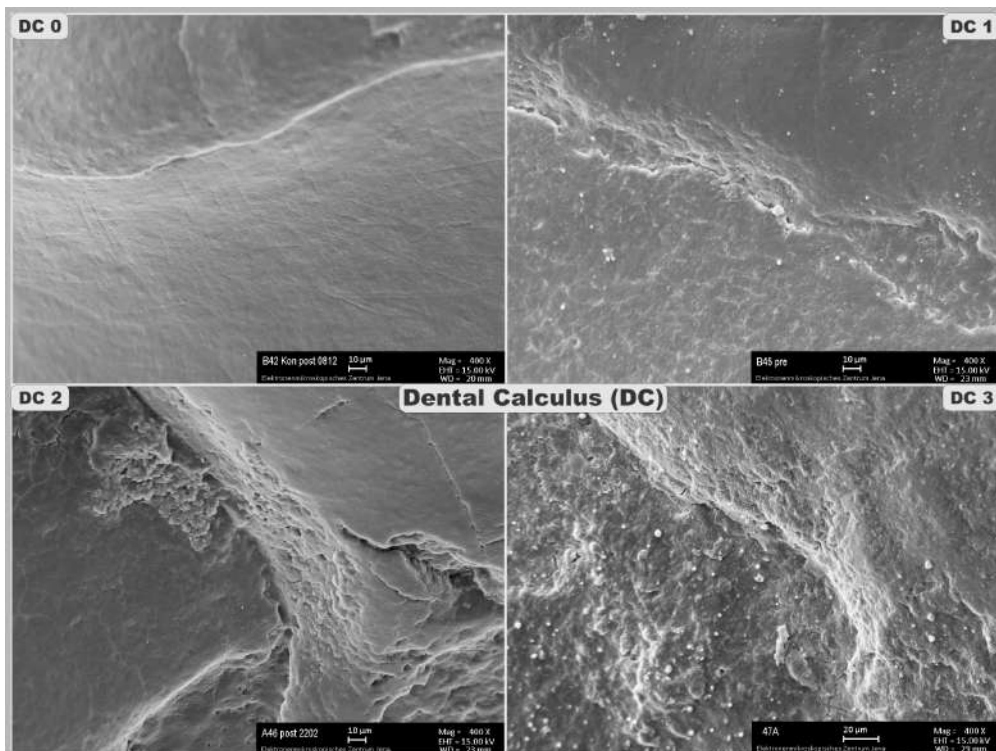


Figure 33: Dental calculus (DC) coding 0–3, SEM magnification 400x. DC 0: No calculus; DC 1: Few calculus remnants (< 30% of tooth area); DC 2: Some calculus islands (30–60% of tooth area); DC 3: Heavy calculus formation (> 60% of tooth area).

5.1.7 Peninsula formation (PF)

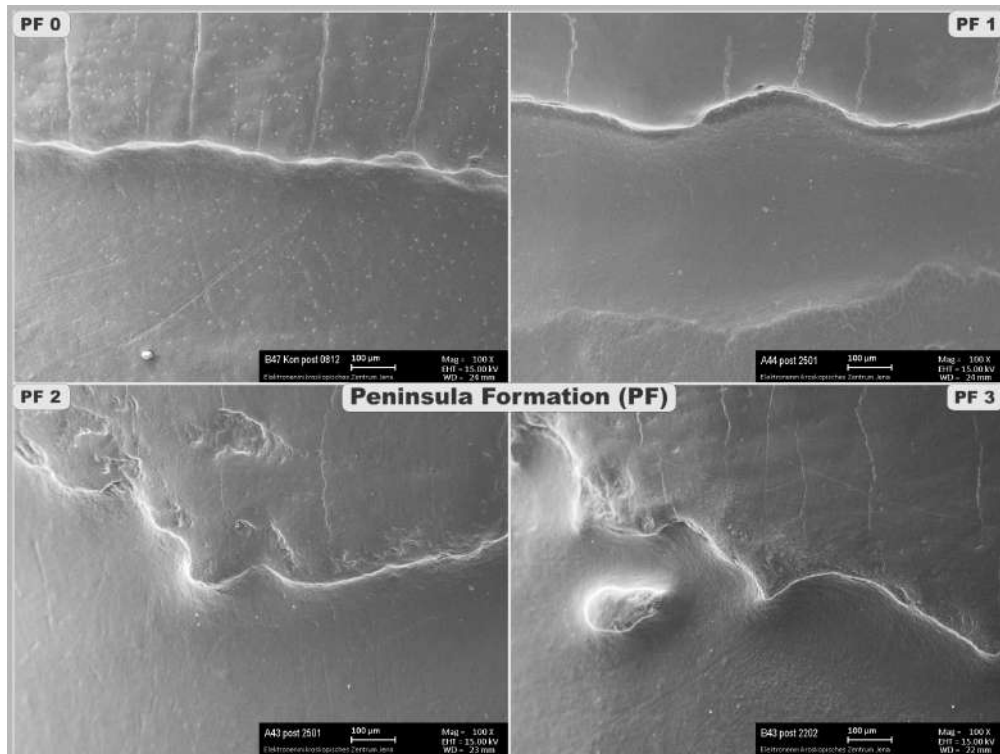


Figure 34: Peninsula formation (PF) coding 0–3, SEM magnification 100x. PF 0: Straight cemento-enamel junction (CEJ); PF 1: Slightly undulating CEJ; PF 2: Undulating CEJ with peninsulas; PF 3: Undulating CEJ with peninsulas and enamel islands.

5.1.8 Cemento-enamel junction types

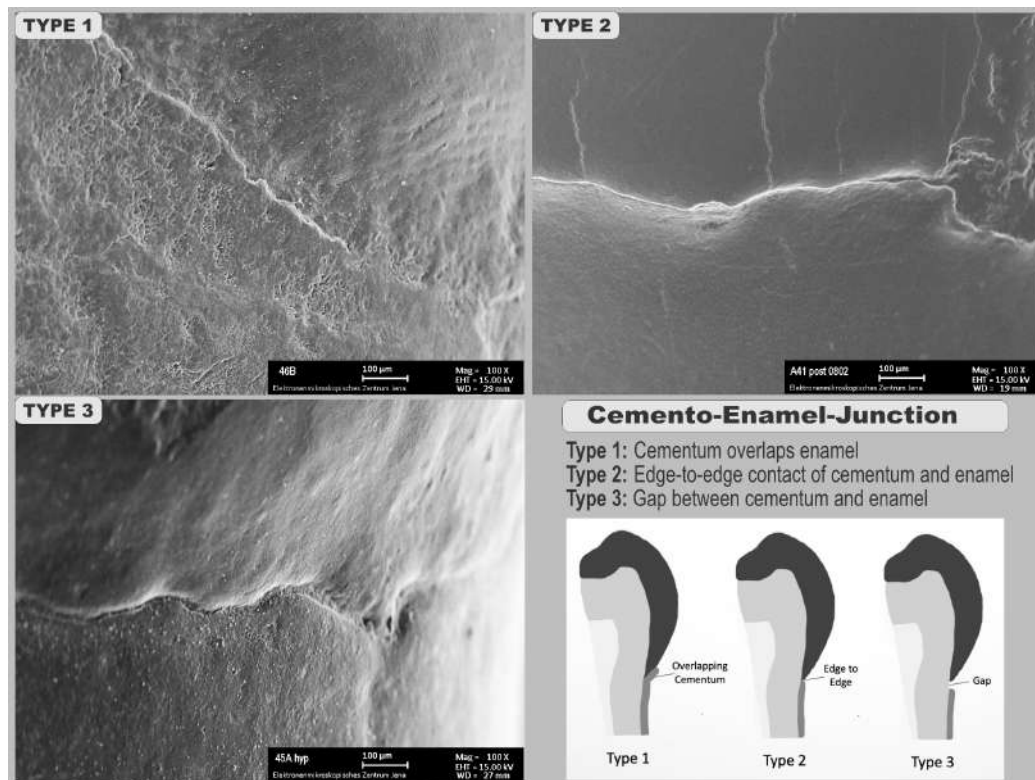


Figure 35: Cemento-enamel junction (CEJ) types 1–3, SEM magnification 100x. Type 1: Cementum overlaps enamel; Type 2: Edge-to-edge contact of cementum and enamel; Type 3: Gap between cementum and enamel.

5.2 Combined wear feature images

5.2.1 Incisor A41 – *Rapid Relief* (flexible neck)

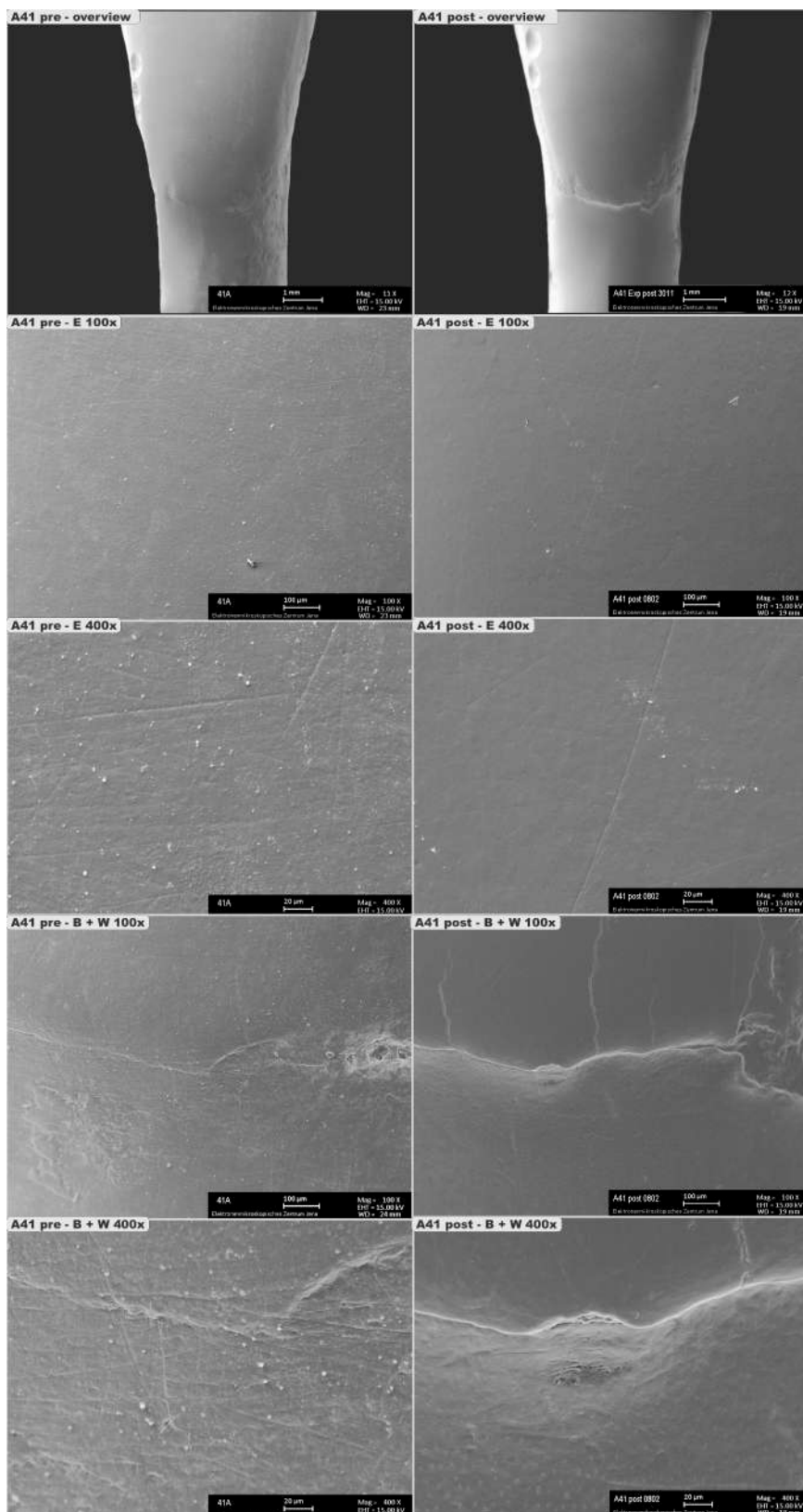


Figure 36: Incisor A41 – combined wear feature image for pre and post comparison. Extraction for periodontal reasons. Age of patient: **55 years**. Coding of morphological features: [Section 5.5.1](#).

Overview (Mag: 12x)

Due to the advanced age of the tooth donor (55 years), it is no longer possible to recognise perikymata. Vertical enamel infractions occur at the cemento-enamel junction. The root surface initially has a rough texture, which is smoothed by tooth brushing.

Planimetry field E: (100x/400x)

The enamel surface above the tooth equator is 100% prismless. There are no infractions in this tooth section. The perikymata are flattened. Many horizontal and oblique abrasion marks can be seen. Afterwards, the enamel surface looks smooth, and the abrasion marks have been reduced. The smear layer has been removed, and only isolated white grains remain.

Planimetry field B+W: (100x/400x)

Several vertical enamel infractions extend through to the cemento-enamel junction (CEJ). Afterwards, the enamel and cementum surfaces are cleaned and polished. Calculus residues have entirely disappeared. The corrugated cervical enamel margin showed some jagged protrusions at baseline, which were afterwards smoothed out. A moon-shaped enamel breakout is visible at the junction, with exposed dentin underneath on the root surface. Edge-to-edge contact of enamel and cementum (CEJ Type 2).

5.2.2 Incisor A42 – Rapid Relief (flexible neck)

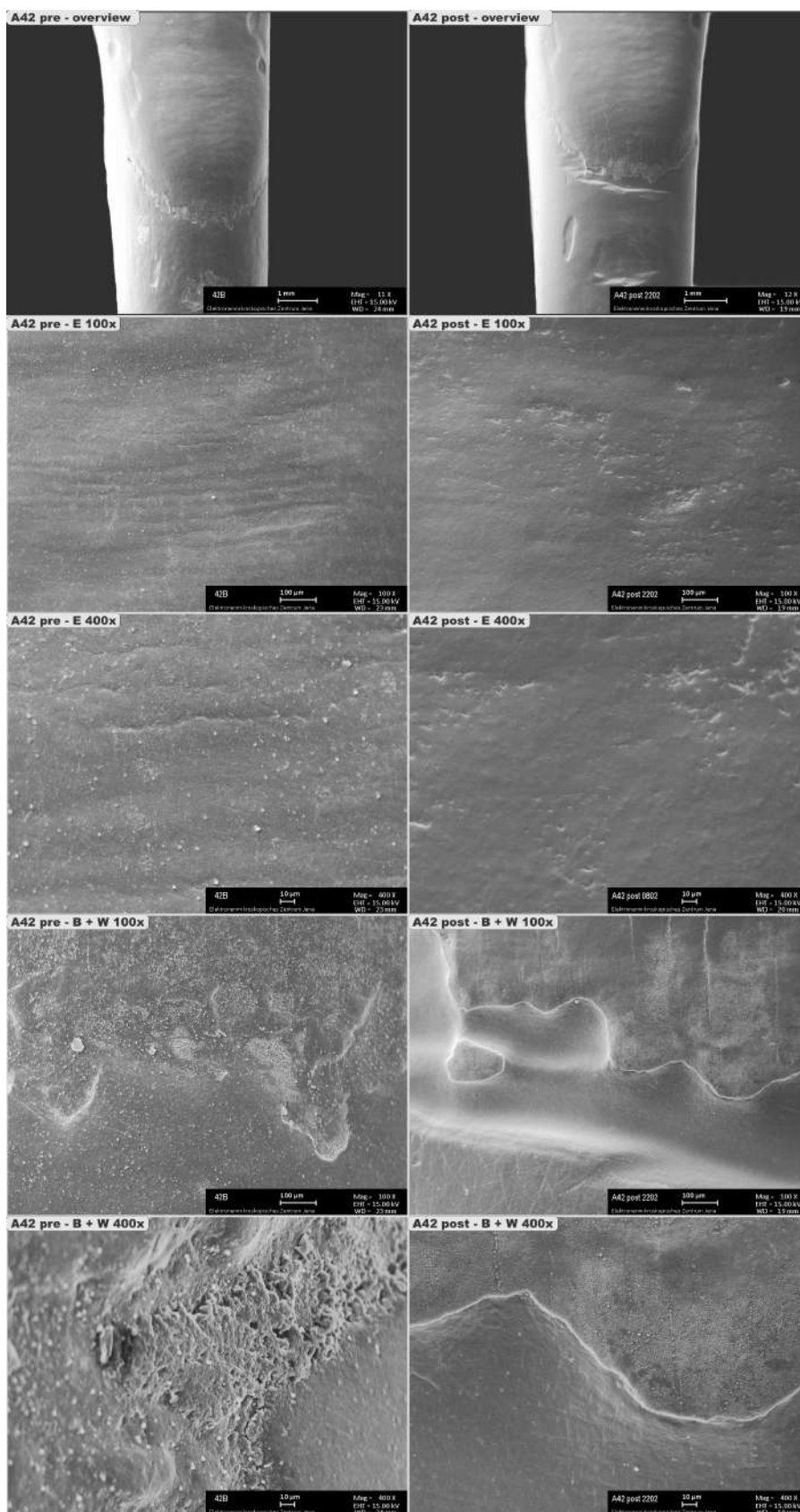


Figure 37: Incisor A42 – combined wear feature image for pre and post comparison. Extraction for periodontal reasons. Age of patient: **40 years**. Coding of morphological features: [Section 5.5.1](#). Volume measurements: [Section 5.4.1](#).

Overview (Mag: 12x)

On the root surface, breakouts caused by the extraction, which were subsequently polished smooth, can be seen. Subtle perikymata are discernible. Several vertical eruptions are visible in the lower third of the tooth crown.

Planimetry field E: (100x/400x)

Slight abrasion marks and minor pits are observable. Perikymata and the enamel surface are leveled and cleansed following the brushing cycle. The infractions do not surpass the dental equator. Residues of a smear layer have dissipated. Subsequently, prismatic enamel was partially exposed (in a ratio of 9:1).

Planimetry field B+W: (100x/400x)

At the baseline, massive calculus had accumulated at the cemento-enamel junction. Removal by toothbrushing resulted in unmasking several criss-cross marks on the root surface. At the baseline, rough, jagged enamel peninsulas extended onto the root surface, which was rounded off afterwards. In addition, an enamel peninsula appeared. A modest cervical lesion formed due to brush abrasion. Edge-to-edge contact of enamel and cementum (CEJ Type 2).

5.2.3 Canine A43 – Rapid Relief (flexible neck)

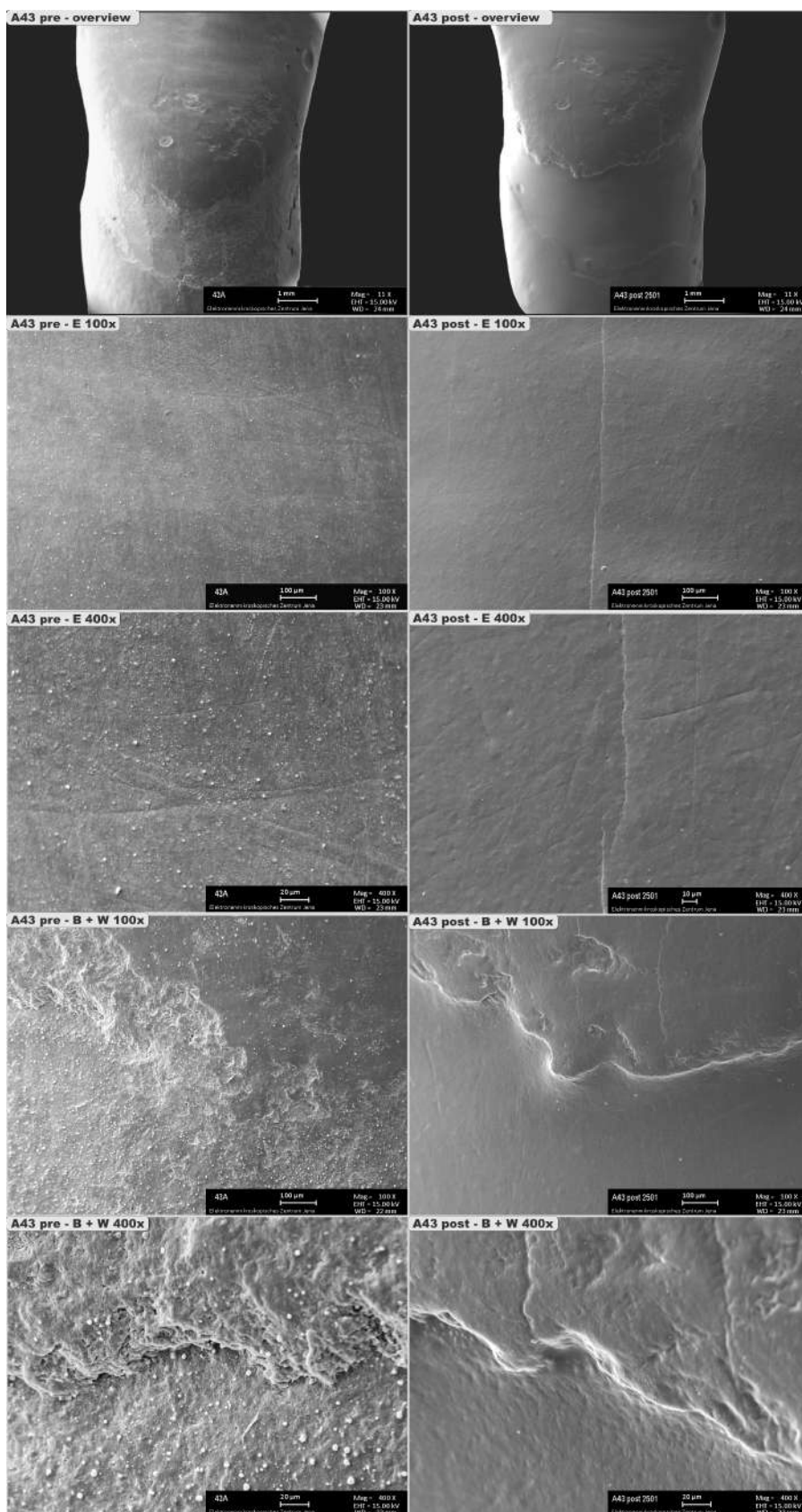


Figure 38: Canine A43 – combined wear feature image for pre and post comparison. Extraction for periodontal reasons. Age of patient: **58 years**. Coding of morphological features: [Section 5.5.1](#).

Overview (Mag: 12x)

Perikymata are worn down. Some vertical enamel infractions in the lower third of the tooth crown. At baseline, the root surface was very roughened, but the texture was smoothed after toothbrushing.

Planimetry field E: (100x/400x)

Removal of the smear layer revealed several criss-cross abrasion marks. Due to the age of the tooth donor (58yrs), the perikymata are no longer recognisable. A vertical enamel infraction crosses the centre of the image. The enamel surface appears 100% prismless.

Planimetry field B+W: (100x/400x)

At baseline, the cervical area of the tooth was covered with massive calculus deposits and roughened. By toothbrushing, the enamel and cementum surfaces were cleaned of all deposits and polished smooth. This revealed masked vertical enamel infractions and enamel peninsulas. The cervical enamel margin became rounded. Edge-to-edge contact of enamel and cementum (CEJ type 2).

5.2.4 Premolar A44 – Rapid Relief (flexible neck)

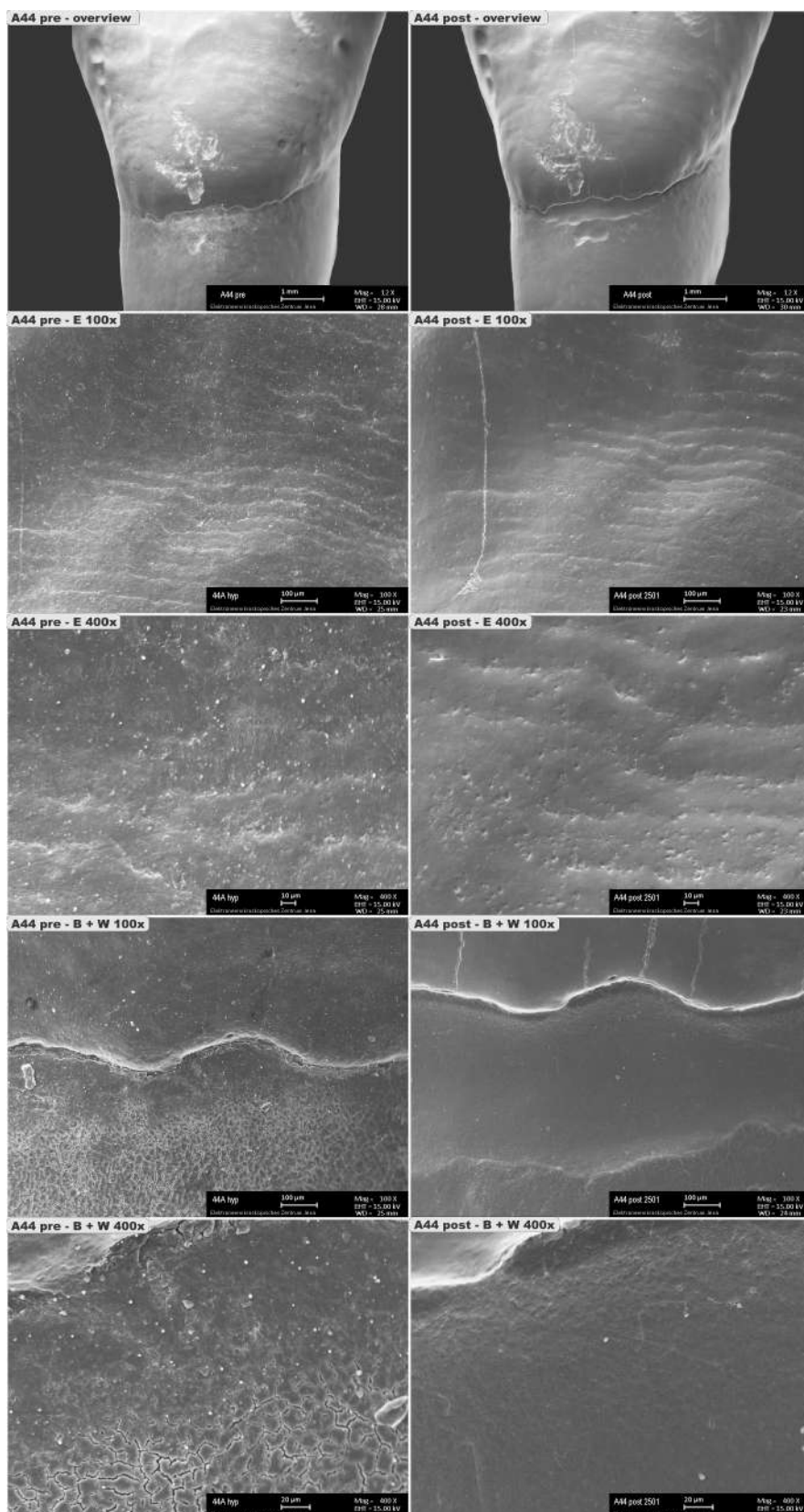


Figure 39: Premolar A44 – combined wear feature image for pre and post comparison. Extraction for orthodontic reasons. Age of patient: **14 years**. Coding of morphological features: [Section 5.5.1](#). Volume measurements: [Section 5.4.2](#).

Overview (Mag: 12x)

Several enamel protrusions appeared above the equator of the tooth. In the lower third of the crown, the enamel has been damaged by the extraction. After brushing, the tooth surface was smoothed. The enamel protrusions and perikymata have remained unchanged.

Planimetry field E: (100x/400x)

Disoriented abrasion marks are only very slightly visible. The smear layer was removed entirely. Several pits were exposed on the enamel surface. The prismatic parts have visibly enlarged due to abrasion (ratio: 8:2). The vertical enamel infraction on the left side has widened.

Planimetry field B+W: (100x/400x)

Several short enamel infractions run perpendicular to the enamel-cementum junction. The surface of the cementum and enamel has been thoroughly cleaned of smear layer and calculus and polished. A slightly undulating CEJ of type 3 appeared at the neck of the tooth. The gap between the enamel and cementum has been deepened and widened by abrasion. No opened dentin tubules are seen.

5.2.5 Premolar A45 – *Rapid Relief* (flexible neck)

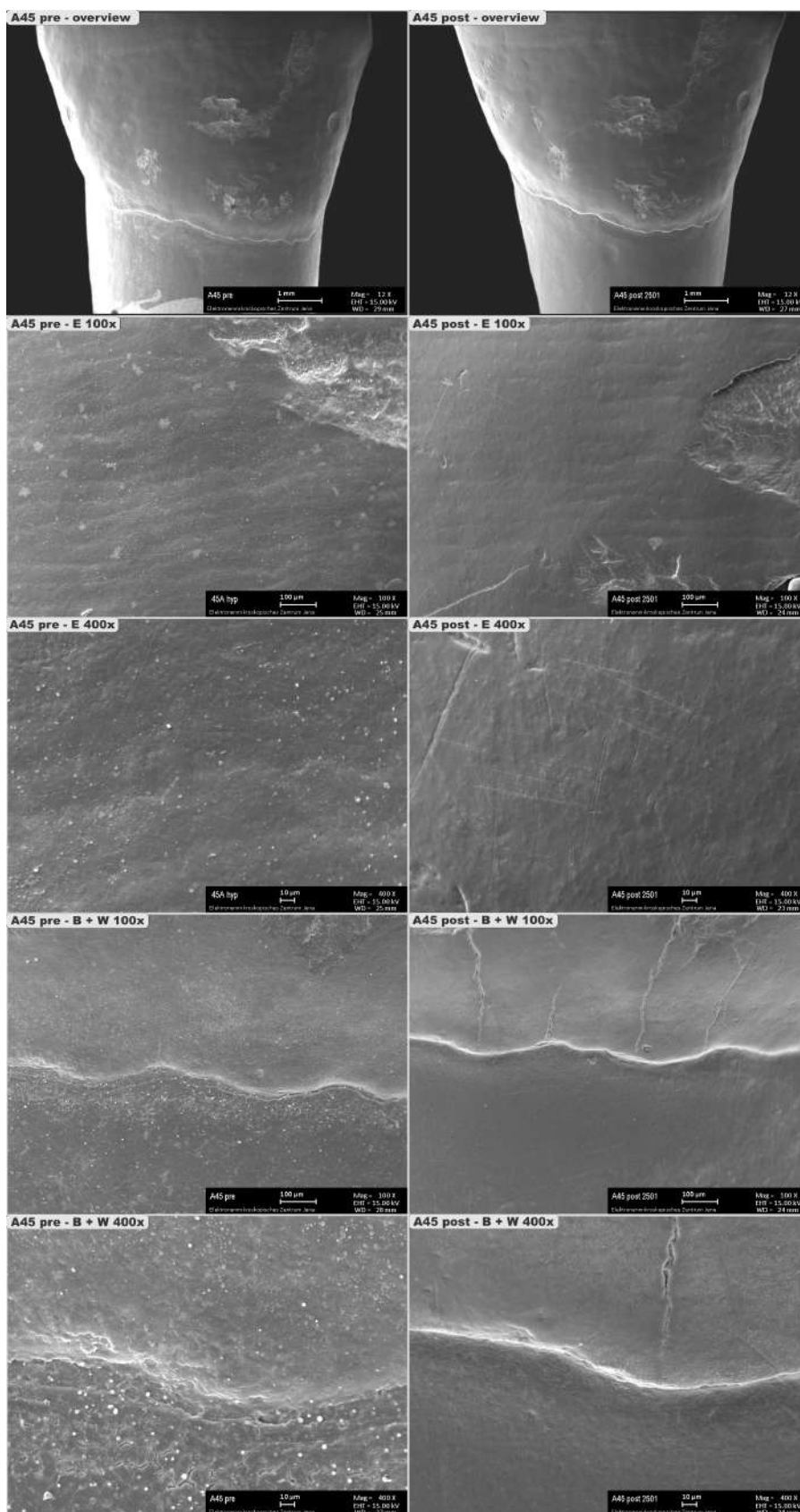


Figure 40: Premolar A45 – combined wear feature image for pre and post comparison. Extraction for orthodontic reasons. Age of patient: **14 years**. Coding of morphological features: Section 5.5.1.

Overview (Mag: 12x)

Enamel defects can be seen at the dental equator through the extraction forceps. Perikymata are still clearly visible in the juvenile premolar. After the toothbrushing cycle, individual enamel infractions have formed in the area of the enamel forceps defects.

Planimetry field E: (100x/400x)

The tooth surface has been cleaned, and the perikymata are now well visible. Several criss-cross abrasion marks have been unmasked. The previously faint oblique infractions are now widened. A prismatic enamel ratio of 1:9 became apparent.

Planimetry field B+W: (100x/400x)

After removing the smear layer and calculus, the enamel and root surface appear clean and polished. Marks of abrasion are only very subtly present. Vertical enamel infractions at the cervical enamel margin have opened up. A gently undulating CEJ type 3 with some suggested enamel peninsulas is current. The narrow gap between the enamel and cementum is now slightly deepened. The enamel margin is rounded.

5.2.6 Molar A46 – Rapid Relief (flexible neck)

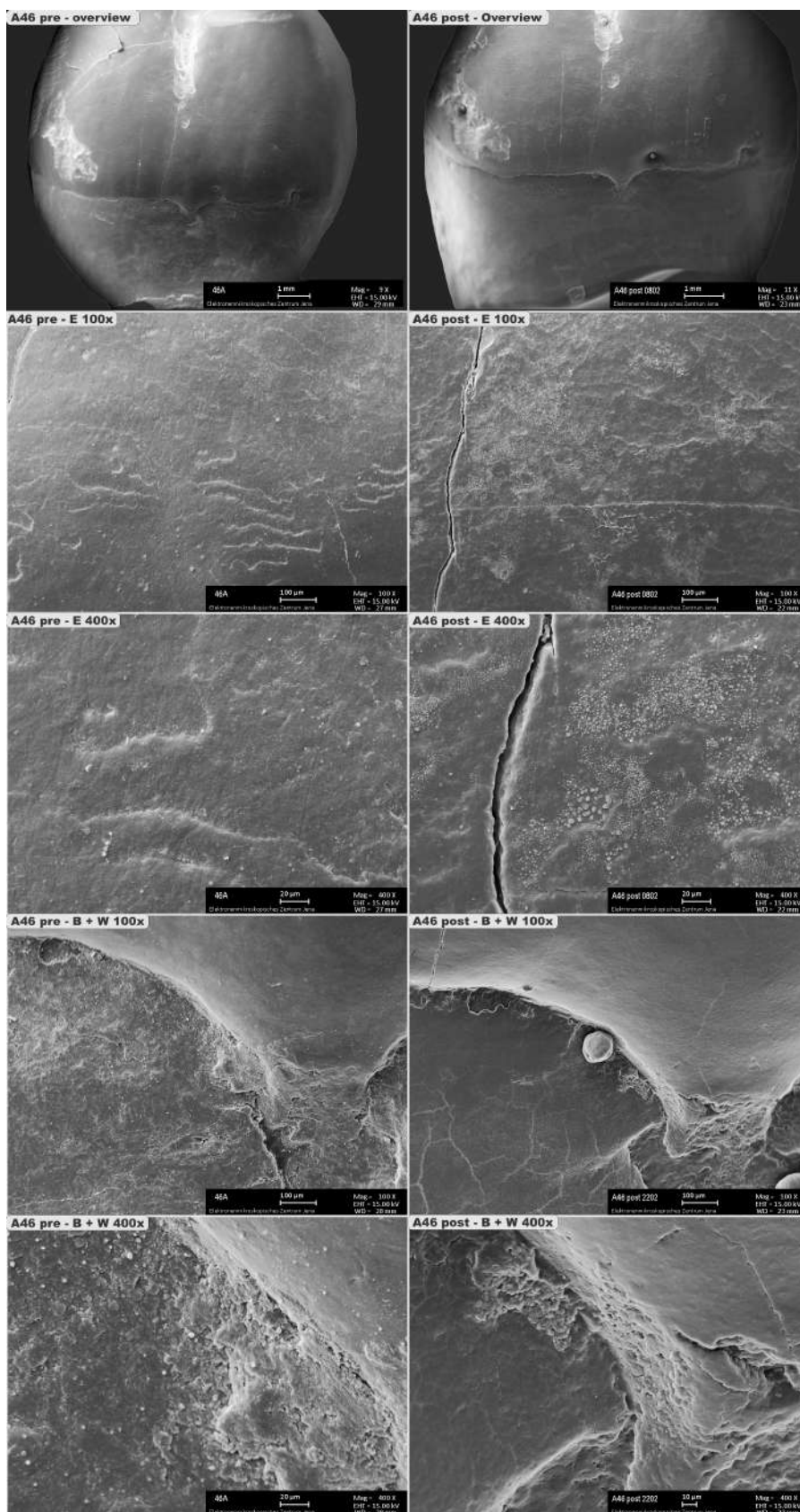


Figure 41: Molar A46 – combined wear feature image for pre and post comparison. Extraction due to caries. Age of patient: **36 years**. Coding of morphological features: [Section 5.5.1](#). Volume measurement: [Section 5.4.3](#).

Overview (Mag: 12x)

Vertical enamel infractions extend to the cemento-enamel junction. An enamel defect runs perpendicular to the tooth axis between the cusps. Larger calculus debris and furrowed, roughened areas are seen on the neck of the tooth. The calculus residues have disappeared mainly after toothbrushing. The root surface in particular has been smoothed.

Planimetry field E: (100x/400x)

Faint criss-cross abrasion marks are visible. The enamel surface is 100% prismless. Perikymata are faintly visible. The vertically running, opened enamel fraction is empty. Afterwards, there are still coccoid deposits on the enamel surface, which could not be removed despite previous surface cleaning.

Planimetry field B+W: (100x/400x)

The cementum appears cracked. The tip of the enamel tongue is fissured. More extensive calculus deposits are on the inter-radicular enamel tongue. There are concretions on the left side. A narrow abrasion groove has formed directly under the enamel margin. The CEJ type 3 is slightly undulating but, overall, relatively straight.

5.2.7 Molar A47 – Rapid Relief (flexible neck)

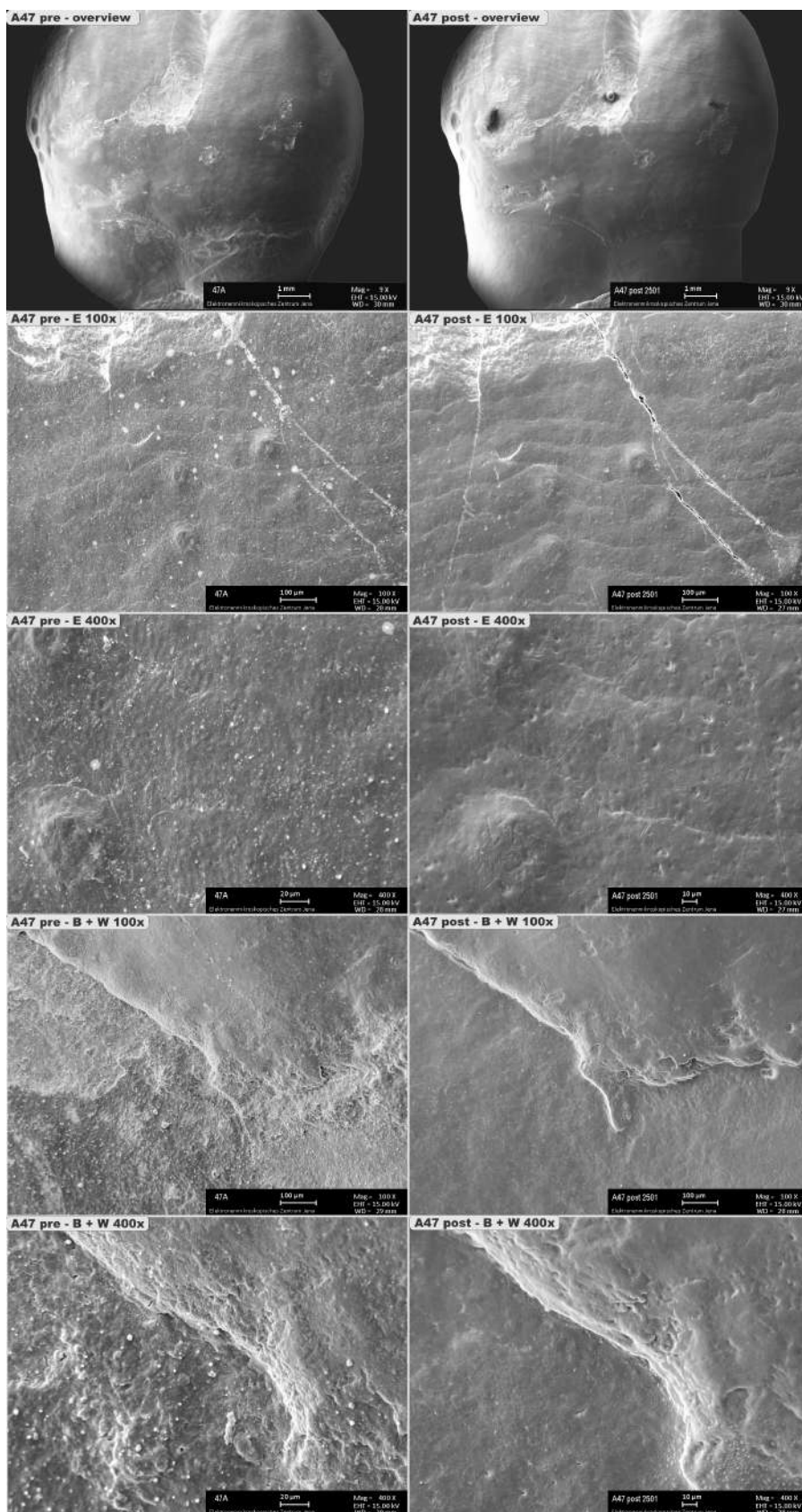


Figure 42: Molar A47 – combined wear feature image for pre and post comparison. Extraction for surgical reasons. Age of patient: **19 years**. Coding of morphological features: [Section 5.5.1](#).

Overview (Mag: 12x)

Extraction-related enamel defects can be seen in the centre of the tooth crown. The perikymata are still visible. Some enamel infractions extend from the cervical enamel margin and the forceps flaw.

Planimetry field E: (100x/400x)

Faint cross-shaped and elongated oblique abrasion marks. Numerous micro-depressions. Individual knobby elevations. Multiple prismatic areas appear on the enamel surface. Ratio 60% prismless / 40% prismatic enamel. Oblique enamel infractions have been widened and emptied. The surface has been polished and cleaned.

Planimetry field B+W: (100x/400x)

Faint, oblique abrasion marks and several micro-pits are visible on the enamel surface. White globules are visible residues of a smear layer. At baseline, there are numerous calculus residues. Several infractions oriented perpendicular to the tooth axis extended from the enamel margin. The cervical enamel margin are rounded by toothbrushing. The root surface was significantly smoothed. The previously hidden enamel peninsulas are unmasked. The CEJ, type 1, with overlapping cementum, is slightly undulated.

5.2.8 Incisor B41 – Jubilee (rigid neck)

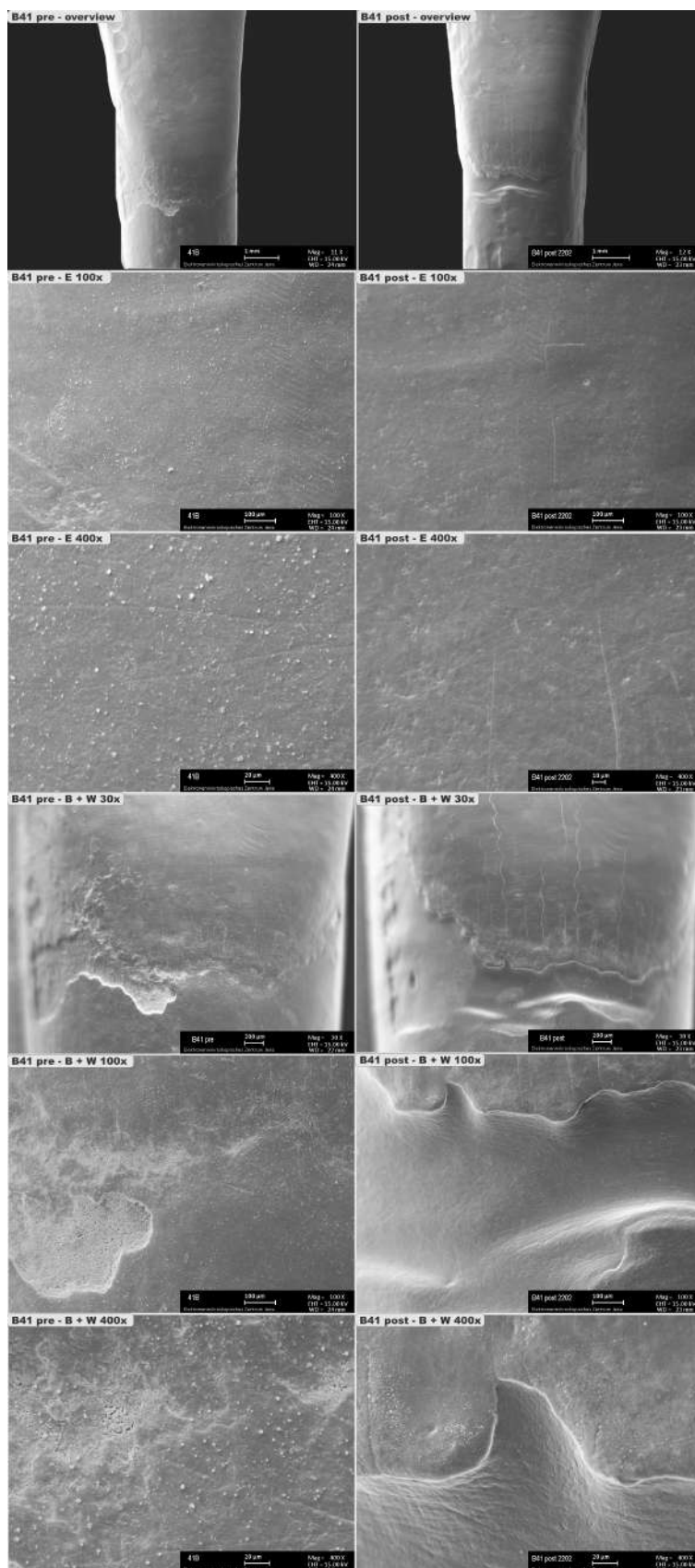


Figure 43: Incisor B41 – combined wear feature image for pre and post comparison. Extraction for periodontal reasons. Age of patient: **40 years**. Coding of morphological features: [Section 5.5.2](#). Volume measurements: [Section 5.4.4](#).

Overview (Mag: 12x)

At the baseline, the tooth surface appeared roughened and brittle at the neck of the tooth. The perikymata are only faintly visible. After toothbrushing, additional enamel infractions extended perpendicularly from the cervical enamel margin.

Planimetry field E: (100x/400x)

Numerous criss-cross abrasion marks on the enamel surface have been levelled by toothbrushing and are fading. Afterwards, the enamel surface showed up to 10% prismatic. A vertical, flat enamel infraction runs perpendicular to the tooth axis in the centre. Remains of a smear layer, and some lumpy calculus, covered the enamel, which was cleansed by toothbrushing.

Planimetry field B+W: (100x/400x)

The course of the CEJ, type 2 edge-to-edge, presents an undulating shape, and abrasion has created an extensive wedge-shaped lesion. No exposed dentin tubules can be seen. Afterwards, the root surface was cleaned and smoothed. There are no more calculus residues. Enamel outbreaks at the cervical margin were rounded off. Enamel peninsulas became more distinct. An impressive shark-shaped cavity has formed.

5.2.9 Incisor B42 – Jubilee (rigid neck)

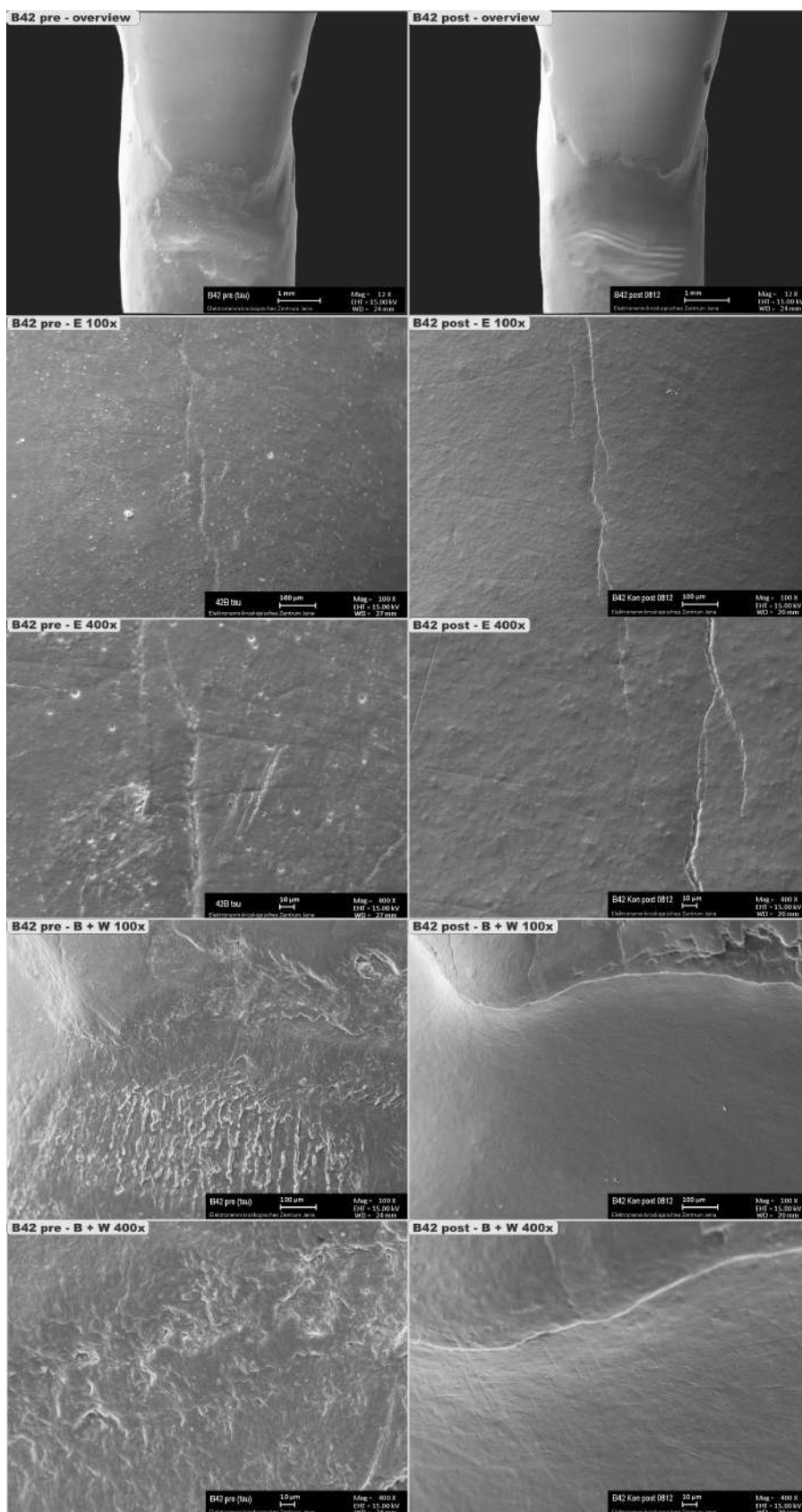


Figure 44: Incisors B42 – combined wear feature image for pre and post comparison. Extraction for periodontal reasons. Age of patient: **61 years**. Coding of morphological features: [Section 5.5.2](#). Volume measurements: [Section 5.4.5](#).

Overview (Mag: 12x)

At the baseline, a saucer-shaped cervical lesion was already present, in which horizontal abrasion grooves had formed on the root surface due to toothbrushing. The senior tooth has a smoothed tooth surface with flattened perikymata. Serrated, widened, but relatively shallow enamel infractions extend outward of the cervical enamel margin.

Planimetry field E: (100x/400x)

Numerous mainly horizontal and deeper vertical abrasion marks. The pits and fissures have been smoothed. No perikymata are evident. The opened, vertical enamel infractions are empty. The edges appear rounded.

Planimetry field B+W: (100x/400x)

At the baseline, numerous enamel eruptions at the cervical enamel margin and a massive loss of cementum and root dentin can be noticed. Several openings of dentin tubules are evident. The type 2 edge-to-edge junction course between enamel and cementum appears straight. Enamel margins have been rounded by brush abrasion. The root surface is now immaculate and polished.

5.2.10 Canine B43 – Jubilee (rigid neck)

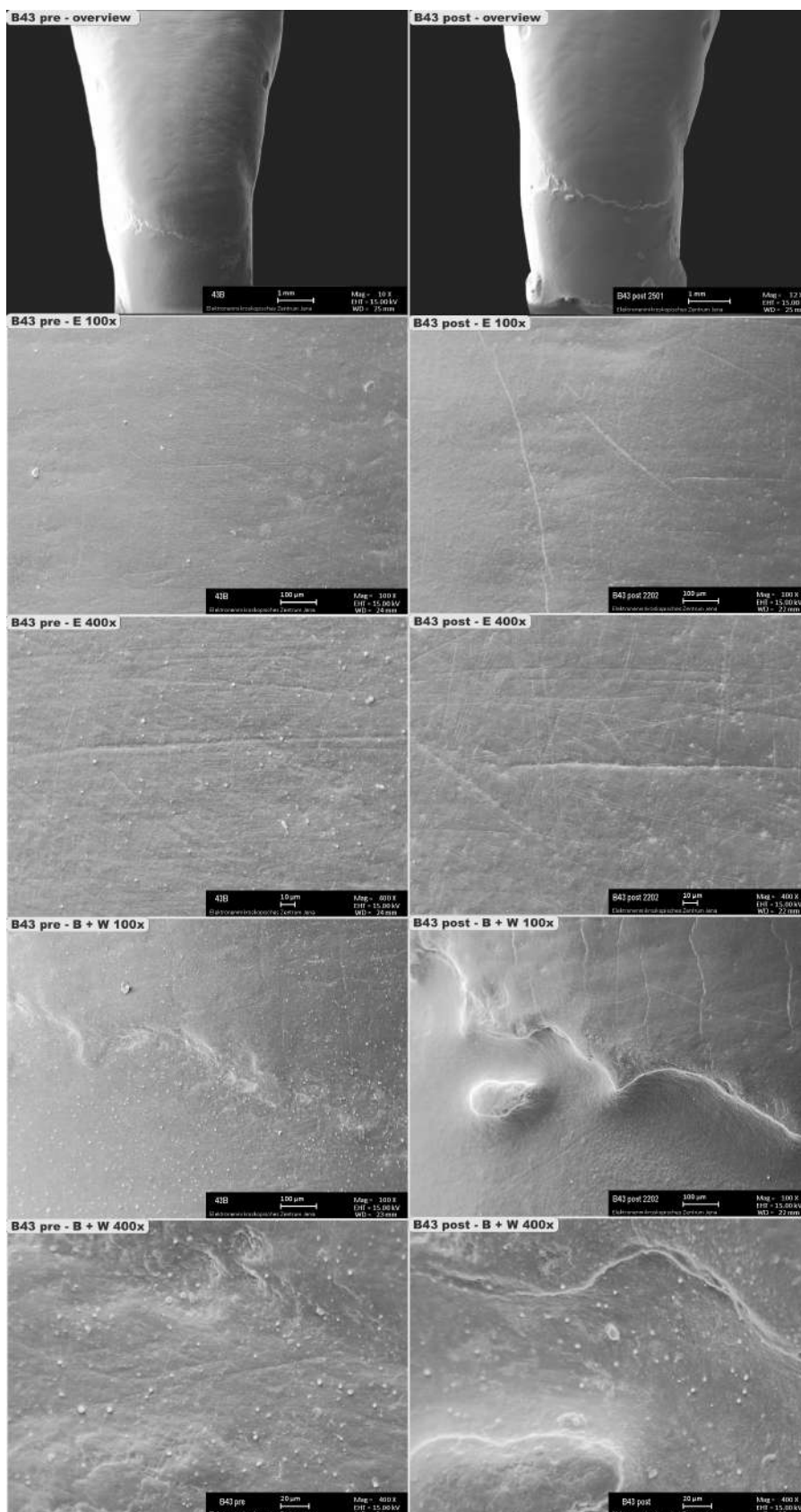


Figure 45: Canine B43 – combined wear feature image. Extraction for periodontal reasons. Age of patient: **58 years**. Coding of morphological features: Section 5.5.2. Volume measurements: Section 5.4.6.

Overview (Mag: 12x)

The tooth surface appears smooth. Signs of perikymata are found in the upper third of the tooth crown. Faintly visible enamel infractions are located in the lower third of the tooth.

Planimetry field E: (100x/400x)

Individual abrasion marks were crosswise with some imposing horizontal scratches. Perikymata were only faintly visible. The enamel surface was 100% prismless. The infraction from the cervical enamel margin did not extend beyond the dental equator. Minor calculus deposits and remnants of a smear layer were visible on the enamel surface during the initial examination, which was subsequently completely removed.

Planimetry field B+W: (100x/400x)

Enamel infractions originating from the cervical enamel margin run perpendicular to the tooth axis. The calculus completely disappeared, but there are still some granules of the smear layer. After abrasion, several peninsulas and an enamel island with a diameter of ~ 100 µm appeared on the root surface. An undulating course of the CEJ of type 2, edge-to-edge contact, can be seen. The enamel margin was rounded, the root surface sloped more steeply.

5.2.11 Premolar B44 – Jubilee (rigid neck)

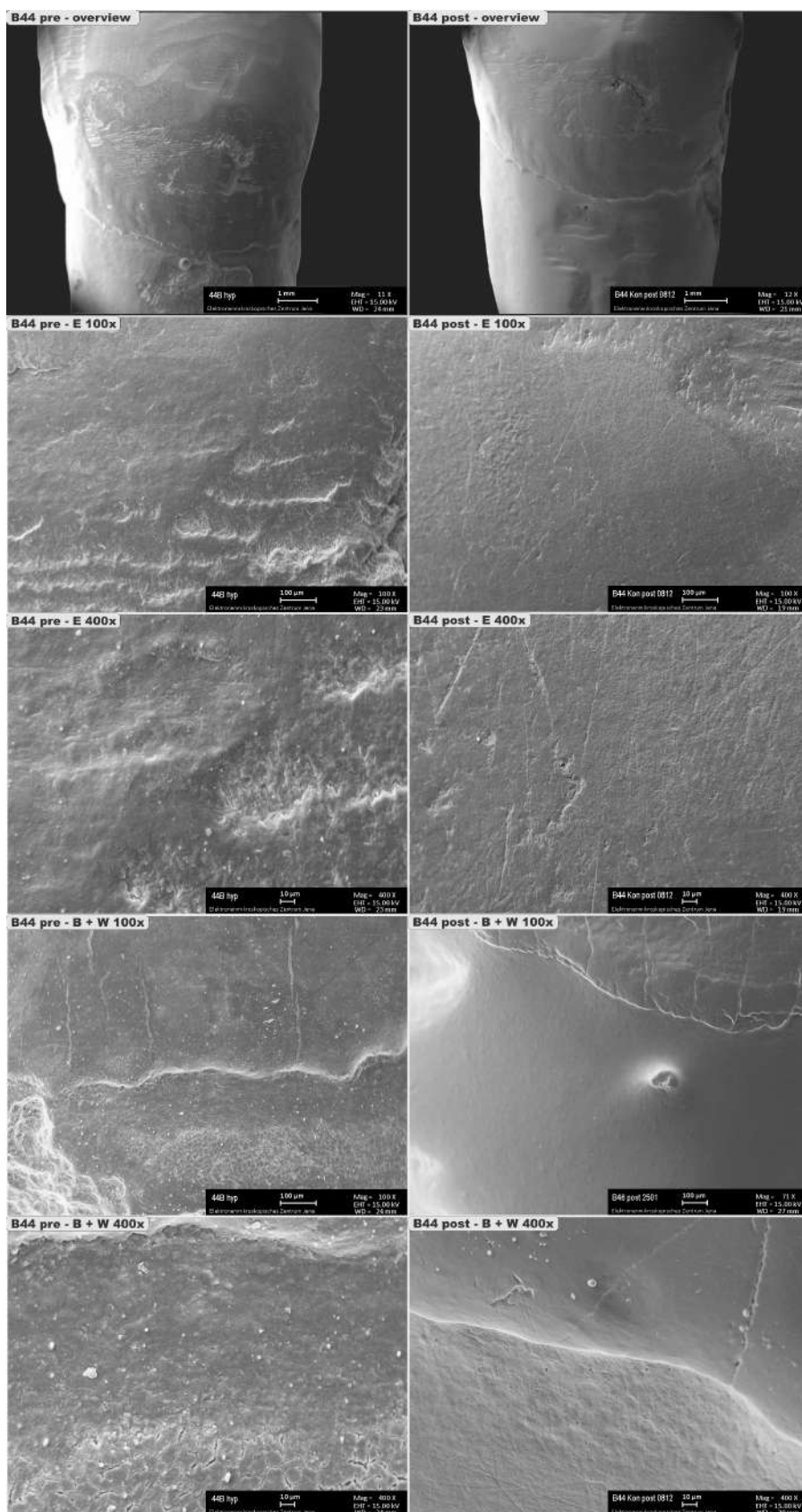


Figure 46: Premolar B44 – combined wear feature image for pre and post comparison. Extraction for orthodontic reasons. Age of patient: **13 years**. Coding of morphological features: [Section 5.5.2](#).

Overview (Mag: 12x)

The premolar was processed with rubber polishers before extraction, damaging the enamel surface. The perikymata were still visible on the juvenile enamel surface despite the damage. Several enamel infractions are evident in the lower third of the tooth.

Planimetry field E: (100x/400x)

There are clear, predominantly vertically aligned abrasion marks. After toothbrushing, up to 25% of the enamel surface has become prismatic. The enamel surface got clean and cleared of particles.

Planimetry field B+W: (100x/400x)

At higher magnification, criss-cross abrasion marks can be seen. On the young root surface, there are dentinal tubules opened by abrasion. The calculus and most of the smear layer residues have disappeared. In addition to the small, grooved enamel peninsula, an enamel island became visible on the root surface. The CEJ type 3 with a gap between enamel and cementum and the previously cracked cementum was visibly smoothed.

5.2.12 Premolar B45 – Jubilee (rigid neck)

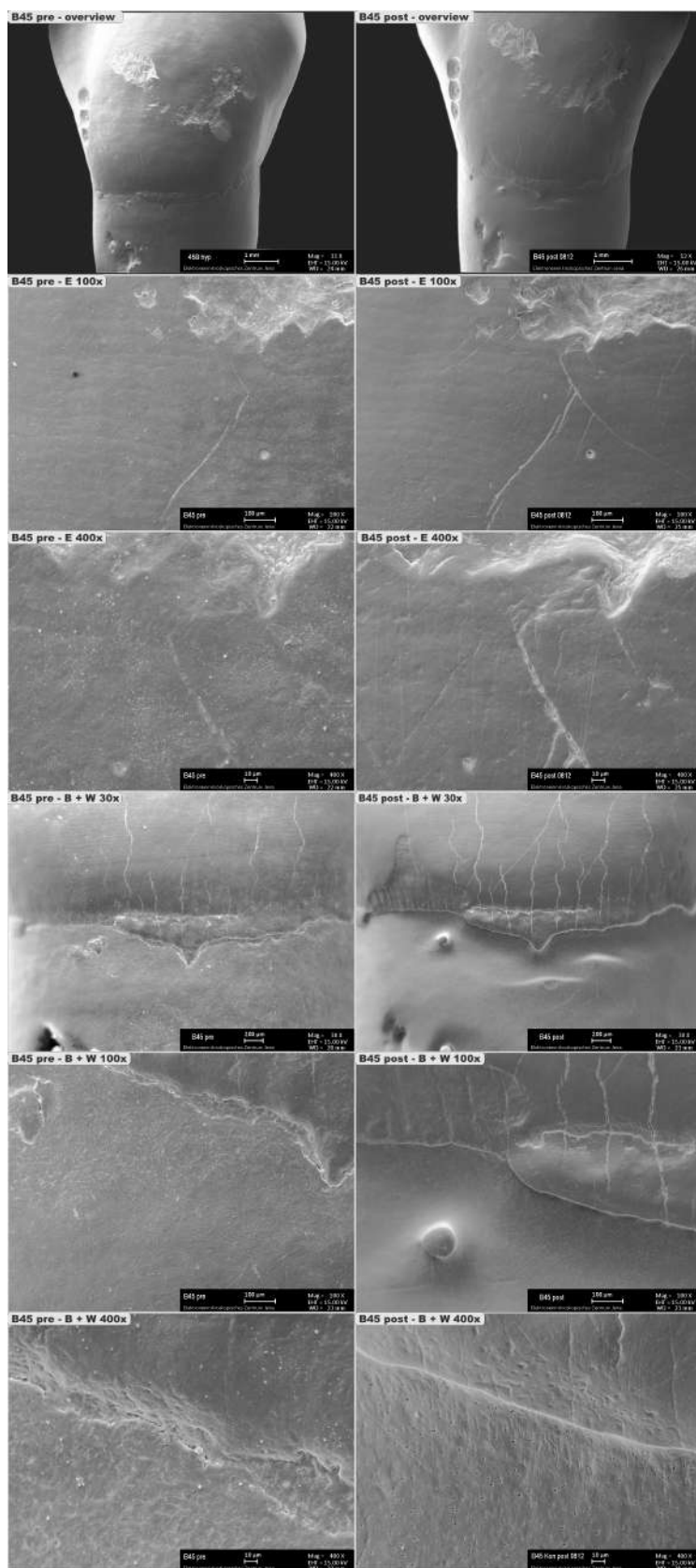


Figure 47: Premolar B45 – combined wear feature image for pre and post comparison. Extraction for orthodontic reasons. Age of patient: **13 years**. Coding of morphological features: [Section 5.5.2](#). Volume measurement: [Section 5.4.7](#).

Overview (Mag: 12x)

An inverted, funnel-shaped abrasion defect appears at the cervical enamel margin. The perikymata are pronounced. Vertical enamel infractions are visible in the lower third of the tooth.

Planimetry field E: (100x/400x)

Numerous vertical, disoriented criss-cross abrasion marks and micro-pits are visible. The enamel surface is 25% prismatic. The vertical enamel infraction has been opened.

Planimetry field B+W: (100x/400x)

Enamel infractions, though opened, are devoid and extend to the cemento-enamel junction. Following toothbrushing, calculus and remnants of the smear layer have vanished. Alongside the significant central enamel peninsula, a small enamel island is revealed on the root surface. The wedge-shaped cervical lesion now presents a rounded appearance, and the undulation of the CEJ type 3 (gap) has been smoothed.

5.2.13 Molar B46 – Jubilee (rigid neck)

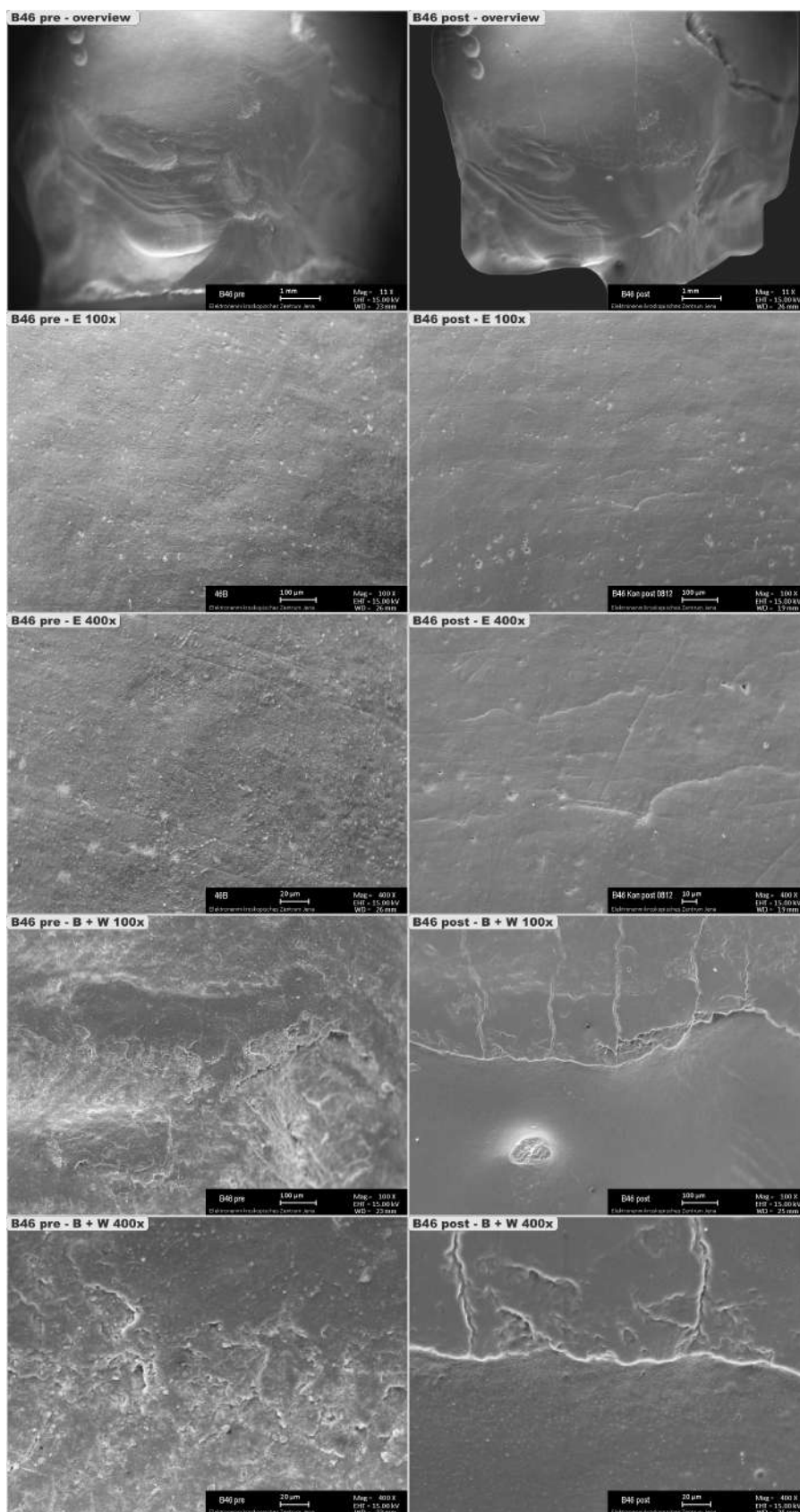


Figure 48: Molar B46 – combined wear feature image for pre and post comparison. Extraction due to caries. Age of patient: **31 years**. Coding of morphological features: [Section 5.5.2](#).

Overview (Mag: 12x)

Distinct, disoriented abrasion marks and indentations are evident on the enamel surface. Root-side defects resulting from extraction have been leveled through tooth-brushing. The perikymata remain distinctly visible. A profound cusp fracture extends through the center of the tooth crown. The deep crater crack is void afterward. Additionally, a vertical enamel infraction is noticeable at the distal cusp.

Planimetry field E: (100x/400x)

The enamel surface exhibits primarily horizontal or vertical abrasion marks, along with some obliquely oriented ones, accompanied by isolated pits. Approximately 10% of the surface manifests a prismatic appearance. Notably, no enamel infractions are apparent in proximity to the tooth equator.

Planimetry field B+W: (100x/400x)

Numerous enamel infractions, visible at magnifications of 100x to 400x, extend to the cervical enamel margin. No evidence of exposed dentinal tubules is observed. The CEJ type 2, with edge-to-edge contact, has been smoothed, preserving its undulating contour. Additionally, a small enamel island has been revealed on the root surface.

5.2.14 Molar B47 – Jubilee (rigid neck)

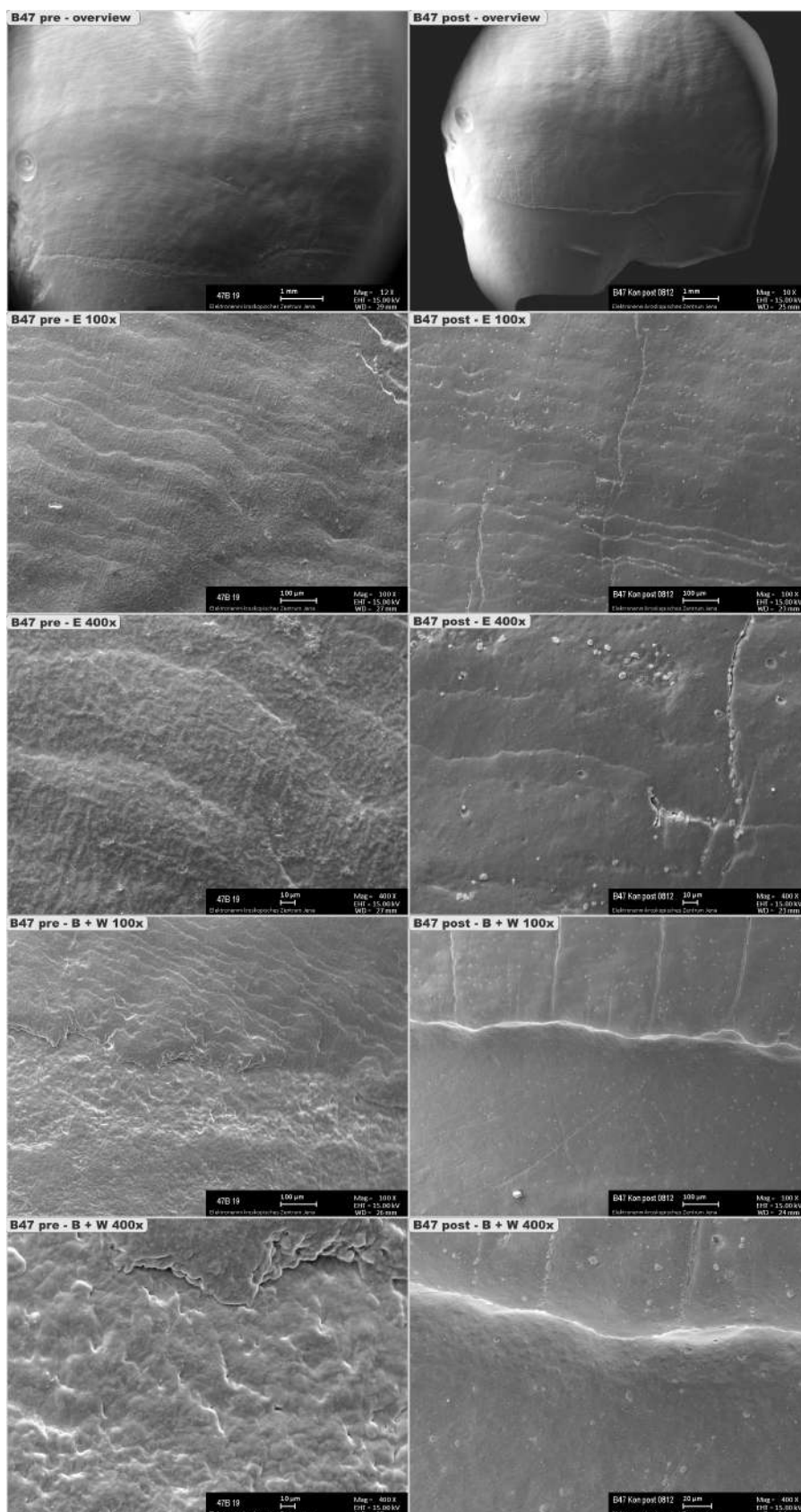


Figure 49: Molar B47 – combined wear feature image for pre and post comparison. Extraction for surgical reasons. Age of patient: **19 years**. Coding of morphological features see [Section 5.5.2](#).

Overview (Mag: 12x)

No discernible abrasion marks are present on the smooth surface. Perikymata are clearly evident, showcasing the tooth's growth patterns. Additionally, enamel infractions are notable in the lower third of the tooth.

Planimetry field E: (100x/400x)

The oblique abrasion marks were leveled through toothbrushing, yet a horizontal break-off edge persisted. This abrasion has exposed certain enamel infractions, with minimal calculus residues discernible within them. Following this, the enamel surface exhibits a 10% prismatic appearance.

Planimetry field B+W: (100x/400x)

Multiple enamel infractions extend to the cervical enamel margin. The enamel appears smoothed, and the margins are rounded. Notably, there are no visible exposed dentinal tubules or peninsula formations. The CEJ type 2, characterized by edge-to-edge contact, has undergone smoothing, resulting in an evened-out undulation.

5.3 Cervical wear lesions

Backscattered electron (BSE) images of pre-brushing and post-brushing cervical lesions.

5.3.1 Incisor A41 – Cervical wear lesion – *Rapid Relief*

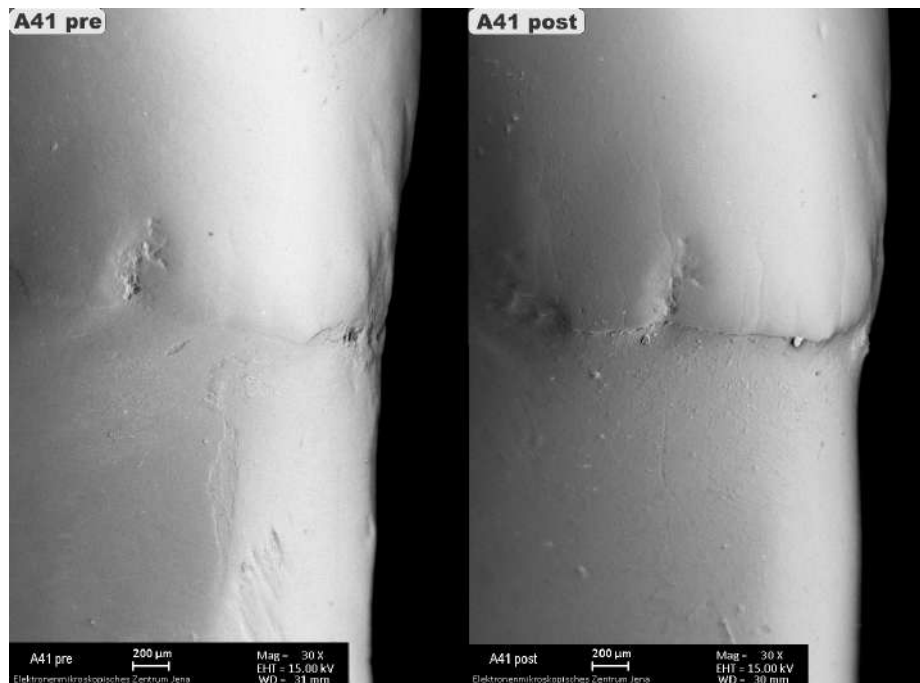


Figure 50: *Incisor A41* exhibits a distinctive cervical lesion at baseline, characterized by dentin loss at the CEJ accompanied by prominent enamel margins, wide open enamel infractions and visible abrasion marks at root dentin. *CEJ type: 1 (pre) and 2 (post)*. Age of patient: 55 years. BSE image.

5.3.2 Incisor A42 – Cervical wear lesion – *Rapid Relief*

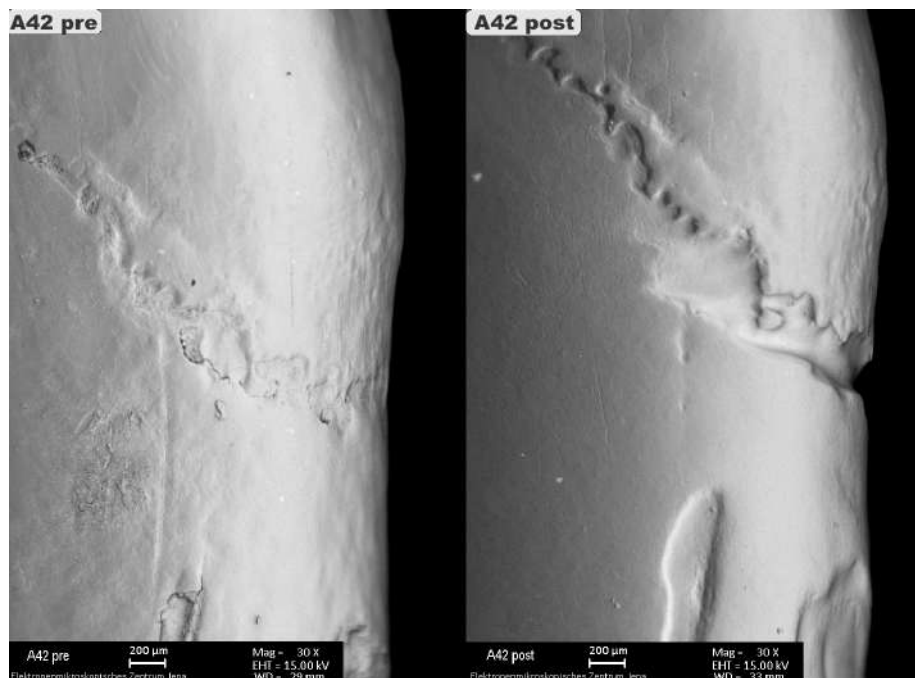


Figure 51: *Incisor A42* initially presents a concealed cervical abrasion lesion and some calculus. Following brushing, dental calculus is removed, revealing sharp enamel margins, loss of root dentin, wide-open enamel infractions, and visible marks on the root dentin. *CEJ type: 2*. Age of patient: 40 years. BSE image.

5.3.3 Canine A43 – Cervical wear lesion – *Rapid Relief*

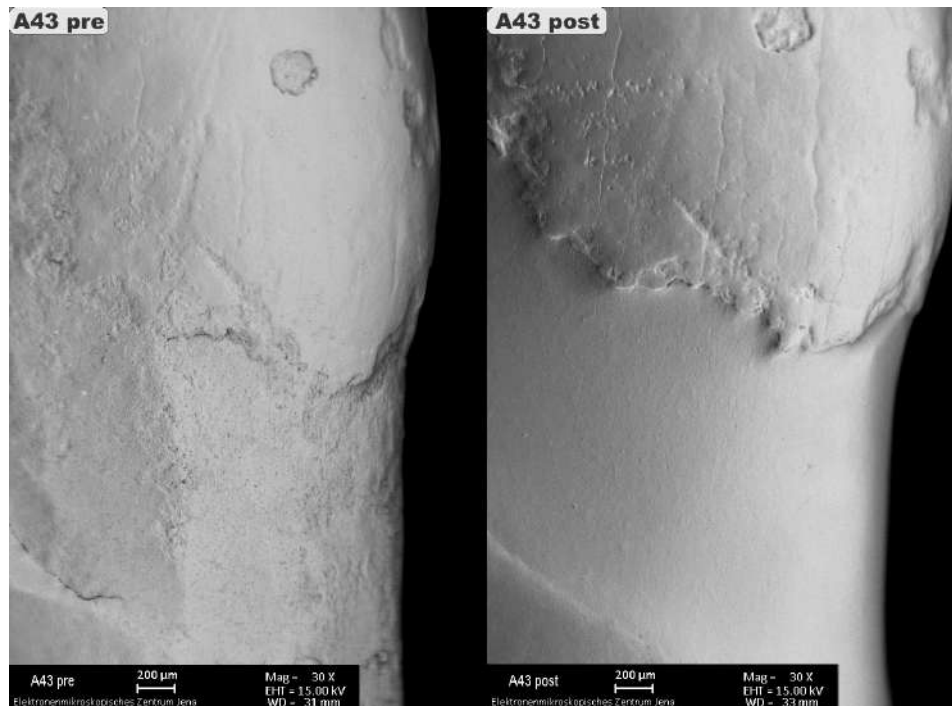


Figure 52: Canine A43 initially displays an extensive cervical lesion filled with remnants of calculus and obscured enamel margins. After the complete removal of dental calculus, sharp enamel margins emerge, revealing some peninsulas with wide-open dental infractions. The clinically smoothed root dentin surface extends down to the cementum layer. **CEJ type: 2.** Age of patient: 58 years. BSE image.

5.3.4 Premolar A44 – Cervical wear lesion – *Rapid Relief*

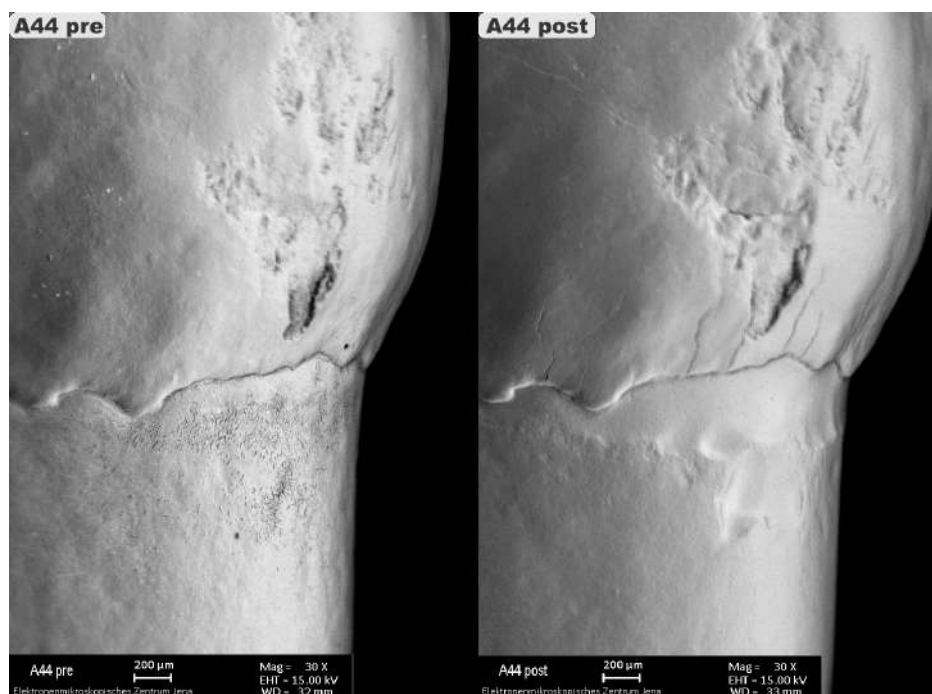


Figure 53: Premolar A44 exhibits extraction damage caused by forceps. Initially, enamel margins show a few peninsulas with no detectable calculus. Post-extraction, there is abrasion of the extraction damage, wide-open enamel infractions, removal of cementum, and the exposure of root dentin, extending up to 200 µm. **CEJ type: 3.** Age of patient: 14 years. BSE image.

5.3.5 Premolar A45 – Cervical wear lesion – *Rapid Relief*

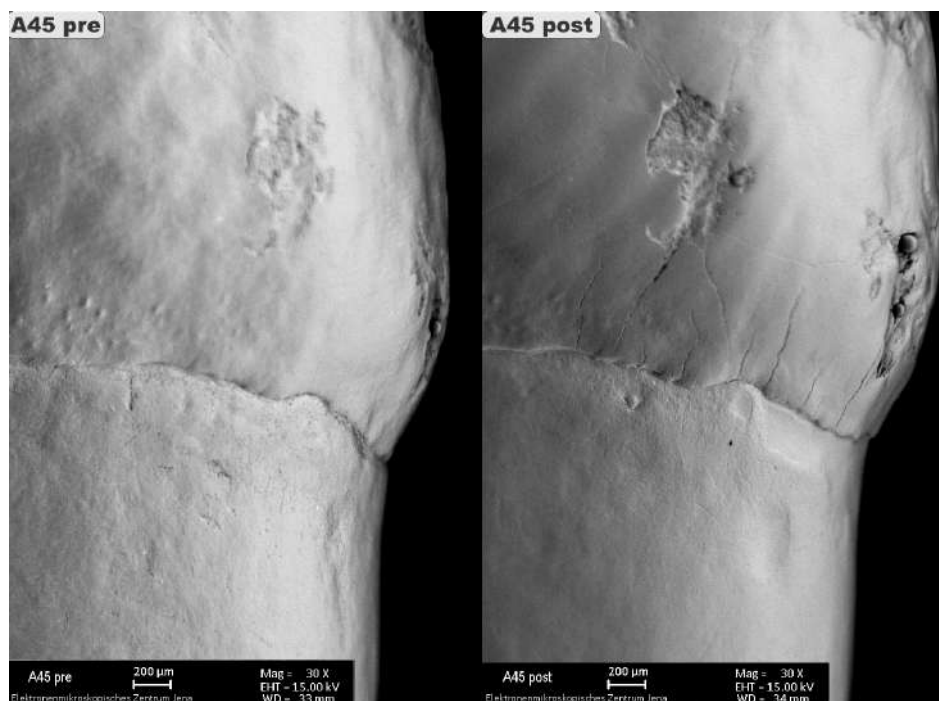


Figure 54: Premolar A45 displays extraction damage with discernible perikymata structures and partly masked sharp enamel margins at baseline. Notably, wide-open enamel infractions and crisp enamel margins are evident. Cementum removal is confined to the buccal site, extending up to 180 µm. **CEJ type: 3.** Age of patient: **14 years.** BSE image.

5.3.6 Molar A46 – Cervical wear lesion – *Rapid Relief*

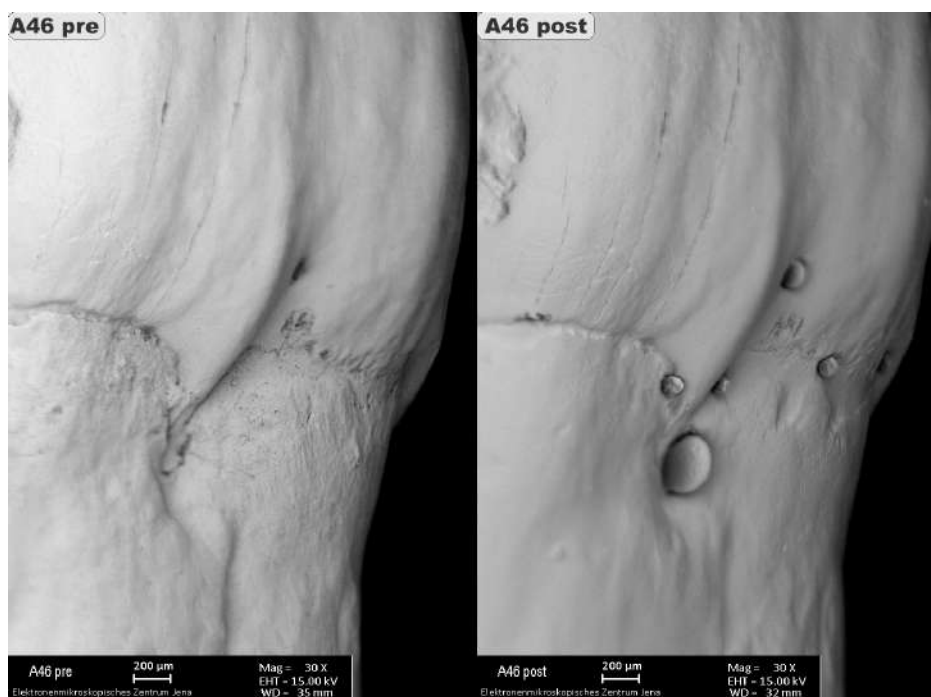


Figure 55: Molar A46 presents with the cemento-enamel junction (CEJ) concealed by dental calculus, featuring a typical enamel fold with a rounded appearance at baseline. Post-abrasion, the enamel fold undergoes abrasion, revealing the opening of enamel infractions. Additionally, there is a somewhat abrasive removal of cementum, showcasing sharp enamel margins. **CEJ type: 3.** Age of patient: **36 years.** BSE image.

5.3.7 Molar A47 – Cervical wear lesion – *Rapid Relief*

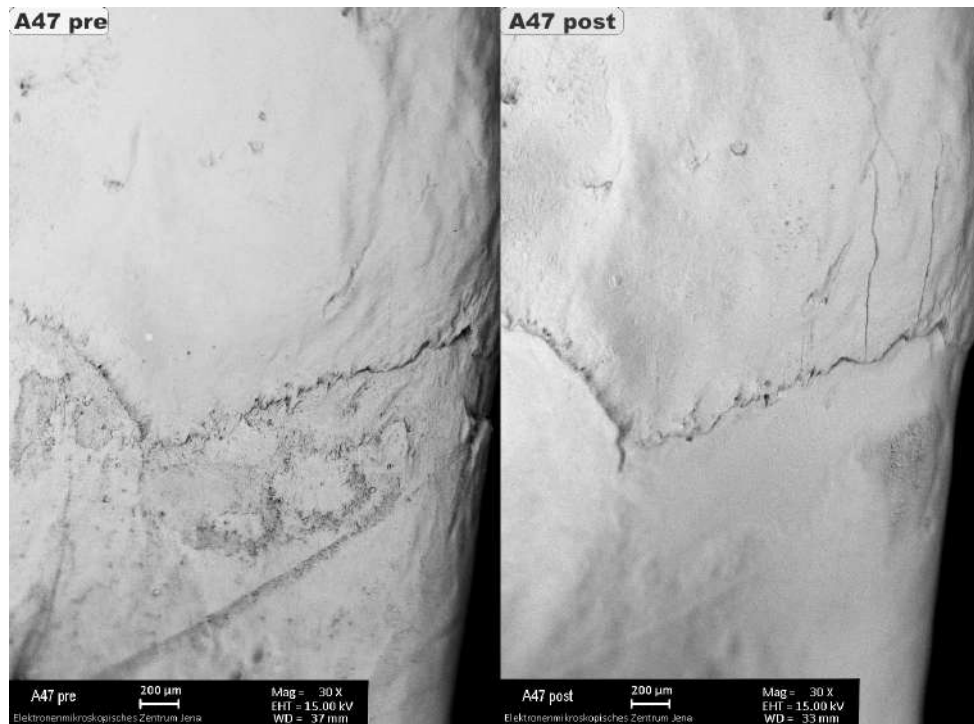


Figure 56: Molar A47 exhibits sharp enamel margins with slight calculus remnants at baseline. Subsequently, the enamel margins take on a rounded form, revealing open enamel infractions, with no detectable removal of cementum. *CEJ type: 1*. Age of patient: 19 years. BSE image.

5.3.8 Incisor B41 – Cervical wear lesion – *Jubilee*

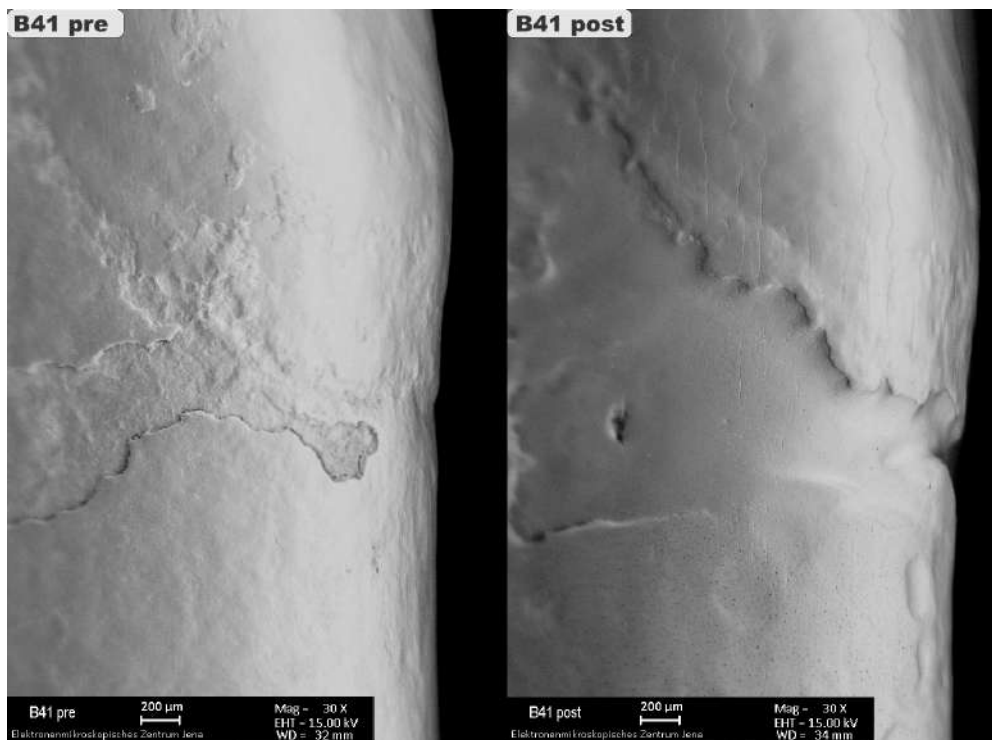


Figure 57: Incisor B41 initially displays calculus remnants and masked enamel margins. Subsequent changes include the opening of sharp enamel margins with peninsulas, thorough cementum removal extending up to 400 µm, leading to underlying root dentin loss. *CEJ type: 2 (post)*. Age of patient: 40 years. BSE image.

5.3.9 Incisor B42 – cervical wear lesion – *Jubilee*

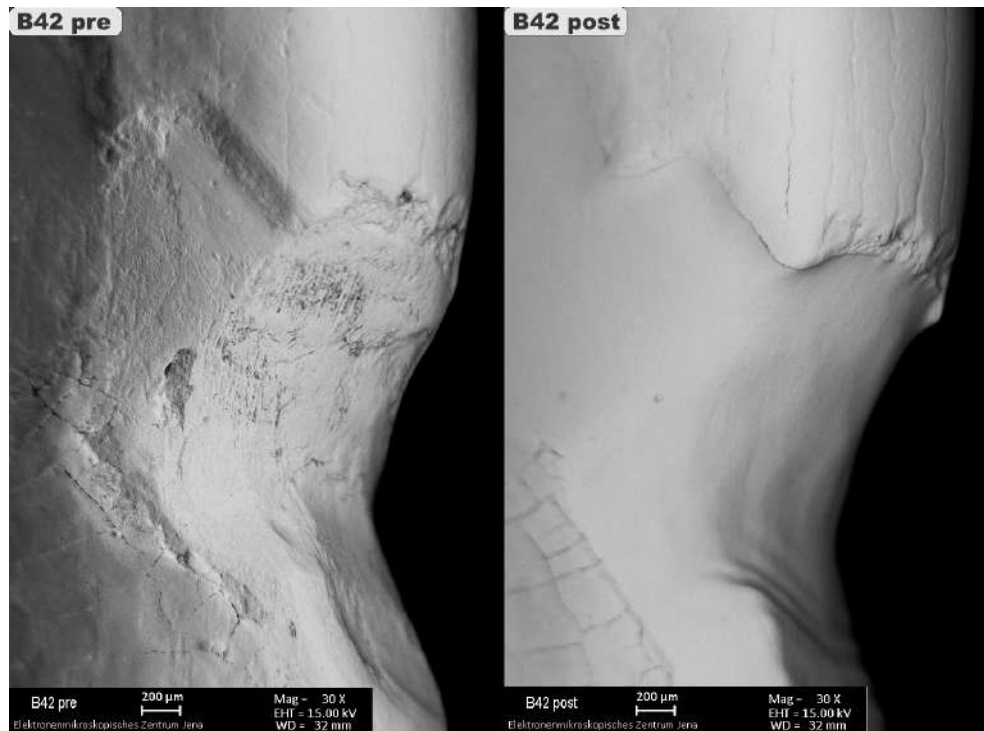


Figure 58: Incisor B42 reveals an extended cervical abrasive lesion penetrating deep into the root dentin, marked by numerous abrasion marks and cementum removal spanning up to 600 µm. Initially, enamel margins are concealed. Post-cervical abrasion, the area is wholly smoothed out, with dentin loss undermining the margins. Additionally, typical brushing grooves are observed on the root surface. **CEJ type: 2.** Age of patient: **61 years.** BSE image.

5.3.10 Canine B43 – Cervical wear lesion – *Jubilee*

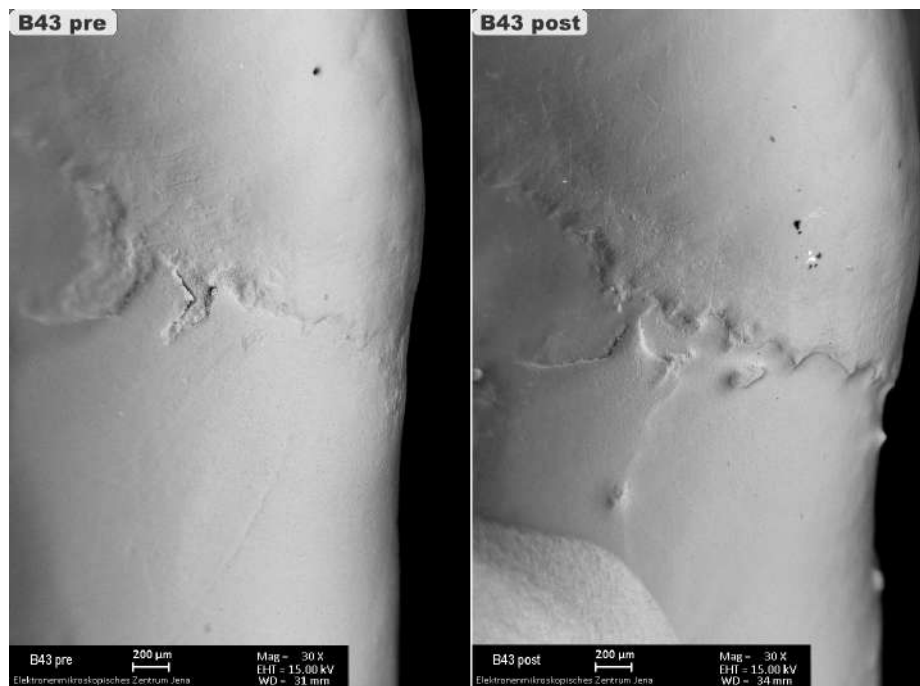


Figure 59: Canine B43 exhibits masked enamel margins and some calculus remnants on the root cementum. The process involves smoothing out with significant cementum dentin loss, revealing unique enamel islands and refining the sharpness of enamel margins. Very few enamel infractions are observed. **CEJ type: 2.** Age of patient: **58 years.** BSE image.

5.3.11 Premolar B44 – Cervical wear lesion – *Jubilee*

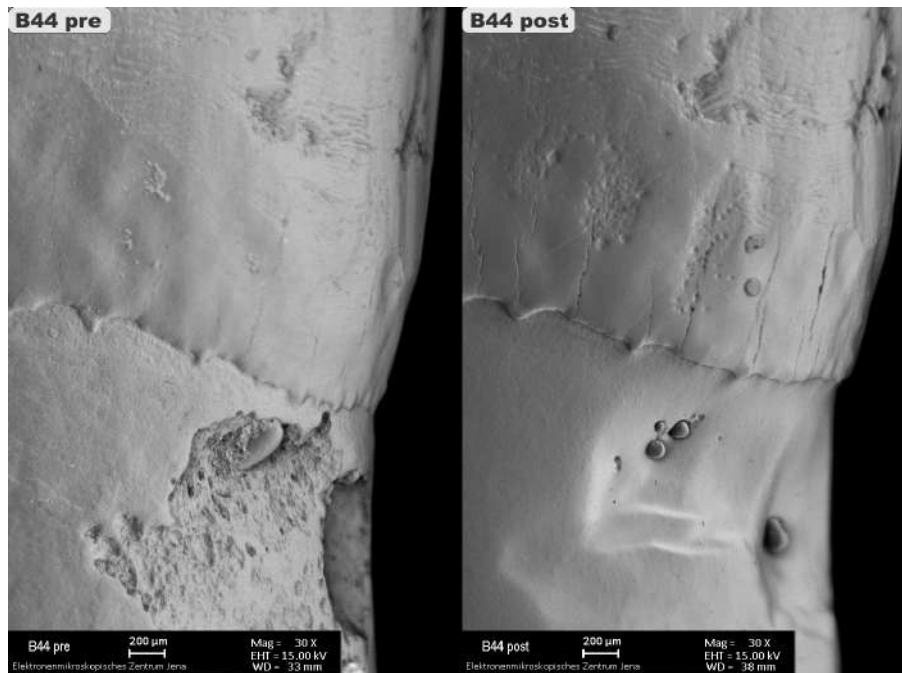


Figure 60: Premolar B44 reveals substantial enamel damage after bracket removal (clinically imperceptible) and root damage due to extraction at baseline. Post-extraction, there is a thorough smoothing out of the root damage, unveiling sharp enamel margins. Additionally, there is a partial smoothing out of post-orthodontic enamel damage, exposing prismatic enamel and wide-open enamel infractions. **CEJ type: 3.** Age of patient: **13 years.** BSE image.

5.3.12 Premolar B45 – Cervical wear lesion – *Jubilee*

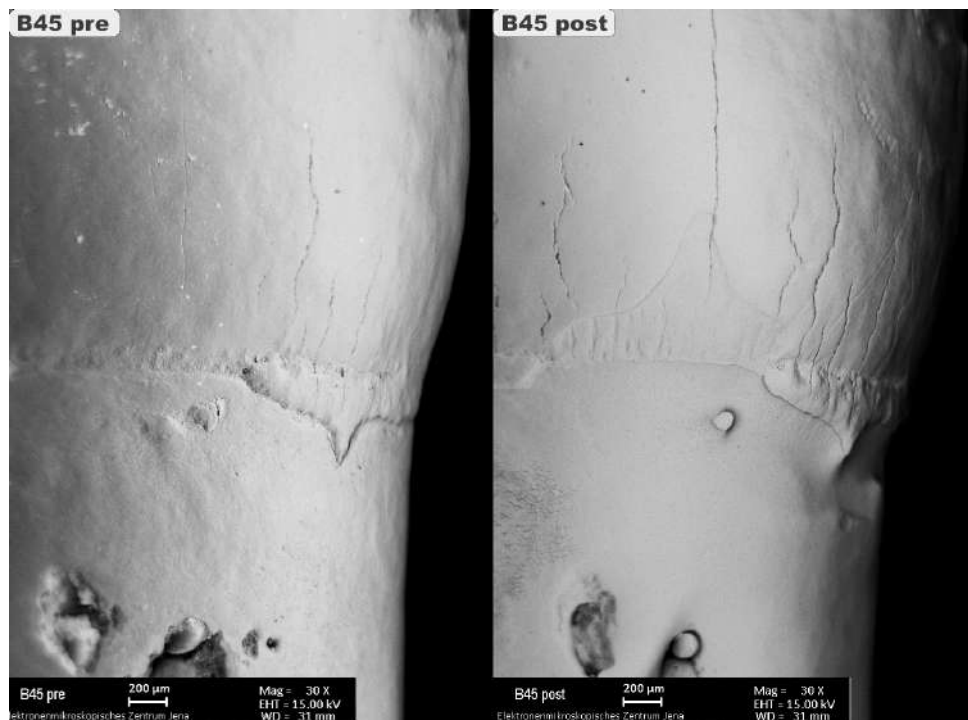


Figure 61: Premolar B45 presents with dental calculus remnants and the masking of enamel margins by cementum at baseline. Notably, an atypical appearance of an enamel peninsula is observed, accompanied by enamel wear. Post-treatment includes the demasking of an enamel island, the presence of wide-open enamel infractions, and a cementum loss extending up to 250 µm. **CEJ type: 3.** Age of patient: **13 years.** BSE image.

5.3.13 Molar B46 – Cervical wear lesion – Jubilee

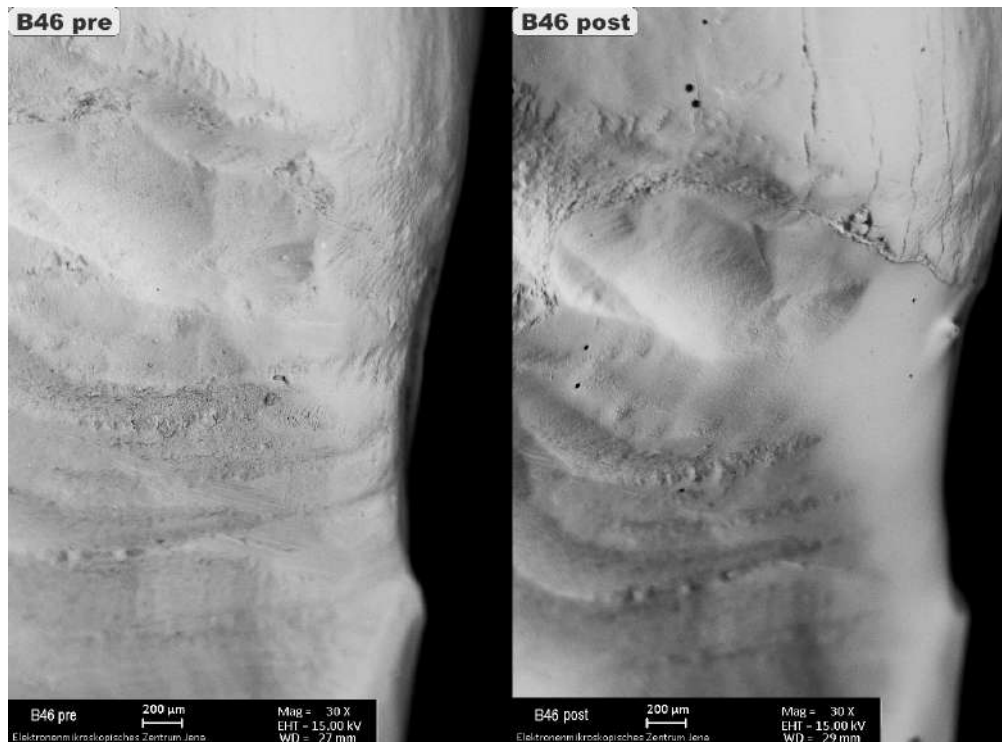


Figure 62: Molar B46 initially exhibits completely masked enamel margins and post-extraction damage at both crown and root. Following cervical abrasion, the tooth reveals sharp enamel margins and the demasking of an enamel island. CEJ type: 2 and 1. Age of patient: 31 years. BSE image.

5.3.14 Molar B47 – Cervical wear lesion – Jubilee

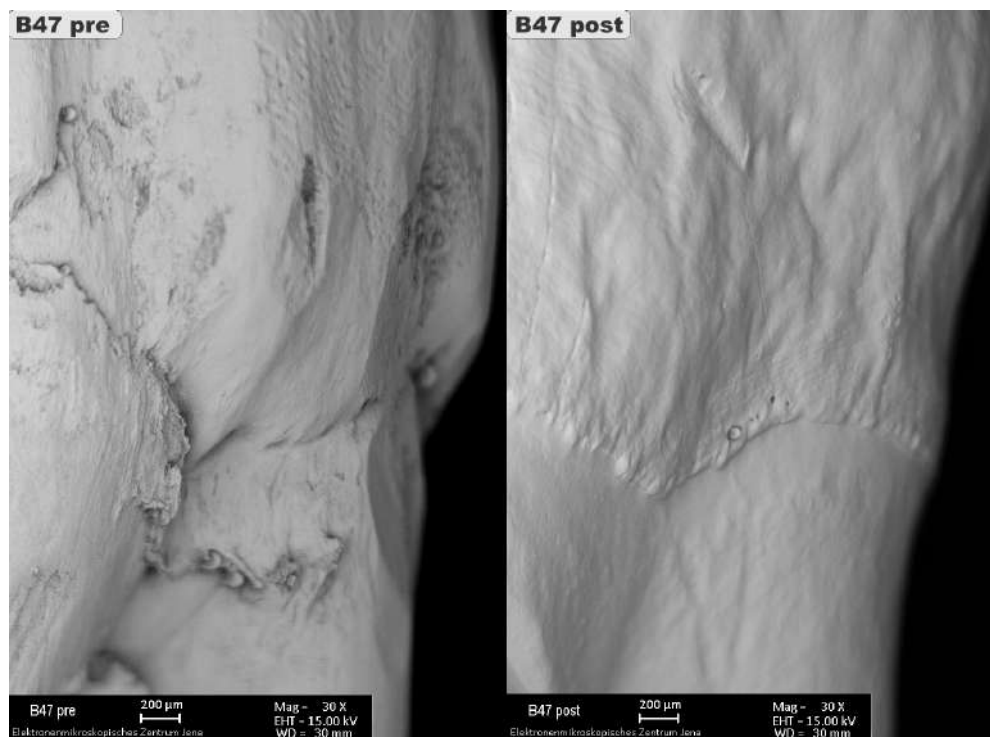


Figure 63: Molar B47 features calculus and tissue remnants (clinically imperceptible) at baseline. Subsequent treatment involves smoothing out and demasking of enamel margins with peninsulas, along with a cementum loss of up to 200 µm. CEJ type: 2. Age of patient: 19 years. BSE image.

5.4 Volume loss

Table 11: Overview of volume loss results

Toothbrush <i>Rapid Relief</i> Ø 34.25 nl					Toothbrush <i>Jubilee</i> Ø 87.75 nl				
Tooth no.	Volume loss (mm ³)	Volume loss (nl)	Altered surface size (mm ²)	Ø µm /mm ²	Tooth no.	Volume loss (mm ³)	Volume loss (nl)	Altered surface size (mm ²)	Ø µm /mm ²
A42	0.043	43	1.538	28	B41	0.055	55	2.000	28
A44	0.050	50	2.033	25	B42	0.188	188	5.142	37
A46m	0.020	20	1.362	15	B43	0.041	41	1.495	27
A46d	0.024	24	1.184	20	B45	0.067	67	2.668	25
Ø mean	0.034	34.25	surface	22	Ø mean	0.087	87.75	surface	29.25

The colour coding of the height scale indicates the difference in height between the pre and post model in positive values.

5.4.1 Incisor A42 – Reshaper 3D

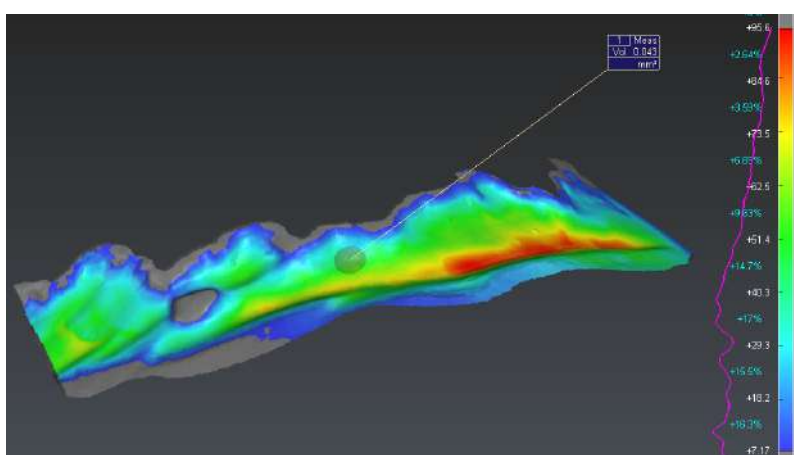


Figure 64: Incisor A42 of a patient aged 40 years – extraction for periodontal reasons. Reshaper surface model. **Result: 43 nl** cervical volume loss after brushing with toothbrush *Rapid Relief*.

Overall volume loss due to cervical wear: **43 nl**

Cervical mesh surface: **1.538 mm²**

Height loss scale

colour coding:

Blue: 5 – 30 µm

Green: 30 – 64 µm

Yellow: 64 – 75 µm

Red: 75 – 98 µm

5.4.2 Premolar A44 – Reshaper 3D

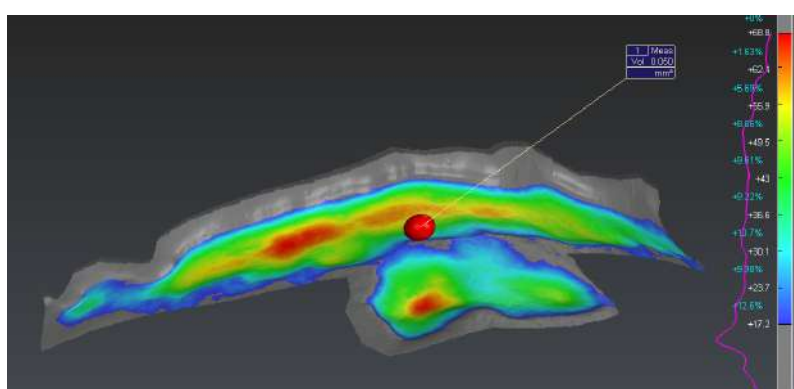


Figure 65: Premolar A44 of a patient aged 14 years – extraction for orthodontic reasons. Reshaper surface model. **Result: 50 nl** cervical volume loss after brushing with toothbrush *Rapid Relief*.

Overall volume loss due to cervical wear: **50 nl**

Cervical mesh surface: **2.033 mm²**

Height loss scale

colour coding:

Blue: 17 – 30 µm

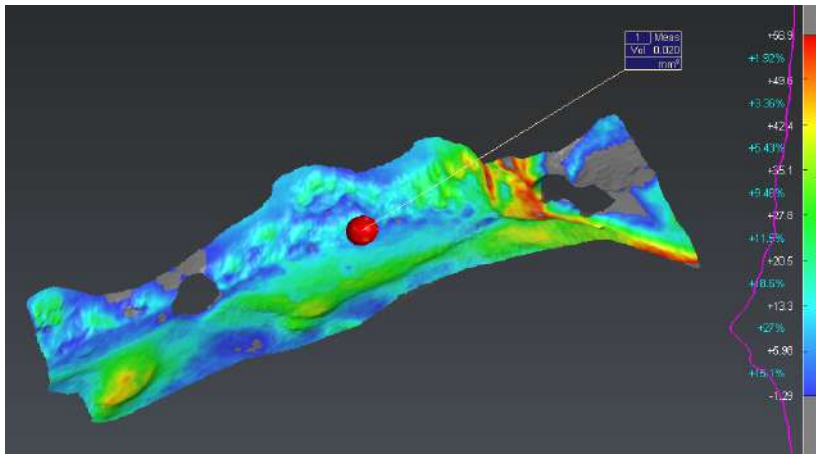
Green: 30 – 50 µm

Yellow: 50 – 63 µm

Red: 63 – 70 µm

5.4.3 Molar A46 – Reshaper 3D

▪ Mesial (right side)



Overall volume loss due to cervical wear: 20 nl

Cervical mesh surface: 1.362 mm²

Height loss scale

colour coding:

Blue: 1 – 13 μ m

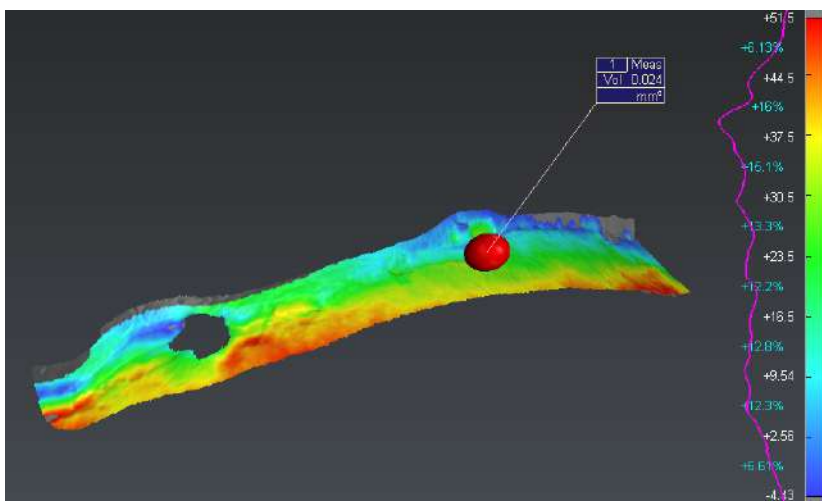
Green: 13 – 35 μ m

Yellow: 35 – 43 μ m

Red: 43 – 57 μ m

Figure 66: Molar A46 of patient aged 36 years, mesial – extraction due to caries. Reshaper surface model. **Result:** 20 nl cervical volume loss after brushing with toothbrush *Rapid Relief*.

▪ Distal (left side)



Overall volume loss due to cervical wear: 24 nl

Cervical mesh surface: 1.184 mm²

Height loss scale

colour coding:

Blue: 4 – 10 μ m

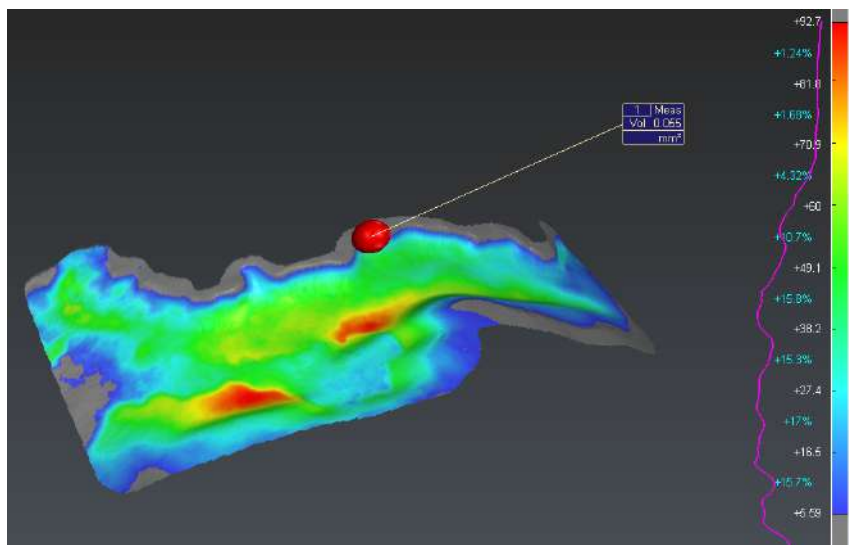
Green: 10 – 30 μ m

Yellow: 30 – 39 μ m

Red: 39 – 52 μ m

Figure 67: Molar A46 of patient aged 36 years, distal – extraction due to caries. Reshaper surface model. **Result:** 24 nl cervical volume loss after brushing with toothbrush *Rapid Relief*.

5.4.4 Incisor B41 – Reshaper 3D



Overall volume loss due to cervical wear: **55 nl**

Cervical mesh surface: **2.000 mm²**

Height loss scale

colour coding:

Blue: 5 – 27 μm

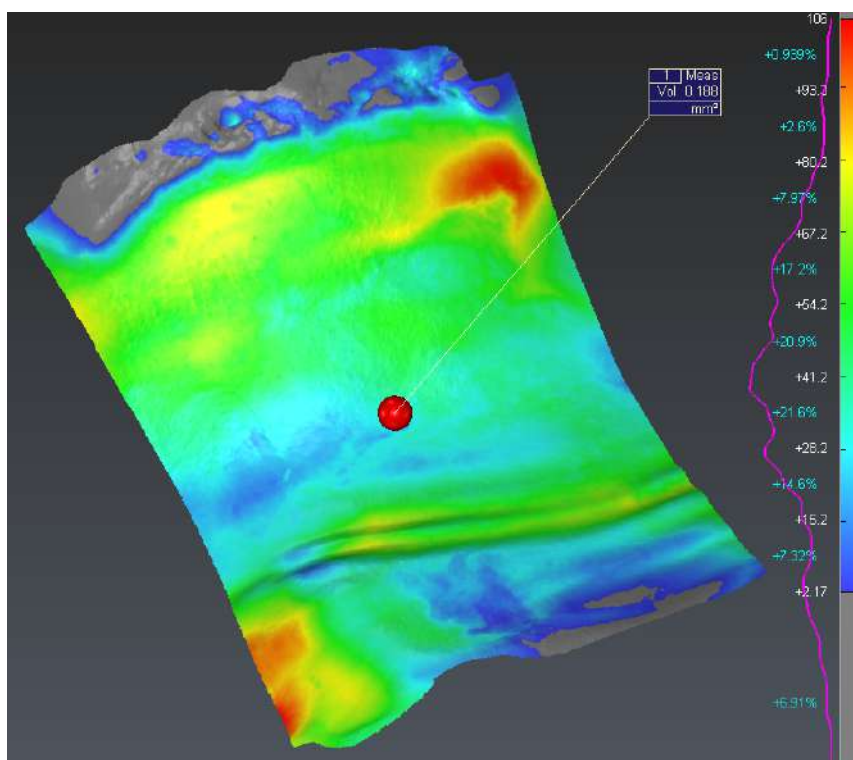
Green: 27 – 60 μm

Yellow: 60 – 72 μm

Red: 72 – 93 μm

Figure 68: Incisor B41 of a patient aged 40 years – extraction for periodontal reasons. Reshaper surface model. **Result:** 55 nl cervical volume loss after brushing with toothbrush Jubilee.

5.4.5 Incisor B42 – Reshaper 3D



Overall volume loss due to cervical wear: **188 nl**

Cervical mesh surface: **5.142 mm²**

Height loss scale

colour coding:

Blue: 2– 28 μm

Green: 28 – 67 μm

Yellow: 67 – 82 μm

Red: 82 – 106 μm

Figure 69: Incisor B42 of a patient aged 61 years – extraction for periodontal reasons. Reshaper surface model. **Result:** 188 nl cervical volume loss after brushing with toothbrush Jubilee.

5.4.6 Canine B43 – Reshaper 3D

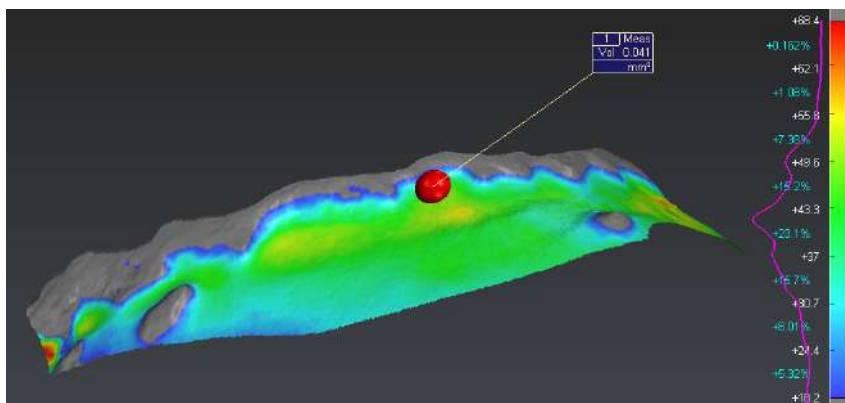


Figure 70: Canine B43 of a patient aged 58 years – extraction for periodontal reasons. **Result:** 41 nl cervical volume loss after brushing with toothbrush Jubilee.

Overall volume loss due to cervical wear: **41 nl**

Cervical mesh surface: **1.495 mm²**

Height loss scale

colour coding:

Blue: 18 – 31 μm

Green: 31 – 50 μm

Yellow: 50 – 56 μm

Red: 56 – 68 μm

5.4.7 Premolar B45 – Reshaper 3D

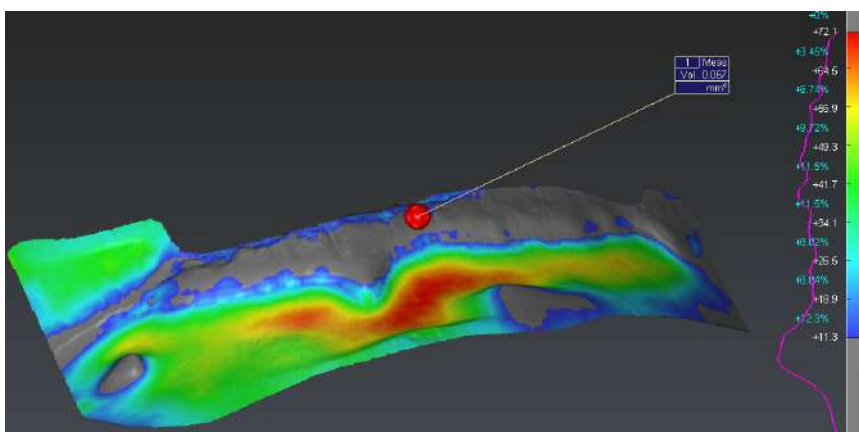


Figure 71: Premolar B45 of a patient aged 13 years – extraction for orthodontic reasons. Reshaper surface model. **Result:** 67 nl cervical volume loss after brushing with the toothbrush Jubilee.

Overall volume loss due to cervical wear: **67 nl**

Cervical mesh surface: **2.668 mm²**

Height loss scale

colour coding:

Blue: 11 – 27 μm

Green: 27 – 50 μm

Yellow: 50 – 58 μm

Red: 58 – 72 μm

5.5 Tooth comparison

The composite images of each tooth were cross-referenced with visual wear coding panels (Section 5.2). Two investigators, one unblinded (KW) and one blinded (PG), evaluated each abrasion pattern before and after the brushing cycle. The results are presented in Tables 12 and 13.

5.5.1 Coding of abrasion patterns per tooth: Toothbrush *Rapid Relief*

Table 12: Human teeth model A



Human teeth A41–A47
in anatomical position.

Incisor A41 (55 y – Paro)	Pre	Post
FAM	2	1
AP	3	3
EPE	0	0
EI	1	2
ODT	0	2
DC	1	0
PF	0	2
CEJ	Type 1	Type 2

Incisor A42 (40 y – Paro)	Pre	Post
FAM	1	0
AP	1	2
EPE	0	1
EI	1	2
ODT	0	1
DC	3	0
PF	2	3
CEJ	Type 2	Type 2

Canine A43 (58 y – Paro)	Pre	Post
FAM	2	1
AP	3	3
EPE	0	0
EI	1	1
ODT	0	0
DC	3	0
PF	2	2
CEJ	Type 2	Type 2

Premolar A44 (14 y – Ortho)	Pre	Post
FAM	1	0
AP	0	0
EPE	1	2
EI	1	2
ODT	0	0
DC	1	0
PF	1	1
CEJ	Type 3	Type 3

Premolar A45 (14 y – Ortho)	Pre	Post
FAM	1	2
AP	1	1
EPE	1	1
EI	1	2
ODT	0	0
DC	1	0
PF	1	1
CEJ	Type 3	Type 3

Molar A46 (36 y – Caries)	Pre	Post
FAM	1	1
AP	2	2
EPE	1	1
EI	3	3
ODT	0	0
DC	3	2
PF	0	0
CEJ	Type 3	Type 3

Molar A47 (19 y – 3rd)	Pre	Post
FAM	1	1
AP	0	0
EPE	3	3
EI	3	3
ODT	0	1
DC	3	1
PF	2	2
CEJ	Type 1	Type 1

3D analysis:

Tooth	Volume loss results*	
A42:	0.043 mm ³	43 nl
A44:	0.050 mm ³	50 nl
A4 mesial:	0.020 mm ³	0.044 mm ³
A46 distal:	0.024 mm ³	
		20 nl
		24 nl

*For visualisation: 1 mm of a G30 endo irrigation needle contains 20 nanolitres.

5.5.2 Coding of abrasion patterns per tooth: Toothbrush *Jubilee*

Table 13: Human teeth model B



Human teeth B41–B47
in anatomical position.

Incisor B41 (40 y – Paro)	Pre	Post
FAM	1	1
AP	3	3
EPE	0	1
EI	1	1
ODT	0	0
DC	3	0
PF	1	2
CEJ	Type 2	Type 2

Incisor B42 (61 y – Paro)	Pre	Post
FAM	3	1
AP	3	3
EPE	0	0
EI	2	2
ODT	0	0
DC	3	0
PF	2	2
CEJ	Type 2	Type 2

Canine B43 (58 y – Paro)	Pre	Post
FAM	2	2
AP	3	3
EPE	0	1
EI	1	2
ODT	0	0
DC	2	1
PF	2	3
CEJ	Type 2	Type 2

Premo- lar B44 (13 y – Ortho)	Pre	Post
FAM	2	1
AP	1	2
EPE	2	3
EI	2	2
ODT	0	1
DC	1	0
PF	2	3
CEJ	Type 3	Type 3

Premolar B45 (13 y – Ortho)	Pre	Post
FAM	0	2
AP	0	1
EPE	0	2
EI	2	3
ODT	0	2
DC	1	0
PF	2	3
CEJ	Type 3	Type 3

Molar B46 (31 y – Caries)	Pre	Post
FAM	2	2
AP	2	2
EPE	1	2
EI	1	2
ODT	0	0
DC	3	0
PF	1	3
CEJ	Type 1	Type 2

Molar B47 (19 y – 3rd)	Pre	Post
FAM	0	0
AP	0	1
EPE	0	2
EI	1	2
ODT	0	0
DC	2	0
PF	0	0
CEJ	Type 2	Type 2

3D analysis

Tooth	Volume loss re- sults*	
B41:	0.055 mm ³	55 nl
B42:	0.188 mm ³	188 nl
B43:	0.041 mm ³	41 nl
B45:	0.067 mm ³	67 nl

*For visualisation: 1 mm of a G30 endo irrigation needle contains 20 nanolitres.

5.6 Descriptive analysis of abrasion patterns

This section examines the morphological alterations induced by abrasion, encompassing shifts in surface texture, infractions, exposure of dentin tubules, and an analysis of calculus accumulation and the exposed root surface.

5.6.1 Functional abrasion marks (FAM)

In middle-aged incisors and canines (41–43), both *Rapid Relief* and *Jubilee* toothbrushes resulted in a one-code smoothing of the enamel surface after the brushing procedure (Fig. 72). Within each group, one juvenile premolar experienced a one-code smoothing, while its counterpart exhibited more scratches post-cleaning. Young adulthood molars showed no significant changes in abrasion marks on the enamel surface due to the cleaning process. Abrasion marks on the smooth surfaces of all tested teeth lost their superficial masking, but complete disappearance occurred only in the case of one old incisor, A42.

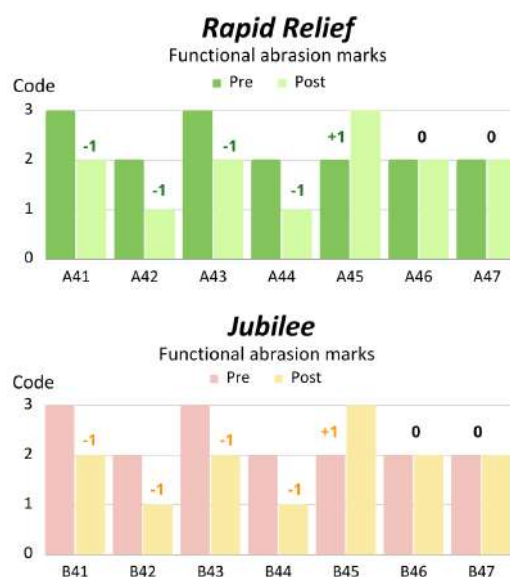


Figure 72: Bar charts showing the difference of functional abrasion marks (FAM) pre and post brushing.

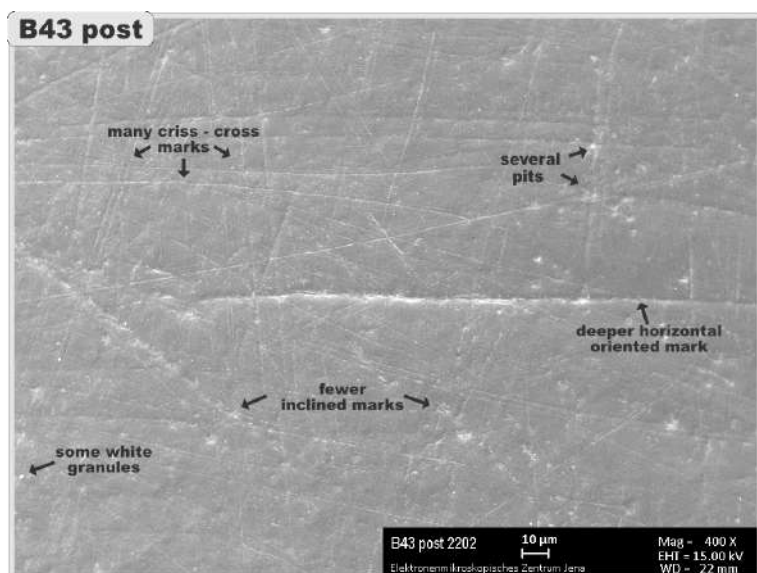


Figure 73: Canine B43 of a 58 years old patient - post brushing with *Jubilee*: Functional abrasion marks (FAM 2) show several small pits, many criss-cross marks, some oblique marks, a clear horizontal, more profound mark and white granules of unknown origin. **Mag: 400x**

SEM provides a high-resolution visualization of microwear consequences, revealing abrasion marks of varied degrees on tooth surfaces. These encompass horizontal, vertical, or transverse abrasion marks, as well as long scratches and iso-diametric pits. Illustrated in Fig. 73 is tooth B43 from a 58-year-old individual, showcasing a distinctive criss-cross abrasion pattern with individual deeper horizontally oriented marks. Notably, perikymata and exposed prisms are no longer visible. The diverse orientations of abrasion marks in horizontal, vertical, or oblique directions can be attributed to the three distinct brushing programs.

5.6.2 Appearance perikymata (AP)

The appearance of perikymata remained nearly unchanged in both toothbrushes, as depicted in Fig. 74. A subtle levelling out of perikymata was observed only in the middle-aged incisor A42 and juvenile premolar B44. Notably, toothbrush *Jubilee* effectively levelled the damaged enamel surface of premolar B44 after orthodontic bracket removal, a detail not visible under typical clinical conditions. This observation could hold significance for post-orthodontic oral hygiene recommendations. Over the years, natural wear processes have contributed to the flattening of perikymata, accompanied by a decline in the proportion of prismatic enamel, a phenomenon associated with aging.

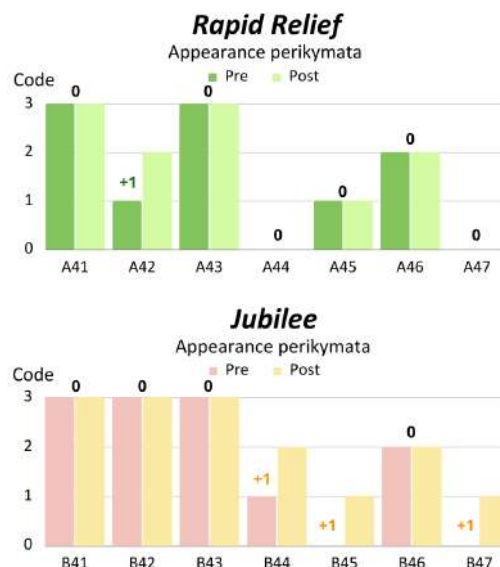


Figure 74: Bar charts showing the difference of appearance perikymata (AP) pre and post brushing.

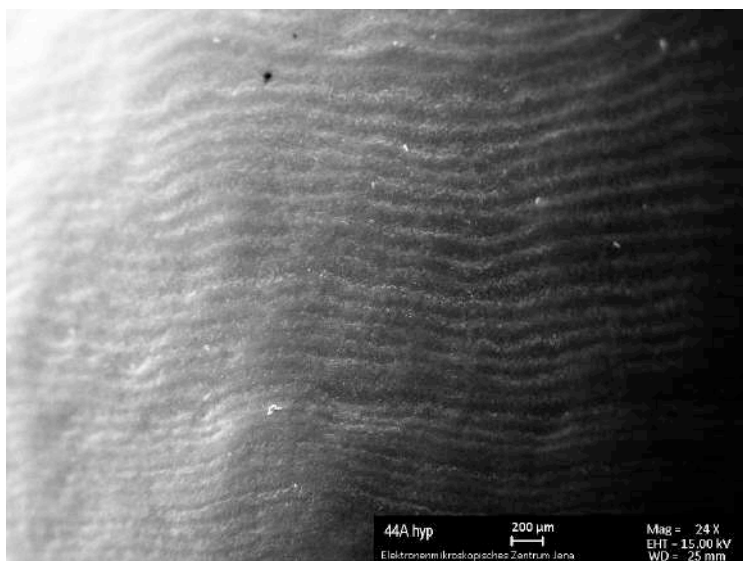


Figure 75: Premolar A44 of a 14 years old patient at baseline – Numerous incremental lines, the perikymata, are visible on the buccal tooth surface of the juvenile premolar, getting denser towards the cervical region. **Mag: 24x**

The perikymata are most densely packed towards the neck and decrease in density towards the occlusal or incisal edge of the surface (Fig. 75). These typically sinuous formations run in closed circles around the tooth and are even more compact on isolated enamel peninsulas that extend into the cementum. The most remarkable irregularities in the appearance of perikymata are observed in the cervical region.

5.6.3 Exposed prismatic enamel (EPE)

Following toothbrushing with *Jubilee*, a higher exposure of enamel prisms was evident compared to the use of *Rapid Relief*. Significantly increased wear of aprismatic enamel was observed after cleaning with the Jubilee toothbrush. In contrast, the baseline situation did not show remarkable changes after brushing with the Rapid Relief toothbrush (Fig. 76).

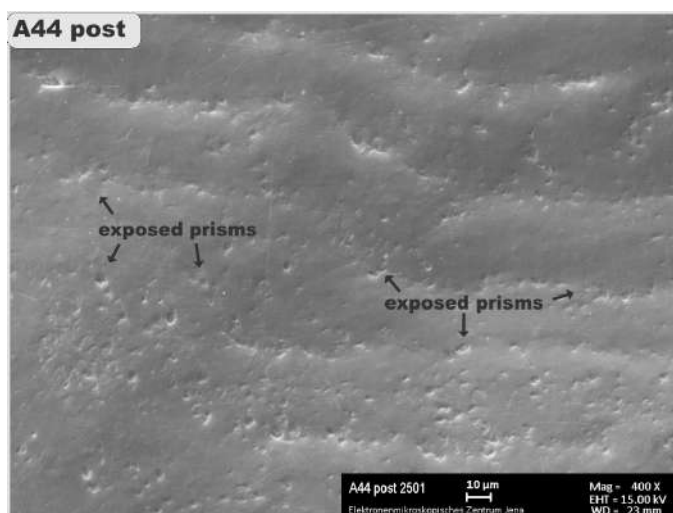


Figure 77: Premolar A44 of a 14 years old patient - post brushing with *Rapid Relief*: Exposure of prismatic enamel occurs because the immature aprismatic layer, which covers juvenile teeth, remains fragile shortly after tooth eruption and can be easily removed through intensive toothbrushing. **Mag: 400x**

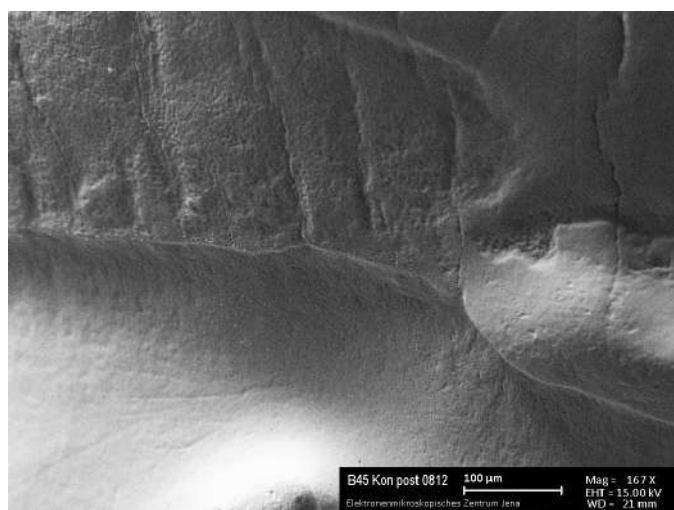


Figure 78: Premolar B45 of a 13 years old patient - post brushing with *Jubilee*: Numerous tiny indentations on the cervical enamel margin indicate exposed prismatic enamel. **Mag: 167x**

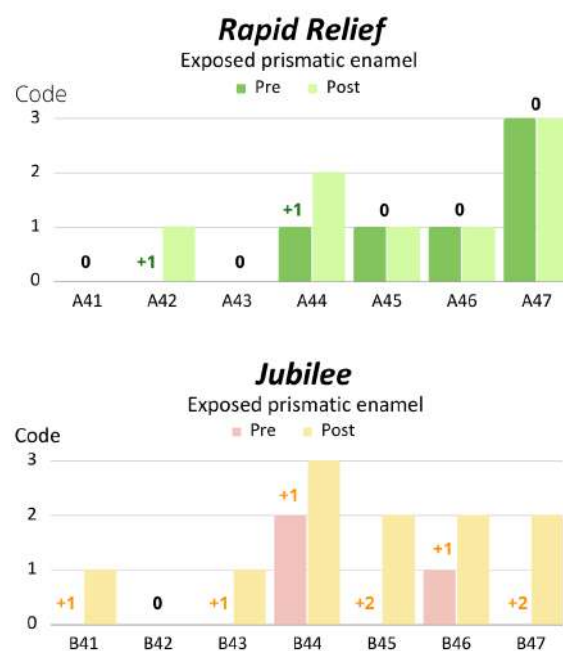


Figure 76: Bar charts showing the difference of exposed prismatic enamel (EPE) pre and post brushing.

As post-eruptive enamel maturation advances, the overall thickness of the aprismatic layer increases due to surface mineralization. Especially in juvenile teeth, prismatic areas are still expected, while middle-aged teeth are likely to have a predominantly aprismatic enamel surface (Gängler et al. 2005). For instance, in the juvenile premolar A44 (Fig. 77), abrasion removed the aprismatic layer in some areas, revealing the underlying prismatic structure. The microscopic examination of tiny indentations, averaging 6 µm in diameter, suggests a correspondence with the structures of enamel rod ends. Microscopic studies by Steiniger et al. (2010) have demonstrated that ameloblasts removed from a freshly erupted enamel surface leave hexagonal indentations in the enamel matrix with their tome extensions (Fig. 78).

5.6.4 Enamel infractions (EI)

In all teeth of both groups, the most significant changes were observed in enamel infractions (Fig. 79). Previously concealed and closed enamel cracks were exposed after abrasion in all teeth, with many widenings more than their original state. This phenomenon is especially pronounced near the cemento-enamel junction (CEJ), where the majority of enamel cracks were located. Despite preserving all teeth in a 0.1% thymol / 0.9% saline solution outside the scanning electron microscope (SEM), it is acknowledged that methodological factors may have contributed to the opening of enamel infractions.

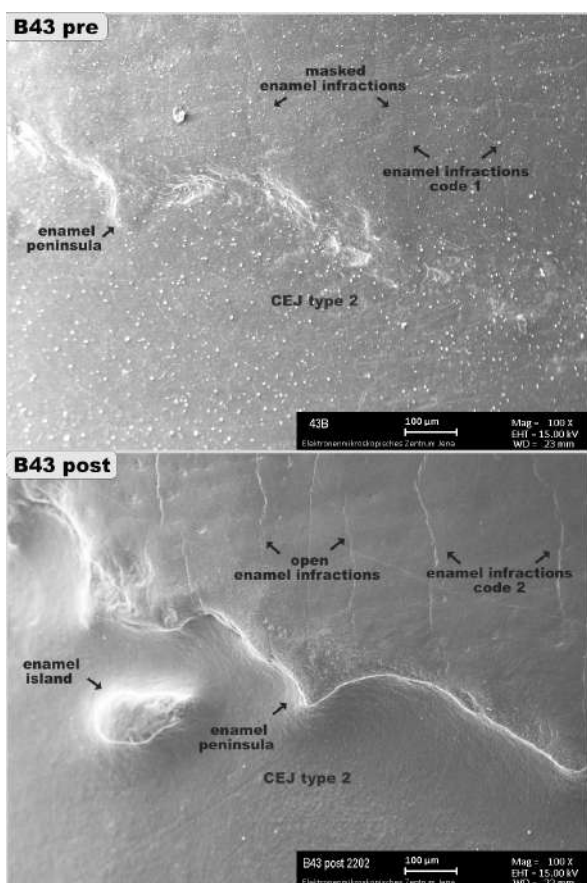


Figure 80: Canine B43 (58 yrs) pre and post brushing with toothbrush Jubilee: At baseline there were already numerous vertical enamel infractions on the cervical part of the tooth. Numerous vertical enamel infractions were already present on the cervical part of the tooth. Subsequent brushing exposed and slightly widened these infractions. Enamel peninsulas became more pronounced and defined, while sporadic enamel islands were unveiled on the root surface. **Mag: 100x**



Figure 79: Bar charts showing the difference of enamel infractions (EI) pre and post brushing.

Several studies affirm that teeth frequently exhibit vertical infractions in the enamel, often inconsequential and frequently unnoticed. The majority of these infractions are so inconspicuous that they are barely visible under direct illumination and remain undetectable on routine intraoral images, leading to a frequent clinical underestimation of their prevalence. The formation of enamel infractions is presumed to be associated with intrinsic defects that manifest during tooth development. Most identified vertical infractions in these studies ranged from 100 to 1,000 μm in length, with longer infractions generally more extensive than shorter ones. The width varied between 1 μm and 5 μm . Notably, in this particular sample, none of these infractions extended to the occlusal surface (Fig. 80).

5.6.5 Open dentin tubules (ODT)

No distinct pattern has been identified. Among *Rapid Relief* teeth, dentin tubules were exposed in two middle-aged incisors (A41, A42) and in a young adult molar (A47). In *Jubilee* teeth, open dentin tubules were observed in the two juvenile premolars (B44 and B45).

Morphological characterization of these sample teeth rarely revealed exposed dentinal tubules (Fig. 81). However, when the cervical abrasion lesion extended into the lower root regions, exposed dentinal tubules became visible within the depths of wedge-shaped lesions.

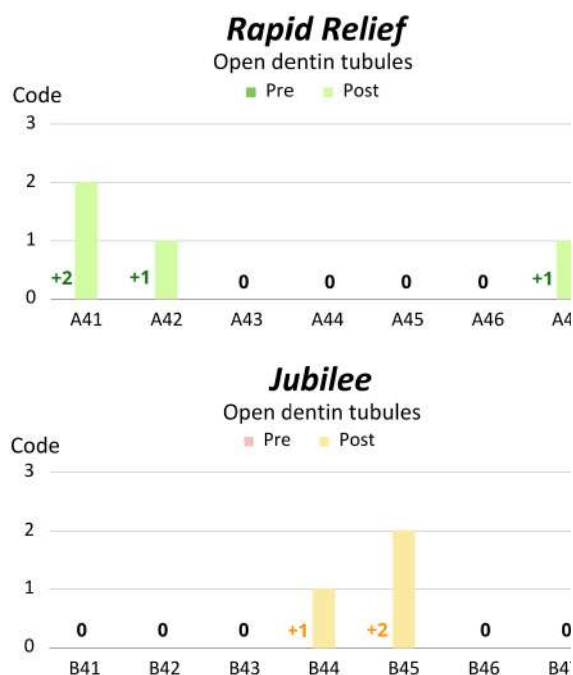


Figure 81: Bar charts showing the difference of open dentin tubules (ODT) pre and post brushing.

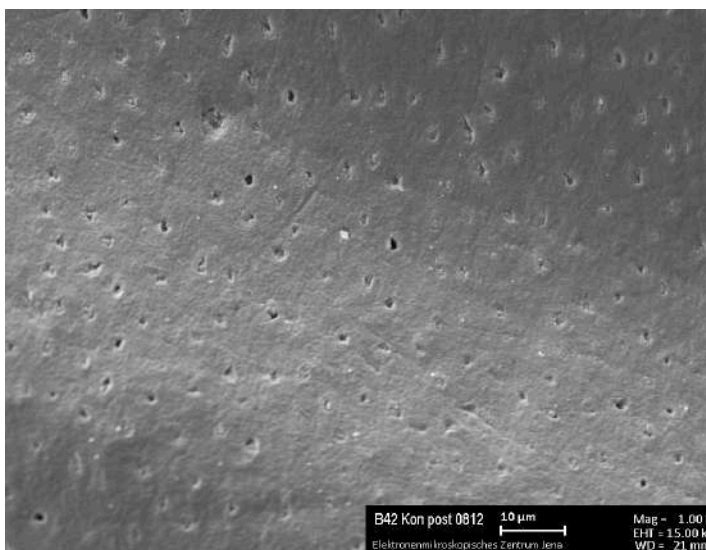


Figure 82: Incisor B42 (61 yrs) post brushing with toothbrush *Jubilee*: Following the three-year toothbrushing cycle, dentinal tubules were exposed and opened at various spots on the root surface. **Mag: 1000x**

Incisor B42 exhibits a uniform distribution of open dentin tubules on the abraded root surface after the tooth-brushing cycle (Fig. 82). Moreover, numerous abrasion marks are discernible. Upon closer inspection at higher magnification, variations in the diameter of dentinal tubule openings become evident. Some entrances are wide open, others narrowed, and some appear to be completely closed.

5.6.6 Dental calculus (DC)

All teeth brushed by *Rapid Relief* and *Jubilee* exhibited typical surface changes and reduced dental calculus even in concealed areas after the abrasion cycle (Fig. 83). Notably, at the cemento-enamel junction, dental calculus was effectively removed, underscoring the contribution of brushing to calculus residue elimination. This holds clinical significance as it visibly reduces plaque attachment in vulnerable areas. As demonstrated in this thesis, regular toothbrushing plays a crucial role in smoothing tooth surfaces, minimizing plaque deposition, and promoting overall healthy periodontal care. Examples in Fig. 84 and Fig. 85 illustrate a significant reduction in calculus in the cervical area due to toothbrushing.

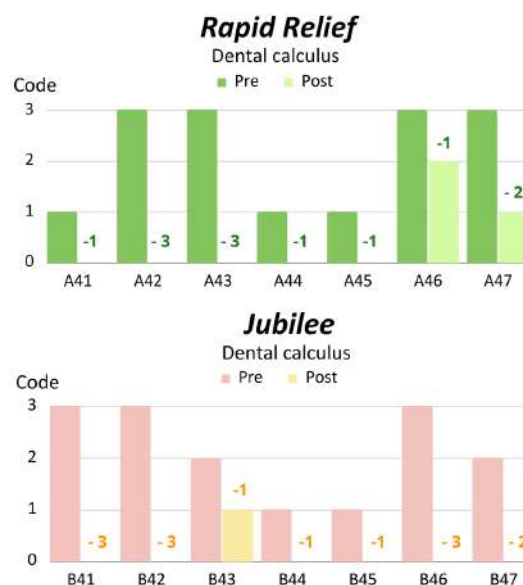


Figure 83: Bar charts showing the difference of dental calculus (DC) pre and post brushing.

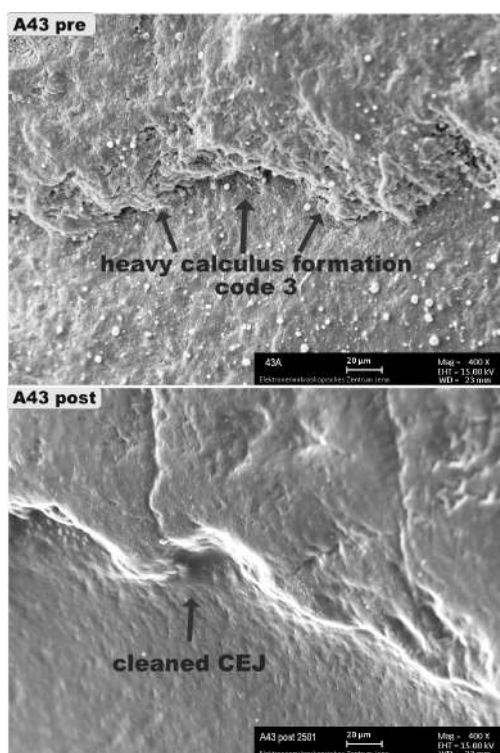


Figure 84: Canine A43 (58 yrs) - pre and post brushing with the *Rapid Relief* toothbrush: At baseline, the cervical area was obscured by a substantial layer of calculus and smear layer. However, after three years of toothbrushing, these deposits were entirely removed, resulting in a rounded and refined cemento-enamel junction. **Mag: 400x**

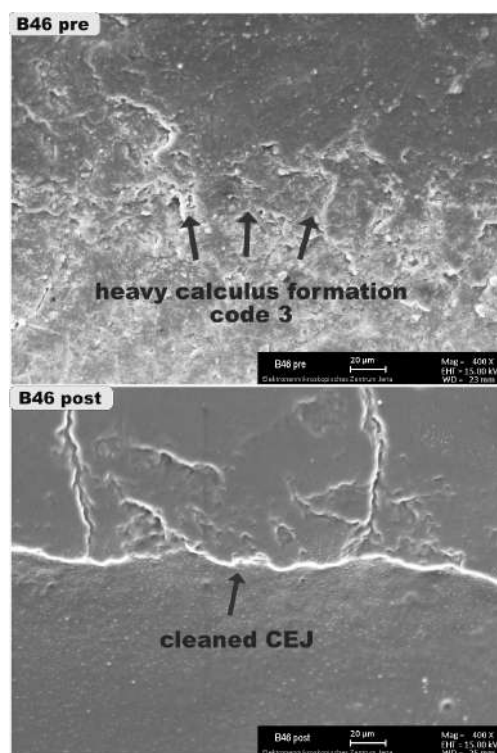


Figure 85: Molar B46 (31 yrs) - pre and post brushing with the *Jubilee* toothbrush: At baseline, a severe formation (DC Code 3) was deposited on the tooth neck. Following the three-year toothbrush approach, the cemento-enamel junction was thoroughly cleaned of calculus and exhibited a rounded appearance. **Mag: 400x**

5.6.7 Peninsula formation (PF)

In the *Rapid Relief* teeth, two middle-aged incisors, A41 and A42, demonstrated signs of wear in the enamel peninsula overlapping root dentin. Almost all of the *Jubilee* teeth, with the exception of one middle-aged anterior incisor (B42) and the wisdom tooth (B47), also showed changes to the enamel peninsula overlying the root dentin, which can be attributed to abrasion by the toothbrush (*Fig. 86*). The demasking of peninsulas and especially enamel islands overlapping the root dentin by toothbrushing abrasion is described for the first time. Enamel islands appeared on teeth A42, B43, B44, B45, and B46.

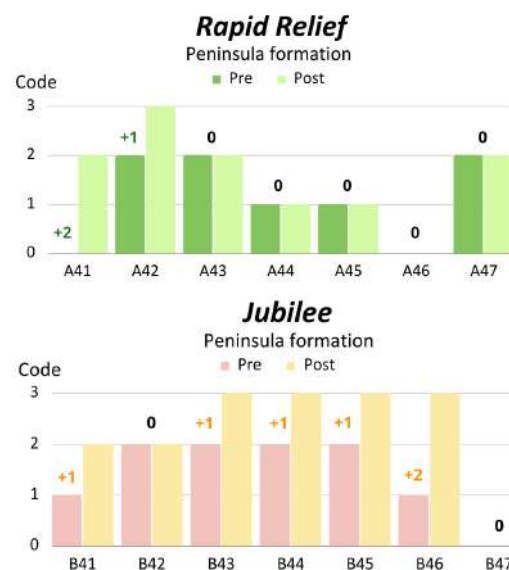


Figure 86: Bar charts showing the difference of peninsula formation (PF) pre and post brushing.

From a clinical perspective, enamel peninsulas and enamel islands pose a heightened risk of cervical abrasion due to their hardness. Moreover, they may contribute to biofilm attachment, establishing a new area of abrasion risk, along with the entire margin along the cementum-(dentin)-enamel interface. Two instances of enamel islands emerging as a consequence of toothbrushing are illustrated in *Fig. 87*.

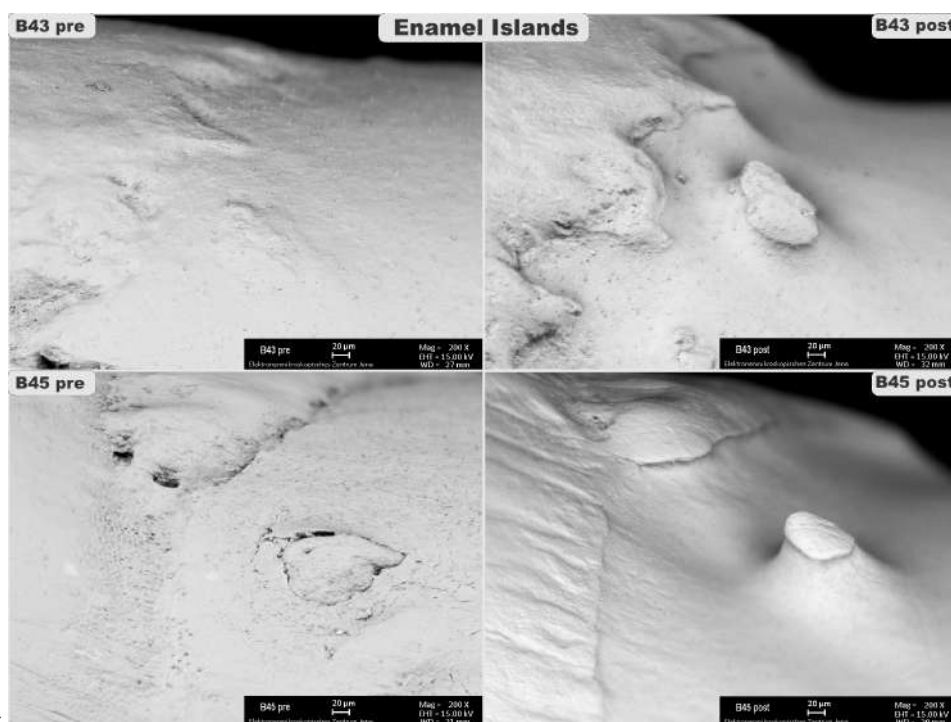
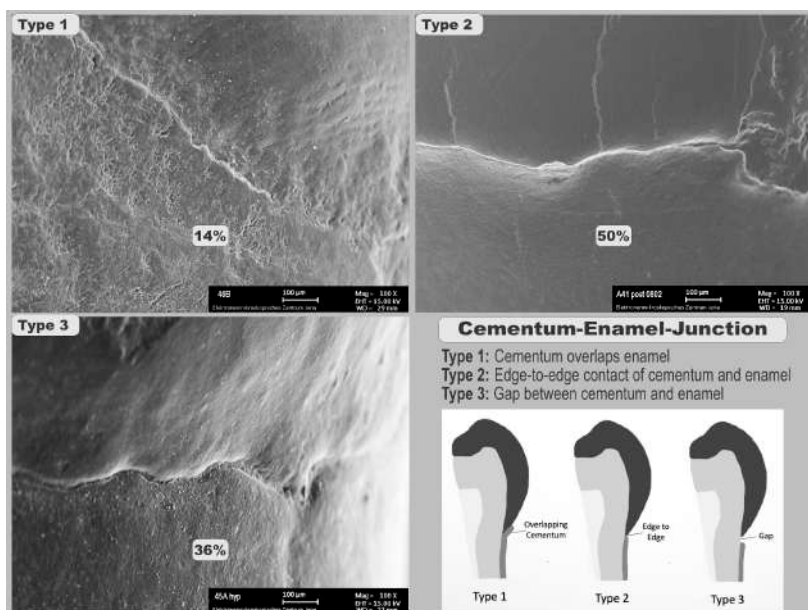


Figure 87: Canine B43 (58 yrs) and premolar B45 (13 yrs) after brushing with the *Jubilee* toothbrush: Previously concealed enamel islands were unveiled on the root surface, protruding impressively after three years of tooth brushing. **Mag:** 200x

5.6.8 Cemento-enamel junction types (CEJ)

The CEJ forms the interface between the enamel-covered crown and the cement-covered root surface and is susceptible to environmental influences, including abrasion and erosion.



The enamel layer in this area is fragile, barely 0.2 mm (Aw et al. 2002). Three anatomical variants of CEJ have been described in the past (Gängler et al. 2005).

1. **Type 1: 60%** Cementum overlapping enamel.
2. **Type 2: 30%** Cementum is in edge-to-edge contact with the enamel.
3. **Type 3: 10%** A gap between cementum and enamel.

Figure 88: Cemento-enamel junction types: The most common type in this sample was type 2 (edge-to-edge) with 50%, followed by type 3 with 36% (a gap between cementum and enamel). Type 1 (cementum overlapping enamel) occurred least frequently with 14%. **Mag: 100x**

All three forms are shown in Figure 88.

The percentages of CEJ types in the sample teeth is (see 7.1 Contingency table) Edge-to-edge (type 2): 50% > Gap (type 3): 36% > Cementum overlapping enamel (type 1): 14%



Figure 89: Gap (type 3) on juvenile premolar A45. The groove of the gap shows tiny depressions, which are considered a typical morphological pattern of enamel in the cervical region. Despite this groove, no dentin is exposed (Enlarged section from Fig 88.).

The most prevalent type of cemento-enamel junction observed was the edge-to-edge contact (type 2), followed by the gap (type 3). The gap type was particularly prominent in juvenile premolars, and tooth A46, also displaying a gap type, belonged to a young adulthood patient (36 yrs). Overlapping cementum (type 1) was identified in only four out of 28 tooth specimens. Specifically, overlapping cementum was present in one middle-aged tooth (A41, 55 yrs), one young adulthood tooth (B46, 31 yrs), and one juvenile tooth (A47, 19 yrs). After brushing, middle-aged and young adulthood teeth transitioned to edge-to-edge contact (Fig. 89). Despite previous reports indicating that cementum overlapping enamel (type 1) is common in human teeth, this type was infrequently represented in this study.

5.6.9 Morphology of cervical abrasion lesions

The three-year toothbrushing cycle revealed that abrasion resulted in a loss of cervical tooth structure, primarily manifesting as wedge-shaped lesions (Fig. 90). However, at the observed stage, the lesions are still in their early phase, making it challenging to anticipate their eventual shape. Most cervical lesions tend to progress gradually in depth, irrespective of their initial form. Consequently, this study observed a notable alteration in the morphology of the cemento-enamel junction over time. The enamel margin shifted slightly coronally due to wear processes, even with the use of a low-abrasive dentifrice and a manual toothbrush with a flexible ball joint neck and tapered bristles.

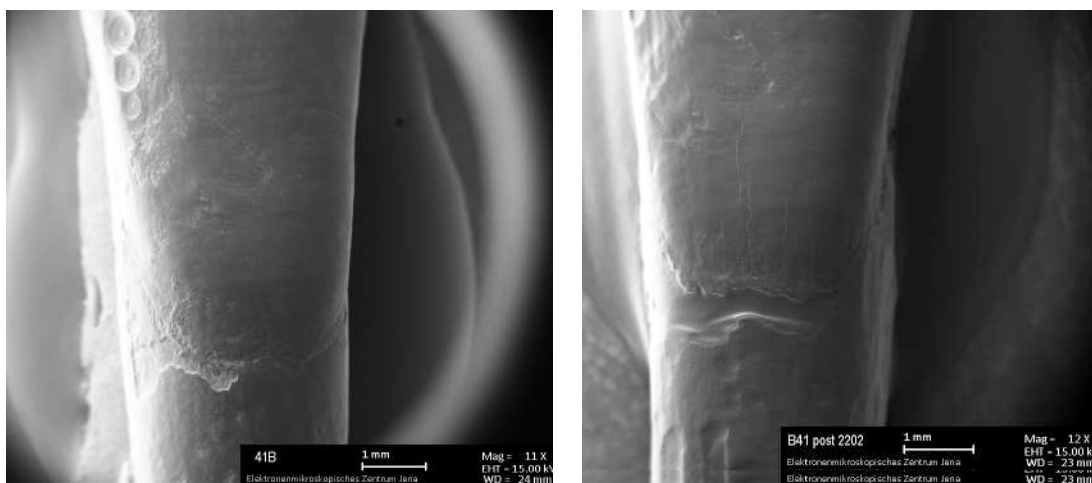


Figure 90: Incisor B41 (40 yrs) - pre and post brushing with Jubilee toothbrush: The friable, superficially furrowed cervical region was smoothed by toothbrushing, yet it also developed a more pronounced, deepened wedge-shaped lesion. A distinctive characteristic of wedge-shaped lesions is a concave coronal and an apical convex surface. **Mag: 11/12x**

A single saucer-shaped cervical lesion, pre-existing at baseline, underwent widening due to toothbrushing (Fig. 91). Following the three-year toothbrushing cycle, this saucer-shaped lesion exhibited noticeable horizontal grooves on the root surface. Horizontal, smooth grooves ranging from 5 to 250 μm can be interpreted as indicative of abrasion and/or erosion.

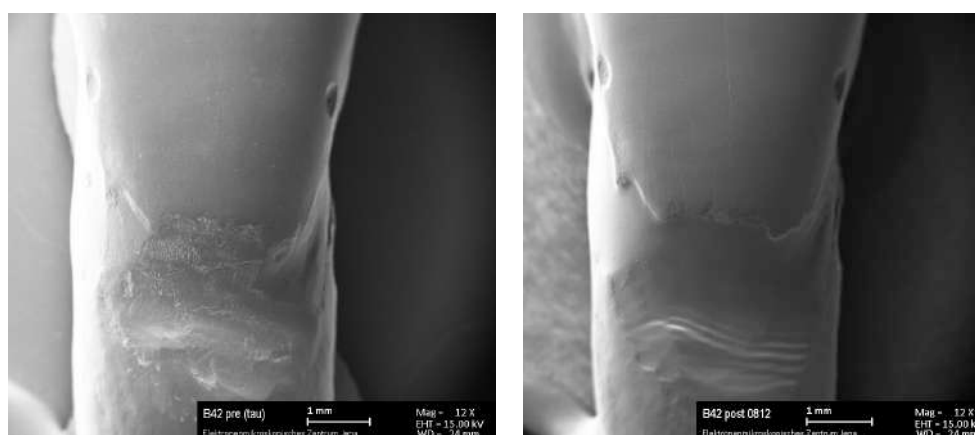


Figure 91: Incisor B42 (61 yrs) pre and post brushing with Jubilee toothbrush: The saucer-shaped cervical lesion initially displayed a rough, furrowed surface, which was subsequently smoothed and exhibited distinct horizontal grooves in the apical region due to abrasion from toothbrushing. **Mag: 12x**

5.7 Statistical evaluation

The comparison of the abrasion patterns before and after tooth brushing is of particular interest and requires unpolished human teeth with natural surface morphology of different ages to be able to determine clinically relevant changes.

Contingency table 14: Manual toothbrush *Rapid Relief*

Tooth	FAM	AP	EPE	EI	ODT	DC	PF	CEJ	Σ	Diff.
A41	PRE	2	3	0	1	0	1	Type 1	7	+3
	POST	1	3	0	2	2	0	Type 2	10	
A42	PRE	1	1	0	1	0	3	Type 2	8	+1
	POST	0	2	1	2	1	0	Type 2	9	
A43	PRE	2	3	0	1	0	3	Type 2	11	-4
	POST	1	3	0	1	0	0	Type 2	7	
A44	PRE	1	0	1	1	0	1	Type 3	5	0
	POST	0	0	2	2	0	0	Type 3	5	
A45	PRE	1	1	1	1	0	1	Type 3	6	+1
	POST	2	1	1	2	0	0	Type 3	7	
A46	PRE	1	2	1	3	0	3	Type 3	10	0
	POST	1	2	1	3	0	2	Type 3	9	
A47	PRE	1	0	3	3	0	3	Type 1	10	-1
	POST	1	0	3	3	1	1	Type 1	9	
Σ	PRE	9	10	6	11	0	15	3xT2 / 3xT3 / 1xT1	T Ø in %*	
	POST	6	11	8	15	4	3	3xT2 / 3xT3 / 1xT1		
Diff.		-3	+1	+2	+4	+4	-12	+3	*43% T2 / 43% T3 / 14% T1	

Contingency table 15: Manual toothbrush *Jubilee*

Tooth	FAM	AP	EPE	EI	ODT	DC	PF	CEJ	Σ	Diff.
B41	PRE	1	3	0	1	0	3	Type 2	9	-1
	POST	1	3	1	1	0	0	Type 2	8	
B42	PRE	3	3	0	2	0	3	Type 2	13	-5
	POST	1	3	0	2	0	0	Type 2	8	
B43	PRE	2	3	0	1	0	2	Type 2	10	+2
	POST	2	3	1	2	0	1	Type 2	12	
B44	PRE	2	1	2	2	0	1	Type 3	10	+2
	POST	1	2	3	2	1	0	Type 3	12	
B45	PRE	0	0	0	2	0	1	Type 3	5	+8
	POST	2	1	2	3	2	0	Type 3	13	
B46	PRE	2	2	1	1	0	3	Type 1	10	+1
	POST	2	2	2	2	0	0	Type 2	11	
B47	PRE	0	0	0	1	0	2	Type 2	3	+2
	POST	0	1	2	2	0	0	Type 2	5	
Σ	PRE	10	12	3	10	0	15	4xT2 / 2xT3 / 1xT1	T Ø in %*	
	POST	9	15	11	14	3	1	5x T2 / 2x T3 / --		
Diff.		-1	+3	+8	+4	+3	-14	+6	*56% T2 / 28% T3 / 14% T1	

5.7.1 Absolute and relative frequency

Table 16: Absolute and relative frequency of abrasion patterns - *Rapid Relief*

Code	Model A: <i>Rapid Relief</i>	Absolute frequency				Relative frequency				
		0	1	2	3	0	1	2	3	
FAM	PRE	1 1 1 1 1 2 2	0	5	2	0	0%	71%	29%	0%
	POST	0 0 1 1 1 1 2	2	4	1	0	29%	57%	14%	0%
AP	PRE	0 0 1 1 2 3 3	2	2	1	2	29%	29%	14%	29%
	POST	0 0 1 2 2 3 3	2	1	2	2	29%	14%	29%	29%
EPE	PRE	0 0 0 1 1 1 3	3	3	0	1	43%	43%	0%	14%
	POST	0 0 1 1 1 2 3	2	3	1	1	29%	43%	14%	14%
EI	PRE	1 1 1 1 1 3 3	0	5	0	2	0%	71%	0%	29%
	POST	1 2 2 2 2 3 3	0	1	4	2	0%	14%	43%	29%
ODT	PRE	0 0 0 0 0 0 0	7	0	0	0	100%	0%	0%	0%
	POST	0 0 0 0 1 1 2	4	2	1	0	57%	29%	14%	0%
DC	PRE	1 1 1 3 3 3 3	0	3	0	4	0%	43%	0%	57%
	POST	1 2 0 0 0 0 0	5	1	1	0	71%	14%	14%	0%
PF	PRE	0 0 1 1 2 2 2	2	2	3	0	29%	29%	43%	0%
	POST	0 1 1 2 2 2 3	1	2	3	1	14%	29%	43%	14%

grey = minor values; dark green = max value (pre); light green = max value (post)

Table 17: Absolute and relative frequency of abrasion patterns - *Jubilee*

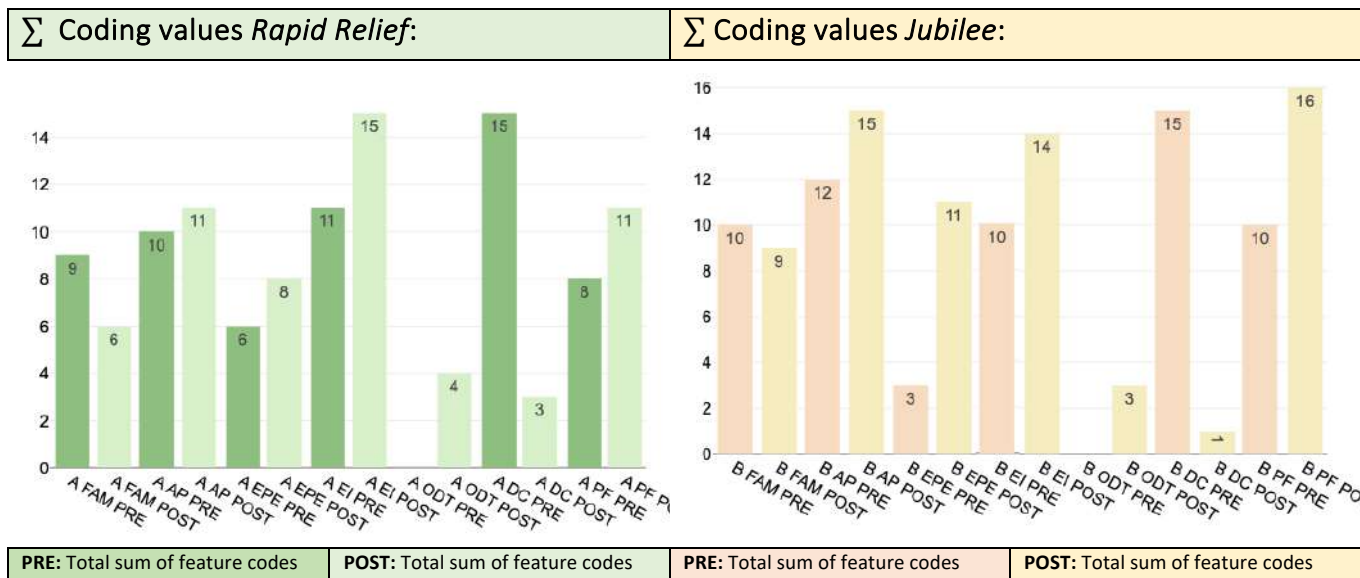
Code	Model B: <i>Jubilee</i>	Absolute frequency				Relative frequency				
		0	1	2	3	0	1	2	3	
FAM	PRE	0 0 1 2 2 2 3	2	1	3	1	29%	14%	43%	14%
	POST	0 1 1 1 2 2 2	1	3	3	0	14%	43%	43%	0%
AP	PRE	0 0 1 2 3 3 3	2	1	1	3	29%	14%	14%	43%
	POST	1 1 2 2 3 3 3	0	2	2	3	0%	29%	29%	43%
EPE	PRE	0 0 0 0 0 1 2	5	1	1	0	71%	14%	14%	0%
	POST	0 1 1 2 2 2 3	1	2	3	1	14%	29%	43%	14%
EI	PRE	1 1 1 1 2 2 2	0	4	3	0	0%	57%	43%	0%
	POST	1 2 2 2 2 2 3	0	1	5	1	0%	14%	71%	14%
ODT	PRE	0 0 0 0 0 0 0	7	0	0	0	100%	0%	0%	0%
	POST	0 0 0 0 0 1 2	5	1	1	0	71%	14%	14%	0%
DC	PRE	1 1 2 2 3 3 3	2	2	2	3	29%	29%	29%	43%
	POST	0 0 0 0 0 0 1	6	1	0	0	86%	14%	0%	0%
PF	PRE	0 1 1 2 2 2 2	1	2	4	0	14%	29%	57%	0%
	POST	0 2 2 3 3 3 3	1	0	2	4	14%	0%	29%	57%

grey = minor values; pale red = max value (pre); yellow = max value (post)

The contingency tables and frequencies (Tables 14–17) were used to get an overview of the categorical variables. CEJ type means in %: Type 2 (edge): 50% > Type 3 (gap): 36% > Type 1 (overlap): 14%.

5.7.2 Bar chart coding sum comparison

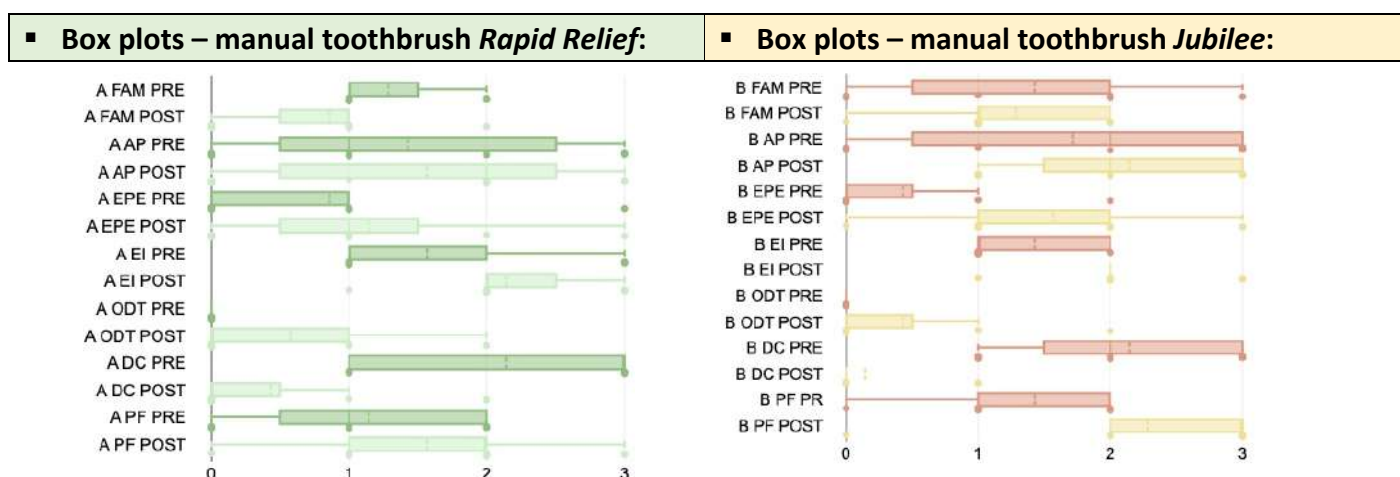
The bar charts illustrate in dark green/pale red the cumulative coding levels of the respective abrasion patterns before and in light green/yellow after the three-year toothbrushing cycle.



Comparing the two samples shows that in the case of *Jubilee*, some post-brushing abrasion patterns were more pronounced than in the *Rapid Relief* sample. These include **functional abrasion marks (FAM)**, **exposed prismatic enamel (EPE)** and **peninsular formation (PF)**. The following statistical tests were intended to verify whether the differences between the samples were significant.

5.7.3 Box plot abrasion patterns comparison

Graphical visualisation of the code distribution by quantile distances and the medians.



The medians illustrate the individual distribution of the abrasion patterns within the dentition used for both the *Rapid Relief* and the *Jubilee* toothbrush. In addition, they characterise individual tooth features (incisors, canines, premolars and molars) and the age of the test subjects who donated the teeth.

5.7.4 Mean value, variance, standard deviation and standard error

The empirical standard deviation (SD) is a scatter value that indicates how far measured values of a random experiment scatter around the empiric mean value \bar{x} . A high standard deviation suggests widely spread data and is a measure of the significance of the mean value. SD can also be calculated from the square root of variance. Empirical variance (=sample variance) indicates how widely the feature characteristics are scattered around an expected value μ . This can be used to estimate the variance of a random variable. The smaller the sample size, the weaker the estimation becomes. Dispersion is mostly underestimated. Therefore, a division by $n-1$ was made, reflecting a more accurate population dispersion. Variance is the basis for further calculations, such as hypothesis tests. The standard error (SE) is the empirical standard deviation divided by the root of the number of cases. The standard error approaches zero as the number of cases increases.

▪ **Table 18: Statistical values – manual toothbrush *Rapid Relief***

Rapid Relief	FAM PRE	FAM POST	AP PRE	AP POST	EPE PRE	EPE POST	EI PRE	EI POST	ODT PRE	ODT POST	DC PRE	DC POST	PF PRE	PF POST
Mean \bar{x}	1.29	0.86	1.43	1.57	0.86	1.14	1.57	2.14	0	0.57	2.14	0.43	1.14	1.57
Std D. s_A	0.49	0.69	1.27	1.27	1.07	1.07	0.98	0.69	0	0.79	1.07	0.79	0.90	0.98
Variance s_A^2	0.24	0.48	1.62	1.62	1.14	1.14	0.95	0.48	0	0.62	1.14	0.62	0.81	0.95
SE mean	0.24	0.35	0.64	0.64	0.54	0.54	0.49	0.35	0	0.39	1.07	0.22	0.57	0.79

Arithmetic mean value \bar{x} , empirical variance s^2 , standard deviation s , (corrected $\frac{1}{(n-1)}$); standard error mean = $SE = \frac{s}{\sqrt{n-1}}$

▪ **Table 19: Statistical values – manual toothbrush *Jubilee***

Jubilee	FAM PRE	FAM POST	AP PRE	AP POST	EPE PRE	EPE POST	EI PRE	EI POST	ODT PRE	ODT POST	DC PRE	DC POST	PF PRE	PF POST
Mean \bar{x}	1.43	1.29	1.71	2.14	0.43	1.57	1.43	2	0	0.43	2.14	0.14	1.43	2.29
Std D. s_B	1.13	0.76	1.38	0.9	0.79	0.98	0.53	0.58	0	0.79	0.9	0.38	0.79	1.11
Variance s_B^2	1.29	0.57	1.9	0.81	0.62	0.95	0.29	0.33	0	0.62	0.81	0.14	0.62	1.24
SE mean	0.57	0.38	0.69	0.45	0.40	0.49	0.27	0.29	0	0.40	0.45	0.19	0.40	0.56

Arithmetic mean value \bar{x} , empirical variance s^2 , standard deviation s , (corrected $\frac{1}{(n-1)}$); standard error mean = $SE = \frac{s}{\sqrt{n-1}}$

The means with relatively high standard deviations and consequently high standard error demonstrated the individual distribution of abrasion pattern codes in the dentition used for the toothbrush *Rapid Relief* and toothbrush *Jubilee* tests, characterising individual tooth characteristics (incisors, canines, premolars and molars) and the age of the subjects donating the teeth.

5.7.5 Hypothesis testing of abrasion patterns

Descriptive statistics of abrasion patterns coded for the first time in this report (*Section 5.5 and 7.1*) are, from a clinical point of view, most important. However, hypothesis testing was executed for pre- and post-brushing results (*Wilcoxon signed-rank test*) and manual toothbrush comparison (*Rapid Relief vs Jubilee*) with the *Mann–Whitney U test*.

▪ Wilcoxon signed-rank test (paired samples)

To measure the significance of changes in abrasion patterns within a model pre- and post-brushing cycle, the *Wilcoxon signed-rank test* was applied. This test is the non-parametric counterpart to the paired samples t-test. The advantage of the *Wilcoxon signed-rank test* is that it can be used even when the sample size is small and variables are ordinally scaled, as in this case. The *Wilcoxon signed-rank test* is often applied to medical scores.

H_0 = There is **no** difference in grading of abrasion patterns of teeth pre and post toothbrushing.

H_1 = There is a difference in grading of abrasion patterns of teeth pre and post toothbrushing.

▪ Table 20: W-test statistic of abrasion patterns

Rapid Relief				Jubilee			
	W_+	W_-	p		W_+	W_-	p
FAM	6.5	21.5	0.1875	FAM	23	5	0.5
AP	17.5	10.5	0.5	AP	23	5	0.125
EPE	20.5	7.5	0.25	EPE	27.5	0.5	0.015625
EI	25	3	0.0625	EI	25	3	0.0625
ODT	23	5	0.125	ODT	20.5	7.5	0.25
DC	0	28	0.0078125	DC	0	28	0.0078125
PF	20.5	7.5	0.25	PF	26.5	1.5	0.03125

$n = 7$; $\alpha = 0.05$ (one-tailed), $W_{crit} < 3$

The *Wilcoxon signed-rank test* ($n = 7$; $\alpha = 0.05$, o.t.) demonstrated for both toothbrushes significant differences for **dental calculus** removal ($p_{DC} = 0.0078$) (*Fig. 4 – Calculus removal*). The control toothbrush also showed significant differences in the W-test for **exposed prismatic enamel** ($p_{EPE} = 0.0156$) and **peninsula formation** ($p_{PF} = 0.0313$).

Due to numerous ties within the codes, tabulated $W_{+/-}$ were too conservative. Therefore, the W-test tended to select the null hypothesis, increasing the probability of a 2nd type error. It can be concluded that toothbrush *Rapid Relief* resulted in fewer wear changes of tooth morphology concerning the sample. In contrast, toothbrush *Jubilee* exposed significantly more prismatic areas in enamel and promoted the demasking of enamel peninsulas and enamel islands by abrasion.

▪ Mann–Whitney U test (independent samples)

Since morphological coding was ordinally scaled, the *non-parametric Mann–Whitney U test* was chosen for hypothesis testing. The *U-test* is the non-parametric counterpart of the *t-test* for independent samples and is distribution-free and, therefore, can be applied without verifying normal distribution. The *Mann–Whitney U test* is based on the idea of ranking data. In other words, it is not calculated with measured values, but these are replaced by ranks with which the actual test is performed. In this case, cross-tabulations were created to determine the *U-test* statistics for each morphological feature. The *Mann–Whitney U test* checks the difference between the two toothbrushes.

H_0 = No distinction between the pre and post difference values of toothbrush *Rapid Relief* and toothbrush *Jubilee* concerning the dependent variable (= investigated abrasion pattern).

H_1 = There is a distinction between the pre and post difference values of toothbrush *Rapid Relief* and toothbrush *Jubilee* concerning the dependent variable (= investigated abrasion pattern).

Expectation value: $\mu_U = \frac{n_1 \cdot n_2}{2} = \frac{49}{2} = 24.5$

If Σ (table values $49 \div 0.5$) = 24.5 indicates that there is no difference between the central tendencies of the toothbrush *Rapid Relief (RR)* sample and toothbrush *Jubilee (J)* sample.

▪ Exposed prismatic enamel (EPE):

EPE _{RR} \ EPE _J	0	1	0	1	0	0	0
1	0	0.5	0	0.5	0	0	0
0	0.5	1	0.5	1	0.5	0.5	0.5
1	0	0.5	0	0.5	0	0	0
1	0	0.5	0	0.5	0	0	0
2	0	0	0	0	0	0	0
1	0	0.5	0	0.5	0	0	0
2	0	0	0	0	0	0	0

$$\sum EPE = 8.5$$

The *Mann–Whitney U test* showed that the difference between *EPE_{RR}* and *EPE_J* with respect to the dependent variable was statistically significant. $U = 8.5$; $p = 0.038$; $r = 0.59$

For larger samples (> 20), the normal distribution could be used as an approximation for calculating **p-values**. For smaller samples, however, the value for **p** has to be calculated precisely.

The test value **U** was tested for significance using the Mann–Whitney table.

Sample number: $n_1 = 7$; $n_2 = 7$; **$U_{crit} = 8$** ;

Level of significance: $\alpha = 0.05$ (two-tailed), applied to all morphological codes.

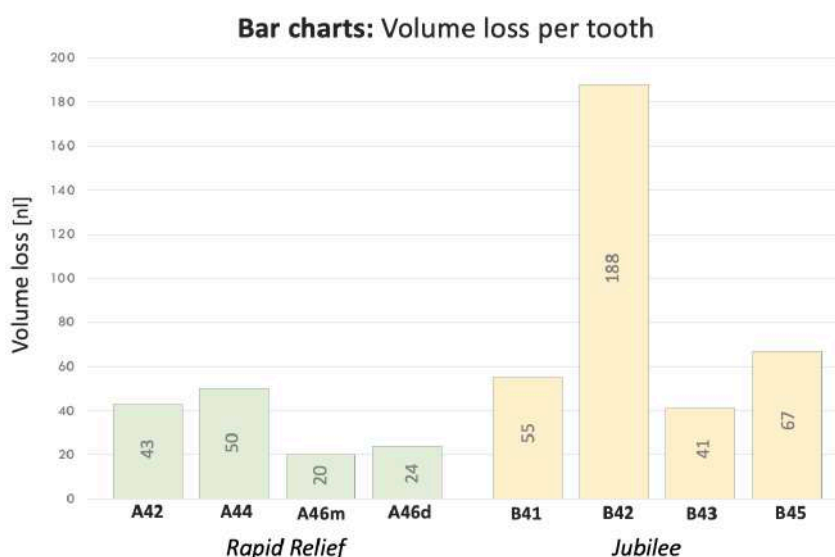
Result: Only the feature exposed prismatic enamel (EPE) reached the critical value of **$U_{crit} = 8$** and **$p = 0.038$** , demonstrating significant difference for *Jubilee* exposing more prismatic enamel compared to *Rapid Relief*.

Thus, the null hypothesis for the abrasion pattern EPE was rejected.

5.7.6 Statistical evaluation of 3D measurements

When assessing the volume loss of specific tooth types—namely, middle-aged anterior teeth A42, B41, canine B43, and juvenile premolars A44 and B45—remarkably similar volume losses were identified in both toothbrush samples. Conversely, a relatively minor loss of substance was observed in a middle-aged molar, likely attributed to the more pronounced convexity of the crown. It is important to note that drawing definitive conclusions from the examination of a single molar is insufficient. Due to its size, the molar had to be divided into two measuring units. The volume loss observed in B42

indicates an outlier. However, it is essential to acknowledge that the cervical lesion of B42 was already considerably more pronounced at baseline of the examination, potentially rendering this tooth more susceptible to abrasion. In general, the volume losses were greater with the Jubilee toothbrush compared to the Rapid Relief toothbrush.



Direct comparison of volume loss results showed considerable differences in mean values, range, standard deviation and variance and the sum of volume loss values. The range (max–min) was very susceptible to outliers, which is why the quartile distance ($q_3 - q_1$) was more suitable.

■ **Table 21: Descriptive statistic *Rapid Relief***

Tooth	Volume loss [nl]	Descriptive values: Toothbrush <i>Rapid Relief</i>	
A42	43	Mean \bar{x}_A	34.25
A44	50	Median \tilde{x}_{med}	33.5
A46m	20	Min–max	20–50 (range: 30)
A46d	24	1 st Quartile: 25% 3 rd Quartile: 75%	q1 = 22 q3 = 46.5
$n_A = 4$	Sum:	Interquartile:	24.5
	137	SD_A	14.51
<u>Sequence values:</u> 20 24 43 50		Variance SD_A^2	211

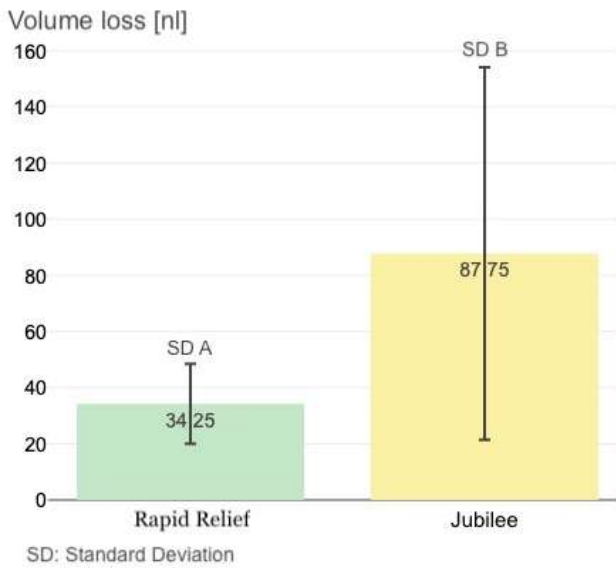
Dark green = max value, grey = min value; SD = Std. deviation

■ **Table 22: Descriptive statistic *Jubilee***

Tooth	Volume loss [nl]	Descriptive values: Toothbrush <i>Jubilee</i>	
B41	55	Mean \bar{x}_B	87.75
B42	188	Median \tilde{x}_{med}	61
B43	41	Min–max	41–188 (range: 147)
B45	67	1 st Quartile: 25% 3 rd Quartile: 75%	q1 = 48 q3 = 127.5
$n_B = 4$	Sum:	Interquartile:	79.5
	351	SD_B	67.67
<u>Sequence values:</u> 41 55 67 188		Variance SD_B^2	4579.58

Pale red = max value, grey = min value; SD = Std. deviation

Bar chart: Mean volume loss and standard deviation



The mean of volume loss due to toothbrush *Rapid Relief* is $\bar{x}_A = 34.25$.

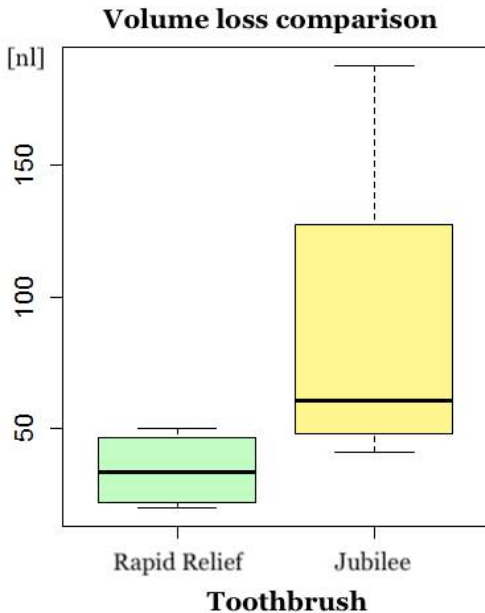
The mean of volume loss due to toothbrush *Jubilee* is $\bar{x}_B = 87.75$.

Difference of means: $\bar{x}_B - \bar{x}_A = 53.5$ nl

On average, the toothbrush *Rapid Relief* removed **53.5 nl less** tooth structure than the toothbrush *Jubilee*. Wear extended 100 – 1,500 μm apical from the cemento-enamel junction. Standard deviation (SD) of *Jubilee* volume loss is larger than in *Rapid Relief* due to the large cervical lesion of incisor B42.

Due to the small sample size, the 95% confidence interval corresponds to the standard deviation. The standard deviation value for the lower value of the volume loss is comparable in both bar charts. However, the difference in the deviation from the maximum value is vast.

Box plot: Volume loss comparison



In the boxplot for the *Jubilee* toothbrush, the median is close to the 1st quartile, while the *Rapid Relief* median is positioned in the middle of its boxplot, represented by a horizontal line inside each box. The size of the boxplots provides an indication of the distribution density. The colored boxes denote the interquartile range, showcasing the spectrum where the middle 50% of volume loss values for each sample are situated. Notably, due to the pronounced cervical lesion of tooth B42, the Jubilee toothbrush boxplot is substantially larger than the Rapid Relief toothbrush boxplot. This visualizes how the resulting volume losses with the Rapid Relief toothbrush were more closely grouped together. The whiskers extend from the 5% to the 95% quantile.

The lower and upper whisker is simply the lowest and highest volume loss value with only four samples: $q_{0.05} = x_{[0.2]+1} = x_1$; $q_{0.95} = x_{[3.8]+1} = x_4$

5.7.7 Shapiro–Wilk test

The Shapiro–Wilk test has high statistical power compared to other normal distribution tests and can be used for sample sizes as small as three observations. As a test statistic, the quotients of two estimates are formed for variance. The *Shapiro–Wilk* estimator = b . The *Shapiro–Wilk* coefficients for four samples are: $a_1 = 0.6872$; $a_2 = 0.1677$

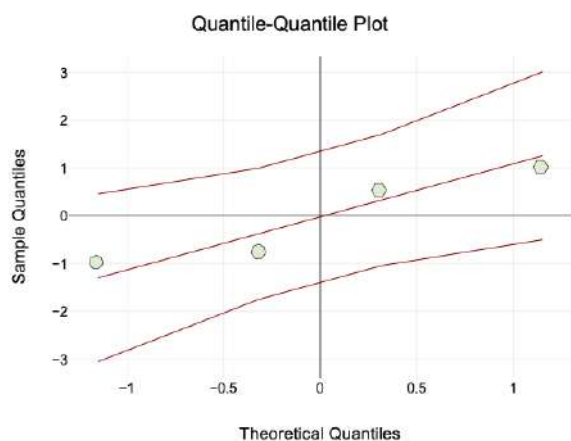
$$W_A = \frac{b^2}{(n-1)s_x^2} = \frac{23.8023^2}{632.75} = \mathbf{0.895}; W_B = \frac{b^2}{(n-1)s_x^2} = \frac{103.0308^2}{13739} = \mathbf{0.773}$$

With a significance level of 0.05 and $n=4$, $W_{krit} = \mathbf{0.748}$. Since $W_{krit} \leq W_{A,B}$ the H_0 hypothesis cannot be rejected. Therefore, the assumption is that there is a normal distribution.

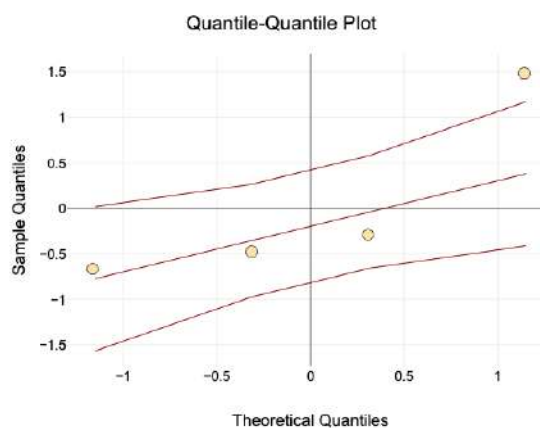
5.7.8 Quantile–quantile plot

The quantile–quantile plot was used to illustrate the distribution of the measured volume loss values, as testing for normal distribution is fragile due to the small sample size.

Quantile–quantile plot of *Rapid Relief*



Quantile–quantile plot of *Jubilee*



The quantile–quantile plot compares the theoretical quantiles of a normal distribution with the quantiles of the measured values. If data is normally distributed, all points will lie approximately on the middle line. The upper quantile for manual toothbrush *Jubilee* is slightly outside the normal distribution range, while the other quantiles line up near the centre line.

Further statistical analysis is precluded by the limited number of human tooth samples in this explorative study. While the distinct mean values suggest a subtle advantage for the *Rapid Relief* toothbrush in preserving tooth structure over the *Jubilee* toothbrush, this hypothesis awaits confirmation in subsequent studies. Nonetheless, the study does affirm that brushing results in the loss of dentin and cementum, yet concurrently contributes to oral health by eliminating calculus and mitigating iatrogenic damage to the tooth surface. It is noteworthy that most toothbrushes exhibit therapeutic effects when used appropriately, underscoring the vital role of brushing in sustaining optimal oral hygiene.

5.7.9 ANOVA: Young vs old teeth

ANOVA (analysis of variance) is a hypothesis test that verifies whether the mean values of more than two groups differ statistically significantly from each other. Independent two-factorial ANOVA can be used to examine two factors within groups. This is interesting for this study because not only the type of toothbrush but also the age of the teeth or a combination of toothbrush type and age of teeth could influence the volume loss due to abrasion. As prerequisites for ANOVA, the measured values must be independent, and the dependent variable, in this case the measured volume loss, must be at least interval scaled. In addition, collected measurements should be generally distributed in all groups, and the variance among each group should be homogeneous. However, if the group size is over 30, ANOVA can be applied without normal distribution. ANOVA cannot be used for the data collected in this pilot study because of the lack of homogeneity of variance between the two samples and the fact that volume measurements were only performed on a limited number of good teeth to verify the new methodology. However, based on the available data, it is worth considering an appropriate 2x2 design for an ANOVA in a follow-up study. To demonstrate a suitable concept, the measured volume losses of a young premolar and an old tooth of the respective manual toothbrush are considered hypothetical mean values of a larger sample. In the case of the toothbrush **Rapid Relief**, the juvenile premolar A44 (14 yrs) with 50 nl and the middle-aged tooth A42 (40 yrs) with 43 nl volume loss were used as hypothetical mean values. For the toothbrush **Jubilee**, the juvenile premolar B45 (13 yrs) with 67 nl and the middle-aged tooth B41 (40 yrs) with 55 nl volume loss were selected as hypothetical mean values. ANOVA tests the error variance, i.e., the variance resulting from unknown influences and the effect variance caused by the independent variables.

1st main factor: The average volume loss through toothbrush **Rapid Relief (RR)** compared to **Jubilee**.

2nd main factor: The average volume loss on juvenile teeth compared to that on older teeth.

3rd main factor: The interaction effect between young and old in the respective toothbrush groups.

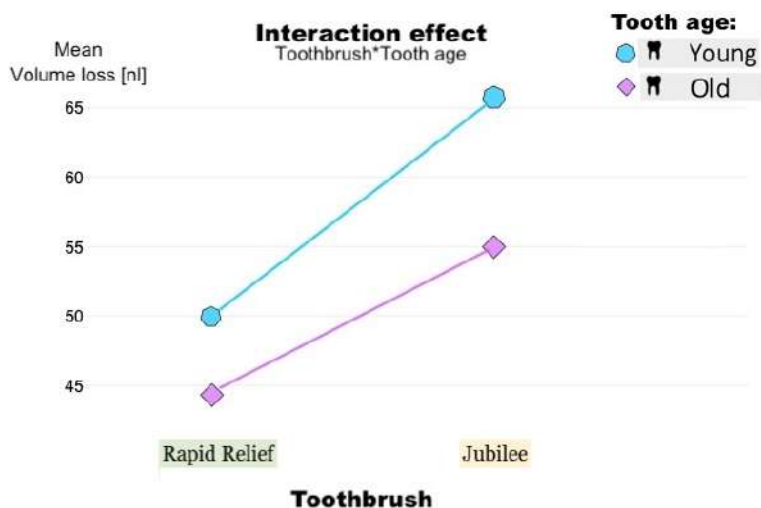
▪ **Table 23: The 2x2 design table**

Sample size: n > 15	Rapid Relief (RR) \bar{x} Volume loss [nl]	Jubilee \bar{x} Volume loss [nl]	\emptyset Means \bar{x} Volume loss [nl]	
☞ Young	50	67	$\emptyset \bar{x}_{young} = 58.2 \text{ nl}$	$\emptyset \bar{x}_{young} - \emptyset \bar{x}_{old}$ = 10 nl.
☞ Old	43	55	$\emptyset \bar{x}_{old} = 48.2 \text{ nl}$	
\emptyset Means	$\emptyset \bar{x}_{RR} = 46 \text{ nl}$	$\emptyset \bar{x}_{Jubilee} = 61 \text{ nl}$	$\emptyset \bar{x}_{Jubilee} - \emptyset \bar{x}_{RR} = 15 \text{ nl}$	

The bottom line represents the average of the two mean values (young and old) of the volume losses in the tooth brushing cycle of the respective manual toothbrush. This describes the first main factor. This factor was previously examined using a t-test on the total sample. It shows that the toothbrush **Rapid Relief** removed on average 15 nl less tooth structure than toothbrush **Jubilee**. The right column in Table 18 describes the second main factor. Accordingly, the average volume loss in the juvenile teeth of both groups was more significant than the average substance loss in the older teeth of

both groups. This could be related to the more resistant aprismatic enamel layer in older teeth, which results from recurrent remineralisation processes. Consequently, 10 nl more substance was removed from juvenile teeth than from older teeth across both toothbrush samples. Whether this difference is random or significant would need to be investigated in a study with a larger selection. Of particular interest is the interaction effect, which is explored here for the sample data using a graph. When the lines drift apart in this diagram, it is called an **ordinal interaction**.

In this case, the choice of toothbrush seems to have a greater influence on substance loss in the



juvenile teeth than in the older teeth. Usually, the **corresponding confidence interval** is also included in the chart. If substantial confidence intervals overlap, rejecting the hypothesis of an interaction between the two main factors would be necessary. The graph again makes it evident that in the case of this exemplary sample, the brushing cycle with the **Rapid Relief** resulted in less volume loss in both age categories (Fig. 92).

Figure 92: The interaction effect indicates that the volume loss by the flat trim toothbrush Jubilee increases compared to the volume loss by the toothbrush Rapid Relief with a flexible neck, especially in the juvenile teeth.

The results from the two-factorial ANOVA provide an opportunity to draw additional conclusions regarding the potential impact of tooth age, the choice of toothbrush, and/or the interaction between these factors. These findings can be further tested using appropriate post-hoc methods. Exploring this observation in follow-up studies with a representative sample would be intriguing.

6 Discussion

6.1 Replication technique

The replication technique has been a well-established method in scanning electron microscopy (SEM) for decades, enabling the repeated examination of identical tooth specimens at various time points (Roulet et al. 1989, Dietz et al. 2008, 2014, Montag et al. 2018). This approach offers the advantage of enabling the observation of environmental effects, such as temperature fluctuations, erosion, or abrasion, over extended periods.

Therefore, the replication technique is considered a valuable diagnostic tool for monitoring the progression of tooth wear and quantifying the volume loss due to wear (Bartlett 2003, Schlueter et al. 2005, Preis et al. 2018). Any process involving the dehydration and desiccation of teeth results in artifacts (Fig. 93), making the indirect method of SEM investigations of teeth the recommended approach (Roulet & Michellod 1984). The replication method has proven to be a simple, reproducible method for the non-invasive examination of micromorphological changes in the cervical tooth region (Bevenius and Hulthenby 1991).

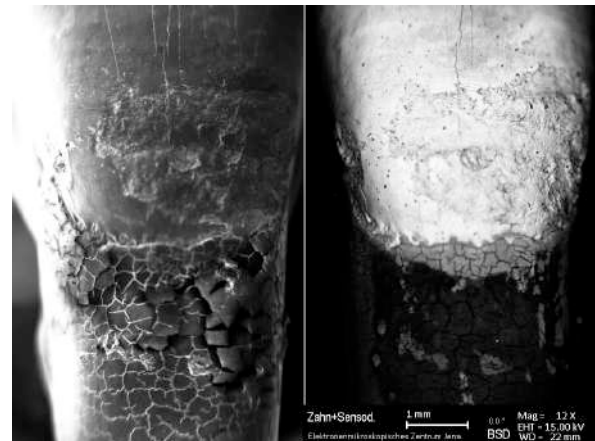


Figure 93: On the left an anterior tooth is shown whose root surface has become cracked and brittle due to the drying process required for direct SEM imaging. On the right an EDX image of the same tooth is shown.

6.1.1 Storage and pre-cleaning of human teeth

The experimental set-up with unprocessed human teeth is rarely chosen, as most classical evaluation methods require flattening and grinding of the tooth samples (Shellis et al. 2011, Ishak et al. 2021). However, the grinding process destroys the enamel's natural roughness. The exposed tooth structure, which originates from deeper layers, does not correspond to the naturally exposed tooth surface in the oral cavity (Camboni and Donnet 2016). The plant-derived phenol *thymol* has been used in research as a storage solution for extracted teeth, due to its disinfecting effect. Thymol has both a fungicidal and a bacteriostatic effect, particularly effective in concentrations of 0.2% and above. However, the effectiveness of 0.1% thymol as a disinfectant is low, ranging from 0% to 13.3%, and there are some gaps in the spectrum of effectiveness (Nawrocka and Łukomska-Szymańska 2019). Therefore, we used a solution of 1 g thymol in 50 ml 100% ethanol, and 950 ml distilled water for the initial storage after teeth extraction. After pre-cleaning and polymerisation on model pins, teeth were finally stored in 0.1% thymol with 0.9% saline at 4–6°C, comparable to the study by Witecy et al. (2021). To remove stubborn residues from the cervical region of the tooth, especially in the juvenile premolars, we used 2% NaOCl solution, which was brushed onto the cervical region of the tooth

for 5 minutes. Long-term treatment (> 16h) with 5% NaOCl can increase the number of focal holes in the enamel and remove unmineralised precementum. However, on enamel surfaces treated with 5% sodium hypochlorite for only 10 minutes, the integrity and morphology remained unchanged (Fejerskov et al. 1984). Therefore, Schroeder & Scherle (1988) as well as Bevenius & Hultenby (1991) immersed tooth samples in 10% sodium hypochlorite for 20 minutes to remove adhering tissue residues. Vossen et al. (1985) and Teaford and Oyen (1989) used 3% sodium hypochlorite for this purpose. Absi et al. (1989) applied 1% sodium hypochlorite to exposed cervical dentin to remove organic debris and promote infiltration of impression material into the dentinal tubules. The samples were rinsed under running water immediately after applying NaOCl, as Risnes et al. (2019) recommended to prevent surface alteration. To remove debris from the tooth surface a scavenger impression was taken as described by Bevenius and Hultenby (1991). It is assumed that cleaning with a prophylaxis brush and soap or water has no effect on the surface condition of the tooth structure (Risnes et al. 2019). Our first scanning electron microscopy examination revealed that even after brushing with a prophylactic brush and scavenger impression, several teeth replicas still showed fine mineral granules of unknown origin on their surface. Therefore, *Tubulicid Blue* with 0.2% EDTA and benzalkonium chloride was integrated for purification before the impression. This product reduces surface tension and thus improves surface connectivity. Moreover, EDTA removes the smear layer, plaque, bacteria and debris without opening or widening the dentinal tubules (Brännström et al. 1980). The substance is considered harmless for both teeth and gums (van Dijken and Hörstedt 1987). Immediately after conditioning with EDTA, the tooth samples were rinsed under running water to remove acid residues from the sample. Initially, the cleaning protocol also involved placing the teeth in distilled water in an ultrasonic device for approximately 5 minutes. This procedure was adopted from an earlier standard operating procedure for replication technology. However, it is suspected that there is a positive correlation between ultrasound treatment and the number of focal holes on enamel surfaces (Fejerskov et al. 1984). Therefore, this step was abandoned as it proved to be rather ineffective and may damage fine structures and thin extensions of the enamel mantle towards the root if repeatedly used (Risnes et al. 2019).

6.1.2 Adaptation of the replication technique

In earlier replication studies, mainly *Epon 812* according to the recipe of Luft (1961) was used (Craig et al. 1962, Lee and Neville 1967). *Epon 812* penetrates quickly into the tissue while providing high contrast. It is easy to cut and remains stable under an electron beam. After production of the original *Epon 812* formulation ceased in 1984 (*Epon 812, Shell Chemical Company, Houston, United States*), numerous other manufacturers produced substitute products and sold them as equivalents. However, the various formulations sometimes deviate considerably from the original chemical composition. Some of these new equivalence products have even been improved in their properties and continue to deliver excellent results in embedding and infiltrating tissue samples for SEM (Ellis 2014).

In studies by Dietz et al. (2014) and Montag et al. (2018), Serva's product (*Glycidether 100, Serva, Heidelberg, Germany; CAS Number: 90529-77-4, 1,2,3-Propanetriol glycidyl ether GE 100*) was chosen as an *Epon 812* equivalent, which allowed detailed imaging of the delicate tooth structures in the scale of 0.1 μm . Because Serva's epoxy resin was unavailable at the beginning of this study, a choice was initially made for an alternative *Epon 812* substitute (*Epoxy embedding kit, Sigma-Aldrich, St. Louis, Missouri, United States; CAS Number: 25038-04-4; 1,2,3-Propanetriol, polymer with 2-(chloromethyl)oxirane*). The polymerisation of *Epon 812* equivalents takes place at 60°C for at least 48 hours. Although the steps from previous studies were followed precisely, unexpected problems occurred, as shown in *Figures 94–96*.

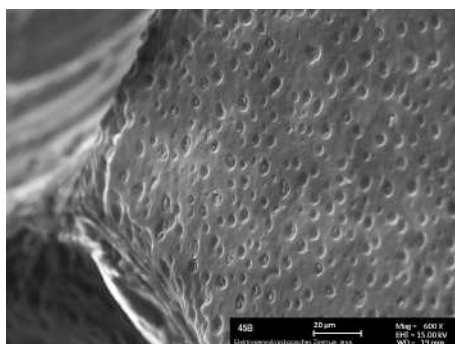


Figure 94: When using the A-silicone Panasil (Panasil initial contact X-Light, Kettenbach, Eschenburg, Germany), leaked silicone oil caused round depressions on the surface of the replica, which prohibited a morphological assessment.

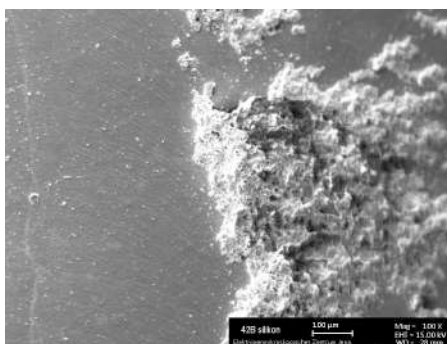


Figure 95: If alcohol was used to dry the surface, silicone was torn out during de-vesting after curing at 60°C, which stuck to the replica surface.

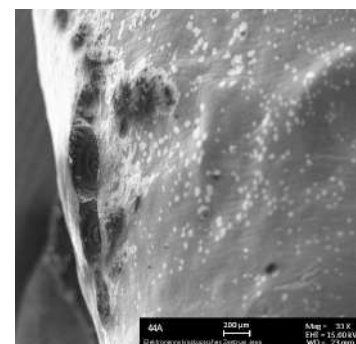


Figure 96: On some replications, white spots or black tufts of indistinct origin appeared on the sputtered surfaces.

To ensure impressions to be taken in patients' mouths, various A-silicones and polyethers used in dentistry were tested for their potential suitability for the replication technique. The clinical advantages of an automated dispensing system for the addition of silicone elastomer impression materials have already been described by Craig (1985) and Keck (1985). Ultimately, *Affinis (Affinis Putty Soft and Affinis light body, Coltene Holding AG, Altstätten, Switzerland)* was selected, as this A-silicone consistently delivered the most reliable and detailed results. Its compatibility with polyurethane and epoxy resin was confirmed in the instruction manual (*Fig. 93*). The suspicion arose that contemporary dental impression materials might establish a chemical bond with the epoxy resin at the necessary curing temperature of 60°C, potentially causing silicone residues to adhere to the tooth replicas during deformation (*Fig. 94*). Therefore, multiple experiments were conducted using various cold-curing epoxy resins. Recent advancements in replication techniques also indicate a shift towards the use of cold-curing replication materials. Roulet et al. (1989) and Stricker and Göhring (2006) used *Stycast (Stycast 1266; Emerson & Cuming, Westerlo, Belgium)* as an epoxy resin for the replication technique. In Schlueter et al. (2005), the epoxy resin *Blue Star* was designed explicitly for model fabrication. Behr et al. (2009) used *Epoxy Die (VP 1031, Ivoclar-Vivadent, Schaan, Liechtenstein)* for replication to compare the marginal adaptation of three self-adhesive resin types. Dental materials and

teeth were repeatedly examined for wear in a chewing simulator at the University of Regensburg. Traditional methods with *Epon 812* were used for their SEM evaluation. More recently, however, also a cold-curing epoxy resin (*Rencast, CW 2215, RenShapes Solutions – Huntsman Corporation, Salt Lake City, United States*) has been adopted for the replication technique (Aschenbrenner et al. 2012). Frankenberger et al. (2012) used a polyurethane (*AlphaDie MF, Schuetzdental, Rosbach v.d. Höhe, Germany*) to replicate third molars to evaluate the marginal quality of CAD/CAM glass-ceramic inlays. However, most of these products have since been withdrawn from the market by the suppliers and were unavailable for this trial. Therefore, we started our material tests for replication. The first cold-curing epoxy resin (*Epoxy Minute Adhesive, Weicon, Münster, Germany*) showed striation during our pilot testing, and the bucket preparation (*Casting resin MS 1000, Weicon, Münster, Germany*) exhibited bubbles during mixing despite a vacuum. Hence, the decision was made to transition to a cartridge system, similar to impression material. However, the polyurethane cartridge system (*Easy Mix PU Crystal, Weicon, Münster, Germany*) did not meet expectations. Ultimately, the preference was for unfilled epoxy resin (*Easy-Mix N 5000, Weicon, Münster, Germany*), which exhibited superior detail accuracy when compared directly with the reproduced coins (*Fig. 26; Section 4.9*). The reproducibility of the replication technique was ensured by providing a detailed standard operating procedure. However, it must be taken into account that replicating tooth surfaces with impressions before scanning microscopy adds an additional source of error. In addition, the accuracy of scanning and software alignment methods also affects the process's overall accuracy (DeLong et al. 2003). In accordance with Lambrechts et al. (1984), inaccuracies in results often stem from flawed replication techniques, repositioning challenges, and limitations in measurement equipment. Consequently, considerable attention was dedicated to refining these parameters in the current study.

6.2 Advantages of the robot simulation

The notable benefit of employing a robot-assisted in vitro method lies in its capacity to examine extended tooth wear processes within a condensed timeframe and standardized conditions. This ensures the comparability and reproducibility of the recorded wear outcomes. Parry et al. (2008) have outlined a set of crucial parameters to be controlled in in vitro toothbrushing simulations, as these factors markedly influence the resultant tooth wear (*Table 5; Section 4.5 and Appendix 10*). In general, the use of a combined toothbrush/dentifrice abrasion concept is recommended (Wiegand et al. 2009). Given the ability to control specific aspects, their impact can be investigated independently of other factors (Wiegand and Attin 2011, Lee et al. 2012, Hamza et al. 2021). These include the abrasiveness and composition of the dentifrice, the configuration and filament stiffness of the toothbrush (soft, medium, hard) and the behavioural aspects, such as brushing technique, brushing force applied, brushing speed, brushing temperature (impact on slurry viscosity and particle suspension), number of brush strokes and frequency of brushing.

6.2.1 Brushing machines

Various brushing machines and wear test concepts were employed, differing significantly in crucial parameters like force, contact geometry, and lubrication. This divergence posed challenges for conducting a comprehensive comparative analysis of the wear data (Heintze 2006). The original British Standard (*BS5136: 1981*) requires a flat-bed toothbrush simulator for wear testing. Thus the horizontal brushing *Grabenstetter V-8 brushing machine* was used frequently in the past (Grabenstetter et al. 1958, Hefferren 1976, Ledder et al. 2019). Subsequently, other brushing machines were devised, incorporating innovations such as vertical strokes (Björn and Lindhe 1966) or a rotating brushing motion (Harrington et al. 1982). Ernst et al. (1997) employed a six-axis robot to evaluate the efficacy of electric toothbrushes in plaque removal. The clinically validated robot used in this study was designed to allow rapid and reproducible in vitro testing of both manual and electric toothbrushes with different toothbrushing programmes. In combination with computer-assisted planimetric plaque assessment, it became possible to review new prototypes with reference toothbrushes for their cleaning efficiency (Gängler et al. 2013, Lang et al. 2014, Acherkouk et al. 2022). The quantitative investigation of tooth wear in this study represents a further area of application for the established robot system. Depending on the brush movement applied, whether horizontal, vertical or rotating, the resulting abrasive volume loss could be different. Parry et al. (2003) concluded that a rotating brushing machine observed the most remarkable and most reproducible abrasion depth. However, this observation cannot necessarily be transferred to our robot, as each brushing machine has its own distinctive brushing pattern. This once again highlights the technical challenges of accurately mimicking brushing in vivo.

6.2.2 Alternative: In vivo models

In vivo wear studies use devices with tooth samples that can be worn inside the mouth but brushed and examined outside. This allows an investigation of the multifactorial wear behaviour on teeth under natural formation of a salivary pellicle while preserving the sensitivity of laboratory analyses and interactions with other toothbrushing parameters (Jaeggi and Lussi 1999). The drawback of this method lies in its time-consuming and costly nature, with results prone to significant variations due to patient-related factors (Hara et al. 2014, 2021). Tooth wear is a slow process, influenced by participant compliance. Standardizing brushing behaviour is crucial for a clinical study, ensuring homogeneity. Dietary factors also play a key role during extended appliance wear (Lewis and Dwyer-Joyce 2005). Mechanisms such as erosion and abrasion can co-occur to varying degrees, making it challenging to isolate decisive factors influencing the wear process (Lewis and Dwyer-Joyce 2005). Individual differences in oral hygiene habits and tooth alignment or saliva composition can significantly influence the outcome. By contrast, the in vitro method allows precise control of the environment and the variables that influence the wear process of the tooth structure and materials (Lambrechts et al. 2006, Lee et al. 2012).

6.2.3 Average brushing duration

An old study by Macgregor and Rugg-Gunn (1985) found an average toothbrushing time of 33s in young adults, and Beals et al. (2000) reported 46s. Several more recent video studies have however observed a significant increase in average tooth brushing time. Over the last 20–30 years, oral hygiene in industrialised countries has improved significantly and most people brush their teeth twice a day for about 90 to 120 seconds on average (Saxer and Yankell 1997). This is in line with the recommendation of the German *Bundeszahnärztekammer* (DGZMK). Ganss et al. (2009) recorded an average brushing time of 96.6s and Eidenhardt et al. (2021) 196s. When participants were asked to brush their teeth to maximum cleanliness, toothbrushing time was more than 120s in Winterfeld et al. (2015), 135s in Ganss et al. (2018) and 200s in Deinzer et al. (2018). In interpreting observational study results, it's crucial to consider the Hawthorne effect, where participants modify behaviour when aware of being observed. Nevertheless, findings indicate that conscientious individuals invest more time in tooth brushing. The ongoing debate questions whether excessive brushing results in heightened tooth wear with no added benefits (Wiegand and Schlueter 2014). Van der Weijden et al. (1993) found that, even with brushing times extending to 6 minutes, no significantly improved plaque control was observed compared to a 2-minute duration. This is due to a lack of systematic toothbrushing. If brushing time is increased, the same tooth surfaces are usually brushed repeatedly and unnecessarily (Petker-Jung et al. 2019, 2022). Addy and Hunter (2003) showed that abrasion is a time-dependent process. Van der Weijden Ga et al. (1993) and Jaeggi T and Lussi (1999) recommended a toothbrushing time of 30–45 seconds per quadrant for optimal cleaning efficiency with minimal abrasion impact. Recommended cleaning times vary depending on the region, from 120s in Europe (Jordan et al. 2014) to 180s in the USA (ADA.org 2017). Nassar et al. (2018) found that brushing teeth three or more times a day increases abrasion on tooth surfaces. Accordingly, this study is based on the general recommendation to brush teeth for 120s twice daily.

6.2.4 Brushed tooth surfaces

One noticeable aspect of video observation studies was that the brushing time is not evenly distributed across all tooth surfaces. It is often observed that the inner surfaces of teeth are greatly neglected (Macgregor and Rugg-Gunn 1979, Ganss et al. 2018). Winterfeld et al. (2015) found that participants brushed buccal surfaces approximately twice as long as the lingual surfaces. Schlueter et al.'s (2018) video observation studies could consistently demonstrate that subjects rarely show systemic brushing of all tooth surfaces. Therefore, the collected data on brushing movements mainly reflect the brushing behaviour of the buccal tooth surfaces, followed by the occlusal surfaces. This is consistent with our video observations. Subjects switched unsystematically between different regions of the dentition and focused mainly on brushing the buccal surfaces of the teeth.

6.2.5 Toothbrush motion frequency

The extensively cited Heath and Wilson (1974) study reported an average toothbrush motion speed of **4.5 Hz**. More recent Japanese studies, such as Tosaka et al. (2014) using a strain gauge and accelerometer, recorded average brushing motion speeds of 4.53 Hz buccally and 4.23 Hz lingually, aligning with our findings. Inada et al. (2015) utilized a 3D optical motion analyzer, measuring an average frequency of **3.91–4.56 Hz**, varying by brushed region. Huang and Lin (2016) recorded toothbrushing movements using various sensors, with a peak elbow movement frequency of **4.5 Hz**. These results align with our video observation study, demonstrating average movement speeds of **4.2 Hz** for rotating, **4.5 Hz** for horizontal, **3.5 Hz** for vertical. Concerning the wear results, the robot's lower motion frequency is negligible, as confirmed Parry et al. (2008), where variations in brushing speed showed no significant impact on dentin abrasion depth.

6.2.6 Calculation of brushing strokes

The literature displays considerable variability in the reported number of brush strokes per tooth. For instance, Addy et al. (2002) estimated an average brushing time of 10 seconds for the buccal surface based on video observations. This aligns with the assumption by Schlueter et al. (2018), who observed that at least half of the time, brushing is predominantly buccal. Ten seconds is half the recommended brushing time (20s) for a sextant (Rodriguez and Bartlett 2010). This resulted in **31,680 strokes in one year** and a total of **95,040 strokes per buccal tooth surface** during the simulated **three-year** toothbrushing period. Sabrah et al. (2018) and Turssi et al. (2019) simulated ten years of toothbrushing with a total of 55,000 double strokes on tooth samples. The assumption is that during a brushing time of 20 seconds per sextant, each tooth surface (buccal, lingual, occlusal) is brushed for about 6 seconds in equivalent proportions. The 6 seconds per surface is claimed to result in **15 brushing strokes** per tooth surface per day, resulting in **5,475 brushing strokes/tooth surface/year** (Turssi et al. 2019a). But an average motion speed of **4.5 Hz** would result in **27 brushing strokes** per tooth surface. The study also assumed that teeth are brushed **three times a day**. This would result in 81 strokes per tooth surface/day. In a subsequent investigation Mazzolani et al. (2019) it was assumed that there were 15 brushing strokes per surface during each brushing cycle, twice daily, resulting in approximately 10,950 brushing strokes per tooth surface per year. However, the clinical extrapolation of the performed brushing strokes remains unclear and inconsistent. Notably, a Swedish study group (Liljeborg et al. 2010, Tellefsen et al. 2011, Johannsen et al. 2013) also cited 15 brushing strokes per tooth surface per brushing cycle, referring to the study by Sexson and Phillips (1951). It is crucial to recognize that the quoted study investigated denture acrylic wear over time due to brushing and various cleaning agents, observing that denture owners cleaned their dentures twice daily with approximately 15 brush strokes each time. Therefore, this reference may be misleading when justifying the assumption of 15 strokes per tooth surface per day. Wiegand and Attin (2011) similarly assumed that during a single session, each tooth surface is brushed for 15

strokes or less than 5 seconds using an electric toothbrush under clinical conditions. Nassar et al. (2014) concluded, based on several of their pilot studies, that an average toothbrushing session involves approximately **50 brushing strokes per tooth**, assuming a motion speed of **3.3 Hz**. Given that many individuals are unlikely to adhere to the recommended 20 seconds for brushing a sextant in their daily oral hygiene routine, adopting half the recommended time may offer a more accurate representation for the general population. However, this study aimed to quantify the abrasion at maximum utilisation of the recommended brushing time. However, extrapolation from in vitro data to the clinical situation should be interpreted with caution. In vitro studies tend to result in higher wear than clinical ones. Therefore, in vitro methods represent a worst-case scenario for the abrasion caused by toothbrushing (Hunter et al. 2002). This is partly because biological factors such as salivary flow and protective pellicle effects cannot adequately be simulated in vitro because of the lack of recovery periods between brush cycles (Wiegand and Attin 2011).

6.2.7 Frequency of toothbrushing techniques

The choice of brushing technique significantly impacts both the cleaning effectiveness and the abrasion process (Heasman et al. 2015). Historically, horizontal brushing was widely employed (Rugg-Gunn et al. 1979). However, horizontal brushing is now recognized as potentially harmful, more frequently causing gingival injuries. As a result, it is only recommended for children up to the age of 3, who may lack the manual dexterity for a gentler technique (Mierau et al. 1989, Mierau 1992). According to Bergström and Lavstedt (1979), significantly more subjects were affected by wedge-shaped cervical lesions when brushing their teeth with the horizontal technique. With an escalation in the frequency of daily toothbrushing, there was a corresponding rise in the severity of cervical abrasion lesions. Attin (1999) hypothesised that hard tooth tissue reacts particularly sensitively to horizontal brushing due to its specific properties. This assumption was later confirmed by Dzakovich and Oslak (2008). Nevertheless, the elevated abrasion of tooth structure associated with this technique may be attributed to the typically greater force applied in the horizontal method. As a result, the DGZMK recommends the modified Bass or rotating Fones technique for daily oral hygiene practices (Schiffner 1995). However, participants lacking prior guidance on tooth brushing were more inclined to adopt the horizontal brushing method. In a recent study by Ganss et al. (2018), horizontal movements were observed during almost 60% of the brushing time in clinical practice, while rotating or vertical movements accounted for only about 30% and 2% of the brushing time, respectively. Similarly, in Deinzer et al.'s (2018) sample, 40% of the outer surfaces were brushed using horizontal strokes. Eidenhardt et al. (2021) also found that despite years of promoted knowledge, young people predominantly employ horizontal movements when brushing their teeth. Therefore, the robot executed the horizontal scrubbing program for almost twice the duration (34 seconds) compared to the rotating (19 seconds) or vertical (22 seconds) brushing programs. However, with increasing age, the willingness to brush the outer surfaces with rotating movements increases (Ganss et al. 2018). In our

video observation study, the brushing techniques were observed with the following frequencies: 40% rotation, 29% horizontal, 10% vertical, and 22% mixed. This aligns with current observational studies (Schlueter et al. 2021, Petker-Jung et al. 2022). Therefore, for future studies, it may be considered to enhance the number of rotating movements executed by the robot.

6.2.8 Brushing force

Patients with commendable oral hygiene frequently encounter heightened gingival recession and tooth wear (Burgett and Ash 1974). It is presumed that individuals with more severe effects also exert greater force during tooth brushing. Phaneuf et al. (1962) illustrated a correlation between the force applied during brushing and the loss of tooth structure. In an in vitro study by Hotz (1983), equivalent substance removal was accomplished by either doubling the brushing force or doubling the brushing time. Mierau and Spindle (1984) observed a median force of **3.75 Newton (N)** in a group with multiple gingival recessions. Völk et al. (1987) found that individuals with wedge-shaped cervical lesions performed brushing with an average force of **2.9 ± 0.4 N**, while the average force of probands without cervical abrasion lesions was **2.1 ± 0.3 N**. Van der Weijden et al. (1998) established an average toothbrushing force of **3.23 N**, with individual variances ranging from **1.7–7.01 N**. Elevated contact forces correlated with greater gingival recession, consequently fostering cervical abrasion lesions. Heasman et al. (1999) observed a median force of **2.97 N** with the manual toothbrush. One of the electric test toothbrushes featured a controlled pressure system. The threshold for the “click force”, at which the brush head bent back with a loud click, was set at **2.6 N**. Claydon (2008) also observed that several of his probands brushed their teeth with more than **3.0 N**. Ganss et al. (2009) reported that 70% of the probands brushed their teeth with a mean total force of between **1.6 and 2.8 N**, while as many as 17.5% used **3.0 N** or more. Men, on average, applied a significantly higher maximum brushing force of **♂ 5.7 ± 1.9 N**, whereas women, on average, only applied a **maximum force of ♀ 4.9 ± 1.4 N**. On average, a brushing force of **♂ 2.5 ± 0.8 N** and **♀ 2.1 ± 0.7 N** was applied. Since abrasion of tooth structure is related to brushing force, this could be a reason why men tend to be more affected by cervical abrasion lesions (Parry et al. 2008). Demarco et al.’s (2021) conducted a multilevel data analysis, affirming that women exhibit a lower prevalence of non-carious cervical lesions compared to men. Additionally, smokers demonstrated a significantly heightened occurrence of wedge-shaped lesions. This may be attributed to the use of more abrasive dentifrice for discoloration removal and the application of greater brushing forces to eliminate staining. Moreover, Addy et al. (1987, 1990) and Tezel et al. (2001) delved into the impact of handedness. Nevertheless, perspectives on this matter diverge, with Ganss et al. (2009) subsequently refuting the hypothesis regarding the influence of handedness. However, according to (Van Der Weijden et al. 1996, Van der Weijden et al. 1998, Lang et al. 2014) it was found that an increase in efficiency of plaque removal is evident only up to **about 4 N**. Elevated brushing force solely amplifies tooth wear without conferring additional benefits. This phenomenon is ascribed to the dispersion of brush filaments

under higher forces, resulting in diminished cleaning efficacy. Mierau et al. (1989) found no detectable abrasion lesions from brushing at forces **less than 2 N**. Kramer and Klemke (1995) therefore proclaimed a general cleaning force below **2 N** to avoid long-term tooth wear damage. Patients struggling with pressure control may find electric toothbrushes with pressure sensors to be beneficial (Klocke et al. 2015). Ganss et al. (2009) have shown that even demineralised organic dentin matrix is remarkably resistant to mechanical impact at a force under **2 N**. Japanese people generally brush their teeth with significantly lower forces of about **1 N** due to the pen-like holding of a toothbrush (Hasegawa et al. 1992, Tosaka et al. 2014). In summary, most users of manual toothbrushes typically apply a brushing force of about **1.5 to 3.75 N**. Therefore, in this study, a clinically relevant contact force of **3.5 N** was defined based on the available data to ensure the measurability and reproducibility of wear results (Hamza et al. 2022).

6.2.9 Artificial oral cavity

The abrasiveness of various dentifrice suspensions on tooth structure has been studied for several decades (Stookey and Muhler 1968). There is a consensus that the risk–benefit ratio favours today’s dentifrices if commonly used (Addy and Hunter 2003). In vitro model studies have indicated that lifelong toothbrushing causes negligible abrasion on the surface of sound enamel (Addy and Hunter 2003). However, the scenario changes with enamel that has been softened by erosion (Attin et al. 1997). Additionally, dentin, in particular, has been proven to be much more susceptible to the abrasiveness of dentifrice (Hooper et al. 2003, Lippert et al. 2017). Excessive brushing or using highly abrasive dentifrices has been shown to increase tooth wear and dentin hypersensitivity in numerous erosion studies (Radentz et al. 1976, Addy 2005, González-Cabezas et al. 2013). Both the abrasiveness of dentifrice as well as its fluoride content are considered relevant parameters for the observed extent of erosion and abrasion (Wiegand and Attin 2011). When using fluoride-containing dentifrice, some authors showed the protective effect against tooth wear (Davis and Winter 1977). Especially in erosion studies, less wear of dentin and eroded enamel was recorded when fluoridated dentifrice was used (Bartlett et al. 1994, Hara et al. 2009). Since most dentifrices on international markets contain fluoride, it is reasonable to use fluoride-containing dentifrices when simulating clinical conditions in an in vitro abrasion study. The abrasiveness of dentifrices is traditionally determined by the relative enamel abrasivity (REA) (Wiegand et al. 2008), and relative dentin abrasivity (RDA) values (Imfeld 2010). An RDA value of 151–250 is considered highly abrasive, 70–150 moderately abrasive and < 70 less abrasive (Giles et al. 2009). With an RDA value of 50–60, the dentifrice *Sensodyne extra fresh* is classified as low-abrasive and gentle on tooth substance. In in vitro studies, dentifrices are commonly used as slurries, as they are diluted by saliva in the clinical situation (González-Cabezas et al. 2013). The usual mixing ratio between dentifrice and water is 1:2 to 1:4. In this study, a slurry ratio of 1:3 was used, just as by Wiegand et al. (2013). Controlled temperature settings and straight teeth rinsing reproduce the oral cavity’s physiological conditions. The experimental set-up in this study was

designed to simulate 1 g of dentifrice on teeth for 2 minutes, corresponding to the average dentifrice consumption per brushing session (Saxer et al. 1998). To keep abrasive particles in suspension, the slurry was regularly agitated in addition to a peristaltic pump to ensure homogeneity. Simultaneously, foaming due to excessive stirring should be avoided (Parry et al. 2008). Litonjua et al. (2004) developed a similar principle, where the sludge was applied through a tube on the toothbrush head. Joiner et al. (2008) suggested using sodium carboxymethyl cellulose to prevent slurry particles from precipitating. In Wiegand et al. (2008), silicone antifoam was added to slurries to avoid foaming during brushing. However, the use of additives in the slurry could alter its properties, impacting clinical transferability. Hence, no additives were introduced in this study, maintaining a pH value of 7.4 to eliminate unintentional erosive effects on tooth surfaces. It's noteworthy that silica and calcium carbonate dentifrices led to increased enamel abrasion in specific cases with rising temperature (Parry et al. 2008). Therefore, room temperature was kept constant at 22°C.

6.2.10 Manual toothbrushes

Modern dentistry has brought many innovations in oral hygiene products. Despite the many new electric toothbrush models, manual toothbrushes remain popular due to long-standing habits. According to a recent survey from Oral Care (2021), more than half of the respondents in Switzerland are still using manual toothbrushes. And according to the latest representative population survey by (Zimmer and Lieding 2014), 53% of respondents in Germany reported using manual toothbrushes. Relevant mechanical properties and potential impacts of commercial toothbrushes include the configuration of the bristle filaments, the ability to maintain tooth-to-surface contact and the potential for injury to the gums (Niemi et al. 1984, Imfeld et al. 2000). Breitenmoser et al. (1979) found that trimmed bristle ends caused significantly more gum injuries than rounded bristle ends. Danser et al. (1998) demonstrated that bristle end curvature influences the toothbrush's abrasive effect. In 2016 the American Dental Association recommended rounded bristle ends as they provide a gentler cleaning of the tooth surface. Most of the filaments used in toothbrushes originate from the brand manufacturer *DuPont*. The manual toothbrushes, *Rapid Relief* and *Jubilee*, were crafted with rounded bristle filaments, both labelled as soft. Assessing the actual hardness of these toothbrushes, categorized as hard, medium, or soft, poses challenges due to the absence of industry-standard parameters. Typically, filaments labelled as hard have a larger diameter. Certain studies propose that soft toothbrushes may expedite the wear process, possibly due to their denser packing, leading to an increased effective contact area with the tooth surface (Dyer et al. 2000, Wiegand et al. 2008, 2009, Bizhang et al. 2016). But based on these results, the stiffness of toothbrush filaments has only minor significance for abrasion. However, alternative studies have suggested that the use of hard toothbrushes may elevate dentin wear, contributing to the emergence of cervical abrasion lesions (De Boer et al. 1985, Lippert et al. 2017). According to Hamza et al. (2021, 2022), soft bristles, once the brushing force reaches 4 N, are deflected further with higher brushing force and therefore contribute fewer

abrasive particles to the dentin surface than medium bristles. Thus, the recommendation is that a soft toothbrush is safer for preventing gingival recessions and tooth wear. In summary, it can be assumed that the abrasiveness of the dentifrice is the most crucial influencing parameter for abrasion of the tooth structure, with the toothbrush acting only as a carrier and thus transporting the effect of the abrasive depending on filament arrangement (Addy 2005, Wiegand et al. 2008, 2009). Tooth wear could also be influenced by the arrangement of the artificial gingival margin, which may deflect brush filaments in different patterns (Litonjua et al. 2004). In addition, the toothbrush **Rapid Relief** has been equipped with tapered bristle filaments. Bizhang et al. (2017) and Turssi et al. (2019) found that flat-trimmed toothbrushes caused more abrasion lesions than tapered toothbrushes. Tapered filaments are considered more flexible and gentle on the gingiva and tooth structure due to their thin, pointed ends (Versteeg et al. 2008). In addition, tapered filaments reach difficult-to-reach areas such as fissures on the occlusal surface or the approximal margin better than other configurations of bristle ends (Hoogteijling et al. 2018). Innovations in developing new toothbrush models also focus on the shape of brush heads and filaments and the design of brush handles and necks. To prevent harmful effects from excessive force, the toothbrush **Rapid Relief** has a flexible neck design to moderate exerted force when brushing. Acherkouk et al. (2022) showed that manual toothbrushes with flexible necks flexed 2.0 to 2.5 times more than reference toothbrushes with rigid necks under the same force applied to the toothbrush head. In addition, the flexible neck due to a ball joint improved biophysical brushing action and is designed to reduce the risk of tooth wear, gum recession and dentine hypersensitivity.

6.3 Toothbrushing-induced morphological changes

Due to tooth wear mechanisms, the morphology and contours of tooth surfaces change over time. These mechanisms include enamel infractions, non-carious cervical lesions and exposure of dentin (Eccles 1979). Various coding systems were historically employed to assess tooth surfaces (*refer to Table 24*), often focusing on specific aspects such as the development of abrasion marks or infractions resulting from different polishing methods (Donachie and Walls 1995, Bartlett et al. 2005). Human teeth continually undergo transformations due to aging and environmental factors, resulting in notable differences between older and younger teeth.

Table 24: Examples of SEM investigations of tooth surfaces and indices for assessing surface features

<i>Index name</i>	<i>Description</i>	<i>Reference</i>
	Evaluation of the appearance of perikymata and prismatic portions on teeth of various ages using replicas under SEM.	(Scott et al. 1949)
<i>Enamel surface index (ESI)</i>	Five-stage score for assessing the enamel surface under SEM after debonding brackets and applying different polishing techniques. But also, for determination of irregularities on the enamel surface of aged teeth.	(Zachrisson and Arthun 1979) (Zachrisson et al. 1980)
<i>Surface roughness index (SRI)</i>	For the evaluation of enamel surface after various bracket debonding procedures under SEM. Grade A–D. Focus on changes in abrasion marks.	(Howell and Weekes 1990, Hong and Lew 1995)
<i>Enamel damage index (EDI)</i>	For the evaluation of enamel surface after various bracket debonding procedures under SEM. Grade 0–3. Focus on changes in abrasion marks, but also taking into account the perikymata.	(Schuler and van Waes 2003)
<i>Enamel score</i>	Three scoring grades for the assessment of abrasion marks on the enamel surface in the SEM.	(Kontturi-Närhi et al. 1990)
<i>Cementum score</i>	Three scoring grades for the assessment of abrasion marks on the root surface in the SEM.	(Horning et al. 1987)
<i>Enamel, cementum and debris score</i>	Combination of Enamel and Cementum Score for the evaluation of tooth surface under SEM after the use of different polishing systems.	(Chowdhary and Mohan 2018)
	Evaluation of early enamel and dentin cracks under a dental operating microscope at 16x magnification and classification into three types of different severity.	(Clark et al. 2003)
<i>Tooth surface comparison index</i>	To assess the surface smoothness, the presence of abrasion marks and debris under SEM after the use of different polishing systems.	(Camboni and Donnet 2016)
	Classification of infractions into three different types (horizontal, vertical, complex) using optical coherence tomography.	(Segarra et al. 2017)

6.3.1 Functional abrasion marks (FAM)

Brasch et al. (1969) employed the replication technique to assess dentifrice abrasiveness by examining abrasion marks on enamel surfaces. Wright (1969) demonstrated that hard abrasive particles generate distinct abrasion marks. Rajstein et al. (1979) systematically brushed teeth using a brushing machine with dentifrice or saline solution and evaluated resulting abrasion marks through SEM. Enamel exhibited minimal changes in abrasion marks, whereas cementum saw an increase with brushing duration, attributed to the hardness of abrasion particles. This led to the conclusion that dentifrice primarily causes abrasion marks, with saline brushing exerting only a minor influence (Litonjua et al. 2003). On tooth surfaces, features of the worn surface have already been found to varying degrees in previous studies. These include abrasion marks running horizontally, vertically or transversely, elongated infractions or even rough isodiametric pits (Walker et al. 1978). Mechanical

wear of the tooth surface removes tiny amounts of material from tooth surfaces, accumulating over time and becoming visible as macroscopic wear. Microwear can already occur at forces of 1 mN or less (Lucas and van Casteren 2015). The occurrence of abrasion marks and infractions depends on various factors, including mechanical stress, individual brushing habits, different compositions of hard tissues and the age of teeth. Tiny, sharp particles with a greater hardness than enamel, such as sand and grains, can also cause abrasion marks when gliding over the surface. Some research groups have made efforts to deduce the community's diet based on micro-abrasion marks on fossil teeth (Ungar et al. 2006, Constantino et al. 2010). A static indentation creates a dimple (pit), while an additional translational movement leads to an abrasion scratch. However, scratches seem much easier to create than pits (Sharp et al. 1993, Lucas and Omar 2012). Coarse abrasive particles in some dentifrices can also cause abrasion marks, especially when teeth are brushed with great force. According to Scott et al. (1949), the percentage of abrasion marks on tooth surfaces has remained relatively constant over the years. In a comprehensive study of the appearance of the tooth surface in various age groups, Mannerberg (1961, 1964) determined that changes in morphological features were associated more with toothbrushing habits than age. Additionally, Mannerberg concluded that alterations in the extent of abrasion marks could be attributed to enamel remineralization processes. Saxton (1976), in an assessment of a two-week toothbrushing program, observed the continuous emergence of new abrasion marks alongside the disappearance of previous ones. Remineralization of superficial abrasion marks is facilitated by the precipitation of minerals from saliva or oral hygiene products penetrating the intercrystallite space (Rivera et al. 2013). In a study by Borrero-Lopez et al. (2014), remineralisation of abrasion marks within 48 hours resulted in a reduction of their length by up to 10%. However, as new ones are generated, the proportion of abrasion marks remains relatively constant (Ten Cate and Arends 1980). Based on this knowledge, numerous studies are currently investigating the remineralisation potential of reagent additives in dentifrice. From age 35, a natural levelling of the occlusal fissure relief and tooth surfaces can be assumed. Therefore, natural abrasion leads to a reduction in predilection sites and thus reduces the risk of caries (Shellis 2010). Toothbrushing's polishing effect is advantageous as it hinders subsequent plaque accumulation (Schemehorn et al. 2011). The research by O'Toole et al. (2021) demonstrated that brushing with a low-abrasive dentifrice smoothed the tooth surface, whereas using an abrasive toothpaste led to a rougher surface, facilitating undesirable plaque accumulation. Thus, achieving the correct balance between cleaning and polishing abrasiveness, along with substance protection, is crucial (Birke 2016). The findings from this study indicate that both manual toothbrushes and low-abrasive dentifrices can effectively smooth buccal tooth surfaces and cervical margins, leading to a reduction in plaque adhesion and, consequently, a decrease in the risk of caries formation. The vanishing abrasion marks can be attributed to continuous diffuse abrasion and remineralization processes occurring on the tooth surface.

6.3.2 Appearance perikymata (AP)

Perikymata, representing Retzius lines, manifest as discernible markings on lateral enamel surfaces. These lines present as irregularly curved circles encompassing the tooth surface, gradually diminishing in prominence from the equatorial circumference towards the cusps and incisal edges. The highest density of perikymata is observed in the cervical tooth region, as reported by Fejerskov et al. (1984). Perikymata are an indicator of tooth growth and have special characteristics within a species. In human teeth, the typical depth of the perikymata range between 2 and 5 μm in depth and exhibit a spatial distribution at intervals of 50 to 100 μm (Elhechmi et al. 2013). In forensic contexts, the count of perikymata becomes a valuable tool for estimating the date of death, especially when the formation of the dental crown was still in progress at the time of the individual's demise (Bromage and Dean 1985). As a result of physiological tooth wear, the average enamel thickness in a 65-year-old has decreased by approximately one-third. This process also contributes to the flattening of perikymata and the gradual disappearance of microporosities with advancing age (Kidd et al. 1984). Mannerberg (1961) discovered that by the age of 20, approximately 20% of tooth surfaces exhibit such significant wear that individual perikymata are no longer distinguishable. Overall, the characteristic features of perikymata gradually diminish with age, giving way to a predominantly abrasion-marked appearance. Perikymata on the molars and premolars tend to be preserved longer than those on the corresponding surfaces of the canines and incisors. Notably, the cervical tooth region is the last to lose these distinctive structural features, as noted by (Scott et al. 1949).

6.3.3 Exposed prismatic enamel (EPE)

As outlined by Kunin et al. (2015) before eruption, permanent teeth predominantly exhibit a prismatic surface, which transitions to an aprismatic character post-eruption. The parallel arrangement of aprismatic crystals contributes to heightened mineralization of the tooth surface, enhancing resistance to abrasion and acid solubility (Robinson et al. 1971, Park et al. 2008). In prismatic enamel, by contrast, the orientation of crystals often changes abruptly at prismatic boundaries and are intertwined in a "decussation" pattern, which reduces the tendency for infraction propagation (Borrero-Lopez et al. 2021). As post-eruptive enamel maturation progresses, the overall thickness of the aprismatic layer increases due to the surface mineralisation (Gängler et al. 2005). The thickness of the aprismatic layer is influenced by the chewing process, salivary mineral adsorption, and regular fluoridation. Consequently, prismatic areas are still anticipated in juvenile teeth, while in older teeth, the enamel surface predominantly exhibits an aprismatic character (Thompson 2020). Per Camboni and Donnet (2016), the typical thickness of an aprismatic layer ranges from 10 to 30 μm . Aprismatic enamel may either entirely cover the enamel surface or exhibit gaps, allowing prismatic enamel to protrude. The distinctive "honeycomb" appearance of prisms following acid etching has been vividly demonstrated in numerous studies (Mannerberg 1961, Gängler et al. 2005).

6.3.4 Enamel infractions (EI)

Owing to its inorganic structure, tooth enamel stands as the hardest substance in the human body. However, despite its formidable hardness enamel exhibits a notably low modulus of elasticity (70 to 110 GPa), comparable to the elasticity of glass (40 to 90 GPa) (Segarra et al. 2017). Therefore, deformation leads to infractions in the brittle enamel, which can sometimes develop into fractures (Cuy et al. 2002). Numerous studies indicate the presence of vertical infractions in tooth enamel, typically remaining inconsequential due to the decussation limiting their propagation within the crystal microstructure. The majority of these infractions are so subtle that they are barely visible under direct illumination and often escape detection on routine intraoral images (Kim et al. 2020). Hence, their prevalence is frequently underestimated in clinical assessments. According to Scott et al. (1949), enamel infractions were identified in over 90% of examined surfaces across various age groups, with the majority originating at the cemento-enamel junction (CEJ), even in teeth that had not yet erupted. In the study by Zachrisson et al. (1980), vertical infractions were observed in 60–70% of cases, primarily in the cervical third of the teeth. Enamel infractions are believed to arise from intrinsic imperfections formed during tooth development, known as lamellae. Originating from the dentin-enamel junction and penetrating about one-third of the enamel thickness between tufts, these features become apparent first in the thin cervical enamel layer. This concept of intrinsic weakness, common in biomaterials, enhances fracture toughness, similar to the prevention of crack propagation in nacre layers and fibrous bone microtissue by organic nodes (Evans et al. 2001, Borrero-Lopez et al. 2020). Hence, the majority of enamel infractions are natural occurrences that typically do not penetrate significantly into the dentin (Lee et al. 2011). However, under prolonged or increasing loads, infractions may expand (He and Swain 2008). Mastication loads and rapid thermal changes can cause enamel infractions by disrupting crystal bonds. Front teeth, particularly middle incisors, are vulnerable due to pronounced thermal fluctuations during activities like eating (Zachrisson et al. 1980). First molars, located in the masticatory centre, are also susceptible (Despain et al. 1974, Bachmann and Lutz 1976). The width of typical infractions ranges between 1 μm and 5 μm , as demonstrated in this study (*Section 5.6.4*). Dental enamel exhibits relatively high toughness against infractions running perpendicular to prisms. In contrast, infractions that run horizontally or transversely are considered more critical, potentially indicating a higher susceptibility to fracture (Xu et al. 1998). The development of enamel infractions is also influenced by the thickness of the enamel layer, which averages 1.4–1.8 mm for molars and 1.3 mm for incisors. Thicker enamel layers contribute to a higher degree of decussation, serving as a protective factor against fractures and wear effects, especially during prolonged loading (Lucas and van Casteren 2015, Wilmers and Bargmann 2020).

6.3.5 Open dentin tubules (ODT)

Dentin's morphological structure, characterized by tubules, includes highly mineralized peritubular dentin. SEM reveals distinct mineralization zones (*mantle, globular, interglobular, granular dentin*) and primarily distinguishes two dentin forms (*secondary and tertiary*) (Schaffner et al. 2016, Karteva et al. 2019). Erosive attacks dissolve peri- and intertubular material, revealing dentinal tubules that can appear open, narrowed, or completely closed under SEM (Wang et al. 2010). Dentinal tubule diameter and density vary by layer. Near the pulp, density reaches around 40,000 tubules per mm², decreasing to 17,000–20,000 per mm² towards the dentin-enamel junction (Pashley et al. 1985). The average count ranges from 8,000 to 29,000 per mm² (Daley et al. 2009), with tubules having a diameter of 0.8 to 1.2 µm and spacing of approximately 10 µm (Thompson 2020). The etching process doesn't immediately result in a volume loss of dentin, as organic components are initially preserved. However, these can be easily removed by mechanical forces (Breschi et al. 2002). Natural abrasion facets of dentin typically lack open tubules, as these close over time due to the gradual sclerotization process (Ketterl 1983). In cases of toothbrush abrasion, hypersensitivity in the cervical region is reported, strongly correlating with the frequency of open dentinal tubules (Lussi et al. 1993). However, the risk of dentin hypersensitivity notably decreases after the age of around 60 (Carvalho and Lussi 2017). In our study, younger teeth showed more open dentin tubules due to abrasion. As cervical abrasion deepened, isolated exposed dentin was observed in the wedge-shaped lesions of older anterior teeth (*Section 5.6.5*).

6.3.6 Dental calculus (DC)

The mechanical removal of dental calculus through scaling and root planning can result in surface roughness, significantly impacting microorganism colonization and thereby promoting the progression of caries and periodontal disease (Walker and Ash 1976, Leknes et al. 1994). A smooth tooth surface, less susceptible to plaque accumulation, is achievable through polishing following (ultra-) scaling. This study illustrates the impact of tooth brushing on surface roughness, particularly achieving explicit smoothing of the CEJ and root cementum in the cervical region of all sample teeth (*Section 5.6.6*). Dental polishing is a crucial aspect of clinical dentistry, receiving significant attention in the literature for finishing restorative materials. As demonstrated in this study, regular toothbrushing contributes to surface smoothing, minimizing plaque accumulation, and promoting effective periodontal care.

6.3.7 Peninsula formation (PF)

Schroeder and Scherle (1988) and Grossman and Hargreaves (1991) were pioneers in identifying the prevalent undulating (scalloping) pattern of the cemento-enamel junction as a distinctive feature of human teeth. When this contour is accentuated by abrasion, it can result in the formation of enamel peninsulas. Additionally, toothbrushing contributes to rounding off sharp edges along the cemento-enamel junction. Another remarkable feature is the occurrence of enamel islands, which form sporadically on the root surface. While enamel islands are rarely discussed in the literature, this study observed their presence in 5 out of 14 teeth, suggesting that it is not a rare phenomenon (*Section 5.5.7*).

6.3.8 Cemento-enamel junction (CEJ)

The scanning electron microscope provides precise images of the cemento-enamel junction's morphological features and the structural relationships among dentin, cementum, and enamel, owing to its high accuracy (Akai et al. 1978). With increasing age, continuous passive eruption, compensating for occlusal wear, gradually exposes cemento-enamel junction (CEJ) structures to the oral environment, subjecting them to physical influences like toothbrushing. This may result in morphological changes, occasionally with notable clinical implications. Given the thin cervical enamel layer (< 0.2 mm) and the susceptibility of cementum and dentin to environmental influences, this area is highly prone to wear (Aw et al. 2002). The CEJ is crucial for diagnosing periodontal attachment loss. Additionally, the cervical region exhibits an exceptionally high prevalence of cervical caries and dentin hypersensitivity (Walters 2005). Previous studies documented Cemento-Enamel Junction (CEJ) frequencies: Cementum overlapping enamel (type 1) 60-65% > edge-to-edge (Type 2) 30% > and gap (Type 3) 10% (Cloquet 1899, Nanci and Ten Cate 2017). A later addition introduced enamel overlapping cementum (Arambawatta et al. 2009). Our study observed CEJ frequencies: Edge-to-edge (type 2) 50% > Gap (type 3) 36% > cementum overlap (type 1) 14%, consistent with recent findings (*Table 25*). While some studies have adjusted the numbering to: Edge-to-edge (Type I) > Gap (Type II) > Cement overlapping enamel (Type III) > Enamel overlapping cement (Type IV) (Araveti et al. 2020), this study maintains the old order for clarity. The gap-type at the cemento-enamel junction was previously associated with susceptibility to wear, hypersensitivity, and caries (Arambawatta et al. 2009). This study, however, found the gap CEJ predominantly in juvenile premolars with minimal oral exposure, making external factors like abrasion or erosion less likely. It is suggested that the cemento-enamel junction relationship may shift from a gap to an edge-to-edge or cementum overlap type due to cementum apposition, as long as the area is covered by gingival tissue (Astekar et al. 2014). This transformation halts once the CEJ is exposed to the oral environment (Smith 1998). However, enamel overlapping cementum (type 1), previously described as the most common type and occurring in only 14% of teeth in this study, was observed even less frequently in some recent studies. For example, with a frequency of 7% in Astekar et al. (2014) and a frequency of 6% in Araveti et al. (2020). The

cementum overlapping the enamel is commonly known as coronal cementum. But in contrast to the multi-layered dentin-enamel junction, the coronal cementum overlapping enamel is only weakly micromechanically bonded to the enamel and therefore tends to flake off and is also considered highly susceptible to tooth wear (Ho et al. 2009). Boyde (2005) attributes the shift in frequencies for cementum overlapping enamel (type 1) to three factors: 1. Natural variations in the length of coronal cementum around a crown result in different CEJ types within a tooth, depending on the sectioning plane. 2. Extraction procedures can significantly damage or tear off the fragile coronal cementum due to ligament traction. 3. Located above the gingiva, toothbrushing and dental hygiene actions can cause relatively rapid loss of the less mineralized coronal cementum. The CEJ's enamel and dentin are often covered by a collagen-free matrix known as acellular afibrillar cementum, characterized by a relatively high organic content and, consequently, a low elastic modulus (Hassan and Mohamed 2015). Araveti et al. (2020) speculated that **overlapping cementum** occurs mainly in juvenile premolars because the teeth were extracted early for orthodontic reasons. Therefore, the coronal cementum remained protected from wear by gingival tissue. However, this study cannot confirm this observation, as the juvenile premolars here predominantly presented the **gap (type 3)**. Conversely, **overlapping cementum** was found in the young adulthood wisdom tooth A47, the middle-aged molar B46 and an old incisor A41. The rare occurrence of enamel overlapping cementum (type 4) is difficult to explain from an embryological point of view, as cementum formation begins only after enamel formation is complete. Muller and van Wyk (1984) interpreted type 4 as an optical illusion due to the thickness of sections. Subsequent authors considered type 4 an artefact caused by the grinding process during the preparation of the specimens (Smith 1998, Astekar et al. 2014). However, if the enamel islands described above are considered type 4 remnants, then the type of enamel overlapping cementum would be found in 5 of the 14 teeth in this study. Finally, the CEJ shows an enormous morphological diversity in the same tooth (Schroeder & Scherle 1988, Grossman & Hargreaves 1991). Due to the variability of all three tooth-hard substances in the cervical region, it has already been suggested that the junction should better be referred to as the dentin-cemento-enamel junction (Neuvald and Consolaro 2000, Arambawatta et al. 2009, Nanci and Ten Cate 2017).

■ **Table 25: Overview: Cemento-enamel junction type distribution**

Overview: Examination with light microscope (LM) and SEM	Reference
<p>60–65% overlapping cementum > 30% edge-to-edge > 10% gap type</p> <p><i>In 1899, Cloquet was the first to describe three morphological types of CEJ using light microscopy. However, the interpretation of the features was still difficult.</i></p>	Cloquet (1899)
<p><i>Thorsen et al. (1917) data are in agreement with the study results of Cloquet (1899) and are henceforth included in most textbooks of oral histology.</i></p> <p><i>The overlapping cementum was attributed by Thorsen to a methodological and interpretative error. Thorsen also described enamel overlapping cementum (type 4).</i></p>	Thorsen (1917) Nanci and Ten Cate (2017)
<p>44% enamel overlapping cementum > 30% edge-to-edge > 16% gap type > 10% overlapping cementum</p> <p><i>Birrer (1952) reported that dentin exposure was more frequent on the buccal sides of teeth (23.1% buccal, 11.4% lingual). This observation was confirmed in the studies by Schroeder et al. (1988) and Arambawatta et al. (2009).</i></p>	Birrer (1952) 143 teeth
<p><i>Incisors: 49% edge-to-edge > 33% overlapping cementum > 18% gap type</i></p> <p><i>Premolars: 65% edge-to-edge > 31% overlapping cementum > 4% gap type</i></p> <p><i>Molars: 46% edge-to-edge > 42% overlapping cementum > 12% gap type</i></p> <p><i>Dentin exposure frequently more on the buccal side.</i></p>	Muller and van Wyk (1984) 150- μ m-thick sections from 152 teeth
<p>Premolars: 68% edge-to-edge > 30% overlapping cementum > 1% gap type</p> <p>Molars: 52% overlapping cementum > 43% edge-to-edge > 5% gap type</p> <p><i>In the wisdom teeth, 50% were found to have overlapping cementum.</i></p> <p><i>Schroeder and Scherle found that the relationship of the three hard tissues in the CEJ region on a single tooth is unpredictable and irregular.</i></p>	Schroeder (1988) 8 juvenile premolars 6 third molars SEM combined with LM
<p><i>Grossmann describes the overlapping cementum as the predominant CEJ type and again subdivides it into three subtypes. Exposed dentin surfaces occurred in only five teeth. Grossmann described the conspicuous “scaloping” of the CEJ as a striking morphological feature. Furthermore, the CEJ types varied in a single tooth.</i></p>	Grossman and Hargreaves (1991) 18 teeth of one man
<p>76% edge-to-edge > 14% overlapping cementum > 10% gap type</p> <p><i>What appeared to be a gap between enamel and cementum at low magnification (10x) turned out to be just a groove in cementum. No exposed dentin was observed in the SEM in this area.</i></p> <p><i>Overlapping of cementum with the enamel was less frequent than previously reported.</i></p>	(Bevenius et al. 1993) 50 juvenile premolars SEM with polarisation microscopy
<p>50% edge-to-edge > 36% overlapping cementum > 10% gap type</p> <p>Enamel overlapping cementum (type 4)</p>	Neuvald and Consolaro (2000) 198 teeth
<p>55.1% edge-to-edge > 30.7% gap type > 12.6% overlapping cementum</p> <p>1.6% enamel overlapping cementum (type 4)</p> <p><i>Overlapping cementum was found much less than previously reported. Enamel overlapping cementum (type IV) was found in only a very small proportion of the sample.</i></p>	Arambawatta et al. (2009) 67 juvenile premolars
<p><i>Teodorovici et al. (2010) reported that the gap type with exposed dentin is more common in maxillary incisors. The most common CEJ relationship was edge-to-edge type, followed by the gap type and the overlapping cementum. Dentin was exposed more frequently buccally and lingually (about 22–24%) than mesially and distally (about 13%). It has been suggested by Araveti et al. (2019) that this is because the proximal surfaces are better preserved from external factors such as abrasion and erosion.</i></p>	Teodorovici et al. (2010)
<p>52.5% edge-to-edge > 40% gap type > 7.5% overlapping cementum</p> <p>0% enamel overlapping cementum (type 4), photomicrograph of ground sections.</p> <p><i>The gap type was seen more frequently on the buccal and lingual surfaces of teeth.</i></p>	Astekar et al. (2014) 80 permanent teeth 38 ant., 42 post.
<p>50% edge-to-edge > 36% overlapping cementum > 10% gap type</p> <p>4% enamel overlapping cementum (type 4)</p>	Hassan and Mohamed (2015) 50 juv. premolars
<p>56.8% edge-to-edge > 36.5% gap type > 6.4% overlapping cementum</p> <p>0.3% enamel overlapping cementum (type 4)</p>	Araveti et al. (2020) 100 permanent teeth

6.3.9 Morphology of cervical abrasion lesions

Brady and Woody's (1977) SEM investigation classified cervical abrasion lesions as either round and shallow or angular and deep. Bevenius et al. (1993) further categorized them as saucer or wedge-shaped lesions. Litonjua et al. (2004) expanded the classification to include wedge-shaped, saucer-shaped, or a mixture of both. Walter et al. (2014) proposed that wedge-shaped lesions primarily result from occlusal attrition or "abfraction," noting increased plaque accumulation and sharp-edged margins attributed to microfractures. Conversely, saucer-shaped lesions, nearly plaque-free with more groove lines, support the theory of abrasion due to toothbrushing. However, Daley et al. (2009) found no histopathological evidence for abfraction in wedge-shaped lesions, identifying multiple horizontal grooves as indicative of toothbrush abrasion. Litonjua et al. (2004) suggested that toothbrushing alone can induce various defect forms, including wedge-shaped lesions, where slight enamel undermining causes sharp angles on the cemento-enamel junction, leading to edge breakage. Dzakovich and Oslak (2008) reproduced cervical lesions with sharp line angles through repeated horizontal toothbrushing movements using an abrasive dentifrice. They hypothesized that the type of toothbrush filaments influences the development of various forms of cervical lesions. In our study, we observed sharp-edged enamel margins on the cervical enamel in some cases, despite the teeth not being exposed to any occlusal load (*Figure 43, p. 43*). Therefore, the observation of sharp edges does not exclude abrasion as a factor. Manly and Schickner (1944) observed that horizontal brushing initially formed linear grooves, evolving into wedge-shaped lesions as abrasion advanced. They noted that abrasion predominantly occurred in the grooves, not on the crests. The development of cervical wedge-shaped lesions was identified as a fundamental feature of dentin abrasion by abrasive brushing, with abrasion progressing most rapidly at the bottom of the notch. This process is analogous to mechanical abrasion by water, creating clefts that deepen gradually and contribute to significant soil loss. Even gentle pressure on the toothbrush causes filaments to slide over pre-existing lesions, concentrating force on the areas already worn down the most. Exploring the impact of different bristle configurations on cervical lesion development is also of interest.

6.4 Advantages 3D-SEM

A standardized method for reliably quantifying the progression of tooth wear has not been established. Current research methods vary from contact or non-contact profilometry to radiotracer and complex computer-generated 3D images using digital laser microscopy (Schlueter et al. 2011). The challenge lies in quantifying profile or volume loss on the reference-free, curved, and complex surface of undamaged teeth with irregular peaks and valleys. Consequently, tooth wear processes are primarily assessed on flat, polished enamel surfaces conforming to ISO standards for analysing step heights (O'Toole et al. 2021). However, polished enamel surfaces react differently to wear than natural enamel and are therefore not directly transferable to the clinical situation (Ganss et al. 2000, Mylonas et al. 2018). Wright (1969) suggested that enamel wear from toothbrushing could be 0.2 mm over a lifetime. According to Zachrisson and Arthun (1979), enamel wear amounts to approximately 2 μm per year. In modern times, the use of toothpastes with reduced abrasive particles suggests lower wear on tooth structure due to toothbrushing. Overall, enamel wear attributed to brushing is considered minimal (Addy and Hunter 2003). Pickles et al. (2005) reported enamel abrasion from dentifrice to be less than 0.5 μm after 24 weeks in an in-situ investigation. In recent years, modern technologies have greatly improved the accuracy of tooth wear measurements. However, even O'Toole et al. (2021) reported that the accuracy is not yet sufficient to detect the minute differences in wear on the lateral surfaces between successive tooth surface scans. Occlusal wear rate is easier to measure, as stable side surfaces of teeth can be used as reference surfaces. The primary objective of this study was to determine the average wear rate of buccal enamel after three years of toothbrushing using lateral reference holes. However, the observed wear rates fell below the measurement inaccuracies of the system, reaching the limits of the measurement method and its reproducibility. Furthermore, there are biologically determined differences in the susceptibility to wear between tooth samples from different donors (Uhlen et al. 2016). On the contrary, dentin exhibited a significantly greater susceptibility to wear from toothbrushing (Hooper et al. 2003, Wiegand and Attin 2011). Addy et al. (2002) anticipated dentin abrasion of up to 1 mm over a lifetime. Kodaka et al. (2001) utilized an intraoral device to brush dentin specimens daily with a low-abrasive dentifrice. Laser scanning microscope measurements revealed an abrasion ranging from 80 to 140 μm . Hence, our study emphasized the quantitative measurement of volume loss attributed to abrasion in the cervical tooth region.

6.4.1 Comparative analysis of volume loss in publications

Volume loss is the preferred parameter for quantifying tooth wear as it progresses linearly with time, unlike one-dimensional step depth (DeLong 2006). To facilitate comparison across various study designs, volume changes must be normalized to the affected area. The International Organization for Standardization outlines the determination of tissue loss in polished dentin or enamel samples by calculating the mean depth profilometrically (BS EN ISO 11609: 1998).

After **95,040 buccal strokes** per tooth over the three-year toothbrushing cycle in this study, the volume loss ranged from **0.020–0.188 mm³** with an extrapolated step height per mm² of **15–37 $\frac{\mu\text{m}}{\text{mm}^2}$** ; \emptyset **25.6 $\frac{\mu\text{m}}{\text{mm}^2}$** . In this context, the volume loss is normalized by the reference area to compute the average depth of wear. This abrasion depth value facilitates comparison with profilometric studies (Table 26).

▪ **Table 26: Overview for comparison of volume loss results**

Reference	Volume loss	Step depth	Method
This study: Wilke (2022)	0.020–0.188 mm ³ after 95,040 buccal strokes under a brush force of 3.5 N	15–37 $\frac{\mu\text{m}}{\text{mm}^2}$; \emptyset 25.6 $\frac{\mu\text{m}}{\text{mm}^2}$	28 epoxy replicas 4Q - BSE SEM
Dyer et al. (2000)	Toothbrush Hard: 3.19 μm ; Medium: 4.30 μm ; Soft: 5.29 μm after 20,000 strokes under a brush force of 200 g (2 N) .	15–25 $\frac{\mu\text{m}}{\text{mm}^2}$	Polymethyl methacrylate Contact profilometer
Addy et al. (2002)	Step depth of 0.96–2.43 μm after 3 months intraoral device; 7x/day 60sec; 10 days	12–29 $\frac{\mu\text{m}}{\text{mm}^2}$	10 ground dentin samples Contact profilometer
Rodriguez & Bartlett (2010)	0.02–0.07 mm ³ after 2,000 strokes under a brush force of 200 g (2 N) . <i>Toothbrushing machine (Abrasion testing machine No. 8. The Pepsodent Co. USA).</i>	18–47 $\frac{\mu\text{m}}{\text{mm}^2}$	80 ground enamel samples Addition silicone impression Non-contacting laser profilometers Taicaan™
Liljeborg et al. (2010)	1.39–9.68 mm ³ after 12,000 double strokes under a brush force of 2.35 N <i>Brushing machine; reciprocating movement of 85 mm, 2,000 double strokes per hour.</i>	55–383 $\frac{\mu\text{m}}{\text{mm}^2}$	Acrylic plates with hardness similar to dentin Contact profilometer Stylus tip radius: 2 μm
Sabrah et al. (2018)	1.12–4.19 mm ³ after 65,000 strokes under a brush force of 200 g (2 N) . <i>V-8 brushing machine (horizontal brushing)</i>	90–340 $\frac{\mu\text{m}}{\text{mm}^2}$	16 human premolars Vinyl polysiloxane 3D optical profilometer <i>Proscan 2000, Scantron, Taunton, UK.</i>
Turssi et al. (2019b)	A: 3.81 mm³; B: 2.56–2.92 mm³ after 55,000 double strokes under a brush force of 3 N <i>V-8 brushing machine (horizontal brushing)</i> <i>*A: flat-trim manual toothbrush; B: cross-angled multileveled or feathered toothbrushes.</i>	<i>Not possible</i>	16 human premolars Vinyl polysiloxane 3D optical profilometer <i>Proscan 2000, Scantron, Taunton, UK.</i>

Results from Turssi et al. (2019b) suggested that using a tapered toothbrush may be beneficial compared to a regular flat-trim toothbrush. Fluoride can increase the dentin's resistance to abrasion caused by toothbrushing (Bartlett et al. 1994, Hara et al. 2009). When assessing wear rates, it's crucial to acknowledge that the measurement inaccuracy of recording systems frequently exceeded the recorded substance removal. For instance, Rodriguez et al. (2012b) reported a measurement accuracy of about 15 μm , with only 22% of the 30 tooth samples having a value above the measuring error. Sabrah et al. (2018) reported a combined error, both between and within examiners, of $\pm 0.24 \text{ mm}^3$. In future studies, it may be worthwhile to record volume changes within a standardized measurement area to ensure reproducibility and comparability of results (O'Toole et al. 2020b).

6.4.2 Imaging errors of 3D SEM

The calibration protocol for the 3D scanning electron microscope (4Q BSE detectors) allowed correction for most imaging errors. Using a multifunctional reference body, paired replicas of a tooth before and after brushing were captured within the same calibration. Despite this, some distortion in the recorded data persisted, particularly at the image edges. To mitigate the issue, cervical lesions were cropped out, resulting in a potential underestimation of volume loss. However, as the model teeth were in proximal contact, significant substance abrasion in marginal areas was not anticipated.

6.4.3 Sputter coat

During the accuracy test with replicas of the reference body, it was found that the 4Q-BSE detectors underestimated the depth of the reference groove with a thin sputter coating of 20 nm Au (*original depth: 328.7 μm vs 164.2 μm with 25 nm Au and 222.5 μm with 50 nm Au*). Sputtering with a gold layer of 15–20 nm is common and has been applied in comparable dental studies (Camboni and Donnet 2016). Therefore, this technical phenomenon, possibly caused by a phase transition between different material densities (gold vs epoxy resin), still needs to be clarified. Subsequently, tooth replicas were sputtered with an additional 80 nm of gold, as only with a thicker coating did the measurement accurately reflect the actual depth of the reference groove. Therefore, replicas were sputtered with a total of 100 nm of gold for 3D SEM measurements. In contrast, the morphological evaluation of characteristic features was carried out in advance with a 15–20 nm sputtering layer.

6.4.4 Software alignment

The accurate alignment of corresponding surfaces significantly influences measurement precision (DeLong 2006). Previously, *in vivo* quantitative tooth wear assessment necessitated fixed reference points. Rodriguez and Bartlett (2010), for instance, employed three drilled enamel reference points to superimpose models. However, alignment challenges arose due to the absence of unchanged reference points detected by the software in more than half of the teeth. *In situ* studies often faced issues with metal markers getting lost during examination, rendering affected teeth untraceable for evaluation (Schlueter et al. 2005, Huysmans et al. 2011). Subsequent to its initial applications, advancements in technology and software have facilitated the execution of measurements without the necessity of attached reference points (Mitchell and Chadwick 1998). The intricacies captured by scanning electron microscopy (SEM) have enabled the meticulous overlay of data networks in this study. This overlay is grounded in the natural roughness of the enamel surface and the cervical enamel margin, ensuring a reliable and comprehensive analysis. The alignment method selected plays a crucial role in shaping measurement outcomes (Besl and McKay 1992). Historically, a standardized best-fit algorithm has been employed, aiming to achieve the optimal mathematical approximation of the data. In instances where best-fit methods are utilized without reference points, alignment accuracy reports have indicated a range of 15–25 μm (Rodriguez et al. 2012a, Wulfman et al. 2018). However, this *iterative closest point (ICP) algorithm* to merge maps to the best possible

alignment does not consider whether the proposed alignment solution is biologically appropriate (Mitchell and Chadwick 1998). The best-fit alignment method effectively minimizes mesh spacing errors between two datasets; however, it may consequently lead to an underestimation of the magnitude of differences in that specific area (O'Toole et al. 2019). Upon visualizing the best-fit alignment in the 3D-Reshaper software, it became evident that the algorithm struggled to optimally align curved tooth surfaces. This limitation is evident in the computed negative and positive differences. Negative differences are indicative of wear, whereas positive differences imply an improbable increase in tooth structure. To rectify this, all points with positive values on the z-axis, representing measurement errors, were adjusted to zero. The same principle was applied by Rodriguez et al. (2012). By initially isolating the cervical lesion area and placing landmarks at distinctive points, we reduce calculation errors. Following the validated approach by O'Toole et al. (2019), our study adopts reference alignment, significantly minimizing errors and enhancing measurement accuracy. Manual correction of model inclinations ensures optimal alignment. However, operator input influenced alignment outcomes, potentially causing varied volume loss determinations. To ensure consistency, all alignments were performed by a single operator (KW) and repeated on different days, yielding an average deviation of $\pm 0.0011 \text{ mm}^3$. Future studies could explore differences in recorded volume losses among different operators for additional insights.

6.4.5 Measurement inaccuracies

Measurement inaccuracies of **0.6 μm** in depth (z-axis), **6 μm** in length and **0.007 mm^3** in volume calculation were observed concerning the known geometric dimensions of the reference body. Rodriguez and Bartlett (2010) used a 3.9 mm^3 titanium cone as a reference, achieving 0.9 μm accuracy for step height and 0.001 mm^3 for volume. Our system demonstrated superior z-axis accuracy, but the volume measurement (0.007 mm^3) was slightly less accurate than Bartlett's method. While standard geometric reference bodies are commonly used to assess measurement accuracy, they may not adequately capture the geometric intricacies of teeth. Rodriguez et al. (2012) addressed this by crafting true-to-scale reference bodies resembling tooth onlays. The findings revealed that the system's measurement accuracy varied between complex tooth-like structures and simple geometric figures, highlighting the limitations of using standard reference bodies for assessing accuracy in dental contexts. Moreover, the individuality of natural enamel surface topography is heightened by factors such as perikymata, functional abrasion marks, pits, and enamel caps. This inherent complexity introduces challenges in accurately measuring natural enamel surface features, as measurement errors often arise when scanning intricate and curved surfaces (Austin et al. 2015). O'Toole et al. (2021) advocated for a detection accuracy of less than 50 μm in measuring tooth wear. In a study by Hayashi et al. (2022) found that the width/depth ratio increased by more than 50 μm in half of the cervical lesions studied, but rarely became deeper than 50 μm .

6.5 Statistical limitations

In this exploratory study, our primary focus was on characterizing morphological features, assessing abrasion severity, and evaluating a novel technique for measuring volume loss after three years of robotic toothbrushing on unpolished teeth, utilizing 3D SEM. The careful selection of tooth samples, guided by well-defined criteria, allowed for the creation of a comprehensive catalogue of pathobiological abrasion patterns. The decision to initially forego detailed case number planning was driven by uncertainties about observable effects and the substantial effort dedicated to method development. Nevertheless, biological interpretation frequently presents challenges, with individual characteristics influencing the observed differences in assessments. Instances involving teeth with periodontitis and exposed roots, coupled with variations in donors' brushing habits, may yield significantly larger cervical abrasion lesions. Confounding variables like gender, age, and specific medical conditions are viewed as random disturbance factors. These confounders can be addressed through exclusion or levelled out via randomization. Therefore, achieving statistical differentiation of volume results is highly intricate and cannot provide a reliable outcome given the limited number of human tooth samples. The small and non-representative sample size precludes the extrapolation of findings from both descriptive and confirmatory statistics to the broader population. Consequently, assertions are confined to the available dataset. However, specific abrasion patterns showed statistical significance, suggesting a trend where the *Rapid Relief* toothbrush, with its flexible neck, contributed to significantly lower abrasion compared to the *Jubilee* toothbrush. The insights derived from the current data could lay the groundwork for formulating future working hypotheses. When comparing abrasion patterns among two or more brushes in different groups, the conventional t-test becomes invalid when variances are not homogeneous, as observed in this sample. However, Welch's t-test, which does not assume equal standard deviations in the groups, can be applied in such cases. The homogeneity of variances can be assessed using Levene's test for variance homogeneity. In toothbrush studies, there is often an assumption of encountering a normal distribution of results. Although larger subject numbers can tend to normalize the mean, it is crucial, especially in studies with a limited number of subjects and non-normally distributed results, to consider abnormal distributions such as skewness. It is imperative to provide mean values, standard deviation, standard error, and variance. Procedures involving morphological characterization, relying on descriptive terms like few, some, and extended, which are then converted into a numerical system for statistical assessment, are prone to errors. The statistical evaluation of numerically rated criteria is inherently subjective. Thus, it is crucial to provide appropriate training and calibration for evaluators to minimize subjective errors. In this study, two professional assessors conducted the abrasion patterns assessments. One evaluator, blinded and devoid of additional information about the tooth samples, ensured unbiased evaluations, as expectations could otherwise influence the outcome. Furthermore, a panel of images accompanied by respective codes for each abrasion pattern was generated to facilitate future evaluators in achieving as objective a classification as possible.

6.6 Alternative methods

According to Nawrocka et al. (2021), the most common techniques for tooth wear investigations are currently confocal laser scanning microscopy (CLSM), scanning electron microscopy (SEM), transmission electron microscopy (TEM) and atomic force microscopy (AFM). The following is a brief overview of common technologies for examining tooth wear.

6.6.1 Profilometry

The measurement of tooth wear by profilometric analysis has been established for decades and can be used both in vitro and in vivo (Davis and Winter 1976, Addy et al. 2002, González-Cabezas et al. 2013). A distinction was made between the mechanical profilometer (Krämer and Kunzelmann, 1995) and the optical, non-contact profilometry (Ganss et al. 2007b). The measuring accuracy is determined by the size of the diamond tip of the stylus, which has a radius between 0.1 and 25 μm (Radhakrishnan 1970). Another disadvantage of contact profilometry is that mechanical scanning of softer surfaces can lead to damage in the form of scratches or surface destruction, resulting in further measurement inaccuracies (Chuenarrom and Benjakul 2008). (Attin et al. 2009) stated an accuracy of 0.105 μm as the lower limit for contact profilometry. To create optimal conditions for profilometry, samples should be flattened and polished before the examination (O'Toole et al. 2021).

6.6.2 Non-contacting profilometry and confocal laser scanning microscopy

Unlike a mechanical tactile profilometer, employing non-contact and digital laser profilometry yields higher resolution (Rodriguez et al. 2012a, Wulfman et al. 2018). A commonly referenced device for assessing tooth wear is the optical profilometer *Proscan 2000* (Scantron, Taunton, UK), designed specifically for surface measurements in the dental industry (Turssi et al. 2019b). Since its inception, a multitude of optical scanners has entered the market. For instance, O'Toole et al. (2019) achieved an accuracy of < 10 μm using a dental model scanner (*Rexcan DS2, Europac 3D, Crewe, UK*). Certain digital profilometers incorporate the confocal laser scanning microscopy principle, offering a non-destructive measurement method that enables follow-up examinations (Mullan et al. 2018). Hara et al. (2021) reported an accuracy of 0.1%, a precision (SD) of ± 0.06 mm and a detection limit of < 0.3 mm using a white light scanning confocal profilometer. Nevertheless, it's important to note that the mentioned measurement accuracies are applicable solely to flattened polished tooth samples (Charalambous et al. 2021).

6.6.3 Digital laser microscope (Keyence)

Keyence's laser scanning digital microscopes (VK-X3000 series, Osaka, Japan) integrate three distinct measurement principles - confocal laser, focus variation, and white light interferometry - offering versatility depending on the application. Focus variation, also known as focus stacking, involves capturing images at various focusing planes. Subsequently, an image combination algorithm merges the

two-dimensional image stacks, resulting in a three-dimensional image with an enhanced depth of field. Widely employed in light microscopy across fields such as materials science, forensic medicine, and biological and geosciences, this technique has previously been tested for evaluating erosive tooth wear (Chuenarrom and Benjakul 2008). White-light interferometry, utilizing the principle of moiré stripe patterns, has demonstrated high accuracy and precision in measuring both flat and naturally curved surfaces. This non-invasive method was initially described by Holme et al. (2005) and has since found frequent application in studies on tooth wear.

The accuracy of this technique is reported to be $0.1\ \mu\text{m}$ and the precision $0.05\ \mu\text{m}$. On natural enamel surfaces, the measurement accuracy decreases to about $0.3\ \mu\text{m}$ (Stenhagen et al. 2019). According to the manufacturer, Keyence's laser scanning digital microscope offers a fast acquisition on uneven shapes, a precise, high-resolution scan to capture detailed structures with a height resolution of $0.01\ \text{nm}$ and a linear resolution of $0.1\ \text{nm}$ (Fig. 97, 98). In addition, telecentric lenses promise to minimise distortion at the edges of the screen. Teeth can be examined directly and non-destructively and would no

longer require replication. The detection of reflective surfaces, e.g., a wet tooth, should be possible with high accuracy. Therefore, teeth would not need to be excessively dried before scanning, avoiding artefacts.

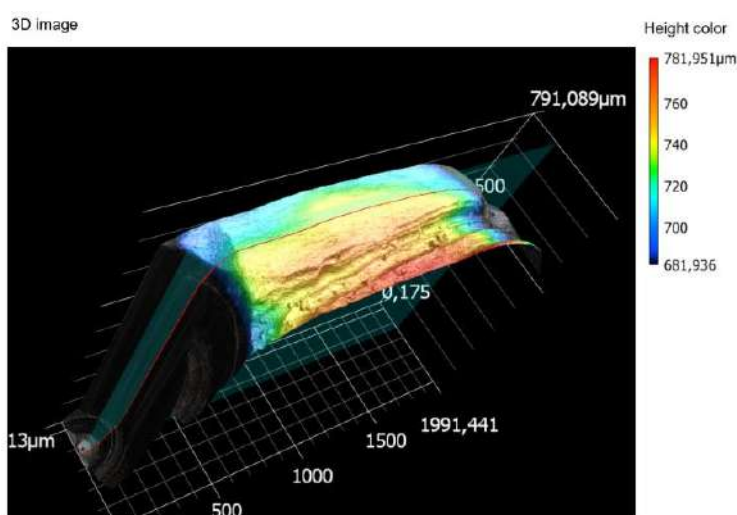


Figure 97: Keyence surface model: For testing, an intact anterior tooth was positioned on the carriage of the Keyence laser scanner, and a 3D surface image of the buccal tooth surface, along with the laterally attached reference mark, was captured. The color-coded height relief and depth information are presented in μm .

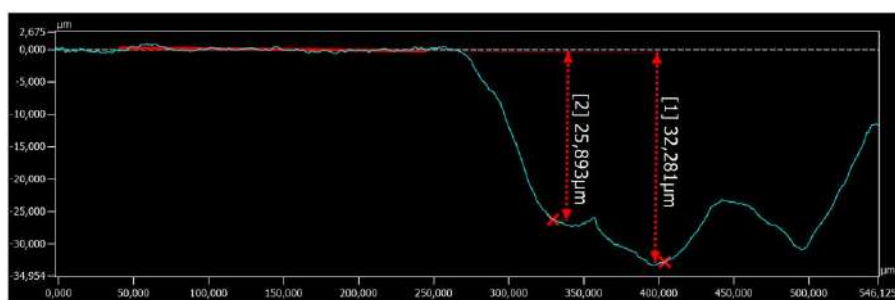


Figure 98: The profilometric display shows the depth of the lateral reference mark in relation to the tooth surface in μm .

6.6.4 Optical coherence tomography (OCT)

Optical coherence tomography (OCT) is a non-invasive method for examining natural tooth surfaces (Machoy et al. 2017, Shimada et al. 2020). Araveti et al. (2020) used OCT to assess dentin thickness, while Mylonas et al. (2019) applied it for early enamel surface changes, achieving a $1\ \mu\text{m}$ resolution. However, reflections may occur due to the high refractive index of dental hard tissue (Chan et al. 2013). The Medical Laser Centre Lübeck is actively advancing OCT in dentistry.

6.6.5 Atomic force microscopy (AFM)

Commercially introduced in 1998, atomic force microscopy (AFM) is useful in dentistry for evaluating surface roughness and nanomechanical properties without requiring sample drying or coating (Tsenova-Ilieva and Karova 2020). AFM employs a flexible cantilever scanning probe to image surfaces at the atomic level, utilizing a piezoelectric scanner and a photodiode as a detector. Nanoindentation, a refinement of microhardness testing, applies a gentle force (0.25–5 μN) with a Berkovich diamond tip to the tooth surface, resulting in an indentation depth of around 100 nm. However, AFM has limitations, including a scanned observation area capped at 240 $\mu\text{m} \times 240 \mu\text{m}$ and a time-consuming scanning process (Tsenova-Ilieva and Karova 2020).

6.6.6 Reflectometer (SRI)

The reflectometer (SRI) uses an optical device to measure changes in reflectance intensity on enamel surfaces. Initially validated for both ground and natural tooth surfaces (Lussi et al. 2012, Carvalho et al. 2016a), it has evolved into a smaller pen-size device for direct oral cavity application (Rakhmatullina et al. 2013). It demonstrated over 64% sensitivity and a high specificity of at least 84% in diagnosing erosive lesions on permanent teeth (Stenhagen et al. 2019).

6.6.7 Intra-oral scanners (IOS)

Various approaches advocate for the use of intra-oral scanners (IOS) as the preferred method for in vivo 3D measurement of tooth wear (Ganss and Lussi 2014, Travassos da Rosa Moreira Bastos et al. 2021). Initially designed for the digital fabrication of CAD/CAM restorations, intra-oral scanners (IOS) are "area devices" that utilize technologies such as laser triangulation, active waveform scanning, or moiré fringe patterns to detect optical interactions on the surface. These interactions are then transformed into surface dots with dot spacing typically ranging from approximately 50 to 150 μm . Wulfman et al. (2018) assessed the accuracy and precision of a maximum of 30 μm of IOS under in vitro conditions as insufficient for determining tooth wear. Chiu et al. (2020) described a scanning resolution of 33 μm for *Trios 3 (3Shape, Denmark)*. IOS scans also experience increased standard deviations, which can be explained by a lower point cloud density, resulting in a stronger smoothing effect that further limits their resolution. In addition, clinical conditions (e.g. saliva, reflections, patient movement) can influence data acquisition of IOS and reduce optical measurement precision (Charalambous et al. 2021). Another limitation is that the analysis is primarily confined to vertical height loss on flat enamel samples (Witecy et al. 2021). Presently, intra-oral scanners (IOS) are regarded as less accurate than alternative methods for measuring tooth wear. Further advancements are needed before recommending IOS for quantitative studies of tooth wear (O'Toole et al. 2019, 2020a).

6.6.8 Other approaches to quantify tooth wear

Huysmans and Thijssen (2000) explored ultrasonic pulses to determine enamel thickness, but the method lacked precision for changes under 0.33 mm (Louwerse et al. 2004). Chadwick and Mitchell (2001) used electrically conductive replicas for digital mapping, and a recent study applied fractal analysis to classify erosive tooth surface features (Hara et al. 2021). Longbottom et al. (2021) utilized bioluminescence to image Ca²⁺ ions on enamel surfaces, studying demineralization patterns from caries or erosion.

6.6.9 Alternative software

Mountains Map 8 (*Digital Surf, Besançon, France*) is a commonly cited software in dental studies, integrating profilometry with SEM data analysis for both 2D and 3D evaluation of tooth surfaces (Hara et al. 2021). Another software worth mentioning is **GomInspect** (*SR1; GOM GmbH, Braunschweig, Germany*), recently employed by Witecy et al. (2021) to monitor erosive tooth wear. While the program yielded favourable results, its usage was characterized as time-consuming and necessitated specific skills from the user. Bartlett's team initially used **Truegauge** (*TrueMap, United States*) but later decided in favour of **Geomagic Control** (*Artec, Senningerberg, Luxembourg*) as the new gold standard for measuring tooth wear (O'Toole et al. 2020a). Subsequently, a dedicated software for quantifying tooth wear was created. Known as **WearCompare** (*University of Leeds, UK*), it is likened to *Geomagic* in its ability to quantify tooth wear and is designed to offer user-friendly free software with additional applicable measurement parameters. (O'Toole et al. 2019). Most intraoral scanners have now implemented a software application for direct wear measurement, which enables chair-side matching of two data sets. The alignment typically relies on a best-fit algorithm and undergoes continuous refinement and development (Kumar et al. 2019). The swift progress in artificial intelligence is anticipated to lead to ongoing enhancements in user-friendly, precise, and validated software for surface matching and volume measurements.

7 Conclusions

Occlusal and cervical wear represent intricate dental phenomena with notable clinical implications. The study illustrates that tooth wear is a distinct dental occurrence, exhibiting variations between individual teeth and across age groups. Hygiene products operate through dual mechanisms: they contribute to oral health by reducing plaque formation, while conversely, causing mechanical abrasion that can lead to enamel, dentin, and cementum loss. Acknowledging this dual role, future research assessments should comprehensively examine both the positive and negative impacts on teeth across all age groups. Therefore, a new standardised laboratory procedure was developed by integrating SEM with three years of robotic simulated tooth brushing in an artificial oral cavity designed to reflect clinical conditions.

- The standard operating procedure involve human teeth in their anatomical position, subjected to wet brushing with clinically validated movements, force, and time. According to the video observation study, the number of brushing strokes per tooth surface is the only biophysical parameter that determines the effectiveness of tooth brushing. The brushing technique and duration, on the other hand, can vary greatly from person to person or even within individuals.
- The application of 3D SEM allowed, for the first time, volumetric quantification of abrasion effects on the cervical tooth, an aspect not achievable with conventional profilometry. Laser scanning microscopy is emerging as a potential alternative to 3D SEM.
- The development of a catalogue of pathobiological abrasion patterns provides deeper insights into the processes of cervical dental abrasion.
- In addition, the design of the toothbrush head and the angle of the bristle field in relation to the tooth surface are other factors that can influence plaque and gingivitis control.
- Both toothbrushes contribute to oral health by removing residual calculus that masks the cemento-enamel junction and smoothing traumatic and iatrogenic damage to the tooth surface.
- Harmful alterations encompassed slight enamel loss on the smooth surface, depletion of cervical cementum, and substantial loss of root dentin. These changes resulted from the combined mechanical abrasion induced by the bristle configuration of the toothbrushes and the dentifrices employed. The manual toothbrush with a flexible brush head could contribute to less abrasion of the tooth neck (\varnothing 34 nl) compared to a flat toothbrush with a rigid brush neck (\varnothing 87 nl).
- The cemento-enamel junction showed considerable morphological diversity. A noteworthy observation, reported here for the first time, involved the unveiling of distinct enamel islands on the root surfaces. This revelation identifies a previously unrecognized risk area. Moreover, a subtle widening of the vertical enamel infractions at the cemento-enamel junction (CEJ) is observed.

- Descriptive statistics are employed to characterize and compare the distinct abrasion behaviour exhibited by the two toothbrushes. However, the limited sample size of two sets of seven human tooth samples and the intricate complexity of morphological features constrain statistically significant differentiation.
- Despite the limited sample size, there is a clear trend showing less harmful cervical wear with the ball-joint manual toothbrush, attributed to its unique biophysical brushing mechanism compared to a rigid toothbrush under identical brushing conditions.

The physical lifetime risk of tooth wear

Occlusal wear, mainly due to abrasion and attrition in omnivorous animals, including humans, is a natural phenomenon that contributes to lifelong functional adaptation and the prevention of dental caries. In contrast, lifelong physical wear on smooth tooth surfaces, especially the cervical tooth region, is a risk for dentin hypersensitivity and fractures. It is caused exclusively by toothbrushing and abrasive dentifrices (combined with chemical erosion).

The results of the present study contribute to the characterisation of dynamic cervical wear changes in permanent dentition during life:

- **Juvenile:** The enamel shows no or minimal signs of wear. In premolars of juvenile patients (10-15 years old), the root cementum is thinly developed, and the immature enamel reveals exposed prismatic structures following the simulated three-year toothbrushing cycle.
- **Young adults:** Molars in young adult patients, aged 18 to 35 years, face a notable risk of gingival recession due to cementum wear. This wear can undermine enamel margins and expose dentinal tubules, leading to potential hypersensitivity. These teeth typically exhibit a combination of aprismatic and prismatic enamel, along with hypermineralised root dentin containing remnants of cementum.
- **Adults:** In middle-aged patients (40-65 years old), the incisors and canines exhibited mature enamel. Periodontitis led to gradual gingival recession and exposed root surfaces. Wear processes resulted in undermining enamel margins, hypermineralised root dentin with occluded open dentin tubules, and occasional deep grooves on the root surface. The wear extended apically from 100 μm to 1.5 mm.

A continuation of the investigation of the identified morphological characteristics with an extended sample would be beneficial. The expansion of the catalogue of pathobiological abrasion patterns has the potential to enrich the fields of oral anatomy, periodontology and preventive dentistry and thus contribute to a deeper understanding of dental abrasion.

8 Summary

Tooth wear is a complex dental phenomenon with significant clinical implications. Hygiene products, while crucial for plaque removal, can also cause mechanical wear on enamel, dentin, and cementum. Given this multifaceted functionality, research assessments should encompass both positive and negative effects across diverse age groups. To address this, a novel laboratory standard has been devised, integrating toothbrushing tests with a robot-simulated toothbrushing cycle within an artificial oral cavity. This innovative approach aims to ascertain alterations in morphological features and quantify the extent of cervical wear lesions resulting from toothbrush abrasion. In assessing this novel method, we investigated the abrasive impact of two manual toothbrushes on tooth structure, hypothesizing that the flexible ball-jointed toothbrush with tapered filaments would be less abrasive than a rigid toothbrush with flat-trimmed bristles. To ensure ethical considerations, the study underwent scrutiny by the Ethics Committee of the University of Witten-Herdecke, receiving a positive vote on 3 May 2021 (application number: SR-67/2021). Subsequently, an amendment for an additional video observation study aimed at determining the average number of toothbrushing strokes per time and the toothbrushing technique of 50 subjects was granted approval on 8 January 2022.

In the robot-simulated toothbrushing cycle, teeth from various age groups were extracted and stored in 0.1% thymol. Fourteen human teeth were polymerized on pins and mounted anatomically in two dental arches to mimic the physiological arrangement of a eugnathic dentition. Employing a validated six-axis robot (FS02N, Kawasaki) enabled the accurate simulation of human toothbrushing movements. Clinical parameters such as force, technique, and time were incorporated for clinically validated and homogeneous study conditions. The random toothbrushing program integrated three common techniques: 2x horizontal (17 s), 1x rotating (19 s), and 1x vertical brushing (22 s), executed in an artificial oral cavity with a brushing force of 3.5 N. Assuming a twice-daily brushing frequency on average, the cycle was reiterated 60 times per month, accumulating a total of 95,040 brush strokes per tooth over the simulated three-year period. The buccal surfaces of teeth were moulded using A-silicone (*Affinis Putty Soft and Affinis light body, Coltene Holding AG, Altstätten, Switzerland*) and replicated with epoxy resin (*Easy-Mix N 5000 Epoxyd, Weicon, Münster, Germany*). Abrasion patterns of enamel, dentin, and cementum were scrutinized using scanning electron microscopy (*LEO-1450, Zeiss, Oberkochen, Germany*). Three-dimensional scanning electron microscopy analyses were conducted with 4Q-BSE detectors (*SEM-515, Philips; Point Electronic, Halle, Germany*). Volume loss was assessed using Leica's Reshaper software (*Leica Geosystems, Heerbrugg, Switzerland*).

We implemented a novel morphological feature coding system, categorizing features into four enamel patterns (functional abrasion marks, perikymata, exposed prismatic enamel, infractions), one dentin pattern (open dentin tubules), and four cervical patterns (dental calculus, overlapping cementum or enamel, gaps between enamel and cementum, enamel islands on the root surface). Abrasion levels from 0 to 3 were assigned for each pattern using image coding panels (*Section 5.1*). The combined image boards, depicting abrasion patterns for each tooth, were systematically compared with the coding panels and independently scored by two examiners: one non-blinded (KW) and one blinded (PG) (*Section 5.2*). Furthermore, we utilized backscattered electron (BSE) images to generate lateral views of the cervical abrasion lesions (*Section 5.3*). This study revealed that effective oral hygiene significantly contributed to the smoothing of buccal tooth surfaces and cervical margins, resulting in reduced plaque adhesion and subsequent caries formation. Abrasion, notably, tended to expose open dentinal tubules, particularly in younger teeth. Additionally, a noteworthy observation was the emergence of enamel islands on the root surface. Furthermore, considerable morphological diversity was observed at the cemento-enamel junction, even within the same tooth. Hypothesis tests were performed for both pre- and post-brushing results using the *Wilcoxon signed-rank test*, and toothbrush comparisons were conducted using the *Mann–Whitney U test*. The manual toothbrush **Rapid Relief** with a flexible neck resulted in fewer changes in tooth abrasion patterns. In contrast, the **Jubilee** manual toothbrush, which is characterised by a rigid neck and flat-trimmed bristles, exposed an increased number of prismatic areas in the enamel and resulted in the unmasking of enamel islands on the root surface. Both toothbrushes showed significant differences in the removal of calculus and the straightening of traumatic and iatrogenic damage. Toothbrushing-induced abrasion led to the loss of cervical tooth structure. On average, Rapid Relief (24 – 50 nl) removed 53.5 nl less tooth structure than Jubilee (41 – 188 nl). Wear was mainly concentrated within the range of 100 – 1,500 µm from the cemento-enamel junction to the apical region (*Section 5.4*).

In this study, 3D secondary electron microscopy was effectively used for the first time to measure the volume of cervical abrasion lesions. Both 2D-SEM and 3D-SEM revealed micromorphological details showing both detrimental and beneficial effects on oral health. Further research is required to validate and refine the methodology with a larger dataset. Improving measurement quality involves minimizing replicas, standardizing calibration procedures, and optimizing scanner settings. Continuous monitoring of tooth wear rates is crucial to understand wear processes and enhance clinical prevention. Notably, the methodology for longitudinally assessing cervical wear differs from occlusal and approximal tooth wear.

9 References

- ABSI EG, ADDY M, ADAMS D. Dentine hypersensitivity. The development and evaluation of a replica technique to study sensitive and non-sensitive cervical dentine. *J Clin Periodontol* 1989; 16: 190–195.
- ACHERKOUK A, GÖTZE M, KIESOW A, RAMAKRISHNAN SS, LANG T, GÄNGLER P. Robot and mechanical testing of a specialist manual toothbrush for cleaning efficacy and improved force control. *BMC Oral Health* 2022; 22
- ADA.ORG. American Dental Association. General Recommendations for the Prevention of Caries and Gingivitis. 2017
- ADDY M, MOSTAFA P, NEWCOMBE RG. Dentine hypersensitivity: the distribution of recession, sensitivity and plaque. *J Dent* 1987; 15: 242–248.
- ADDY M, DUMMER PM, HUNTER ML, KINGDON A, SHAW WC. The effect of toothbrushing frequency, toothbrushing hand, sex and social class on the incidence of plaque, gingivitis and pocketing in adolescents: a longitudinal cohort study. *Community Dent Health* 1990; 7: 237–247.
- ADDY M, HUGHES J, PICKLES MJ, JOINER A, HUNTINGTON E. Development of a method in situ to study toothpaste abrasion of dentine. Comparison of 2 products. *J Clin Periodontol* 2002; 29: 896–900.
- ADDY M, HUNTER ML. Can tooth brushing damage your health? Effects on oral and dental tissues. *Int Dent J* 2003; 53 Suppl 3: 177–186.
- ADDY M. Tooth brushing, tooth wear and dentine hypersensitivity--are they associated? *Int Dent J* 2005; 55: 261–267.
- AINAMO A, AINAMO J. The dentition is intended to last a lifetime. *Int Dent J* 1984; 34: 87–92.
- AKAI M, NAKATA T, YAMAMOTO K, FUJIWARA J, TSUJI Y, KITANO E. Scanning electron microscopy of cemento-enamel junction. *J Osaka Univ Dent Sch* 1978; 18: 83–94.
- AKKUS A, KARASIK D, ROBERTO R. Correlation between micro-hardness and mineral content in healthy human enamel. *J Clin Exp Dent* 2017; 9: 569–573.
- AMAECHE BT, ABDULAZEES PA, OKOYE LO, MEYER F, ENAX J. Comparison of hydroxyapatite and fluoride oral care gels for remineralization of initial caries: a pH-cycling study. *BDJ Open* 2020; 6: 9.
- AN B, WANG R, AROLA D, ZHANG D. The role of property gradients on the mechanical behavior of human enamel. *J Mech Behav Biomed Mater* 2012; 9: 63–72.
- ARAMBAWATTA K, PEIRIS R, NANAYAKKARA D. Morphology of the cemento-enamel junction in premolar teeth. *J Oral Sci* 2009; 51: 623–627.
- ARAVETI SK, HIRAIISHI N, KOMINAMI N, OTSUKI M, SUMI Y, YIU CKY, ET AL. Swept-source optical coherence tomographic observation on prevalence and variations of cemento-enamel junction morphology. *Lasers Med Sci* 2020; 35: 213–219.
- ARNOLD W. Mikromorphologie und Molekularbiologie der Dentinogenese und Amelogenese. *Dtsch. Zahnärztl. Z*; 2006;524–534.
- AROLA DD, GAO S, ZHANG H, MASRI R. The tooth: its structure and properties. *Dent Clin North Am* 2017; 61: 651–668.
- ASCHENBRENNER CM, LANG R, HANDEL G, BEHR M. Analysis of marginal adaptation and sealing to enamel and dentin of four self-adhesive resin cements. *Clin Oral Investig* 2012; 16: 191–200.
- ASTEKAR M, KAUR P, DHAKAR N, SINGH J. Comparison of hard tissue interrelationships at the cervical region of teeth based on tooth type and gender difference. *J Forensic Dent Sci* 2014; 6: 86–91.
- ATTIN T, KOIDL U, BUCHALLA W, SCHALLER HG, KIELBASSA AM, HELLWIG E. Correlation of microhardness and wear in differently eroded bovine dental enamel. *Arch Oral Biol* 1997; 42: 243–250
- ATTIN T. Erosion und Abrasion von Zahnhartsubstanz- Einflußfaktoren, Pathogenese und Therapie. *Deutscher Zahnärztekalendar* 1999; 58: 1-31.
- ATTIN T, BECKER K, ROOS M, ATTIN R, PAQUÉ F. Impact of storage conditions on profilometry of eroded dental hard tissue. *Clin Oral Investig* 2009; 13: 473–478.
- AUBRY M, MAFART B, DONAT B, BRAU JJ. Brief communication: Study of noncarious cervical tooth lesions in samples of prehistoric, historic, and modern populations from the South of France. *Am J Phys Anthropol* 2003; 121: 10–14.
- AUSTIN RS, MULLEN F, BARTLETT DW. Surface texture measurement for dental wear applications. *Surf. Topogr.: Metrol. Prop.* 2015; 3: 023002.
- AW T, LEPE X, JOHNSON GH, MANCL L. Characteristics of noncarious cervical lesions: a clinical investigation. *J Am Dent Assoc* 2002; 133: 725–733.
- BACHMANN A, LUTZ F. Schmelzsprünge durch die Sensibilitätsprüfung mit CO₂-Schnee und Dichlordifluormethan - eine vergleichende In-vivo-Untersuchung. *SSO Schweiz Monatsschr Zahnheilkd* 1976; 86: 1042–1059.

- BADER JD, LEVITCH LC, SHUGARS DA, HEYMANN HO, McCLURE F. How dentists classified and treated non-carious cervical lesions. *J Am Dent Assoc* 1993; 124: 46–54.
- BADER JD, McCLURE F, SCURRIA MS, SHUGARS DA, HEYMANN HO. Case-control study of non-carious cervical lesions. *Community Dent Oral Epidemiol* 1996; 24: 286–291.
- BARDSLEY PF. The evolution of tooth wear indices. *Clin Oral Investig* 2008; 12 Suppl 1: 15–19.
- BARTLETT D, SMITH BG, WILSON RF. Comparison of the effect of fluoride and non-fluoride toothpaste on tooth wear in vitro and the influence of enamel fluoride concentration and hardness of enamel. *Br Dent J* 1994; 176: 346–348.
- BARTLETT D, EVANS D, SMITH B. The relationship between gastro-oesophageal reflux disease and dental erosion. *J Oral Rehabil* 1996; 23: 289–297.
- BARTLETT D, PHILLIPS K, SMITH B. A difference in perspective--the North American and European interpretations of tooth wear. *Int J Prosthodont* 1999; 12: 401–408.
- BARTLETT D. Retrospective long term monitoring of tooth wear using study models. *Br Dent J* 2003; 194: 211–213.
- BARTLETT D. The implication of laboratory research on tooth wear and erosion. *Oral Dis* 2005; 11: 3–6.
- BARTLETT D, PALMER I, SHAH P. An audit of study casts used to monitor tooth wear in general practice. *Br Dent J* 2005; 199: 143–145.
- BARTLETT D. Intrinsic causes of erosion. *Monogr Oral Sci* 2006; 20: 119–139.
- BARTLETT D, GANSS C, LUSSI A. Tooth wear and aging. *Clin Oral Investig* 2008; 12 Suppl 1: 65–68.
- BARTLETT D, HARDING M, SHERRIFF M, SHIRODARIA S, WHELTON H. A new index to measure tooth wear--methodolgy and practical advice. *Community Dent Health* 2011; 28: 182–187.
- BARTLETT D, LUSSI A, WEST NX, BOUCHARD P, SANZ M, BOURGEOIS D. Prevalence of tooth wear on buccal and lingual surfaces and possible risk factors in young European adults. *J Dent* 2013; 41: 1007–1013.
- BARTLETT D, O'TOOLE S. Tooth wear and aging. *Aust Dent J* 2019; 64 Suppl 1: 59–62.
- BARTLETT D, O'TOOLE S. Tooth wear: best evidence consensus statement. *J Prosthodont* 2021; 30: 20–25.
- BEALS D, NGO T, FENG Y, COOK D, GRAU DG, WEBER DA. Development and laboratory evaluation of a new toothbrush with a novel brush head design. *Am J Dent* 2000; 13: 5–14.
- BEHR M, HANSMANN M, ROSENTRITT M, HANDEL G. Marginal adaptation of three self-adhesive resin cements vs. a well-tried adhesive luting agent. *Clin Oral Investig* 2009; 13: 459–464.
- BERGSTRÖM J, LAVSTEDT S. An epidemiologic approach to toothbrushing and dental abrasion. *Community Dent Oral Epidemiol* 1979; 7: 57–64.
- BESL PJ, MCKAY ND. A method for registration of 3-D shapes. *IEEE Trans. Pattern Anal. Mach. Intell.* 1992; 14: 239–256.
- BEVENIUS J, HULTENBY K. In vitro and in vivo replication for scanning electron microscopy of the cervical region of human teeth. *Scanning Microsc* 1991; 5: 731–740.
- BEVENIUS J, LINDSKOG S, HULTENBY K. The amelocemental junction in young premolar teeth. A replica study by scanning electron microscopy. *Acta Odontol Scand* 1993; 51: 135–142.
- BHUNDIA S, BARTLETT D, O'TOOLE S. Non-carious cervical lesions - can terminology influence our clinical assessment? *Br Dent J* 2019; 227: 985–988.
- BIRKE C. Plaque-Kontrolle durch drei unterschiedlich abrasive Zahnputzmittel mit einer Handzahnbürste, eine randomisierte klinische kontrollierte Studie [Zahnmed. Diss.]. 2016. Universität Witten/Herdecke.
- BIRRRER H. Zur Kenntnis der Schmelz-Zement-Zone des menschlichen Zahnes. *Acta Anat (Basel)* 1952; 15: 228–242.
- BIZHANG M, RIEMER K, ARNOLD WH, DOMIN J, ZIMMER S. Influence of bristle stiffness of manual toothbrushes on eroded and sound human dentin - an in vitro study. *PLoS One* 2016; 11: e0153250.
- BIZHANG M, SCHMIDT I, CHUN Y-HP, ARNOLD WH, ZIMMER S. Toothbrush abrasivity in a long-term simulation on human dentin depends on brushing mode and bristle arrangement. *PLoS One* 2017; 12: e0172060.
- BJÖRN H, LINDHE J. Abrasion of dentine by toothbrush and dentifrice. A methodological study. *Odontol Revy* 1966; 17: 17–27.
- BLEICHER F. Odontoblast physiology. *Exp Cell Res* 2014; 325: 65–71.
- BORRERO-LOPEZ O, PAJARES A, CONSTANTINO PJ, LAWN BR. A model for predicting wear rates in tooth enamel. *J Mech Behav Biomed Mater* 2014; 37: 226–234.
- BORRERO-LOPEZ O, CONSTANTINO PJ, BUSH MB, LAWN BR. On the vital role of enamel prism interfaces and graded properties in human tooth survival. *Biol Lett* 2020; 16: 20200498.

- BORRERO-LOPEZ O, RODRIGUEZ-ROJAS F, CONSTANTINO PJ, LAWN BR. Fundamental mechanics of tooth fracture and wear: implications for humans and other primates. *Interface Focus* 2021; 11 (5): 20200070.
- BOYDE A. Understanding the structure of the mammalian mineralised tissues through their development. *MRS Online Proceedings Library (OPL)* 2005; 898: 0898-L03-01
- BRADY JM, WOODY RD. Scanning microscopy of cervical erosion. *J Am Dent Assoc* 1977; 94: 726–729.
- BRÄNNSTRÖM M, NORDENVALL KJ, GLANTZ PO. The effect of EDTA-containing surface-active solutions on the morphology of prepared dentin: an in vivo study. *J Dent Res* 1980; 59: 1127–1131.
- BRASCH SV, LAZAROU J, VAN ABBÉ NJ, FORREST JO. The assessment of dentifrice abrasivity in vivo. *Br Dent J* 1969; 127: 119–124.
- BREITENMOSER J, MÖRMANN W, MÜHLEMANN HR. Damaging effects of toothbrush bristle end form on gingiva. *J Periodontol* 1979; 50: 212–216.
- BRESCHI L, GOBBI P, MAZZOTTI G, FALCONI M, ELLIS TH, STANGEL I. High resolution SEM evaluation of dentin etched with maleic and citric acid. *Dent Mater* 2002; 18: 26–35.
- BROMAGE TG, DEAN MC. Re-evaluation of the age at death of immature fossil hominids. *Nature* 1985; 317: 525–527.
- BURGETT F, ASH M. Comparative study of the pressure of brushing with three types of toothbrushes. *J Periodontol* 1974; 45: 410–413.
- CAMBONI S, DONNET M. Tooth surface comparison after air polishing and rubber cup: a scanning electron microscopy study. *J Clin Dent* 2016; 27: 13–18.
- CARLSSON G, EGERMARK I, MAGNUSSON T. Predictors of bruxism, other oral parafunctions, and tooth wear over a 20-year follow-up period. *J Orofac Pain* 2003; 17: 50–57.
- CARVALHO TS, BAUMANN T, LUSSI A. A new hand-held optical reflectometer to measure enamel erosion: correlation with surface hardness and calcium release. *Sci Rep* 2016a; 6: 25259.
- CARVALHO TS, COLON P, GANSS C, HUYSMANS M-C, LUSSI A, SCHLUETER N, ET AL. Consensus report of the European Federation of conservative dentistry: erosive tooth wear - diagnosis and management. *Swiss Dent J* 2016b; 126 (4): 342–346.
- CARVALHO TS, LUSSI A. Age-related morphological, histological and functional changes in teeth. *J Oral Rehabil* 2017; 44: 291–298.
- CERUTI P, MENICUCCI G, MARIANI GD, PITTONI D, GASSINO G. Non carious cervical lesions. A review. *Minerva Stomatol* 2006; 55: 43–57.
- CHADWICK RG, MITCHELL HL. Conduct of an algorithm in quantifying simulated palatal surface tooth erosion. *J Oral Rehabil* 2001; 28: 450–456.
- CHAN KH, CHAN AC, DARLING CL, FRIED D. Methods for monitoring erosion using optical coherence tomography. *Proc SPIE Int Soc Opt Eng* 2013; 8566: 856606.
- CHARALAMBOUS P, O'TOOLE S, BULL T, BARTLETT D, AUSTIN R. The measurement threshold and limitations of an intra-oral scanner on polished human enamel. *Dent Mater* 2021; 37: 648–654.
- CHIU A, CHEN Y-W, HAYASHI J, SADR A. Accuracy of CAD/CAM digital impressions with different intraoral scanner parameters. *Sensors (Basel)* 2020; 20: 1157.
- CHOWDHARY Z, MOHAN R. Efficiency of three different polishing methods on enamel and cementum: a scanning electron microscope study. *J Indian Soc Periodontol* 2018; 22: 18–24.
- CHUENARROM C, BENJAKUL P. Comparison between a profilometer and a measuring microscope for measurement of enamel erosion. *J Oral Sci* 2008; 50: 475–479.
- CLARK DJ, SHEETS CG, PAQUETTE JM. Definitive diagnosis of early enamel and dentin cracks based on microscopic evaluation. *J Esthet Restor Dent* 2003; 15: 391–401; discussion 401.
- CLAYDON NC. Current concepts in toothbrushing and interdental cleaning. *Periodontol 2000* 2008; 48: 10–22.
- CLOQUET M. Notes about the anatomical relationship's existent in the human dentition between the enamel and the cementum. *Odontologie* 1899; 8
- CONSTANTINO PJ, LEE JJ-W, CHAI H, ZIPFEL B, ZISCOVICI C, LAWN BR, ET AL. Tooth chipping can reveal the diet and bite forces of fossil hominins. *Biol Lett* 2010; 6: 826–829.
- CRAIG EL, FRAJOLA WJ, GREIDER MH. An embedding technique for electron microscopy using EPON 812. *J Cell Biol* 1962; 12: 190–194.
- CRAIG RG. Evaluation of an automatic mixing system for an addition silicone impression material. *J Am Dent Assoc* 1985; 110: 213–215.
- CUY JL, MANN AB, LIVI KJ, TEAFORD MF, WEIHS TP. Nanoindentation mapping of the mechanical properties of human molar tooth enamel. *Arch Oral Biol* 2002; 47: 281–291.
- DACULSI G, MENANTEAU J, KEREBEL LM, MITRE D. Length and shape of enamel crystals. *Calcif Tissue Int* 1984; 36: 550–555.

- DALEY TJ, HARBROW DJ, KAHLER B, YOUNG WG. The cervical wedge-shaped lesion in teeth: a light and electron microscopic study. *Aust Dent J* 2009; 54: 212–219.
- DANSER MM, TIMMERMAN MF, IJZERMAN Y, BULTHUIS H, VAN DER VELDEN U, VAN DER WEIJDEN GA. Evaluation of the incidence of gingival abrasion as a result of toothbrushing. *J Clin Periodontol* 1998; 25: 701–706.
- DAVIS WB, WINTER PJ. Measurement in vitro of enamel abrasion by dentifrice. *J Dent Res* 1976; 55: 970–975.
- DAVIS WB, WINTER PJ. Dietary erosion of adult dentine and enamel. Protection with a fluoride toothpaste. *Br Dent J* 1977; 143: 116–119.
- DE BOER P, DUINKERKE AS, ARENDS J. Influence of tooth paste particle size and tooth brush stiffness on dentine abrasion in vitro. *Caries Res* 1985; 19: 232–239.
- DEAN MC. A comparative study of cross striation spacings in cuspal enamel and of four methods of estimating the time taken to grow molar cuspal enamel in Pan, Pongo and Homo. *J Hum Evol* 1998; 35: 449–462.
- DEINZER R, EBEL S, BLÄTTERMANN H, WEIK U, MARGRAF-STIKSRUD J. Toothbrushing: to the best of one's abilities is possibly not good enough. *BMC Oral Health* 2018; 18: 167.
- DELONG R, HEINZEN M, HODGES JS, KO C-C, DOUGLAS WH. Accuracy of a system for creating 3D computer models of dental arches. *J Dent Res* 2003; 82: 438–442.
- DELONG R. Intra-oral restorative materials wear: rethinking the current approaches: how to measure wear. *Dent Mater* 2006; 22: 702–711.
- DEMARCO FF, CADEMARTORI MG, HARTWIG AD, LUND RG, AZEVEDO MS, HORTA BL, ET AL. Non-cariou cervical lesions (NCCLs) and associated factors: a multilevel analysis in a cohort study in southern Brazil. *J Clin Periodontol* 2021; 49: 48–58.
- DESPAIN RR, LLOYD BA, BROWN WS. Scanning electron microscope investigation of cracks in teeth through replication. *J Am Dent Assoc* 1974; 88: 580–584.
- DIETZ W, MEINEBER S, HOYER I, MONTAG R. Quantitative evaluation of the long-term marginal behaviour of filling restorations of human teeth using three-dimensional scanning electron microscopy. *EMC* 2008; 2: 729–730.
- DIETZ W. Longitudinale mikromorphologische 15-Jahres-Bewertung von Kompositfüllungen im Seitenzahnbereich unter Anwendung dreidimensionaler Rasterelektronenmikroskopie [Thesis]. 2012. Universität Witten/Herdecke.
- DIETZ W, MONTAG R, KRAFT U, WALTHER M, SIGUSCH BW, GÄNGLER P. Longitudinal micromorphological 15-year results of posterior composite restorations using three-dimensional scanning electron microscopy. *J Dent* 2014; 42: 959–969.
- VAN DIJKEN JW, HÖRSTEDT P. Effect of 5% sodium hypochlorite or Tubulicid pretreatment in vivo on the marginal adaptation of dental adhesives and glass ionomer cements. *Dent Mater* 1987; 3: 303–306.
- DIXON B, SHARIF MO, AHMED F, SMITH AB, SEYMOUR D, BRUNTON PA. Evaluation of the basic erosive wear examination (BEWE) for use in general dental practice. *Br Dent J* 2012; 213: E4.
- DONACHIE MA, WALLS AW. Assessment of tooth wear in an ageing population. *J Dent* 1995; 23: 157–164.
- DOURDA AO, MOULE AJ, YOUNG WG. A morphometric analysis of the cross-sectional area of dentine occupied by dentinal tubules in human third molar teeth. *Int Endod J* 1994; 27: 184–189.
- DYER D, ADDY M, NEWCOMBE RG. Studies in vitro of abrasion by different manual toothbrush heads and a standard toothpaste. *J Clin Periodontol* 2000; 27: 99–103.
- DZAKOVICH JJ, OSLAK RR. In vitro reproduction of noncariou cervical lesions. *J Prosthet Dent* 2008; 100: 1–10.
- ECCLES JD. Dental erosion of nonindustrial origin. A clinical survey and classification. *J Prosthet Dent* 1979; 42: 649–653.
- ECCLES JD. Tooth surface loss from abrasion, attrition and erosion. *Dent Update* 1982; 9: 373–374, 376–378, 380–381.
- EIDENHARDT Z, RITSERT A, SHANKAR-SUBRAMANIAN S, EBEL S, MARGRAF-STIKSRUD J, DEINZER R. Tooth brushing performance in adolescents as compared to the best-practice demonstrated in group prophylaxis programs: an observational study. *BMC Oral Health* 2021; 21: 359.
- ELHECHMI I, BRAGA J, DASGUPTA G, GHARBI T. Accelerated measurement of perikymata by an optical instrument. *Biomed Opt Express* 2013; 4: 2124–2137.
- ELHENNAWY K, MANTON DJ, CROMBIE F, ZASLANSKY P, RADLANSKI RJ, JOST-BRINKMANN P-G, ET AL. Structural, mechanical and chemical evaluation of molar-incisor hypomineralization-affected enamel: A systematic review. *Arch Oral Biol* 2017; 83: 272–281.
- ELLIS E. No more Epon 812: this product does not exist today. *Microscopy Today* 2014; 22: 50–53.
- ERNST CP, WILLERSHAUSEN B, DRIESEN G, WARREN PR, HILFINGER P. A robot system for evaluating plaque removal efficiency of toothbrushes in vitro. *Quintessence Int* 1997; 28: 441–445.

- EVANS AG, SUO Z, WANG RZ, AKSAY IA, HE MY, HUTCHINSON JW. Model for the robust mechanical behavior of nacre. *J. Mater. Res.* 2001; 16: 2475–2484.
- FARES J, SHIRODARIA S, CHIU K, AHMAD N, SHERRIFF M, BARTLETT D. A new index of tooth wear. Reproducibility and application to a sample of 18- to 30-year-old university students. *Caries Res* 2009; 43: 119–125.
- FEJERSKOV O, JOSEPHSEN K, NYVAD B. Surface ultrastructure of unerupted mature human enamel. *Caries Res* 1984; 18: 302–314.
- FRANKENBERGER R, HEHN J, HAJTO J, KRÄMER N, NAUMANN M, KOCH A, ET AL. Effect of proximal box elevation with resin composite on marginal quality of ceramic inlays in vitro. *Clinical Oral Investigations* 2012; 17
- GÄNGLER P. Klinische und experimentelle Aspekte der vergleichenden Odontologie und Periodontologie. *Nova Acta Leopoldina NF* 262 1986; 58: 525–537.
- GÄNGLER P. Lehrbuch der konservierenden Zahnheilkunde. 3. Auflage. 1995. Ullstein Mosby Verlag, Berlin/Wiesbaden.
- GÄNGLER P, HOFFMANN T, WILLERSHAUSEN B, SCHWENZER N, EHRENFELD M, GRIMM G. Konservierende Zahnheilkunde und Parodontologie. 2. Auflage. 2005. Thieme, Stuttgart.
- GÄNGLER P, LANG T, JENNES B. Computer-assisted planimetric plaque assessment of robot tested toothbrushing. *J Dent Res.* 2013; 92.
- GANSS C, KLIMEK J, SCHWARZ N. A comparative profilometric in vitro study of the susceptibility of polished and natural human enamel and dentine surfaces to erosive demineralization. *Arch Oral Biol* 2000; 45: 897–902.
- GANSS C, KLIMEK J, LUSSI A. Accuracy and consistency of the visual diagnosis of exposed dentine on worn occlusal/incisal surfaces. *Caries Res* 2006; 40: 208–212.
- GANSS C, SCHLUETER N, FRIEDRICH D, KLIMEK J. Efficacy of waiting periods and topical fluoride treatment on toothbrush abrasion of eroded enamel in situ. *Caries Res* 2007a; 41: 146–151.
- GANSS C, SCHLUETER N, HARDT M, VON HINCKELDEY J, KLIMEK J. Effects of toothbrushing on eroded dentine. *Eur J Oral Sci* 2007b; 115: 390–396.
- GANSS C, LUSSI A, SCHARMANN I, WEIGELT T, HARDT M, KLIMEK J, ET AL. Comparison of calcium analysis, longitudinal microradiography and profilometry for the quantitative assessment of erosion in dentine. *Caries Res* 2009a; 43: 422–429.
- GANSS C, PREISS S, KLIMEK J. Tooth brushing habits in uninstructed adults—frequency, technique, duration and force. *Clin Oral Investig* 2009b; 13: 203–08.
- GANSS C, YOUNG A, LUSSI A. Tooth wear and erosion: methodological issues in epidemiological and public health research and the future research agenda. *Community Dent Health* 2011; 28: 191–195.
- GANSS C, LUSSI A. Diagnosis of erosive tooth wear. *Monogr Oral Sci* 2014; 25: 22–31.
- GANSS C, DURAN R, WINTERFELD T, SCHLUETER N. Tooth brushing motion patterns with manual and powered toothbrushes—a randomised video observation study. *Clin Oral Investig* 2018; 22: 715–720.
- GILES A, CLAYDON NCA, ADDY M, HUGHES N, SUFI F, WEST NX. Clinical in situ study investigating abrasive effects of two commercially available toothpastes. *J Oral Rehabil* 2009; 36: 498–507.
- GONZÁLEZ-CABEZAS C, HARA AT, HEFFERREN J, LIPPERT F. Abrasivity testing of dentifrices - challenges and current state of the art. *Monogr Oral Sci* 2013; 23: 100–107.
- GRABENSTETTER RJ, BROGE RW, JACKSON FL, RADIKE AW. The measurement of the abrasion of human teeth by dentifrice abrasives: a test utilizing radioactive teeth. *J Dent Res* 1958; 37: 1060–1068.
- GRIFFIN SO, REGNIER E, GRIFFIN PM, HUNTLEY V. Effectiveness of fluoride in preventing caries in adults. *J Dent Res* 2007; 86: 410–415.
- GRIPPO JO. Abrasions: a new classification of hard tissue lesions of teeth. *J Esthet Dent* 1991; 3: 14–19.
- GROSS D, LENK C, UTZIG B. Normative Rahmenbedingungen der Rekrutierung und Nutzung extrahierter Zähne in Forschung und Lehre. *Ethik in der Medizin* 2015; 28: 21–31.
- GROSSMAN ES, HARGREAVES JA. Variable cemento-enamel junction in one person. *J Prosthet Dent* 1991; 65: 93–97.
- GUPTA P, KAUR H, SHANKARI G S M, JAWANDA MK, SAHI N. Human age estimation from tooth cementum and dentin. *J Clin Diagn Res* 2014; 8: ZC07-10.
- HABELITZ S, BAI Y. Mechanisms of enamel mineralization guided by amelogenin nanoribbons. *J Dent Res* 2021; 100: 1434–1443.
- HAMZA B, TANNER M, KÖRNER P, ATTIN T, WEGEHAUPT FJ. Effect of toothbrush bristle stiffness and toothbrushing force on the abrasive dentine wear. *Int J Dent Hyg* 2021; 19: 355–359.
- HAMZA B, NIEDZWIECKI M, KÖRNER P, ATTIN T, WEGEHAUPT FJ. Effect of the toothbrush tuft arrangement and bristle stiffness on the abrasive dentin wear. *Sci Rep* 2022; 12: 840.

- HARA AT, GONZÁLEZ-CABEZAS C, CREETH J, PARMAR M, ECKERT GJ, ZERO DT. Interplay between fluoride and abrasivity of dentifrices on dental erosion-abrasion. *J Dent* 2009; 37: 781–785.
- HARA AT, BARLOW AP, ECKERT GJ, ZERO DT. Novel in-situ longitudinal model for the study of dentifrices on dental erosion-abrasion. *Eur J Oral Sci* 2014; 122: 161–167.
- HARA AT, ELKINGTON-STAUSS D, UNGAR PS, LIPPERT F, ECKERT GJ, ZERO DT. Three-dimensional surface texture characterization of In situ simulated erosive tooth wear. *J Dent Res* 2021; 100: 1236–1242.
- HARRINGTON E, JONES PA, FISHER SE, WILSON HJ. Toothbrush-dentifrice abrasion. A suggested standard method. *Br Dent J* 1982; 153: 135–138.
- HARTZ JJ, PROCOPIO A, ATTIN T, WEGEHAUPT FJ. Erosive potential of bottled salad dressings. *Oral Health Prev Dent* 2021; 19: 51–57.
- HASEGAWA K, MACHIDA Y, MATSUZAKI K, ICHINOHE S. The most effective toothbrushing force. *Pediatr Dent J*. 1992: 139–143.
- HASSAN RM, MOHAMED DG. Cementoenamel junction in egyptian maxillary first premolar: scanning electron microscopy and energy-dispersive x-ray analysis study. *Int. J. of Adv. Res.* 2015; 3: 545–556
- HAYASHI M, KUBO S, PEREIRA PNR, IKEDA M, TAKAGAKI T, NIKAIIDO T, ET AL. Progression of non-cariou cervical lesions: 3D morphological analysis. *Clin Oral Investig* 2022; 26: 575–583.
- HE B, HUANG S, ZHANG C, JING J, HAO Y, XIAO L, ET AL. Mineral densities and elemental content in different layers of healthy human enamel with varying teeth age. *Arch Oral Biol* 2011; 56: 997–1004.
- HE LH, SWAIN M. Energy absorption characterization of human enamel using nanoindentation. *J Biomed Mater Res A* 2007; 81: 484–492.
- HE LH, SWAIN M. Understanding the mechanical behaviour of human enamel from its structural and compositional characteristics. *J Mech Behav Biomed Mater* 2008; 1: 18–29.
- HE LH, SWAIN MV. Enamel--a functionally graded natural coating. *J Dent* 2009; 37: 596–603.
- HEASMAN P, STACEY F, HEASMAN L, SELLERS P, MACGREGOR ID, KELLY PJ. A comparative study of the Philips HP 735, Braun/Oral B D7 and the Oral B 35 advantage toothbrushes. *J Clin Periodontol* 1999; 26: 85–90.
- HEASMAN P, HOLLIDAY R, BRYANT A, PRESHAW PM. Evidence for the occurrence of gingival recession and non-cariou cervical lesions as a consequence of traumatic toothbrushing. *J Clin Periodontol* 2015; 42 Suppl 16: 237–255.
- HEATH JR, WILSON HJ. Forces and rates observed during in vivo toothbrushing. *Biomed Eng* 1974; 9: 61–64.
- HEFFERREN JJ. A laboratory method for assessment of dentifrice abrasivity. *J Dent Res* 1976; 55: 563–573.
- HEINTZE SD. How to qualify and validate wear simulation devices and methods. *Dent Mater* 2006; 22: 712–734.
- HO SP, SENKYRIKOVA P, MARSHALL GW, YUN W, WANG Y, KARAN K, ET AL. Structure, chemical composition and mechanical properties of coronal cementum in human deciduous molars. *Dent Mater* 2009; 25: 1195–1204.
- HOLME B, HOVE LH, TVEIT AB. Using white light interferometry to measure etching of dental enamel. *Measurement* 2005; 2: 137–147.
- HONG YH, LEW KK. Quantitative and qualitative assessment of enamel surface following five composite removal methods after bracket debonding. *Eur J Orthod* 1995; 17: 121–128.
- HOOGTEIJLING F, HENNEQUIN-HOENDERDOS NL, VAN DER WEIJDEN GA, SLOT DE. The effect of tapered toothbrush filaments compared to end-rounded filaments on dental plaque, gingivitis and gingival abrasion: a systematic review and meta-analysis. *Int J Dent Hyg* 2018; 16: 3–12.
- HOOPER S, WEST NX, PICKLES MJ, JOINER A, NEWCOMBE RG, ADDY M. Investigation of erosion and abrasion on enamel and dentine: a model in situ using toothpastes of different abrasivity. *J Clin Periodontol* 2003; 30: 802–808.
- HORNING GM, COBB CM, KILLOY WJ. Effect of an air-powder abrasive system on root surfaces in periodontal surgery. *J Clin Periodontol* 1987; 14: 213–220.
- HOTZ PR. Untersuchungen zur Abrasivität von Zahnpasten. *SSO Schweiz Monatsschr Zahnheilkd* 1983; 93: 93–99.
- HOWELL S, WEEKES WT. An electron microscopic evaluation of the enamel surface subsequent to various debonding procedures. *Aust Dent J* 1990; 35: 245–252.
- HU JC, HU Y, SMITH CE, MCKEE MD, WRIGHT JT, YAMAKOSHI Y, ET AL. Enamel defects and ameloblast-specific expression in Enam knock-out/lacz knock-in mice. *J Biol Chem* 2008; 283: 10858–10871.
- HUANG H, LIN S. Toothbrushing Monitoring using Wrist Watch. *Proceedings of the 14th ACM Conference on Embedded Network Sensor Systems CD-ROM* 2016: 202–215
- HUNTER M L., ADDY M, PICKLES M J., JOINER A. The role of toothpastes and toothbrushes in the aetiology of tooth wear. *Int Dent J*. 2002; 52: 399–405.

- HUR B, KIM HC, PARK JK, VERSLUIS A. Characteristics of non-cariou cervical lesions--an ex vivo study using micro computed tomography. *J Oral Rehabil* 2011; 38: 469–474.
- HUYSMANS MC, THUISSEN JM. Ultrasonic measurement of enamel thickness: a tool for monitoring dental erosion? *J Dent* 2000; 28: 187–191.
- HUYSMANS MC, CHEW HP, ELLWOOD RP. Clinical studies of dental erosion and erosive wear. *Caries Res* 2011; 45 Suppl 1: 60–68.
- IMFELD T. Prevention of progression of dental erosion by professional and individual prophylactic measures. *Eur J Oral Sci* 1996; 104: 215–220.
- IMFELD T, SENER B, SIMONOVIC I. In-vitro-Untersuchung der mechanischen Wirkung von handelsüblichen Handzahnbürsten. *Acta Med Dent* 2000; 5: 37–47.
- IMFELD T. Standard operation procedures for the relative dentin abrasion: (RDA) method used at Zurich University. *J Clin Dent* 2010; 21: 11–12.
- INADA E, SAITOH I, YU Y, TOMIYAMA D, MURAKAMI D, TAKEMOTO Y, ET AL. Quantitative evaluation of toothbrush and arm-joint motion during tooth brushing. *Clin Oral Investig* 2015; 19: 1451–1462.
- ISHAK H, FIELD J, GERMAN M. Baseline specimens of erosion and abrasion studies. *Eur J Dent* 2021; 15: 369–378.
- JAEGGI T, LUSSI A. Toothbrush abrasion of erosively altered enamel after intraoral exposure to saliva: an in situ study. *Caries Res* 1999; 33: 455–461.
- JIANG H, DU MQ, HUANG W, PENG B, BIAN Z, TAI BJ. The prevalence of and risk factors for non-cariou cervical lesions in adults in Hubei Province, China. *Community Dent Health* 2011; 28: 22–28.
- JOHANNSEN G, TELLEFSEN G, JOHANNSEN A, LILJEBORG A. The importance of measuring toothpaste abrasivity in both a quantitative and qualitative way. *Acta Odontol Scand* 2013; 71: 508–517.
- JOINER A, SCHWARZ A, PHILPOTTS CJ, COX TF, HUBER K, HANNIG M. The protective nature of pellicle towards toothpaste abrasion on enamel and dentine. *J Dent* 2008; 36: 360–368.
- JORDAN RA, BODECHTEL C, HERTRAMPF K, HOFFMANN T, KOCHER T, NITSCHKE I, ET AL. Fünfte Deutsche Mundgesundheitsstudie (DMS V). *Deutscher Zahnärzte Verlag DÄV*; Köln 2016; Band 35.
- KAIDONIS JA. Tooth wear: the view of the anthropologist. *Clin Oral Investig* 2008; 12 Suppl 1: 21–26.
- KAPAGIANNIDOU D, KOUTRIS M, WETSELAAR P, VISSCHER CM, VAN DER ZAAG J, LOBBEZOO F. Association between polysomnographic parameters of sleep bruxism and attrition-type tooth wear. *J Oral Rehabil* 2021; 48: 687–691.
- KARTEVA E, MANCHOROVA-VELEVA N, DAMYANOV Z, KARTEVA T. Morphology and structural characterization of human enamel and dentin by optical and scanning electron microscopy. *J of IMAB* 2019; 25: 2744–2750.
- KECK SC. Automixing: a new concept in elastomeric impression material delivery systems. *J Prosthet Dent* 1985; 54: 479–483.
- KEREBEL B, DACULSI G, KEREBEL LM. Ultrastructural studies of enamel crystallites. *J Dent Res* 1979; 58: 844–851.
- KETTERL W. Age-induced changes in the teeth and their attachment apparatus. *Int Dent J* 1983; 33: 262–271.
- KIDD EA, RICHARDS A, THYLSTRUP A, FEJERSKOV O. The susceptibility of “young” and “old” human enamel to artificial caries in vitro. *Caries Res* 1984; 18: 226–230.
- KIM J-H, EO S-H, SHRESTHA R, IHM J-J, SEO D-G. Association between longitudinal tooth fractures and visual detection methods in diagnosis. *J Dent* 2020; 101: 103466.
- KLOCKE A, DAVID S, THOMAS B. Elektrische Zahnbürsten – gibt es etwas Neues? *Quintessenz* 2015: 7–19.
- KODAKA T, KUROIWA M, KUROIWA M, OKUMURA J, MORI R, HIRASAWA S, ET AL. Effects of brushing with a dentifrice for sensitive teeth on tubule occlusion and abrasion of dentin. *J Electron Microsc (Tokyo)* 2001; 50: 57–64.
- KONTTURI-NÄRHI V, MARKKANEN S, MARKKANEN H. Effects of airpolishing on dental plaque removal and hard tissues as evaluated by scanning electron microscopy. *J Periodontol* 1990; 61: 334–338.
- KRAMER E, KLEMKE J. Standortbestimmung der zahnärztlichen Prophylaxe. *ZWR* 1995; 9: 634–638.
- KRÄMER N, KUNZELMANN KH. Meßfehler bei der 3D-Erfassung von Oberflächen durch mechanische Profilometrie. *Dtsch. Zahnärztl. Z* 1995; 10: 725–728.
- KREULEN CM, VAN 'T SPIJKER A, RODRIGUEZ JM, BRONKHORST EM, CREUGERS NHJ, BARTLETT DW. Systematic review of the prevalence of tooth wear in children and adolescents. *Caries Res* 2010; 44: 151–159.
- KUMAR S, KEELING A, OSNES C, BARTLETT D, O'TOOLE S. The sensitivity of digital intraoral scanners at measuring early erosive wear. *J Dent* 2019; 81: 39–42.

- KUNIN AA, EVDOKIMOVA AY, MOISEEVA NS. Age-related differences of tooth enamel morphochemistry in health and dental caries. *EPMA J* 2015; 6: 3.
- LACRUZ RS, HABELITZ S, WRIGHT JT, PAINE ML. Dental enamel formation and implications for oral health and disease. *Physiol Rev* 2017; 97: 939–993.
- LAMBRECHTS P, VANHERLE G, VUYLSTEKE M, DAVIDSON CL. Quantitative evaluation of the wear resistance of posterior dental restorations: a new three-dimensional measuring technique. *J Dent* 1984; 12: 252–267.
- LAMBRECHTS P, DEBELS E, VAN LANDUYT K, PEUMANS M, VAN MEERBEEK B. How to simulate wear? Overview of existing methods. *Dent Mater* 2006; 22: 693–701.
- LANG T, STAUFER S, JENNES B, GÄNGLER P. Clinical validation of robot simulation of toothbrushing - comparative plaque removal efficacy. *BMC Oral Health* 2014; 14: 82.
- LARSEN MJ, NYVAD B. Enamel erosion by some soft drinks and orange juices relative to their pH, buffering effect and contents of calcium phosphate. *Caries Res* 1999; 33: 81–87
- LEDDER RG, LATIMER J, FORBES S, PENNEY JL, SREENIVASAN PK, MCBAIN AJ. Visualization and quantification of the oral hygiene effects of brushing, dentifrice use, and brush wear using a tooth brushing simulator. *Front Public Health* 2019; 7: 91.
- LEE A, HE LH, LYONS K, SWAIN MV. Tooth wear and wear investigations in dentistry. *J Oral Rehabil* 2012; 39: 217–225.
- LEE H, NEVILLE K. Handbook of epoxy resins. 1967. McGraw-Hill, New York.
- LEE JW, MORRIS D, CONSTANTINO PJ, LUCAS PW, SMITH TM, LAWN BR. Properties of tooth enamel in great apes. *Acta Biomater* 2010; 6: 4560–4565.
- LEE JW, CONSTANTINO PJ, LUCAS PW, LAWN BR. Fracture in teeth: a diagnostic for inferring bite force and tooth function. *Biol Rev Camb Philos Soc* 2011; 86: 959–974.
- LEE WC, EAKLE WS. Possible role of tensile stress in the etiology of cervical erosive lesions of teeth. *J Prosthet Dent* 1984; 52: 374–380.
- LEHNEN S, GÖTZ W, BAXMANN M, JÄGER A. Immunohistochemical evidence for sclerostin during cementogenesis in mice. *Ann Anat* 2012; 194: 415–421.
- LEKNES KN, LIE T, WIKESJÖ UM, BOGLE GC, SELVIG KA. Influence of tooth instrumentation roughness on subgingival microbial colonization. *J Periodontol* 1994; 65: 303–308.
- LEWIS R, DWYER-JOYCE R. Wear of human teeth: A tribological perspective. *Proceedings of The Institution of Mechanical Engineers Part J: J. Eng. Tr.* 2005; 219: 1–18.
- LILJEBORG A, TELLEFSEN G, JOHANNSEN G. The use of a profilometer for both quantitative and qualitative measurements of toothpaste abrasivity. *Int J Dent Hyg* 2010; 8: 237–243.
- LIPPERT F, ARRAGEG MA, ECKERT GJ, HARA AT. Interaction between toothpaste abrasivity and toothbrush filament stiffness on the development of erosive/abrasive lesions in vitro. *Int Dent J* 2017; 67: 344–350.
- LITONJUA LA, ANDREANA S, BUSH PJ, COHEN RE. Tooth wear: attrition, erosion, and abrasion. *Quintessence Int* 2003; 34: 435–446.
- LITONJUA LA, ANDREANA S, BUSH PJ, TOBIAS TS, COHEN RE. Wedged cervical lesions produced by toothbrushing. *Am J Dent* 2004; 17: 237–240.
- LONGBOTTOM C, VERNON B, PERFECT E, HAUGHEY A-M, CHRISTIE A, PITTS N. Initial investigations of a novel bioluminescence method for imaging dental demineralization. *Clin Exp Dent Res* 2021; 7: 786–794.
- LOOMANS B, OPDAM N, ATTIN T, BARTLETT D, EDELHOFF D, FRANKENBERGER R, ET AL. Severe tooth wear: European consensus statement on management guidelines. *J Adhes Dent* 2017; 19: 111–119.
- LOUWERSE C, KJAEELDGAARD M, HUYSMANS MCDNJM. The reproducibility of ultrasonic enamel thickness measurements: an in vitro study. *J Dent* 2004; 32: 83–89.
- LUCAS PW, OMAR R. New perspectives on tooth wear. *Int J Dent* 2012; 2012:287573.
- LUCAS PW, VAN CASTEREN A. The wear and tear of teeth. *Med Princ Pract* 2015; 24 Suppl 1: 3–13.
- LUFT JH. Improvements in epoxy resin embedding methods. *J Biophys Biochem Cytol* 1961; 9: 409–414.
- LÜLLMANN-RAUCH R. Histologie. 3. Auflage. 2009. Thieme, Stuttgart.
- LUSSI A, SCHAFFNER M, HOTZ P, SUTER P. Epidemiology and risk factors of wedge-shaped defects in a Swiss population. *Schweiz Monatsschr Zahnmed* 1993; 103: 276–280.
- LUSSI A. Dental erosion clinical diagnosis and case history taking. *Eur J Oral Sci* 1996; 104: 191–198.
- LUSSI A, BOSSEN A, HÖSCHELE C, BEYELER B, MEGERT B, MEIER C, ET AL. Effects of enamel abrasion, salivary pellicle, and measurement angle on the optical assessment of dental erosion. *J Biomed Opt* 2012; 17: 97009–97001.

- LUSSI A, CARVALHO TS. Erosive tooth wear: a multifactorial condition of growing concern and increasing knowledge. *Monogr Oral Sci* 2014; 25: 1–15.
- LYNCH CD, O'SULLIVAN VR, DOCKERY P, MCGILLYCUDDY CT, SLOAN AJ. Hunter-Schreger Band patterns in human tooth enamel. *J Anat* 2010; 217: 106–115.
- MACGREGOR I, RUGG-GUNN A. A survey of toothbrushing sequence in children and young adults. *J Periodontal Res* 1979; 14: 225–230.
- MACGREGOR I, RUGG-GUNN A. Toothbrushing duration in 60 uninstructed young adults. *Community Dent Oral Epidemiol* 1985; 13: 121–122.
- MACHOY M, SEELIGER J, SZYSZKA-SOMMERFELD L, KOPROWSKI R, GEDRANGE T, WOŹNIAK K. The use of optical coherence tomography in dental diagnostics: a state-of-the-art review. *J Healthc Eng* 2017; 2017: 7560645.
- MAEDA H. Aging and senescence of dental pulp and hard tissues of the tooth. *Front Cell Dev Biol* 2020; 8: 605996.
- MANLY RS, SCHICKNER FA. Factors influencing tests on the abrasion of dentin by brushing with dentifrices. *J Dent Res* 1944; 23: 59–72.
- MANNERBERG F. Changes in the enamel surface in cases of erosion. A replica study. *Arch Oral Biol* 1961; 4: 59–62.
- MANNERBERG F. The incipient carious lesion as observed in shadowed replicas (en face pictures) and ground sections (profile pictures) of the same teeth. *Acta Odontol Scand* 1964; 22: 343–363.
- MARRO F, DE LAT L, MARTENS L, JACQUET W, BOTTENBERG P. Monitoring the progression of erosive tooth wear (ETW) using BEWE index in casts and their 3D images: A retrospective longitudinal study. *J Dent* 2018; 73: 70–75.
- MARTEN A, FRATZL P, PARIS O, ZASLANSKY P. On the mineral in collagen of human crown dentine. *Biomaterials* 2010; 31: 5479–5490.
- MAZZOLANI MR, MANTILLA TF, FRANÇA FMG, AMARAL FLB, BASTING RT, TURSSI CP. Multibenefit desensitising/whitening toothpastes: a study on abrasion and permeability of root dentine. *Oral Health Prev Dent* 2019; 17: 579–584.
- MCCOY G. The etiology of gingival erosion. *J Oral Implantol* 1982; 10: 361–362.
- MCGUIRE J, SZABO A, JACKSON S, BRADLEY TG, OKUNSERI C. Erosive tooth wear among children in the United States: relationship to race/ethnicity and obesity. *Int J Paediatr Dent* 2009; 19: 91–98.
- MECKEL AH, GRIEBSTEIN WJ, NEAL RJ. Structure of mature human dental enamel as observed by electron microscopy. *Arch Oral Biol* 1965; 10: 775–783.
- MEHTA SB, LOOMANS BAC, BRONKHORST EM, BANERJI S, BARTLETT DW. The impact of e-training on tooth wear assessments using the BEWE. *J Dent* 2020; 100: 103427.
- MEURMAN JH, FRANK RM. Scanning electron microscopic study of the effect of salivary pellicle on enamel erosion. *Caries Res* 1991; 25: 1–6.
- MIERAU HD, SPINDLER T. Beitrag zur Ätiologie der Gingivarezessionen. *Dtsch. Zahnärztl. Z.* 1984; 39: 634–639.
- MIERAU HD, HAUBITZ I, VÖLK W. Gewohnheitsmuster beim Gebrauch der Handzahnbürste. *Dtsch. Zahnärztl. Z.* 1989; 36: 836–841.
- MIERAU HD. Der freiliegende Zahnhals. *Dtsch. Zahnärztl. Z.* 1992; 47: 643–653.
- MILLWARD A, SHAW L, SMITH AJ, RIPPIN JW, HARRINGTON E. The distribution and severity of tooth wear and the relationship between erosion and dietary constituents in a group of children. *Int J Paediatr Dent* 1994; 4: 151–157.
- MITCHELL HL, CHADWICK RG. Mathematical shape matching as a tool in tooth wear assessment—development and conduct. *J Oral Rehabil* 1998; 25: 921–928.
- MOAZZEZ R, SMITH BG, BARTLETT DW. Oral pH and drinking habit during ingestion of a carbonated drink in a group of adolescents with dental erosion. *J Dent* 2000; 28: 395–397.
- MONTAG R, DIETZ W, NIETZSCHE S, LANG T, WEICH K, SIGUSCH BW, ET AL. Clinical and Micromorphologic 29-year Results of Posterior Composite Restorations. *J Dent Res* 2018; 97: 1431–1437.
- MULIC A, TVEIT AB, WANG NJ, HOVE LH, ESPELID I, SKAARE AB. Reliability of two clinical scoring systems for dental erosive wear. *Caries Res* 2010; 44: 294–299.
- MULLAN F, MYLONAS P, PARKINSON C, BARTLETT D, AUSTIN RS. Precision of 655nm Confocal Laser Profilometry for 3D surface texture characterisation of natural human enamel undergoing dietary acid mediated erosive wear. *Dent Mater* 2018; 34: 531–537.
- MULLER CJ, VAN WYK CW. The amelo-cemental junction. *J Dent Assoc S Afr* 1984; 39: 799–803.
- MYLONAS P, AUSTIN RS, MOAZZEZ R, JOINER A, BARTLETT DW. In vitro evaluation of the early erosive lesion in polished and natural human enamel. *Dent Mater* 2018; 34: 1391–1400.
- MYLONAS P, BULL T, MOAZZEZ R, JOINER A, BARTLETT D. Detection threshold of non-contacting laser profilometry and influence of thermal variation on characterisation of early surface form and textural changes in natural human enamel. *Dent Mater* 2019; 35: 140–152.

- NANCI A, TEN CATE AR. Ten Cate's oral histology: development, structure, and function. 9th ed. 2017. Elsevier, St. Louis, Mo.
- NASCIMENTO M, GORDAN V, QVIST V, BADER JD, RINDAL DB, WILLIAMS OD, ET AL. Restoration of noncarious tooth defects by dentists in the dental practice-based research network. *J Am Dent Assoc* 2011; 142: 1368–1375.
- NASSAR HM, LIPPERT F, ECKERT GJ, HARA AT. Dentifrice fluoride and abrasivity interplay on artificial caries lesions. *Caries Res.* 2014; 48: 557–565
- NASSAR HM, LIPPERT F, ECKERT GJ, HARA AT. Impact of toothbrushing frequency and toothpaste fluoride/abrasivity levels on incipient artificial caries lesion abrasion. *J Dent* 2018; 76: 89–92.
- NAWROCKA A, ŁUKOMSKA-SZYMAŃSKA M. Extracted human teeth and their utility in dental research. Recommendations on proper preservation: A literature review. *Dent Med Probl* 2019; 56: 185–190.
- NAWROCKA A, PIWONSKI I, SAURO S, PORCELLI A, HARDAN L, LUKOMSKA-SZYMANSKA M. Traditional microscopic techniques employed in dental adhesion research-applications and protocols of specimen preparation. *Biosensors (Basel)* 2021; 11: 408.
- NAZARI A, BAJAJ D, ZHANG D, ROMBERG E, AROLA D. Aging and the reduction in fracture toughness of human dentin. *J Mech Behav Biomed Mater* 2009; 2: 550–559.
- NEUVALD L, CONSOLARO A. Cementoenamel junction: microscopic analysis and external cervical resorption. *J Endod* 2000; 26: 503–508.
- NIEMI ML, SANDHOLM L, AINAMO J. Frequency of gingival lesions after standardized brushing as related to stiffness of toothbrush and abrasiveness of dentifrice. *J Clin Periodontol* 1984; 11: 254–261.
- OKUNSERI C, WONG MCM, YAU DTW, MCGRATH C, SZABO A. The relationship between consumption of beverages and tooth wear among adults in the United States. *J Public Health Dent* 2015; 75: 274–281.
- OLLEY RC, WILSON R, BARTLETT D, MOAZZEZ R. Validation of the Basic Erosive Wear Examination. *Caries Res* 2014; 48: 51–56.
- ORAL CARE. Konsumentenumfrage in der Schweiz. 2021. Institut für limbische Kommunikation und Strategie.
- OSBORN JW. Variations in structure and development of enamel. *Oral Sci Rev* 1973; 3: 3–83.
- O'TOOLE S, MISTRY M, MUTAHAR M, MOAZZEZ R, BARTLETT D. Sequence of stannous and sodium fluoride solutions to prevent enamel erosion. *J Dent* 2015; 43: 1498–1503.
- O'TOOLE S, KHAN M, PATEL A, PATEL NJ, SHAH N, BARTLETT D, ET AL. Tooth wear risk assessment and care-planning in general dental practice. *Br Dent J* 2018a; 224: 358–362.
- O'TOOLE S, NEWTON T, MOAZZEZ R, HASAN A, BARTLETT D. Randomised controlled clinical trial Investigating the impact of implementation planning on behaviour related to the diet. *Sci Rep* 2018b; 8: 8024.
- O'TOOLE S, OSNES C, BARTLETT D, KEELING A. Investigation into the accuracy and measurement methods of sequential 3D dental scan alignment. *Dent Mater* 2019; 35: 495–500.
- O'TOOLE S, BARTLETT D, KEELING A, MCBRIDE J, BERNABE E, CRINS L, ET AL. Influence of scanner precision and analysis software in quantifying three-dimensional intraoral changes: two-factor factorial experimental design. *J Med Internet Res* 2020a; 22: e17150.
- O'TOOLE S, LAU JS, REES M, WARBURTON F, LOOMANS B, BARTLETT D. Quantitative tooth wear analysis of index teeth compared to complete dentition. *J Dent* 2020b; 97: 103342.
- O'TOOLE S, CHARALAMBOUS P, ALMATRAFI A, MUKAR S, ELSHARKAWY S, BARTLETT D. Progress and limitations of current surface registration methods when measuring natural enamel wear. *J Dent* 2021; 112: 103738.
- PARK S, WANG DH, ZHANG D, ROMBERG E, AROLA D. Mechanical properties of human enamel as a function of age and location in the tooth. *J Mater Sci Mater Med* 2008; 19: 2317–2324.
- PARKER AS, PATEL AN, AL BOTROS R, SNOWDEN ME, MCKELVEY K, UNWIN PR, ET AL. Measurement of the efficacy of calcium silicate for the protection and repair of dental enamel. *J Dent* 2014; 42 Suppl 1: 21–29.
- PARRY J, REES G, SMITH A. Comparison of brushing machines in the in vitro assessment of toothpaste abrasivity. *J Dent Res* 2003; 82: B355.
- PARRY J, HARRINGTON E, REES GD, McNAB R, SMITH AJ. Control of brushing variables for the in vitro assessment of toothpaste abrasivity using a novel laboratory model. *J Dent* 2008; 36: 117–124.
- PASHLEY D, OKABE A, PARHAM P. The relationship between dentin microhardness and tubule density. *Endod Dent Traumatol* 1985; 1: 176–179.
- PETKER-JUNG W, WEIK U, MARGRAF-STIKSRUD J, DEINZER R. Oral cleanliness in daily users of powered vs. manual toothbrushes - a cross-sectional study. *BMC Oral Health* 2019; 19: 96.
- PETKER-JUNG W, WEIK U, MARGRAF-STIKSRUD J, DEINZER R. What characterizes effective tooth brushing of daily users of powered versus manual toothbrushes? *BMC Oral Health* 2022; 22: 10.
- PHANEUF EA, HARRINGTON JH, DALE PP, SHKLAR G. Automatic toothbrush: a new reciprocating action. *J Am Dent Assoc* 1962; 65: 12–25.

- PICKLES MJ, JOINER A, WEADER E, COOPER YL, COX TF. Abrasion of human enamel and dentine caused by toothpastes of differing abrasivity determined using an in situ wear model. *Int Dent J* 2005; 55: 188–193.
- PREIS V, HAHNEL S, BEHR M, ROSENTRITT M. Contact wear of artificial denture teeth. *J Prosthodont Res* 2018; 62: 252–257.
- RADENTZ WH, BARNES GP, CUTRIGHT DE. A survey of factors possibly associated with cervical abrasion of tooth surfaces. *J Periodontol* 1976; 47: 148–154.
- RADHAKRISHNAN V. Effect of stylus radius on the roughness values measured with tracing stylus instruments. *Wear* 1970; 16: 325–335.
- RAJSTEIN J, LUSTMANN J, HERSHKOVITZ J, GEDALIA I. In vitro evaluation of enamel and cementum abrasion after toothbrushing. *Refuat Hapeh Vehashinayim* 1979; 28: 17–20, 15–18.
- RAJU GS, KEERTHI M, NANDAN SRK, RAO TM, KULKARNI PG, REDDY DSP. Cementum as an age determinant: A forensic view. *J Forensic Dent Sci* 2016; 8: 175.
- RAKHMATULLINA E, BOSSEN A, BACHOFNER KK, MEIER C, LUSSI A. Optical pen-size reflectometer for monitoring of early dental erosion in native and polished enamels. *J Biomed Opt* 2013; 18: 117009.
- RIPA LW, GWINNETT AJ, BUONOCORE MG. The “prismless” outer layer of deciduous and permanent enamel. *Arch Oral Biol* 1966; 11: 41–48.
- RISNES S, SAEED M, SEHIC A. Scanning electron microscopy (SEM) methods for dental enamel. *Methods Mol Biol* 2019; 1922: 293–308.
- RIVERA C, AROLA D, OSSA A. Indentation damage and crack repair in human enamel. *J Mech Behav Biomed Mater* 2013; 21: 178–184.
- ROBINSON C, WEATHERELL JA, HALLSWORTH AS. Variatooon in composition of dental enamel within thin ground tooth sections. *Caries Res* 1971; 5: 44–57.
- RODRIGUEZ JM, BARTLETT DW. A comparison of two-dimensional and three-dimensional measurements of wear in a laboratory investigation. *Dent Mater* 2010; 26: e221–e225.
- RODRIGUEZ JM, AUSTIN RS, BARTLETT DW. A method to evaluate profilometric tooth wear measurements. *Dent Mater* 2012a; 28: 245–251.
- RODRIGUEZ JM, AUSTIN RS, BARTLETT DW. In vivo measurements of tooth wear over 12 months. *Caries Res* 2012b; 46: 9–15.
- RONNHOLM E. The amelogenesis of human teeth as revealed by electron microscopy. II. The development of the enamel crystallites - PubMed. *J Ultrastruct Res* 1962; 249–303.
- ROULET JF, MICHELLOD PY. [Desiccation of composite fillings for scanning electron microscopic studies--a methodological study]. *Schweiz Monatsschr Zahnmed* 1984; 94: 1049–1060.
- ROULET JF, REICH T, BLUNCK U, NOACK M. Quantitative margin analysis in the scanning electron microscope. *Scanning Microsc* 1989; 3: 147–159.
- RUGG-GUNN AJ, MACGREGOR ID, EDGAR WM, FERGUSON MW. Toothbrushing behaviour in relation to plaque and gingivitis in adolescent schoolchildren. *J Periodontal Res* 1979; 14: 231–238.
- SAADS CARVALHO T, LUSSI A. Chapter 9: Acidic beverages and foods associated with dental erosion and erosive tooth wear. *Monogr Oral Sci* 2020; 28: 91–98.
- SABRAH AH, TURSSI CP, LIPPERT F, ECKERT GJ, KELLY AB, HARA AT. 3D-Image analysis of the impact of toothpaste abrasivity on the progression of simulated non-cariou cervical lesions. *J Dent* 2018; 73: 14–18.
- SALAS MMS, NASCIMENTO GG, VARGAS-FERREIRA F, TARQUINIO SBC, HUYSMANS MCDNJM, DEMARCO FF. Diet influenced tooth erosion prevalence in children and adolescents: Results of a meta-analysis and meta-regression. *J Dent* 2015; 43: 865–875.
- SANGNES G, GJERMO P. Prevalence of oral soft and hard tissue lesions related to mechanical toothcleansing procedures. *Community Dent Oral Epidemiol* 1976; 4: 77–83.
- SAXER UP, YANKELL SL. Impact of improved toothbrushes on dental diseases. II. *Quintessence Int* 1997; 28: 573–593.
- SAXER UP, BARBAKOW J, YANKELL SL. New studies on estimated and actual toothbrushing times and dentifrice use. *J Clin Dent* 1998; 9: 49–51.
- SAXTON CA. The effects of dentifrices on the appearance of the tooth surface observed with the scanning electron microscope. *J Periodontal Res* 1976; 11: 74–85.
- SCHAFFNER M, STICH H, MEGERT B, LUSSI A. Tertiärdentin: Reaktionsdentin, Reparaturdentin. *Swiss Dent J* 2016; 126: 1028–1029.
- SCHEMEHORN BR, MOORE MH, PUTT MS. Abrasion, polishing, and stain removal characteristics of various commercial dentifrices in vitro. *J Clin Dent* 2011; 22: 11–18.
- SCHIFFNER U. Mechanische und chemische Plaquereduktion. Wissenschaftliche Stellungnahme. 1995. DGZMK.

- SCHLUETER N, GANSS C, DE SANCTIS S, KLIMEK J. Evaluation of a profilometrical method for monitoring erosive tooth wear. *Eur J Oral Sci* 2005; 113: 505–511.
- SCHLUETER N, KLIMEK J, SALESCHKE G, GANSS C. Adoption of a toothbrushing technique: a controlled, randomised clinical trial. *Clin Oral Investig* 2010; 14: 99–106.
- SCHLUETER N, HARA A, SHELLIS RP, GANSS C. Methods for the measurement and characterization of erosion in enamel and dentine. *Caries Res* 2011; 45 Suppl 1: 13–23.
- SCHLUETER N, LUKA B. Erosive tooth wear - a review on global prevalence and on its prevalence in risk groups. *Br Dent J* 2018; 224: 364–370.
- SCHLUETER N, WINTERFELD K, QUERA V, WINTERFELD T, GANSS C. Toothbrushing Systematics Index (TSI) - A new tool for quantifying systematics in toothbrushing behaviour. *PLoS One* 2018; 13: e0196497.
- SCHLUETER N, AMAECHI BT, BARTLETT D, BUZALAF MAR, CARVALHO TS, GANSS C, ET AL. Terminology of erosive tooth wear: consensus report of a workshop organized by the ORCA and the cariology research group of the IADR. *Caries Res* 2020; 54: 2–6.
- SCHLUETER N, FIEDLER S, MUELLER M, WALTER C, DIFLOE-GEISERT JC, VACH K, ET AL. Efficacy of a sonic toothbrush on plaque removal-A video-controlled explorative clinical trial. *PLoS One* 2021; 16: e0261496.
- SCHULER FS, VAN WAES H. SEM-evaluation of enamel surfaces after removal of fixed orthodontic appliances. *Am J Dent* 2003; 16: 390–394.
- SCOTT DB, KAPLAN H, WYCKOFF RWG. Replica studies of changes in tooth surfaces with age. *J Dent Res* 1949; 28: 31–47.
- SEGARRA MS, SHIMADA Y, SADR A, SUMI Y, TAGAMI J. Three-dimensional analysis of enamel crack behavior using optical coherence tomography. *J Dent Res* 2017; 96: 308–314.
- SEONG J, DAVIES M, MACDONALD EL, CLAYDON NC, WEST NX. Randomized clinical trial to determine if changes in dentin tubule occlusion visualized by SEM of replica impressions correlate with pain scores. *Am J Dent* 2018; 31: 189–194.
- SEXSON JC, PHILLIPS RW. Studies on the effects of abrasives on acrylic resins. *J Prosthet Dent* 1951; 1: 454–471.
- SHARP SJ, ASHBY MF, FLECK NA. Material response under static and sliding indentation loads. *Acta Metallurgica et Materialia* 1993; 41: 685–692.
- SHELLIS RP. Formation of caries-like lesions in vitro on the root surfaces of human teeth in solutions simulating plaque fluid. *Caries Res* 2010; 44: 380–389.
- SHELLIS RP, GANSS C, REN Y, ZERO DT, LUSSI A. Methodology and models in erosion research: discussion and conclusions. *Caries Res* 2011; 45 Suppl 1: 69–77.
- SHELLIS RP, FEATHERSTONE JDB, LUSSI A. Understanding the chemistry of dental erosion. *Monogr Oral Sci* 2014; 25: 163–179.
- SHIMADA Y, YOSHIYAMA M, TAGAMI J, SUMI Y. Evaluation of dental caries, tooth crack, and age-related changes in tooth structure using optical coherence tomography. *Jpn Dent Sci Rev* 2020; 56: 109–118.
- SILVA AG, MARTINS CC, ZINA LG, MOREIRA AN, PAIVA SM, PORDEUS IA, ET AL. The association between occlusal factors and noncarious cervical lesions: a systematic review. *J Dent* 2013; 41: 9–16.
- SIMMER JP, PAPAGERAKIS P, SMITH CE, FISHER DC, ROUNTREY AN, ZHENG L, ET AL. Regulation of dental enamel shape and hardness. *J Dent Res* 2010; 89: 1024–1038.
- SMITH BG, KNIGHT JK. An index for measuring the wear of teeth. *Br Dent J* 1984; 156: 435–438.
- SMITH CE. Cellular and chemical events during enamel maturation. *Crit Rev Oral Biol Med* 1998; 9: 128–161.
- STEINIGER B, SCHWARZBACH H, STACHNISS V. *Mikroskopische Anatomie der Zähne und des Parodonts*. 1. 2010. Thieme, Stuttgart.
- STENHAGEN KR, HOLME B, TVEIT AB, LUSSI A, CARVALHO TS. Analytical strategies for clinical studies on dental erosive wear. *BMC Oral Health* 2019; 19: 167.
- STOOKEY GK, MUHLER JC. Laboratory studies concerning the enamel and dentin abrasion properties of common dentifrice polishing agents. *J Dent Res* 1968; 47: 524–532.
- STRICKER EJ, GÖHRING TN. Influence of different posts and cores on marginal adaptation, fracture resistance, and fracture mode of composite resin crowns on human mandibular premolars. An in vitro study. *J Dent* 2006; 34: 326–335.
- TAKEHARA J, TAKANO T, AKHTER R, MORITA M. Correlations of noncarious cervical lesions and occlusal factors determined by using pressure-detecting sheet. *J Dent* 2008; 36: 774–779.
- TEAFORD MF, OYEN OJ. Live primates and dental replication: new problems and new techniques. *Am J Phys Anthropol* 1989; 80: 73–81.
- TEIXEIRA DNR, THOMAS RZ, SOARES PV, CUNE MS, GRESNIGT MMM, SLOT DE. Prevalence of noncarious cervical lesions among adults: A systematic review. *J Dent* 2020; 95: 103285.

- TELLEFSEN G, LILJEBORG A, JOHANNSSEN A, JOHANNSSEN G. The role of the toothbrush in the abrasion process. *Int J Dent Hyg* 2011; 9: 284–290.
- TEN CATE JM, ARENDS J. Remineralization of artificial enamel lesions in vitro: III. A study of the deposition mechanism. *Caries Res* 1980; 14: 351–358.
- TEZEL A, CANAKÇI V, CIÇEK Y, DEMIR T. Evaluation of gingival recession in left- and right-handed adults. *Int J Neurosci* 2001; 110: 135–146.
- THOMPSON VP. The tooth: An analogue for biomimetic materials design and processing. *Dent Mater* 2020; 36: 25–42.
- THORSEN G. The gingival region of the tooth, and in particular the anatomical relation between the enamel and cementum. *Dental Cosmos* 1917; 59: 836.
- TOSAKA Y, NAKAKURA-OHSHIMA K, MURAKAMI N, ISHII R, SAITOH I, IWASE Y, ET AL. Analysis of tooth brushing cycles. *Clin Oral Investig* 2014; 18: 2045–2053.
- TRAVASSOS DA ROSA MOREIRA BASTOS R, TEIXEIRA DA SILVA P, NORMANDO D. Reliability of qualitative occlusal tooth wear evaluation using an intraoral scanner: A pilot study. *PLoS One* 2021; 16: e0249119.
- TSENOVA-ILIEVA I, KAROVA E. Application of atomic force microscopy in dental investigations. *Int. j. sci. res.* 2020; 9: 1319–1326.
- TURSSI CP, BINSALEH F, LIPPERT F, BOTTINO MC, ECKERT GJ, MOSER EAS, ET AL. Interplay between toothbrush stiffness and dentifrice abrasivity on the development of non-carious cervical lesions. *Clin Oral Investig* 2019a; 23: 3551–3556.
- TURSSI CP, KELLY AB, HARA AT. Toothbrush bristle configuration and brushing load: Effect on the development of simulated non-carious cervical lesions. *J Dent* 2019b; 86: 75–80.
- UHLEN MM, MULIC A, HOLME B, TVEIT AB, STENHAGEN KR. The susceptibility to dental erosion differs among individuals. *Caries Res* 2016; 50: 117–123.
- UNGAR PS, GRINE FE, TEAFORD MF, EL ZAATARI S. Dental microwear and diets of African early Homo. *J Hum Evol* 2006; 50: 78–95.
- UNGAR PS. Mammalian dental function and wear: A review. *Biosurface and Biotribology* 2015; 1: 25–41.
- URZÚA I, CABELLO R, RODRÍGUEZ R, SÁNCHEZ J, FALEIROS S, PACHECO A. Absence of non-carious cervical lesions (NCCs) in a Chilean pre-Columbian sample with severe occlusal tooth wear. *Int J Odontostomatol* 2015; 9: 59–64.
- VAN DER WEIJDEN G, TIMMERMAN MF, REIJERSE E, SNOEK CM, VAN DER VELDEN U. Toothbrushing force in relation to plaque removal. *J Clin Periodontol* 1996; 23: 724–729.
- VAN DER WEIJDEN GA, TIMMERMAN MF, DANSER MM, VAN DER VELDEN U. Relationship between the plaque removal efficacy of a manual toothbrush and brushing force. *J Clin Periodontol* 1998; 25: 413–416.
- VERSTEEG PA, PISCAER M, ROSEMA N A. M, TIMMERMAN MF, VAN DER VELDEN U, VAN DER WEIJDEN GA. Tapered toothbrush filaments in relation to gingival abrasion, removal of plaque and treatment of gingivitis. *Int J Dent Hyg* 2008; 6: 174–182.
- VÖLK W, MIERAU HD, BIEHL P, DORNHEIM G, REITHMAYER C. Beitrag Zur Ätiologie der keilförmigen Defekte. *Dtsch. Zahnärztl. Z.* 1987; 42: 499–504.
- VOSSEN ME, LETZEL H, STADHOUDERS AM, HERTEL R, HENRIKS FH. A rapid scanning electron microscopic replication technique for clinical studies of dental restorations. *Dent Mater* 1985; 1: 158–163.
- WALKER A, HOECK HN, PEREZ L. Mecrowear of mammalian teeth as an indicator of diet. *Science* 1978; 201: 908–910.
- WALKER SL, ASH MM. A study of root planning by scanning electron microscopy. *Dent Hyg (Chic)* 1976; 50: 109–114.
- WALTER C, KRESS E, GÖTZ H, TAYLOR K, WILLERSHAUSEN I, ZAMPETIS A. The anatomy of non-carious cervical lesions. *Clin Oral Investig* 2014; 18: 139–146.
- WALTERS PA. Dentinal hypersensitivity: a review. *J Contemp Dent Pract* 2005; 6: 107–117.
- WANG L, GUAN X, YIN H, MORADIAN-OLDAK J, NANCOLLAS GH. Mimicking the self-organized microstructure of tooth enamel. *J Phys Chem C Nanomater Interfaces* 2008; 112: 5892–5899.
- WANG Z, SA Y, SAURO S, CHEN H, XING W, MA X, ET AL. Effect of desensitising toothpastes on dentinal tubule occlusion: a dentine permeability measurement and SEM in vitro study. *J Dent* 2010; 38: 400–410.
- WEATHERELL JA, WEIDMANN SM, EYRE DR. Histological appearance and chemical composition of enamel proteins from mature human molars. *Caries Res* 1968; 2: 281–293.
- WEST NX, SANZ M, LUSSI A, BARTLETT D, BOUCHARD P, BOURGEOIS D. Prevalence of dentine hypersensitivity and study of associated factors: a European population-based cross-sectional study. *J Dent* 2013; 41: 841–851.
- WIEGAND A, SCHWERZMANN M, SENER B, MAGALHAES AC, ROOS M, ZIEBOLZ D, ET AL. Impact of toothpaste slurry abrasivity and toothbrush filament stiffness on abrasion of eroded enamel - an in vitro study. *Acta Odontol Scand* 2008; 66: 231–235.

- WIEGAND A, KUHN M, SENER B, ROOS M, ATTIN T. Abrasion of eroded dentin caused by toothpaste slurries of different abrasivity and toothbrushes of different filament diameter. *J Dent* 2009; 37: 480–484.
- WIEGAND A, ATTIN T. Design of erosion/abrasion studies—insights and rational concepts. *Caries Res* 2011; 45 Suppl 1: 53–59.
- WIEGAND A, BURKHARD JPM, EGGMANN F, ATTIN T. Brushing force of manual and sonic toothbrushes affects dental hard tissue abrasion. *Clin Oral Investig* 2013; 17: 815–822.
- WIEGAND A, SCHLUETER N. The role of oral hygiene: does toothbrushing harm? Monographs in oral science. 2014. Monogr Oral Sci.
- WILBUR EUGENE R, STOCUM D. Part II: Temporomandibular joint (TMJ)-regeneration, degeneration, and adaptation. *Curr Osteoporos Rep. Springer Nature* 2018; Current Osteoporosis Reports: 369–79.
- WILMERS J, BARGMANN S. Nature's design solutions in dental enamel: Uniting high strength and extreme damage resistance. *Acta Biomater* 2020; 107: 1–24.
- WINTERFELD T, SCHLUETER N, HARNACKE D, ILLIG J, MARGRAF-STIKSRUD J, DEINZER R, ET AL. Toothbrushing and flossing behaviour in young adults—a video observation. *Clin Oral Investig* 2015; 19: 851–858.
- WITECY C, GANSS C, WÖSTMANN B, SCHLENZ MB, SCHLENZ MA. Monitoring of erosive tooth wear with intraoral scanners in vitro. *Caries Res* 2021; 55: 215–224.
- WORAWONGVASU R. Scanning electron microscope characterization of noncarious cervical lesions in human teeth. *J Oral Maxillofac Pathol* 2021; 25: 202.
- WRIGHT K. The abrasive wear resistance of human dental tissues. *Wear* 1969;263–284.
- WULFMAN C, KOENIG V, MAINJOT AK. Wear measurement of dental tissues and materials in clinical studies: A systematic review. *Dent Mater* 2018; 34: 825–850.
- XU H, SMITH DT, JAHANMIR S, ROMBERG E, KELLY JR, THOMPSON VP, ET AL. Indentation damage and mechanical properties of human enamel and dentin. *J Dent Res* 1998; 77: 472–480.
- XU H, ZHENG Q, SHAO Y, SONG F, ZHANG L, WANG Q, ET AL. The effects of ageing on the biomechanical properties of root dentine and fracture. *J Dent* 2014; 42: 305–311.
- YADAV U, AHMED J, ONGOLE R, SHENOY N, SUJIR N, NATARAJAN S. Influence of psychosocial factors and parafunctional habits in temporomandibular disorders: a cross-sectional study. *Perm J* 2020; 24: 19.144.
- YETTRAM AL, WRIGHT KW, PICKARD HM. Finite element stress analysis of the crowns of normal and restored teeth. *J Dent Res* 1976; 55: 1004–1011.
- YOUNG RA. Implications of atomic substitutions and other structural details in apatites. *J Dent Res* 1974; 53: 193–203.
- ZACHRISSON BU, ARTHUN J. Enamel surface appearance after various debonding techniques. *Am J Orthod* 1979; 75: 121–127.
- ZACHRISSON BU, SKOGAN O, HÖYMYHR S. Enamel cracks in debonded, debanded, and orthodontically untreated teeth. *Am J Orthod* 1980; 77: 307–319.
- ZENTNER A, DUSCHNER H. Structural changes of acid etched enamel examined under confocal laser scanning microscope. *J Orofac Orthop* 1996; 57: 202–209.
- ZIMMER S, LIEDING L. Gewohnheiten und Kenntnisse zur Mundhygiene in Deutschland – Ergebnisse einer bevölkerungsrepräsentativen Befragung. *Dtsch. Zahnärztl. Z.* 2014; 69: 584–593.

10 Danksagung

Ich möchte **Prof. Dr. Dr. h.c. Peter Gängler** meinen herzlichen Dank aussprechen, da er die Idee für diese Arbeit bereitstellte, den Grundstein legte und mir die Möglichkeit zur Promotion ermöglichte. Besonders schätze ich seine kontinuierliche Unterstützung, herausragende Betreuung, zahlreiche förderliche Ratschläge und die stets offene Tür. Ebenso danke ich **Dr. Tomas Lang** für die Kontaktaufnahme über den Podcast *Intra Dental* und die Vermittlung am Institut *ORMED*.

Frau **Sabine Schön** vom Forschungslaboratorium der Poliklinik für Konservierende Zahnheilkunde und Parodontologie am Universitätsklinikum Jena danke ich herzlich für ihre geduldige Einweisung in die Replikationstechnik trotz begrenzter Zeit. Ebenso gilt mein großer Dank **Dr. Sandor Nietzsche** vom Elektronenmikroskopischen Zentrum des Universitätsklinikums Jena für bereichernde Stunden vor dem REM und die stetige Möglichkeit, Neues zu lernen. Außerdem danke ich **Dr. Matthias Hemmleb** von *point electronics* für seine Unterstützung bei Softwareproblemen.

Ich danke dem Dentallabor von Marcus Rönicke in Hermannsburg für den flexiblen Arbeitsplatz und die Unterstützung bei der Modellherstellung. **Maik Siebler** gebührt mein herzlicher Dank für seine äußerst kompetente Unterstützung und Beratung zu statistischen Themen. Sein herausragendes mathematisches Verständnis hat mir die Grundlagen und Hypothesentests auf anschauliche Weise nähergebracht. Ebenso möchte ich mich für seine unterstützende Begleitung nach Rhodos zur Posterpräsentation und zur abschließenden Verteidigung herzlich bedanken. Ein großer Dank geht an **Markus Ehm** von *Tietgen&Ehm 3D Solutions* für die Einführung und Bereitstellung der Software *Reshaper 3D* zur genauen Vermessung des Abrasionsvolumens.

Außerdem möchte ich noch meinem Lebenspartner **Dr. Jan Linxweiler** danken. Vornehmlich bin ich für sein unermüdliches geduldiges Zuhören, die Bereitstellung der notwendigen Technologien, für seine Rücksichtnahme und uneingeschränkten Aufmunterungen sowie für jede einzelne Umarmung in den schwierigen Phasen dankbar.

Von ganzem Herzen möchte ich zuletzt noch meiner **Mutter Brigitte Wilke** für ihre Geduld, Bereitschaft zum Zuhören und für die unaufhörliche Unterstützung in jeglicher Hinsicht danken. Ohne all diese Unterstützung wäre diese Arbeit nicht möglich gewesen.

Widmen möchte ich die Arbeit meinen Großeltern, meinem **Großvater Dr. Wolfgang Klein**, der mit seinen mittlerweile 102 Lebensjahren schon zahlreiche eigene Bücher veröffentlicht hat und meiner **Großmutter Anneliese Klein** die ihm stets all die Jahre unterstützend zur Seite stand.

11 Curriculum Vitae

▪ Persönliche Daten

Familienname	Wilke
Vorname	Katharina
Anschrift	Am Wasserturm 58 29223 Celle
Geboren am	17.12.1984
Geburtsort	Albstadt
Familienstand	ledig
Staatsangehörigkeit	deutsch

▪ Beruflicher Werdegang

10/2023 – heute	Angestellte Zahnärztin in der Zahnarztpraxis OZeAHN in Didderse
01/2023 – 09/2023	Angestellte Zahnärztin in der Zahnarztpraxis Deneke in Wienhausen
02/2021 – 12/2022	Angestellte Zahnärztin in der Zahnarztpraxis Müden Aller
11/2018 – 11/2020	Assistenz Zahnärztin in der Zahnarztpraxis Behn
03/2015 – 09/2018	Truppenzahnärztin und Orientierungslauf Sportkader bei der Bundeswehr mit Teilnahme an den 6. Military World Games in Südkorea

▪ Bildungsweg

Seit WiSe 2021	Promotionsstudentin an der Universität Witten/Herdecke
23. März 2015	Erteilung der Approbation als Zahnärztin – Regierung Oberbayern
04/2009 – 03/2015	Fortsetzung Studium der Zahnmedizin – Universität Regensburg
01/2009 - 03/2009	Dreimonatige Grundausbildung bei der Bundeswehr
05/2008 - 12/2008	Studium der Zahnmedizin – Universität Regensburg
10/2005 - 04/2008	Studium Biologie und Chemie (Lehramt) - Universität Tübingen
24. Juni 2005	Gymnasium Balingen Schulabschluss allgemeine Hochschulreife

12 Eidesstattliche Erklärung

Katharina Wilke
Am Wasserturm 58
29223 Celle

Eidesstattliche Erklärung

Ich versichere (an Eides statt), dass ich die zur Erlangung des Doktorgrades der Zahnheilkunde vorgelegte Dissertationsschrift mit dem Thema „*Structural pathobiology of cervical wear by robot-simulated three-year toothbrushing*“ *selbstständig* und ohne unerlaubte fremde Hilfe angefertigt und die in der Arbeit verwendete Literatur vollständig zitiert habe.

Die nachfolgend genannten Personen haben mich bei der Methodik, Auswahl und Auswertung des Materials sowie bei der Erstellung des Manuskriptes unterstützt:

Prof. Dr. Dr. h.c. P. Gängler (PG)¹, Dr. Sandor Nietzsche (SN)².

Ich habe diese Dissertation weder in dieser noch in einer ähnlichen Form an einer anderen Hochschule eingereicht.

Celle, der 29.11.2023

Ort, Datum



Unterschrift

¹ Institute for Oral Medicine at the University of Witten/Herdecke, Germany

² Centre for Electron Microscopy, University Hospital Jena, Jena, Germany

Appendix

A.1 Vote of the Ethics Committee

Application number: SR-67/2021

Approval on 3 May 2021

**Ethik-Kommission der
Universität Witten / Herdecke**

Universität Witten/Herdecke - Ethik-Kommission - Alfred-Herrhausen-Str. 50 - D-58448 Witten

Herrn:
Prof. Dr. med. dent. Dr. h. c. Peter Gängler
persönlich/vertraulich
ORMED CEO
Alfred-Herrhausen-Straße 45
54455 Witten

-per Hauspost-

Ethik-Kommission
Alfred-Herrhausen-Str. 50
D-58448 Witten

Sekretariat:
Frau Andrea Plegier
Mo-Fr 8.00-12.00 Uhr
Telefon 02302/926-740
Telefax 02302/926-739
e-mail: sekretariat-ethik@uni-wi.de
Internet: www.ethik-kommission-irah.de

03.05.2021
Ga/eb

cc:
Frau
Katharina Wilke
persönlich/vertraulich
Am Wasserturn 58
59223 Cella

Antrag Nr. SR-67/2021 (bitte stets angeben)
Micromorphology of toothbrush wear and cervical abrasion at the cemento-enamel junction of different human teeth by robot simulation of 3 years brushing

Sehr geehrter Herr Professor Dr. Dr. Gängler,


herzlichen Dank für die mit Mail vom 29.04.2021 übermittelten Unterlagen, Zugang am 30.04.2021.

Mit den vorgenommenen Änderungen bzw. Ergänzungen sind Sie den Hinweisen der Ethik-Kommission in ihrem Schreiben vom 20.04.2021 nachgekommen.

Weitere ethische oder rechtliche Bedenken gegen das Projekt sind nicht ersichtlich.

Für dessen Durchführung wünschen wir der Doktorandin wie auch Ihnen viel Erfolg!

Mit freundlichen Grüßen



i. A.

RA Prof. Dr. med. P. W. Gaidzik
Geschäftsführendes Vorstandsmitglied

Ethik-Kommission der Universität Witten/Herdecke e. V.
Vorstand: Prof. Dr. med. Petra Thümmann (Vorsitzende), Prof. Dr. med. nat. Ulrike Heineke, RA Prof. Dr. med. Peter W. Gaidzik
Sitz des Vereins: Witten, Amtsgericht Witten VR 779; Bank: Sparkasse Witten (BLZ 452 500 35) Konto-Nr. 0050534
IBAN: DE 41 4525 0035 0000 0505 34 SWIFT-BIC: WELADED1WITN

Approval amendment on 8 January 2022

**Ethik-Kommission der
Universität Witten / Herdecke**

Universität Witten/Herdecke - Ethik-Kommission - Alfred-Herrhausen-Str. 50 - D-58448 Witten

Herrn:
Prof. Dr. med. dent. Dr. h. c. Peter Gängler
persönlich/vertraulich
ORMED CEO
Alfred-Herrhausen-Straße 45
54455 Witten

-per Hauspost-

Ethik-Kommission
Alfred-Herrhausen-Str. 50
D-58448 Witten

Sekretariat:
Frau Andrea Plegier
Mo-Fr 8.00-12.00 Uhr
Telefon 02302/926-740
Telefax 02302/926-739
e-mail: sekretariat-ethik@uni-wi.de
Internet: www.ethik-kommission-irah.de

08.01.2022
Ga/wa

cc:
Frau
Katharina Wilke
persönlich/vertraulich
Am Wasserturn 58
59223 Cella

Antrag Nr. SR-67/2021 (bitte stets angeben)
Micromorphology of toothbrush wear and cervical abrasion at the cemento-enamel junction of different human teeth by robot simulation of 3 years brushing


Sehr geehrter Herr Professor Dr. Dr. Gängler,

herzlichen Dank für die mit Mail vom 03.01.2022 übermittelten Unterlagen, Zugang am selben Tag.

Mit den vorgenommenen Änderungen / Ergänzungen sind Sie den Hinweisen der Ethik-Kommission in ihrem Schreiben vom 03.08.2021 nachgekommen.

Für die Durchführung des Promotionsprojektes wünschen wir der Doktorandin wie auch Ihnen viel Erfolg!

Mit freundlichen Grüßen



i. A.

RA Prof. Dr. med. P. W. Gaidzik
Geschäftsführendes Vorstandsmitglied

Ethik-Kommission der Universität Witten/Herdecke e. V.
Vorstand: Prof. Dr. med. Petra Thümmann (Vorsitzende), Prof. Dr. med. nat. Ulrike Heineke, RA Prof. Dr. med. Peter W. Gaidzik
Sitz des Vereins: Witten, Amtsgericht Witten VR 779; Bank: Sparkasse Witten (BLZ 452 500 35) Konto-Nr. 0050534
IBAN: DE 41 4525 0035 0000 0505 34 SWIFT-BIC: WELADED1WITN

A.2 Information for study participants (tooth donation)

Praxisstempel



Information für Studienteilnehmende

Sehr geehrte Studieninteressentin, sehr geehrter Studieninteressent,

Bei Ihnen wurde heute aus **strenger, medizinischer Indikation** heraus ein Zahn gezogen. Aus Sicht Ihres Zahnarztes wäre Ihr extrahierter Zahn / Ihre extrahierten Zähne dazu geeignet, in ein Forschungsprojekt aufgenommen zu werden. Daher möchten wir Sie nach Ihrer Bereitschaft fragen, Ihren extrahierten Zahn / Ihre extrahierten Zähne für dieses Forschungsvorhaben zu spenden.

Ihre Zahnspende wird **anonymisiert** in die Studie aufgenommen. Zu Ihrem Zahn / Ihren Zähnen werden nur ihr Alter und der Extraktionsgrund notiert. Darüber hinaus findet keine Zuordnung personenbezogener Daten statt. Es werden keine gendiagnostischen Untersuchungen vorgenommen. Außerdem erfolgt eine Begutachtung durch die zuständige Ethikkommission.

Ihre Teilnahme an dieser Studie ist **freiwillig**. Sie werden also nur dann einbezogen, wenn Sie dazu schriftlich Ihr Einverständnis erklären. Sofern Sie nicht an der Studie teilnehmen oder später aus ihr ausscheiden möchten (auch ohne Angabe von Gründen), entstehen für Sie keine Nachteile oder Konsequenzen jeglicher Art.

Grundlegende Informationen zur Studie:

Die Studie findet an der Universitätsklinik Witten/Herdecke in Kooperation mit der Friedrich-Schiller-Universität Jena statt und wird im Laufe dieses Jahres durchgeführt.

Der Zweck dieser Studie ist es verschiedene Zahnbürsten auf ihre Abriebkraft an der Zahnhartsubstanz zu testen. Ziel ist es, dadurch in Zukunft Zahnbürsten noch zahnfreundlicher zu gestalten.

Vielen Dank für Ihre Teilnahme!

Folgende Personen stehen für Sie bei Rückfragen zur Verfügung:

Katharina Wilke
ORMED Institut
katie.wilke@gmx.de

A.3 Declaration of consent (tooth donation)

Praxisstempel



ORMED - Alfred-Herrhausen-Str.45 -
58455 Witten - Germany

Einverständniserklärung zur Zahnspende

Die Zahnextraktion erfolgte aus **strenger, medizinischer Indikation** heraus.

Für die Studie werden zu Ihrer Zahnspende nur ihr Alter und der Indikationsgrund notiert.
Ansonsten werden keine personenbezogenen Daten erhoben.

Die Zahnspende wird **anonymisiert** in die Studie aufgenommen und kann Ihnen dann nicht mehr zugeordnet werden.

Es werden dabei keine gendiagnostischen Untersuchungen vorgenommen.

Ihr Einverständnis zur Zahnspende erfolgt **freiwillig**. Es entstehen Ihnen keine Nachteile, wenn Sie dieses widerrufen.

Ich habe eine Kopie der Einverständniserklärung erhalten

Ich verzichte auf eine Kopie der Einverständniserklärung.

**Hiermit erkläre ich mich bereit, meinen extrahierten Zahn für das Forschungsprojekt am ORMED-Institut an der Universitätsklinik Witten/Herdecke zu spenden.
Ich bestätige, dass ich die Informationsschrift erhalten habe und über den Zweck der Studie informiert worden bin.**

Ort, Datum

Unterschrift Patient/in oder gesetzliche/r Vertreter/in

A.4 Method for video observations

Bestimmung der Putzfrequenz



ORMED - Alfred-Herrhausen-Str.45 -
58455 Witten - Germany

Methode zur Bestimmung der Putzfrequenz:

Ermittlung eines Durchschnittswerts

Die Rekrutierung der Probanden erfolgt mittels digitalen Aufrufs über die sozialen Medien. Laut einer Studie (SCHLUETER u. a., 2010) wurde eine **Stichprobengröße von 30 Probanden** als ausreichend erachtet, um Mundhygienetechniken zu erheben. Interessierte Teilnehmer erhalten mündliche und schriftliche Informationen über das Verfahren und den Zweck der Studie. Beim Erstkontakt wird außerdem **eine Einverständniserklärung** zugesandt und die **Einschlusskriterien** abgefragt.

Nach der informierten Zustimmung werden die Probanden gebeten, einen **Fragebogen** zu ihren Putzgewohnheiten auszufüllen und ihre Zähne auf ihre gewohnte Weise mit einer Handzahnbürste und Zahnpasta zu reinigen und sich dabei selbst zu filmen.

Das Zähneputzen **wird 30 Sekunden lang vor einem Spiegel mit Zahnpasta** durchgeführt. Der Proband filmt sich dabei selbst. Der Spiegel soll die Aufnahme erleichtern. Der Proband wird instruiert mit den Außenflächen der rechten Unterkieferzähne zu beginnen und sich dann zu den unteren Frontzähnen vorzuarbeiten, da dass die Region ist, für die der Roboter programmiert wurde. Zur Aufnahme kann ein Smartphone oder ein vergleichbares Gerät verwendet werden.

Einschlusskriterien sind:

- die schriftliche, informierte Einwilligung
- Alter ≥ 18 Jahre, Mitteleuropäer
- ein Gebiss mit mehr als 20 Zähnen
- ein Videoaufnahmegerät
- der Besitz einer manuellen Zahnbürste

Ausschlusskriterien sind:

- festsitzende kieferorthopädische Apparaturen
- geistige oder körperliche Behinderungen, die die Durchführung der Mundhygiene beeinflussen könnten.
- herausnehmbarer Zahnersatz

Die Daten werden **pseudonymisiert** (gemäß Art.4 Nr.5 DS-GVO) erhoben. Dabei werden keine individuellen Fallberichte erstellt, sondern nur ein Durchschnittswert ermittelt.

SCHLUETER, N. ; KLIMEK, J. ; SALESCHKE, G. ; GANSS, C.: Adoption of a toothbrushing technique: a controlled, randomised clinical trial. In: *Clinical Oral Investigations* Bd. 14 (2010), Nr. 1, S. 99–106

A.5 Information for study participants (video observation)

Bestimmung der Putzfrequenz



ORMED - Alfred-Herrhausen-Str.45 -
58455 Witten - Germany

Information für Studienteilnehmer*innen

Die Studie findet an der Universitätsklinik Witten/Herdecke in Kooperation mit der Friedrich-Schiller-Universität Jena statt und wird im Laufe dieses Jahres durchgeführt.

Der **Zweck dieser Studie** ist es, verschiedene Zahnbürsten auf ihre Abriebkraft an der Zahnhartsubstanz zu testen. Ziel ist es, dadurch in Zukunft Zahnbürsten noch zahnfreundlicher zu gestalten.

Das Testprogramm für die Zahnbürsten wird von einem **Sechs-Achsen-Roboter** ausgeführt. Der Roboter dient zur Simulation der Zahnputzbewegungen des Menschen.



Allerdings fehlen in der Literatur bisher eindeutige Daten über die durchschnittliche Geschwindigkeit von Putzbewegungen. Diese Erhebung dient dazu, das Abriebverhalten von Zahnbürsten auf den Zähnen klinisch besser interpretieren zu können.

Deswegen bitten wir Sie darum, sich

30 Sekunden lang beim Zähneputzen zu filmen.

Dafür beginnen Sie bitte mit dem Zähneputzen im rechten Unterkiefer mit den äußeren Flächen der Seitenzähne und arbeiten sich dann zu den unteren Frontzähnen vor.

Das ist die Region, auf die der Roboter programmiert wurde. Bitte achten Sie darauf, dass wir ihre Putzbewegungen auf dem Filmmaterial anschließend erkennen können.

Ihre Daten werden **pseudonymisiert**, d.h. in verschlüsselter Form (*gemäß Art.4 Nr.5 DS-GVO*) in die Studie aufgenommen. Es findet keine Zuordnung personenbezogener Daten statt. Das gilt auch für den beiliegenden Fragebogen. Die Erhebung findet im Rahmen einer Studie statt, die bereits von der Ethik-Kommission begutachtet worden ist.

Ihre Teilnahme an dieser Studie ist **freiwillig**. Sie werden also nur dann einbezogen, wenn Sie dazu schriftlich Ihr Einverständnis erklären. Sofern Sie nicht an der Studie teilnehmen oder später aus ihr ausscheiden möchten (auch ohne Angabe von Gründen), entstehen für Sie keine Nachteile oder Konsequenzen jeglicher Art.

Vielen Dank für Ihre Teilnahme!

Ansprechperson bei Rückfragen:
Katharina Wilke - katie.wilke@gmx.de

A.6 Video observation consent form

Bestimmung der Putzfrequenz



Einverständniserklärung zur Bestimmung der Putzfrequenz

Sie haben sich bereit erklärt, ein **30 Sekunden langes Video** über Ihre Putzgewohnheiten aufzunehmen und es zur Auswertung für die Studie freizugeben.

Für die Studie wird das Video analysiert und es wird ggfs. der dazugehörige Fragebogen ausgewertet. Es werden dabei keine personenbezogenen Daten erhoben.

Die Daten werden **pseudonymisiert**, d.h. in verschlüsselter Form (*gemäß Art.4 Nr.5 DS-GVO*) in die Studie aufgenommen und werden Ihnen dann nicht mehr direkt zugeordnet.

Ihr Einverständnis zur Studienteilnahme erfolgt **freiwillig**. Es entstehen Ihnen keine Nachteile, wenn Sie dieses widerrufen.

- Hiermit erkläre ich mich bereit, meine Videoaufnahme über meine Zahnputzgewohnheiten für das Forschungsprojekt am ORMED-Institut an der Universitätsklinik Witten/Herdecke freizugeben.

- Ich bestätige, dass ich die Informationsschrift erhalten habe und über den Zweck der Studie informiert worden bin.

Ort, Datum

Unterschrift Proband/in oder gesetzliche/r Vertreter/in

A.7 Questionnaire on tooth brushing habits

Bestimmung der Putzfrequenz

Vorname:

Name:



ORMED - Alfred-Herrhausen-Str.45 -
58455 Witten - Germany

Fragebogen zu ihren Zahnputzgewohnheiten

Wurde Ihnen jemals eine Zahnputztechnik vermittelt? Ja Nein

Wenn ja, von wem? _____

Welche? _____

Wie oft putzen Sie ihre Zähne?

3x täglich 2x täglich 1x täglich nicht täglich

Wann putzen Sie ihre Zähne?

Vor dem Frühstück	<input type="checkbox"/>	Nach dem Frühstück	<input type="checkbox"/>
Nach dem Mittagessen	<input type="checkbox"/>	Nach dem Abendessen	<input type="checkbox"/>
Nach Zwischenmahlzeiten	<input type="checkbox"/>	Vor dem ins Bett gehen	<input type="checkbox"/>
Unterschiedlich	<input type="checkbox"/>		

Wie lange putzen Sie ihre Zähne?

~ 30 Sekunden ~ 1 Minute ~ 1,5 Minuten
 ~ 2 Minuten ≥ 3 Minuten

Was ist ihre bevorzugte Putztechnik?

Horizontal (Schrubkend) Rotierend (Kreisend) Vertikal (Rot-Weiß)

Welche Zahnputzmittel verwenden Sie zur Mundhygiene?

Manuelle Zahnbürste	<input type="checkbox"/>	Elektrische Zahnbürste	<input type="checkbox"/>	Zahnpasta	<input type="checkbox"/>
Zahnseide	<input type="checkbox"/>	Zahnstocher	<input type="checkbox"/>	Zahnzwischenraumbürste	<input type="checkbox"/>
Munddusche	<input type="checkbox"/>	Mundspüllösung	<input type="checkbox"/>	Zuckerfreie Kaugummis	<input type="checkbox"/>
Sonstiges:					

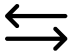
A.8 Video evaluation table


Video evaluation table:


(1 Hertz (Hz) = 1 (Double) stroke per second)

	Coding	Double strokes/s	Brushing technique (buccal)	Questionnaire	♂ ♀
01.	EEd5gd4t	3.6 Hz	Rotating	yes	♀
02.	fPmgGV9U	3.8 Hz	Rotating	no	♀
03.	Uuv6goYB	4.0 Hz	Vertical	yes	♀
04.	jMR9kxRq	4.8 Hz	Horizontal	no	♂
05.	cGmV96f8	3.2 Hz	Rotating & Horizontal	no	♀
06.	UcMPjuL5	3.8 Hz	Horizontal & Pen grip	yes	♂
07.	PWBcYUf2	4.1 Hz	Rotating	yes	♂
08.	Vma2eziZ	5.2 Hz	Vibrating, Rotating	no	♀
09.	V6raDghw	4.1 Hz	Rotating	no	♂
10.	de4EyNSv	3.5 Hz	Rotating	no	♀
11.	fGZYqNA7	4.6 Hz	Horizontal	no	♂
12.	BVRXrPnv	3.3 Hz	Vertical	no	♀
13.	NustDkw5	7.0 Hz	Vibrating, Horizontal	no	♂
14.	ZuudQJNU	3.6 Hz	Horizontal & Vertical	no	♂
15.	6EWYGk6L	5.3 Hz	Horizontal	no	♂
16.	PZTC8nsm	3.7 Hz	Vertical	no	♀
17.	JZ2cvdsa	5.4 Hz	Rotating & Horizontal	no	♂
18.	WQbWQVri	3.8 Hz	Rotating	no	♂
19.	TMAtebLi	4.4 Hz	Rotating	no	♀
20.	w3EMATWB	4.1 Hz	Rotating	no	♀
21.	8uUbhmrA	4.0 Hz	Rotating	yes	♀
22.	nJcWBvyv	4.5 Hz	Horizontal	no	♂
23.	r8JXqdzZ	4.5 Hz	Rotating	yes	♀
24.	Ba9HVUvp	4.5 Hz	Rotating & Horizontal	yes	♀
25.	wc6GRs9h	4.8 Hz	Horizontal	yes	♂
26.	ZV3FwfjT	3.9 Hz	Horizontal	yes	♀
27.	KySmy9FJ	3.8 Hz	Horizontal	no	♀
28.	RUgzFUnh	4.7 Hz	Rotating & Horizontal	no	♂
29.	mnn76mkW	4.0 Hz	Horizontal & Vertical	no	♀
30.	4RKap3PS	4.2 Hz	Rotating	no	♀
31.	eTVRPMLA	4.4 Hz	Rotating	no	♀
32.	us6hXYXT	2.8 Hz	Rotating & Vertical	no	♀
33.	ox3fBRJG	4.5 Hz	Horizontal	no	♀
34.	Ae639VmS	4.2 Hz	Horizontal	no	♀
35.	fzfYFFTD	4.1 Hz	Rotating	no	♀
36.	APCEn4Xr	4.6 Hz	Rotating	yes	♀
37.	PoQG2FNi	4.0 Hz	Rotating	no	♀
38.	GuQsjKvM	4.8 Hz	Vibrating, Vertical	no	♀
39.	LL2CLsEQ	3.5 Hz	Horizontal	no	♀
40.	c8Uv5wT2	4.8 Hz	Rotating & Vertical	no	♀
41.	Pq3EAxjc	4.2 Hz	Rotating	no	♀
42.	NXEHB24m	3.6 Hz	Vertical	yes	♀
43.	JxXm9J9x	4.8 Hz	Rotating	no	♂
44.	yGR7KAnt	4.6 Hz	Rotierend & Vertical	no	♂
45.	BxW3Njpu	4.5 Hz	Rotating	no	♂
46.	5zGbm5LL	4.6 Hz	Rotating & Horizontal	no	♂
47.	QBiNA9aJ	4.9 Hz	Horizontal	no	♂
48.	pXMVmDDB	4.4 Hz	Rotating & Vertical	no	♀
49.	qNAqAigX	4.2 Hz	Rotating	no	♀
50.	5joHJxW	4.3 Hz	Horizontal	no	♀
	Average:	Double strokes/s	Brushing technique (buccal)	Gender: 32 ♀ / 18 ♂	
	Rotating:	4.19 Hz	20x Rotating (40%)	*Mixed distribution:	
	Horizontal:	4.48 Hz	14 x Horizontal (29%)	r + h 5x: 46%	
	Vertical:	3.5 Hz	5x Vertical (10%)	h + v 2x: 18%	
	Insgesamt:	4.14 Hz	11x Mixed (22%) *	r + v 4x: 36%	

A.9 Evaluation of robot tooth brushing programmes

Brushing programme:	1 st Contact phase	2 nd Contact phase
 <p>Horizontal Contact time: 17s Speed: 2.6 Hz (Back and forth)</p>	<p>The robot arm passed through eight different positions.</p> <p>4 horizontal strokes per position in 12 seconds. (8 positions x 4 strokes) ⇒ 32 horizontal strokes</p>	<p>The robot arm passed through three more positions.</p> <p>4 horizontal strokes per position in 5 seconds. (3 positions x 4 strokes) ⇒ 12 horizontal strokes</p>
	<p>Since the horizontal programme was run through twice for each brushing cycle and a half stroke was additionally applied during repositioning, this results in a total of 90 strokes in 17 seconds.</p>	
Evaluation strokes per tooth:	<p>Counting the positions in which the respective tooth was brushed horizontally: 47: 3x, 46: 4x, 45: 4x, 44: 4x, 43: 4x, 42: 4x, 41: 4x</p>	
<p>Each buccal tooth surface experienced 16 horizontal strokes during one cycle. Since the programme is run through twice, this results in a total of 32 horizontal strokes per tooth.</p>		

Brushing programme:	1 st Contact phase	2 nd Contact phase
 <p>Rotating Contact time: 19s Speed: 1.7 Hz (360° rotation)</p>	<p>The robot arm passed through eight different positions.</p> <p>3 rotating strokes per position in 14 seconds. (8 positions x 3 strokes) ⇒ 24 rotating strokes</p>	<p>The robot arm passed through three more positions.</p> <p>3 rotating strokes per position in 5 seconds. (3 positions x 3 strokes) ⇒ 9 rotating strokes</p>
	<p>During the rotating programme, a total of 33 rotating strokes are performed in 19 seconds.</p>	
Evaluation strokes per tooth:	<p>Counting the positions in which the respective tooth was brushed rotationally: 47: 3x, 46: 3x, 45: 3x, 44: 3x, 43: 3x, 42: 3x, 41: 3x</p>	
<p>Each buccal tooth surface experienced 9 rotating strokes during one cycle (\emptyset 3 positions x 3 rotating strokes).</p>		

Brushing programme:	1 st Contact phase	2 nd Contact phase
 <p>Vertical Contact time: 22s Speed: 1.5 Hz (Upward brushing)</p>	<p>The robot arm passed through eight different positions.</p> <p>3 vertical strokes per position in 16 seconds. (8 positions x 3 strokes) ⇒ 24 vertical strokes</p>	<p>The robot arm passed through three more positions.</p> <p>3 vertical strokes per position in 5 seconds. (3 positions x 3 strokes) ⇒ 9 vertical strokes</p>
	<p>During the vertical programme, a total of 33 vertical strokes are performed in 22 seconds.</p>	
Evaluation strokes per tooth:	<p>Counting the positions at which the respective tooth was brushed vertically: 47: 2x, 46: 3x, 45: 3x, 44: 3x, 43: 2x, 42: 3x, 41: 3x</p>	
<p>Each buccal tooth surface experienced 9 vertical strokes during one cycle (\emptyset 3 positions x 3 vertical strokes).</p>		

A.10 3D SEM calibration protocol

	Beam			Mag.			BSE			Scan			Save
Prep.	Fila	Emis	Spot	WD	Disp.	Real	horiz	dark	bright	pixel/ time	sph- cor.	z-cor.	1602 <i>(date)</i>
A42pre	7	60	5	26.7	25.4	23.9	√	√	60%	1024 1:01	11.6	0.915	A42pre_date
A42post	6	40	5	26.7	25.4	23.9	√	√	52%	1024 1:01	11.6	0.915	A42post_date
Fila: Filament (= wire of the glow cathode). Emis: Emission (= number of emitted electrons). Spot: = Diameter of the electron beam. WD: Working distance. Disp: Magnification shown on display. Real: Effective magnification after checking the lateral scaling. horiz: The mean measured value of total yield on a horizontal plane. dark: Zero balancing of all detectors when the primary beam is switched off.							bright: Amplification correction of all four detectors with the primary beam switched on. pixel/time: Resolution 1024 x 1024, raster scan time: 1.01 min (faster by a factor of 4 than 2048). sph-cor: Spherical correction using a horizontal calibration body. Number = radius of the virtual correction sphere. z-cor: Depth calibration by comparison with a calibration notch of known depth. Save: Name of the saved height profile data set.						

Using the control panel of SEM, electron beam was adjusted so that signal output was optimal in terms of our intended usage. First, function of filament (= wire of the incandescent cathode) was checked. As the tungsten wire gets thinner over time and sometimes bends up, the heating current had to be adjusted to possible changes before each application. Emission, i.e., the number of electrons emerging from the wire, is adjusted. The spot describes the probe diameter and was set to five for all following investigations, as this relatively large aperture is well suited for low magnifications.

A.11 Key parameters for in vitro tooth brushing studies

1. The brushing force exerted by each brush head should be accurately and conveniently controlled.
2. The brushing speed should be controlled.
3. A homogeneous paste slurry must be maintained during the test period.
4. It should be possible to test a range of different paste slurries within the same experimental run.
5. Individual specimens should be exposed to the same slurry rather than being individually isolated, the latter being currently the most common design.
6. Wear levels should be sufficient to facilitate the measurement of tissue loss in order to optimise accuracy, precision and resolution.
7. The temperature should be controlled and physiologically relevant.
8. The methodology should be straightforward and require minimal set-up time.

by Parry et al. (2008)